

The foundations of stable isotope geochemistry were laid in 1947 by Urey's classic paper on the thermodynamic properties of isotopic substances and by Nier's development of the ratio mass spectrometer. Before discussing details of the naturally occurring variations in stable isotope ratios, it is useful to describe some generalities that are pertinent to the field of non-radiogenic isotope geochemistry as a whole.

1. Isotope fractionation is pronounced when the mass differences between the isotopes of a specific element are large relative to the mass of the element. Therefore, isotope fractionations are especially large for the light elements. Recent developments in analytical techniques have opened the possibility to detect small variations in elements with much higher mass numbers. The heaviest element for which natural variations have been reported is uranium.
2. All elements that form solid, liquid, and gaseous compounds stable over a wide temperature range are likely to have variations in isotopic composition. Generally, the heavy isotope is concentrated in the solid phase in which it is more tightly bound. Heavier isotopes tend to concentrate in molecules in which they are present in the highest oxidation state.
3. Mass balance effects can cause isotope fractionations because modal proportions of substances can change during a chemical reaction. They are especially important for elements in situations where these coexist in molecules of reduced and oxidized compounds. Conservation of mass in an n component system can be described by

$$\delta_{(\text{system})} = \sum x_i \delta_i \quad (2.1)$$

where " x_i " is the mole fraction of the element in question for each of n phases within the system.

4. Isotopic variations in most biological systems are mostly caused by kinetic effects. During biological reactions (e.g. photosynthesis, bacterial processes) the lighter isotope is very often enriched in the reaction product relative to the

substrate. Most of the fractionations in biological reactions generally take place during the so-called rate determining step, which is the slowest step. It commonly involves a large reservoir, where the material actually used is small compared to the size of the reservoir.

2.1 Hydrogen

Until 1931 it was assumed that hydrogen consists of only one isotope. Urey et al. (1932) detected the presence of a second stable isotope, which was called deuterium. (In addition to these two stable isotopes there is a third naturally occurring but radioactive isotope, ^3H , tritium, with a half-life of approximately 12.5 years.) Rosman and Taylor (1998) gave the following average abundances of the stable hydrogen isotopes:

$$\begin{aligned}^1\text{H}: & 99.9885 \% \\ ^2\text{D}: & 0.0115 \%\end{aligned}$$

The isotope geochemistry of hydrogen is particular interesting, for two reasons:

- (1) Hydrogen is omnipresent in terrestrial environments occurring in different oxidation states in the forms of H_2O , H_3O^+ , OH^- , H_2 and CH_4 , even at great depths within the Earth. Therefore, hydrogen is envisaged to play a major role, directly or indirectly, in a wide variety of naturally occurring geological processes.
- (2) Hydrogen has by far the largest mass difference relative to the mass of the element between its two stable isotopes. Consequently hydrogen exhibits the largest variations in stable isotope ratios of all elements.

The ranges of hydrogen isotope compositions of some geologically important reservoirs are given in Fig. 2.1. It is noteworthy that all rocks on Earth have somewhat similar hydrogen isotope compositions, which is a characteristic feature of hydrogen, but not of the other elements. The reason for this overlap in isotope composition for rocks is likely due to the enormous amounts of water that have been cycled through the outer shell of the Earth.

2.1.1 Methods

Determination of the D/H ratio of water is performed on H_2 -gas. There are two different preparation techniques: (i) equilibration of milliliter-sized samples with gaseous hydrogen gas, followed by mass-spectrometric measurement and back calculation of the D/H of the equilibrated H_2 (Horita 1988). Due to the very large fractionation factor (0.2625 at 25 °C) the measured H_2 is very much depleted in D, which complicates the mass-spectrometric measurement. (ii) water is converted to

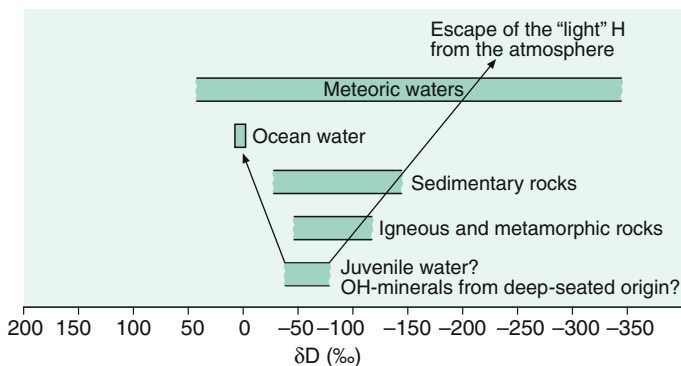


Fig. 2.1 δD variation ranges of geologically important reservoirs (Fig. 2.1, 6th edition, p. 37)

hydrogen by passage over hot metals (uranium: Bigeleisen et al. 1952; Friedman 1953 and Godfrey 1962, zinc: Coleman et al. 1982, chromium: Gehre et al. 1996). This is still the classic method and commonly used.

A difficulty in measuring D/H isotope ratios is that, along with the H_2^+ and HD^+ formation in the ion source, H_3^+ is produced as a by-product of ion-molecule collisions. Therefore, a H_3^+ correction has to be made. The amount of H_3^+ formed is directly proportional to the number of H_2 molecules and H^+ ions. Generally the H_3^+ current measured for hydrogen from ocean water is on the order of 16 % of the total mass 3. The relevant procedures for correction have been evaluated by Brand (2002).

Analytical uncertainty for hydrogen isotope measurements is usually in the range ± 0.5 to ± 3 % depending on different sample materials, preparation techniques and laboratories.

Burgoyne and Hayes (1998) and Sessions et al. (1999) introduced the continuous flow technique for the D/H measurement of individual organic compounds. Quantitative conversion to H_2 is achieved at high temperatures (>1400 °C). The precise measurement of D/H ratios in a He carrier poses a number of analytical problems, related to the tailing from the abundant $^4He^+$ onto the minor HD^+ peak as well as on reactions occurring in the ion source that produce H_3^+ ; these problems have been overcome, however, and precise D/H measurements of individual organic compounds are possible.

An alternative to mass-spectrometry represents the direct measurement of D/H, $^{17}O/^{16}O$ and $^{18}O/^{16}O$ isotope compositions of water vapour by laser absorption spectroscopy, also called Cavity Ring-Down Spectroscopy (CRDS) (Kerstel et al. 2002; Brand et al. 2009a, b; Schmidt et al. 2010 and others). The CRDS technique is fast and easy in operation and allows the direct analysis of water vapour with high precisions comparable to the classic continuous flow techniques (Brand et al. 2009a, b).

Table 2.1 Hydrogen isotope standards

Standards	Description	δ -value
V-SMOW	Vienna standard mean	0
	Ocean water	
GISP	Greenland ice sheet	
	Precipitation	-189.9
V-SLAP	Vienna standard light	
	Antarctic precipitation	-428
NBS-30	Biotite	65

2.1.2 Standards

There is a range of standards for hydrogen isotopes. The primary reference standard, the zero point of the δ -scale, is V-SMOW, which is virtually identical in isotopic composition with the earlier defined SMOW, being a hypothetical water sample originally defined by Craig (1961b).

V-SMOW has a D/H ratio that is higher than most natural samples on Earth, thus δ D-values in the literature are generally negative. The other standards, listed in Table 2.1, are generally used to verify the accuracy of sample preparation and mass spectrometry.

2.1.3 Fractionation Processes

2.1.3.1 Water Fractionations

The most effective processes in the generation of hydrogen isotope variations in the terrestrial environment are phase transitions of water between vapor, liquid, and ice through evaporation/precipitation and/or boiling/condensation in the atmosphere, at the Earth's surface, and in the upper part of the crust. Differences in H-isotopic composition arise due to vapor pressure differences of water and, to a smaller degree, to differences in freezing points. Because the vapor pressure of HDO is slightly lower than that of H₂O, the concentration of D is lower in the vapor than in the liquid phase. In a simple, but elegant experiment Ingraham and Criss (1998) have monitored the effect of vapor pressure on the rate of isotope exchange between water and vapor, which is shown in Fig. 2.1. Two beakers with isotopically differing waters were juxtaposed in a sealed box to monitor the exchange process at different temperatures (in this case 21 and 52 °C). As shown in Fig. 2.1 in the 52 °C experiment the isotopic composition of the water changes rapidly and nearly reaches equilibrium in only 27 days.

Horita and Wesolowski (1994) have summarized experimental results for the hydrogen isotope fractionation between liquid water and water vapor in the temperature range 0–350 °C (see Fig. 2.2). Hydrogen isotope fractionations decrease rapidly with increasing temperatures and become zero at 220–230 °C. Above the

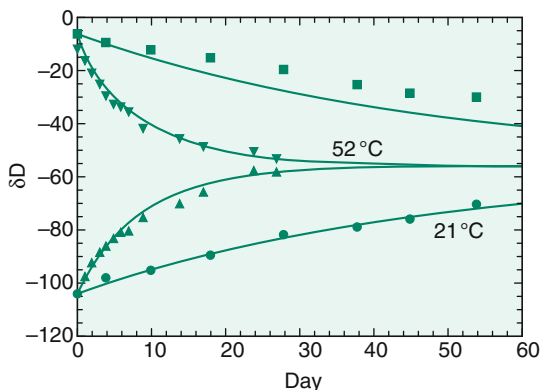


Fig. 2.2 δD -values versus time for two beakers that have equal surface areas and equal volumes undergoing isotopic exchange in sealed systems. In both experiments at 21 and 52 °C isotope ratios progress toward an average value of -56‰ via exchange with ambient vapour: *solid curves* are calculated, *points* are experimental data (after Criss 1999) (Fig. 2.2, 6th edition, p. 39)

crossover temperature, water vapor is more enriched in deuterium than liquid water. Fractionations again approach zero at the critical temperature of water (Fig. 2.2).

From experiments, Lehmann and Siegenthaler (1991) determined the equilibrium H-isotope fractionation between ice and water to be $+21.2\text{‰}$. Under natural conditions, however, ice will not necessarily be formed in isotopic equilibrium with the bulk water, depending mainly on the freezing rate.

In all processes concerning the evaporation and condensation of water, hydrogen isotopes are fractionated in a similar fashion to those of oxygen isotopes, albeit with a different magnitude, because a corresponding difference in vapor pressures exists between H_2O and HDO in one case and $H_2^{16}O$ and $H_2^{18}O$ in the other.

Therefore, the hydrogen and oxygen isotope distributions are correlated for meteoric waters. Craig (1961a) first defined the generalized relationship:

$$\delta D = 8\delta^{18}O + 10,$$

which describes the interdependence of H- and O-isotope ratios in meteoric waters on a global scale.

This relationship, shown in Fig. 2.3, is described in the literature as the “Global Meteoric Water Line (GMWL)”.

Neither the numerical coefficient 8 nor the constant 10, also called the deuterium excess d , are constant in nature. Both may vary depending on the conditions of evaporation, vapor transport and precipitation and, as a result, offer insight into climatic processes. The deuterium excess d is a valuable tool to derive information on relative humidities (see discussion on p. 242).

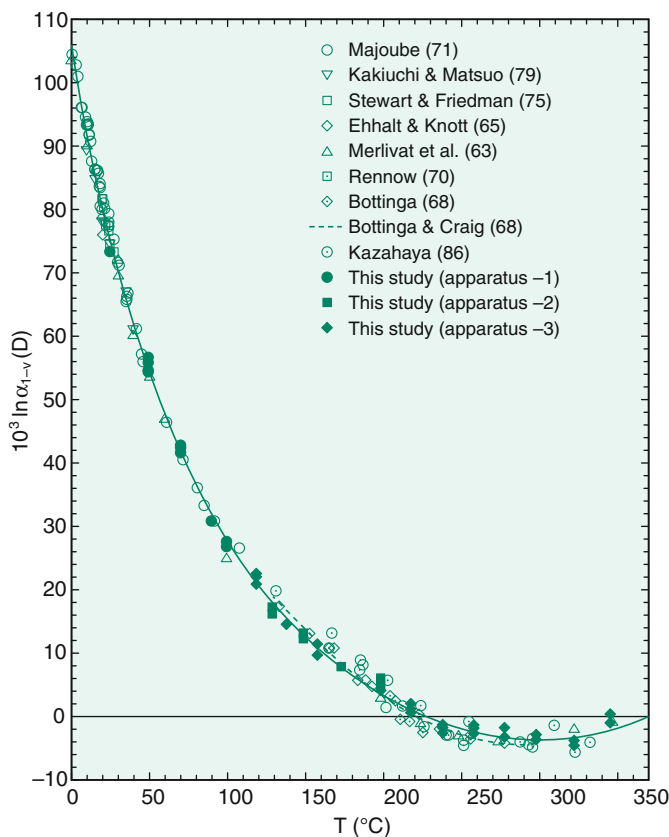


Fig. 2.3 Experimentally determined fractionation factors between liquid water and water vapour from 1 to 350 °C (after Horita and Wesolowski 1994) (Fig. 2.3, 6th edition, p. 39)

2.1.3.2 Equilibrium Reactions

D/H fractionations among gases are extraordinarily large, as calculated by Bottinga (1969) and Richet et al. (1977) and plotted in Fig. 2.4. Even in magmatic systems, fractionation factors are sufficiently large to affect the δD -value of dissolved water in melts during degassing of H_2 , H_2S or CH_4 . The oxidation of H_2 or CH_4 to H_2O and CO_2 may also have an effect on the isotopic composition of water dissolved in melts due to the large fractionation factors (Fig. 2.5).

With respect to mineral-water systems, different experimental studies obtained widely different results for the common hydrous minerals with respect to the absolute magnitude and the temperature dependence of D/H fractionations (Suzuoki and Epstein 1976; Graham et al. 1980; Vennemann and O'Neil 1996; Saccocia et al. 2009). Suzuoki and Epstein (1976) first demonstrated the importance of the chemical composition of the octahedral sites in crystal lattices to the mineral H-isotope composition. Subsequently, isotope exchange experiments by Graham

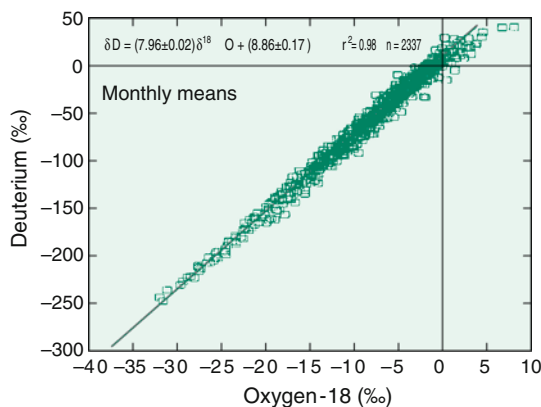
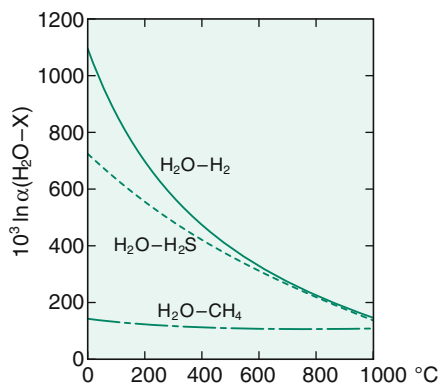


Fig. 2.4 Global relationship between monthly means of δD and $\delta^{18}O$ in precipitation, derived for all stations of the IAEA global network. Line indicates the global Meteoric Water Line (MWL) (after Rozanski et al. 1993) (Fig. 2.4, 6th edition, p. 40)

Fig. 2.5 D/H fractionations between H_2O-H_2 , H_2O-H_2S and H_2O-CH_4 (from calculated data of Richet et al. 1977) (Fig. 2.5, 6th edition, p. 41)



et al. (1980, 1984) suggested that the chemical composition of sites other than the octahedral sites can also affect hydrogen isotope compositions. These authors postulate a qualitative relationship between hydrogen-bond distances and hydrogen isotope fractionations: the shorter the hydrogen bond, the more depleted the mineral is in deuterium.

On the basis of theoretical calculations, Driesner (1997) proposed that many of the discrepancies between the experimental studies were due to pressure differences at which the experiments were carried out. Thus for hydrogen, pressure is a variable that must be taken into account in fluid-bearing systems. Later, Horita et al. (1999) presented experimental evidence for a pressure effect between brucite and water.

Chacko et al. (1999) developed an alternative method for the experimental determination of hydrogen isotope fractionation factors. Instead of using powdered minerals as starting materials, these authors carried out exchange experiments with

large single crystals and then analyzed the exchanged rims with the ion probe. Although the precision of the analytical data is less than that for conventional bulk techniques, the advantage of this technique is that it allows the determination of fractionation factors in experiments in which isotopic exchange occurs by a diffusional process rather than by a combination of diffusion and recrystallization.

In summary, as discussed by Vennemann and O'Neil (1996), discrepancies between published experimental calibrations in individual mineral-water systems are difficult to resolve, which limits the application of D/H fractionations in mineral-water systems to estimate δD -values of coexisting fluids. As shown by Méheut et al. (2010) first-principles calculations of D/H fractionations may reproduce experimental calculations within a range of about 15 ‰. These authors also demonstrated that internal fractionations between inner-surface and inner hydroxyl groups may be large and even opposite in sign.

2.1.3.3 Fractionations During Biosynthesis

Water is the ultimate source of hydrogen in all naturally organic compounds produced by photosynthesis. Thus D/H ratios in organic matter contain information about climate (see Sect. 3.11). During biosynthetic hydrogen conversion of water to organic matter, large H-isotope fractionations with δD -values between -400 and $+200$ ‰ have been observed (Sachse et al. 2012).

δD -variations in individual compounds within a single plant or organism can be related to differences in biosynthesis. Accurate isotope fractionation factors among organic molecules and water are difficult to be determined, although tremendous progress has been achieved through the introduction of the compound specific hydrogen isotope analysis (Sessions et al. 1999; Sauer et al. 2001; Schimmelmann et al. 2006), which allows the δD analysis of individual biochemical compound. Further details are discussed in Sect. 3.10.1.2.

Using a combination of experimental calibration and theoretical calculation Wang et al. (2009a, b) estimated equilibrium factors for various H positions in molecules such as alkanes, ketones, carboxyl acids and alcohols. By summing over individual H positions, equilibrium fractionations relative to water are -90 to -70 ‰ for n-alkanes and about -100 ‰ for pristane and phytane. Wang et al. (2013a, b) extended his approach to cyclic compounds and observed total equilibrium fractionations of -100 to -65 ‰ for typical cyclic paraffins being similar to linear hydrocarbons. These numbers, however, are very different to typical biosynthetic fractionations that are between -300 and -150 ‰ due to kinetic isotope fractionations.

The biosynthesis of lipids as one of the most common group of organic material involves complex enzymatic reactions in which hydrogen may be added, removed or exchanged, all potentially leading to H isotope fractionations. Lipids with the smallest D depletion relative to water are n-alkyl lipids. Isoprenoid lipids show depletions by 200 – 250 ‰ and phytol and related compounds have the largest D-depletion.

2.1.3.4 Other Fractionations

In salt solutions, isotopic fractionations can occur between water in the “hydration sphere” and free water (Truesdell 1974). The effects of dissolved salts on hydrogen isotope activity ratios in salt solutions can be qualitatively interpreted in terms of interactions between ions and water molecules, which appear to be primarily related to their charge and radius. Hydrogen isotope activity ratios of all salt solutions studied so far are appreciably higher than H-isotope composition ratios. As shown by Horita et al. (1993), the D/H ratio of water vapor in isotope equilibrium with a solution increases as salt is added to the solution. Magnitudes of the hydrogen isotope effects are in the order $\text{CaCl}_2 > \text{MgCl}_2 > \text{MgSO}_4 > \text{KCl} \sim \text{NaCl} > \text{NaSO}_4$ at the same molality.

Isotope effects of this kind are relevant for an understanding of the isotope composition of clay minerals and absorption of water on mineral surfaces. The tendency for clays and shales to act as semipermeable membranes is well known. This effect is also known as “ultrafiltration”. Coplen and Hanshaw (1973) postulated that hydrogen isotope fractionations may occur during ultrafiltration in such a way that the residual water is enriched in deuterium due to its preferential adsorption on the clay minerals and its lower diffusivity.

2.2 Lithium

Lithium has two stable isotopes with the following abundances (Rosman and Taylor 1998):

$${}^6\text{Li} \quad 7.59 \%$$

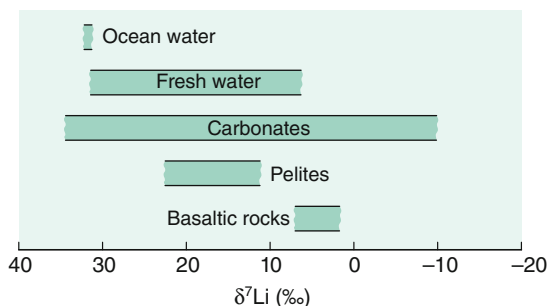
$${}^7\text{Li} \quad 92.41 \%$$

Lithium is one of the rare elements where the lighter isotope is less abundant than the heavier one. In order to be consistent with the other isotope systems lithium isotope ratios are reported as $\delta^7\text{Li}$ -values.

The large relative mass difference between ${}^6\text{Li}$ and ${}^7\text{Li}$ of about 16 % is a favorable condition for their fractionation in nature. Taylor and Urey (1938) found a change of 25 % in the Li-isotope ratio when Li-solutions percolate through a zeolite column. Thus, fractionation of Li-isotopes might be expected in geochemical settings in which cation exchange processes are involved. Li is only present in the +1 valence state, so redox reactions do not influence its isotope composition. A recent review about natural Li isotope variations has been given by Burton and Vigier (2011).

Lithium isotope geochemistry is characterized by a difference close to 30 ‰ between ocean water ($\delta^7\text{Li} +31 \text{ ‰}$) and bulk silicate earth with a $\delta^7\text{Li}$ -value of 3.2 ‰ (Seitz et al. 2007). In this respect lithium isotope geochemistry is very similar to that of boron (see p. 59). The isotopic difference between the mantle and the ocean

Fig. 2.6 Lithium isotope variations in major geological reservoirs (Fig. 2.6, 6th edition, p. 43)



can be used as a powerful tracer to constrain water/rock interactions (Tomaszak 2004). Figure 2.6 gives an overview of Li-isotope variations in major geological reservoirs.

2.2.1 Methods

Early workers had to struggle with serious lithium fractionation effects during mass spectrometric analysis. Li isotopes have been analysed with TIMS (James and Palmer 2000) and ion microprobe (Kasemann et al. 2005a, b). Most workers use the multicollector sector ICP-MS technique first described by Tomascak et al. (1999), modified by Millot et al. (2004) and Jeffcoate et al. (2004). In order to avoid interferences and matrix effects, Li has to be separated from the rest of the sample. During elution, a 100 % yield is necessary, even a small loss of Li may shift the $\delta^7\text{Li}$ value by several ‰.

Unfortunately, there are no internationally accepted Li isotope values for rocks or waters. James and Palmer (2000) have determined nine international rock standards ranging from basalt to shale relative to the so-called NIST L-SVEC standard. In addition, Jeffcoate et al. (2004) and Gao and Casey (2011) presented $\delta^7\text{Li}$ values for other reference materials.

2.2.2 Diffusion

Li isotope variations have been interpreted—like other isotope systems—in terms of isotope equilibrium between minerals and fluids, however, the analysis of natural samples and experimental studies have shown that Li isotope variations may be very often kinetically controlled due to the large differences in ^6Li and ^7Li diffusivities that may far exceed Li isotope variations produced by equilibrium processes. Diffusive Li isotope fractionation has been reported to occur on a meter to micrometer scale during cooling processes (Lundstrom et al. 2005; Teng et al. 2006; Jeffcoate et al. 2007; Parkinson et al. 2007). In silicate minerals ^6Li diffuses 3 % faster than ^7Li , consistent with experiments by Richter et al. (2003). Dohmen

et al. (2010) measured Li diffusion rates in olivine and observed a complex diffusion behaviour, that can be described by a model that partitions Li between two sites: an octahedral and an interstitial site. Published Li isotope data indicate that the interstitial mechanism is unlikely to be the dominant system (Seitz et al. 2004; Jeffcoate et al. 2007).

In summary, diffusion at magmatic temperatures is a very effective mechanism for generating large variations in $^7\text{Li}/^6\text{Li}$ ratios (Lundstrom et al. 2005; Teng et al. 2006; Rudnick and Ionov 2007). Although diffusion profiles will relax with time, the existence of sharp $\delta^7\text{Li}$ -profiles suggest diffusional Li isotope fractionation over short timescales (days to a few months) and therefore diffusion profiles in mantle minerals may be used as geospeedometers (Parkinson et al. 2007). At the same time diffusion may obliterate primary mantle signatures.

2.2.3 Magmatic Rocks

High temperature equilibrium Li isotope fractionations have been investigated experimentally (Wunder et al. 2006, 2007) and theoretically (Kowalski and Jahn 2011). Calculated fractionation factors between staurolite, spodumene, mica and aqueous fluids are in good agreement with experimentally derived fractionation factors.

Mantle-derived basalts have a relatively uniform composition with $\delta^7\text{Li}$ values of 4 ± 2 ‰ (Tomaszak 2004; Elliott et al. 2004), close to undepleted upper mantle (Jeffcoate et al. 2007). The $\delta^7\text{Li}$ range for MORB is relatively narrow, but larger than for mantle peridotites. On the other hand, some peridotites have a wide range in $\delta^7\text{Li}$ values from values as low as -17 ‰ (Nishio et al. 2004) to values as high as $+10$ ‰ (Brooker et al. 2004). This large range might be explained by diffusion controlled Li exchange.

Mantle minerals show a typical order of ^7Li enrichment: olivines and orthopyroxenes have \pm the same isotope composition, whereas clinopyroxenes are enriched in ^7Li and more variable. Olivines generally keep the mantle signatures whereas clinopyroxenes are more sensitive to metasomatic overprint leading to isotope variations, which can be explained by diffusion processes that may affect clinopyroxenes during melt migration (Parkinson et al. 2007).

Because Li isotopes may be used as a tracer to identify the existence of recycled material in the mantle, systematic studies of arc lavas have been undertaken (Moriguti and Nakamura 1998; Tomascak et al. 2000; Leeman et al. 2004 and others). However, most arc lavas have $\delta^7\text{Li}$ values that are indistinguishable from those of MORB. Thus Li seems to be decoupled from other fluid mobile elements, because Li can partition into the Mg-silicates, pyroxene, olivine (Tomascak et al. 2002).

Granites of various origin display an average $\delta^7\text{Li}$ value slightly lighter than the mantle (Teng et al. 2004, 2009). Considering the small Li isotope fractionation at high temperature during igneous differentiation processes (Tomaszak 2004),

pristine continental crust should not be too different in Li isotope composition from the mantle. Because this is not the case, the isotopically light crust must have been modified by secondary processes, such as weathering, hydrothermal alteration and prograde metamorphism (Teng et al. 2007a, b).

Li isotope distribution through the oceanic crust reflects the varying conditions of seawater alteration with depth (Chan et al. 2002; Gao et al. 2012). At low temperatures, altered volcanic rocks have heavier Li isotope compositions than MORB whereas at higher temperatures in deeper parts of the oceanic crust $\delta^7\text{Li}$ -values become similar to MORB. Gao et al. (2012) concluded that the Li isotope pattern in drilled oceanic sections reflects variations in water/rock ratios in combination with increasing downhole temperatures.

During fluid-rock interaction, Li as a fluid-mobile element will enrich in aqueous fluids. It might therefore be expected that $\delta^7\text{Li}$ enriched seawater incorporated into altered oceanic crust should be removed during subduction zone metamorphism. Continuous dehydration of pelagic sediments and altered oceanic crust results in ^7Li -depleted rocks and in ^7Li enriched fluids. A subducting slab therefore should introduce large amounts of ^7Li into the mantle wedge. To quantitatively understand this process Li isotope fractionation factors between minerals and coexisting fluids must be known (Wunder et al. 2006, 2007).

2.2.4 Weathering

Li is relatively mobile during weathering. The best evidence for Li isotope fractionation during weathering is the systematic ^7Li enrichment of natural waters relative to their source rocks (Burton and Vigier 2011). During weathering ^7Li is preferentially mobilized, whereas ^6Li becomes enriched in the weathering residue. The range of $\delta^7\text{Li}$ values in river waters can be quite large (from +6 to +33 ‰, Huh et al. 1998, 2004). The major control of Li isotopic composition is the balance between primary mineral dissolution and secondary mineral formation, where ^6Li is preferentially taken up by the solid, driving the fluid to heavy values (Wimpenny et al. 2010). The magnitude of fractionation seems to depend on the extent of weathering: large Li isotope fractionations seem to occur during superficial weathering while little fractionation is observed during prolonged weathering in stable environments (Millot et al. 2010a, b). Rudnick et al. (2004) have demonstrated that Li isotope fractionation correlates directly with the degree of weathering leading to very light $\delta^7\text{Li}$ -values in soils.

Preferential weathering of primary minerals does not generate significant Li isotope fractionations. Wimpenny et al. (2010) demonstrated that dissolution of basaltic glass and olivine does not result in measurable Li isotope fractionation. Secondary mineral formation and adsorption on mineral surfaces are regarded to be the major process responsible for the high $\delta^7\text{Li}$ values in waters. Considerable Li isotope fractionations, for instance, have been observed during chemical sorption of

Li on the surface of gibbsite (Pistiner and Henderson 2003) or on clay minerals (Zhang et al. 1998; Millot et al. 2010a, b).

2.2.5 Ocean Water

Lithium is a conservative element in the ocean with a residence time of about one million year. Its isotope composition ($\delta^7\text{Li}$: 31 ‰) is maintained by inputs of dissolved Li from rivers (average $\delta^7\text{Li}$ +23 ‰, Huh et al. 1998) and high-temperature hydrothermal fluids at ocean ridges at one hand and low temperature removal of Li into oceanic basalts and marine sediments at the other. Precipitation of carbonates does not play a major role due to the low Li-concentrations of carbonates. This fractionation pattern explains, why the Li isotope composition of seawater is heavier than its primary sources (continental weathering: 23 ‰; Huh et al. 1998) and high-temperature hydrothermal fluids (6–10 ‰, Chan et al. 1993).

In this connection it is interesting to note that ocean water is not the major Li supplier in rainwater (Millot et al. 2010a, b). Rainwater has low Li concentrations, but very variable Li isotope compositions. High $\delta^7\text{Li}$ values have been explained by anthropogenic contamination from fertilizers in agriculture (Millot et al. 2010a, b).

Any variance in Li sources and sinks during geologic history should cause secular variations in the isotope composition of oceanic Li. And indeed Misra and Froelich (2012) reconstructed the Li isotope composition of ocean water for the last 68 Ma and observed an 9 ‰ increase from the Paleocene to the present requiring changes in continental weathering and/or low temperature ocean crust alteration (see p. 268). By extending this approach, Wanner et al. (2014) presented a model that revealed a close relationship between $\delta^7\text{Li}$ and CO_2 consumption by silicate weathering.

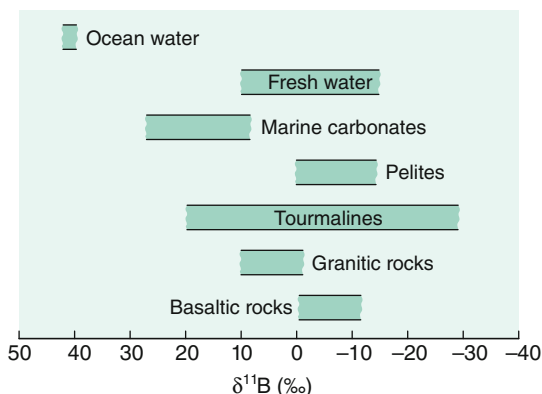
2.3 Boron

Boron has two stable isotopes with the following abundances (Rosman and Taylor 1998).

^{10}B	19.9 ‰
^{11}B	80.1 ‰

The large mass difference between ^{10}B and ^{11}B and large chemical isotope effects between different species (Bigeleisen 1965) make boron a very promising element to study for isotope variations. The utility of boron isotopes as a geochemical tracer stems from the high mobility of boron during high- and low-temperature fluid-related processes, showing a strong affinity for silicate melts

Fig. 2.7 Boron isotope variations in geologically important reservoirs (Fig. 2.7, 6th edition, p. 45)



and aqueous fluids. B is preferentially hosted in phyllosilicates; common mantle and crustal minerals except tourmaline have low B concentrations.

Boron isotope geochemistry is characterized by distinct isotope signatures:

- (i) strong enrichment of ^{11}B in seawater (+39.6 ‰, Foster et al. 2010).
- (ii) depletion of ^{11}B in the continental crust and marine sediments
- (iii) slight depletion of ^{11}B in the upper mantle (Chaussidon and Marty 1995)

The lowest $\delta^{11}\text{B}$ -values of around -70 ‰ have been observed for certain coals (Williams and Hervig 2004), whereas the most enriched ^{11}B -reservoir has been found in brines from Australia and Israel (Dead Sea) which have $\delta^{11}\text{B}$ -values of up to 60 ‰ (Vengosh et al. 1991a, b). A very characteristic feature of boron geochemistry is the isotopic composition of ocean water with a constant $\delta^{11}\text{B}$ -value of 39.6 ‰ (Foster et al. 2010), which is about 50 ‰ heavier than the average continental crust of -10 ± 2 ‰ (Chaussidon and Albarede 1992). Isotope variations of boron in some geological reservoirs are shown in Fig. 2.7.

2.3.1 Methods

In recent years 3 different methods have been used for boron isotope analysis: (i) thermal ionisation mass-spectrometry (TIMS), either with positively charged (P-TIMS) or negatively charged (N-TIMS) ions, (ii) multi-collector-ICP mass spectrometry and (iii) secondary ion mass spectrometry (SIMS).

- (i) Two different methods have been developed for TIMS. The positive thermal ionization technique uses Na_2BO_2^+ ions (McMullen et al. 1961). Subsequently, Spivack and Edmond (1986) modified this technique by using Cs_2BO_2^+ ions (measurement of the masses 308 and 309). The substitution of ^{133}Cs for ^{23}Na increases the molecular mass and reduces the relative mass

difference of its isotopic species, which limits the thermally induced mass dependent isotopic fractionation. This latter method has a precision of about ± 0.25 ‰, which is better by a factor of 10 than the Na_2BO_2^+ method. In negative ion mode (N-TIMS), boron isotopes are analysed as BO_2^- (masses 42 and 43). N-TIMS has the advantage that no chemical separation of boron from the sample matrix is required.

- (ii) Lecuyer et al. (2002) first described the use of MC-ICP-MS for B isotopic measurements of waters, carbonates, phosphates and silicates with an external reproducibility of ± 0.3 ‰, improvement in reproducibility has been achieved by Guerrot et al. (2011) and Louvat et al. (2011). Le Roux et al. (2004) introduced an in situ laser ablation ICP-MS method at the nanogram level. The amount of boron measured are two orders of magnitude lower than P-TIMS and acid solution ICP-MS methods.
- (iii) Chaussidon and Albarede (1992), performed boron isotope determinations with an ion-microprobe having an analytical uncertainty of about ± 2 ‰. Significant improvements with SIMS analysis have been described by Rollion and Erez (2010).

As analytical techniques have been consistently improved in recent years, the number of boron isotope studies has increased rapidly. $\delta^{11}\text{B}$ -values are generally given relative NBS boric acid SRM 951, which is prepared from a Searles Lake borax. This standard has a $^{11}\text{B}/^{10}\text{B}$ ratio of 4.04558 (Palmer and Slack 1989).

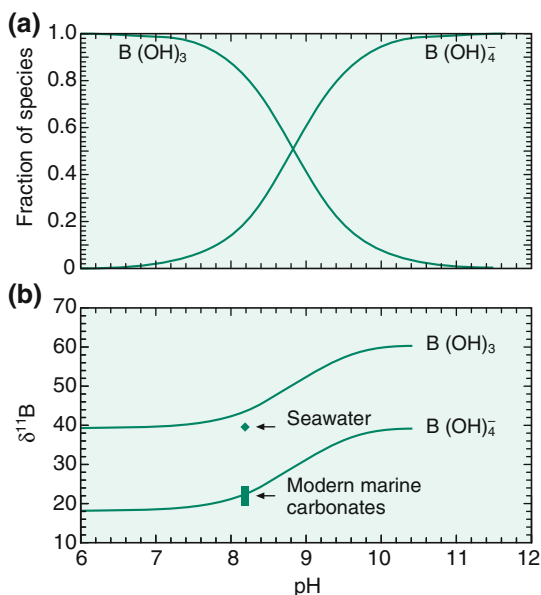
2.3.2 Isotope Fractionation Mechanism

(a) pH dependence of isotope fractionations

Boron is generally bound to oxygen or hydroxyl groups in either triangular (e.g., BO_3) or tetrahedral (e.g., $\text{B}(\text{OH})_4^-$) coordination. The dominant isotope fractionation process occurs in aqueous systems via an equilibrium exchange process between boric acid ($\text{B}(\text{OH})_3$) and coexisting borate anion ($\text{B}(\text{OH})_4^-$). At low pH-values trigonal $\text{B}(\text{OH})_3$ predominates, at high pH-values tetrahedral $\text{B}(\text{OH})_4^-$ is the primary anion. The pH-dependence of the two boron species and their related isotope fractionation is shown in Fig. 2.8 (after Hemming and Hanson 1992). The pH dependence has been used reconstructing past ocean pH-values by measuring the boron isotope composition of carbonates e.g. foraminifera. This relies on the fact that mainly the charged species $\text{B}(\text{OH})_4^-$ is incorporated into carbonate minerals with small to insignificant fractionations (Hemming and Hanson 1992; Sanyal et al. 2000). In corals, Rollion-Bard et al. (2011), however, observed both coordination species in the coral microstructure.

Because of the inability to quantitatively separate the two species in solution, a theoretically calculated fractionation factor of about 1.0194 at 25 °C has been widely used for p_{H} estimates (Kakihana et al. 1977). As recently shown by Zeebe

Fig. 2.8 **a** Distribution of aqueous boron species versus pH; **b** $\delta^{11}\text{B}$ of the two dominant species $\text{B}(\text{OH})_3$ and $\text{B}(\text{OH})_4^-$ versus pH (after Hemming and Hanson 1992)



(2005) and Klochko et al. (2006), the equilibrium fractionation factor appears to be significantly larger than the theoretical value of Kakihana et al. (1977) used in paleo-pH studies. Klochko et al. (2006), for instance, reported a fractionation factor of 1.0272. Furthermore, it has to be assumed that no “vital effect” occurs during incorporation of borate into the carbonate lattice or the species-specific fractionation effect is known and can be corrected for.

This approach has been not only used to indirectly estimate the seawater pH from $\delta^{11}\text{B}$ of foraminifera, but to estimate from the pH proxy the past atmospheric CO_2 concentrations (i.e. Pearson and Palmer 1999, 2000; Pagani et al. 2005). An increase in atmospheric CO_2 results in increased dissolved CO_2 in ocean water, which in turn causes a reduction in oceanic pH , well known as ocean acidification. A note of caution was presented by Lemarchand et al. (2000), who suggested that boron isotope variations in foraminifera depend at least in part on variations in the supply of riverine boron to the ocean during the geologic past. And indeed the boron isotope composition of rivers can be extremely variable (Rose et al. 2000; Lemarchand et al. 2002).

(b) Adsorption

Significant isotope fractionations may occur when aqueous boric acid adsorbs on solid surfaces, as shown by Lemarchand et al. (2005) and others. Boron isotopic compositions are controlled by ion exchange rates at the mineral/water interface. The extent of B isotope fractionation depends on B aqueous speciation and on the structure of surface complexes. High values of B isotope fractionation are observed

at low pH, lower values are observed at high pH, which is due to the change in coordination from trigonal to tetrahedral.

2.3.3 Fractionations at High Temperatures

Experimental studies of boron isotope fractionation between hydrous fluids, melts and minerals have shown that ^{11}B preferentially partitions into the fluid relative to minerals or melts (Palmer et al. 1987; Williams et al. 2001; Wunder et al. 2005; Liebscher et al. 2005), ranging from about 33 ‰ for fluid-clay (Palmer et al. 1987), to about 6 ‰ for fluid-muscovite at 700 °C (Wunder et al. 2005) and to a few ‰ for fluid-melt above 1000 °C (Hervig et al. 2002). The main fractionation effect seems to be due to the change from trigonal boron in neutral pH hydrous fluid to tetrahedrally coordinated boron in most rock forming minerals.

At high temperatures, B isotope fractionations during crystal fractionation and melting are small. Boron like lithium are useful tracers for mass transfer in subduction zones. Both elements are mobilized by fluids and melts and display considerable isotope fractionation during dehydration reactions. Concentrations of B are low in mantle derived materials, whereas they are high in sediments and altered oceanic crust. Any input of fluid and melt from the subducting slab into the overlying mantle has a strong impact on the isotope composition of the mantle wedge and on magmas generated there. Recycled marine boron, for instance, may lead to an enrichment of ^{11}B in sources for arc volcanic rocks (Tonarini et al. 2011).

2.3.4 Tourmaline

Tourmaline is the most abundant reservoir of boron in metamorphic and magmatic rocks. Tourmaline is stable over a very large p-T range and forms where crustal rocks interact with fluids or melts. Thus, its isotope composition provides a record of fluids and melts from which it crystallized. Swihart and Moore (1989), Palmer and Slack (1989), Slack et al. (1993), Smith and Yardley (1996) and Jiang and Palmer (1998) analyzed tourmaline from various geological settings and observed a large range in $\delta^{11}\text{B}$ -values which reflects the different origins of boron and its high mobility during fluid related processes.

Boron isotope compositions of tourmalines vary from about +30 ‰ to values below -20 ‰ (Marschall and Jiang 2011). High $\delta^{11}\text{B}$ -values can be related to seawater, whereas low $\delta^{11}\text{B}$ -values are either derived from nonmarine evaporites or produced by interaction between rocks and fluids during metamorphic dehydration. Tourmalines in most granites and pegmatites show $\delta^{11}\text{B}$ -values around -10 ‰ close to the average composition of the continental crust (Marschall and Jiang 2011).

Since volume diffusion of B isotopes is insignificant in tourmalines (Nakano and Nakamura 2001), isotopic heterogeneities of zoned tourmalines should be preserved up to at least 600 °C. By using the SIMS method, Marschall et al. (2008) demonstrated that boron isotopes in zoned tourmalines, indeed, may reflect different stages of tourmaline growth. Besides, the large chemical variability of tourmaline can be used as a fingerprint for a large number of other isotope systems including O, H, Si, Mg and Li (Marschall and Jiang 2011).

2.3.5 Tracer for Anthropogenic Pollution

Boron is widely used in industry; most commonly in the form of sodium perborate as an oxidative bleaching agent in cleaning products. The abundant use results in boron accumulation in waste effluents. Borate minerals and synthetic borate products are characterized by a narrow range in $\delta^{11}\text{B}$ -values that are distinctly different from boron isotope values in unpolluted groundwater (Vengosh et al. 1994; Barth 1998). Thus, boron isotopes may identify or even quantify contamination of surface waters.

Although the concentration of B in rain water is low, improved analytical techniques have allowed the determination of very precise B isotope data (Chetelat et al. 2009; Millot et al. 2010a, b). $\delta^{11}\text{B}$ values in rain show a large variation depending on the sampling site (coastal vs. inland). Near coastal stations reflect the marine origin of boron, variably influenced by evaporation-condensation fractionation processes. For inland stations, crustal, anthropogenic and biogenic boron sources have to be included.

2.4 Carbon

Carbon occurs in a wide variety of compounds on Earth, from reduced organic compounds in the biosphere to oxidized inorganic compounds like CO_2 and carbonates. The broad spectrum of carbon-bearing compounds involved in low- and high-temperature geological settings can be assessed on the basis of carbon isotope fractionations.

Carbon has two stable isotopes (Rosman and Taylor 1998)

$$^{12}\text{C} = 98.93 \text{ \% (reference mass for atomic weight scale)}$$

$$^{13}\text{C} = 1.07 \text{ \%}$$

The naturally occurring variations in carbon isotope composition are greater than 120 ‰, neglecting extraterrestrial materials. Heavy carbonates with $\delta^{13}\text{C}$ -values $> +20 \text{ ‰}$ and light methane of $< -100 \text{ ‰}$ have been reported in the literature.

Table 2.2 $\delta^{13}\text{C}$ -values of NBS-reference samples relative to V-PDB

NBS-18	Carbonatite	−5.00
NBS-19	Marble	+1.95
NBS-20	Limestone	−1.06
NBS-21	Graphite	−28.10
NBS-22	Oil	−30.03

2.4.1 Analytical Methods

The gases used in $^{13}\text{C}/^{12}\text{C}$ measurements are CO_2 or CO obtained during pyrolysis. For CO_2 the following preparation methods exist:

- Carbonates are reacted with 100 % phosphoric acid at temperatures between 20 and 90 °C (depending on the type of carbonate) to liberate CO_2 (see also “oxygen”).
- Organic compounds are generally oxidized at high temperatures (850–1000 °C) in a stream of oxygen or by an oxidizing agent like CuO . For the analysis of individual compounds in complex organic mixtures, a gas chromatography—combustion—isotope ratio mass-spectrometry (GC-C-IRMS) system is used, first described by Matthews and Hayes (1978). This device can measure individual carbon compounds in mixtures of sub-nanogram samples with a precision of better than ± 0.5 ‰.

2.4.1.1 Standards

As the commonly used international reference standard PDB has been exhausted for several decades, there is a need for introducing new standards. Even though several different standards are in use today, the international standard the δ -values are referred to remains to be the V-PDB-standard (Table 2.2).

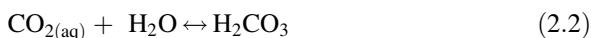
2.4.2 Fractionation Processes

The two main terrestrial carbon reservoirs, organic matter and sedimentary carbonates, have distinctly different isotopic characteristics because of the operation of two different reaction mechanisms:

- Isotope equilibrium exchange reactions within the inorganic carbon system “atmospheric CO_2 —dissolved bicarbonate—solid carbonate” lead to an enrichment of ^{13}C in carbonates.
- Kinetic isotope effects during photosynthesis concentrate the light isotope ^{12}C in the synthesized organic material.

2.4.2.1 Carbonate System

The inorganic carbonate system is comprised of multiple chemical species linked by a series of equilibria:



The carbonate (CO_3^{2-}) ion can combine with divalent cations to form solid minerals, calcite and aragonite being the most common



An isotope fractionation is associated with each of these equilibria, the ^{13}C -differences between the species depend only on temperature, although the relative abundances of the species are strongly dependent on pH. Several authors have reported isotope fractionation factors for the system dissolved inorganic carbon (DIC)—gaseous CO_2 (Vogel et al. 1970; Mook et al. 1974; Zhang et al. 1995). The major problem in the experimental determination of the fractionation factor is the separation of the dissolved carbon phases ($\text{CO}_{2\text{aq}}$, HCO_3^- , CO_3^{2-}) because isotope equilibrium among these phases is reached within seconds. The generally accepted carbon isotope equilibrium values between calcium carbonate and dissolved bicarbonate are derived from inorganic precipitate data of Robinson and Clayton (1969), Emrich et al. (1970), and Turner (1982). What is often not adequately recognized is the fact that systematic C-isotope differences exist between calcite and aragonite. Robinson and Clayton (1969) and Romanek et al. (1992) found calcite and aragonite to be 0.9 and 2.7 ‰ enriched in ^{13}C relative to bicarbonate at 25 °C. Another complicating factor is that shell carbonate—precipitated by marine organisms—is frequently not in isotopic equilibrium with the ambient dissolved bicarbonate. Such so-called “vital” effects can be as large as a few permil (see discussion on p. 307).

Carbon isotope fractionations under equilibrium conditions are important not only at low-temperature, but also at high temperatures within the system carbonate, CO_2 , graphite, and CH_4 . Of these, the calcite-graphite fractionation has become a useful geothermometer (e.g., Valley and O’Neil 1981; Scheele and Hoefs 1992; Kitchen and Valley 1995) (see discussion on p. 339).

Figure 2.9 summarizes carbon isotope fractionations between various geologic materials and gaseous CO_2 (after Chacko et al. 2001).

2.4.2.2 Organic Carbon System

Early reviews by O’Leary (1981) and Farquhar et al. (1989) have provided the biochemical background of carbon isotope fractionations during photosynthesis,

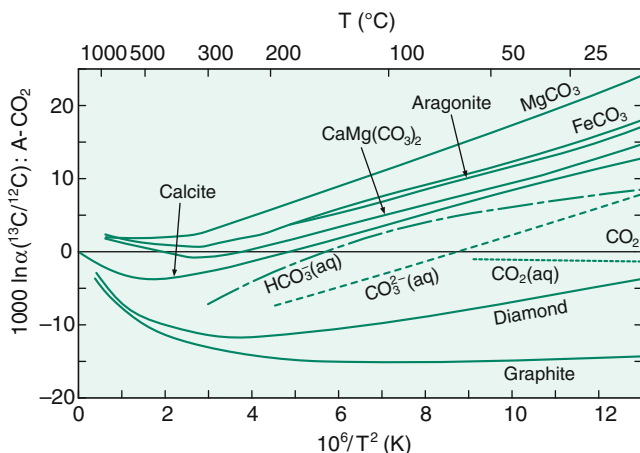
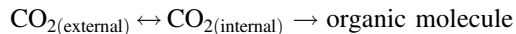


Fig. 2.9 Carbon isotope fractionation between various geologic compounds and CO_2 (after Chacko et al. 2001) (Fig. 2.9, 6th edition, p. 50)

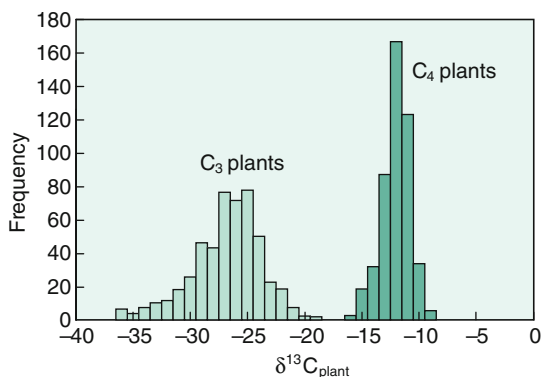
with more recent accounts by Hayes (2001), Freeman (2001) and Galimov (2006). The main isotope-discriminating steps during biological carbon fixation are (i) the uptake and intracellular diffusion of CO_2 and (ii) the biosynthesis of cellular components. Such a two-step model was first proposed by Park and Epstein (1960):



From this simplified scheme, it follows that the diffusional process is reversible, whereas the enzymatic carbon fixation is irreversible. The two-step model of carbon fixation clearly suggests that isotope fractionation is dependent on the partial pressure of CO_2 of the system. With an unlimited amount of CO_2 available to a plant, the enzymatic fractionation will determine the isotopic difference between the inorganic carbon source and the final bioproduct. Under these conditions, ^{13}C fractionations may vary from -17 to -40 ‰ (O’Leary 1981). When the concentration of CO_2 is the limiting factor, the diffusion of CO_2 into the plant is the slow step in the reaction and carbon isotope fractionation of the plant decreases.

Atmospheric CO_2 first moves through the stomata, dissolves into leaf water and enters the outer layer of photosynthetic cells, the mesophyll cell. Mesophyll CO_2 is directly converted by the enzyme ribulose biphosphate carboxylase/oxygenase (“Rubisco”) to a 6 carbon molecule, that is then cleaved into 2 molecules of phosphoglycerate (PGA), each with 3 carbon atoms (plants using this photosynthetic pathway are therefore called C_3 plants). Most PGA is recycled to make ribulose biphosphate, but some is used to make carbohydrates. Free exchange between external and mesophyll CO_2 makes the carbon fixation process less efficient, which causes the observed large ^{13}C -depletions of C_3 plants.

Fig. 2.10 Histogram of $\delta^{13}\text{C}$ values of C_3 and C_4 plants (after Cerling and Harris 1999) (Fig. 2.10, eth edition, p. 52)



C_4 plants incorporate CO_2 by the carboxylation of phosphoenolpyruvate (PEP) via the enzyme PEP carboxylase to make the molecule oxaloacetate which has 4 carbon atoms (hence C_4). The carboxylation product is transported from the outer layer of mesophyll cells to the inner layer of bundle sheath cells, which are able to concentrate CO_2 , so that most of the CO_2 is fixed with relatively little carbon fractionation.

In conclusion, the main controls on carbon fractionation in plants are the action of a particular enzyme and the “leakiness” of cells. Because mesophyll cells are permeable and bundle sheath cells are less permeable, C_3 versus C_4 plants have ^{13}C -depletions of -18‰ versus -4‰ relative to atmospheric CO_2 (see Fig. 2.10).

The final carbon isotope composition of naturally synthesized organic matter depends on a complex set of parameters. (i) the ^{13}C -content of the carbon source, (ii) isotope effects associated with the assimilation of carbon, (iii) isotope effects associated with metabolism and biosynthesis and (iv) cellular carbon budgets (Hayes 1993, 2001).

Even more complex is C-isotope fractionation in aquatic plants. Factors that control the $\delta^{13}\text{C}$ of phytoplankton include temperature, availability of $\text{CO}_{2(\text{aq})}$, light intensity, nutrient availability, pH and physiological factors such as cell size and growth rate (Laws et al. 1995, 1997; Bidigare et al. 1997; Popp et al. 1998 and others). In particular the relationship between C-isotope composition of phytoplankton and concentration of oceanic dissolved CO_2 has been subject of considerable debate because of its potential as a palaeo- CO_2 barometer (see discussion p. 278).

Since the pioneering work of Park and Epstein (1960) and Abelson and Hoering (1961), it is well known that ^{13}C is not uniformly distributed among the total organic matter of plant material, but varies between carbohydrates, proteins and lipids. The latter class of compounds is considerably depleted in ^{13}C relative to the other products of biosynthesis. Although the causes of these ^{13}C -differences are not entirely clear, kinetic isotope effects seem to be more plausible (De Niro and Epstein 1977; Monson and Hayes 1982) than thermodynamic equilibrium effects (Galimov 1985a, 2006). The latter author argued that ^{13}C -concentrations at

individual carbon positions within organic molecules are principally controlled by structural factors. Approximate calculations suggested that reduced C–H bonded positions are systematically depleted in ^{13}C , while oxidized C–O bonded positions are enriched in ^{13}C . Many of the observed relationships are qualitatively consistent with that concept. However, it is difficult to identify any general mechanism by which thermodynamic factors should be able to control chemical equilibrium within a complex organic structure. Experimental evidence presented by Monson and Hayes (1982) suggests that kinetic effects will be dominant in most biological systems.

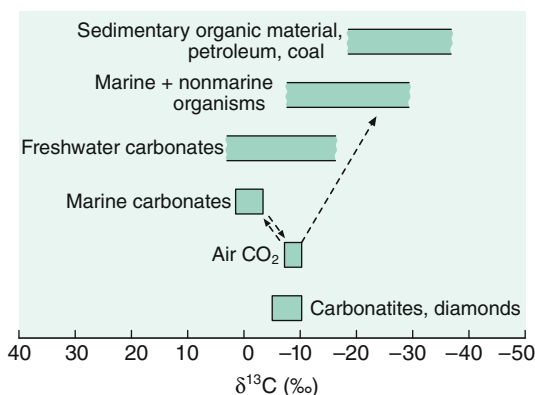
2.4.2.3 Interactions Between Carbonate-Carbon and Organic Carbon

Variations in ^{13}C content of some important carbon compounds are schematically demonstrated in Fig. 2.11: The two most important carbon reservoirs on Earth, marine carbonates and the biogenic organic matter, are characterized by very different isotopic compositions: the carbonates being isotopically heavy with a mean $\delta^{13}\text{C}$ -value around 0 ‰ and organic matter being isotopically light with a mean $\delta^{13}\text{C}$ -value around –25 ‰. For these two sedimentary carbon reservoirs an isotope mass balance must exist such that:

$$\delta^{13}\text{C}_{\text{input}} = f_{\text{org}} \delta^{13}\text{C}_{\text{org}} + (1 - f_{\text{org}}) \delta^{13}\text{C}_{\text{carb}} \quad (2.6)$$

If δ_{input} , δ_{org} , δ_{carb} can be determined for a specific geologic time, f_{org} can be calculated, where f_{org} is the fraction of organic carbon entering the sediments. It should be noted that f_{org} is defined in terms of the global mass balance and is independent of biological productivity referring to the burial rather than the synthesis of organic material. That means that large f_{org} values might be a result of high productivity and average levels of preservation of organic material or of low levels of productivity and high levels of preservation.

Fig. 2.11 $\delta^{13}\text{C}$ -values of important geological reservoirs (Fig. 2.11, 6th edition, p. 53)



The $\delta^{13}\text{C}$ -value for the input carbon cannot be measured precisely but can be estimated with a high degree of certainty. As will be shown later, mantle carbon has an isotopic composition around -5‰ and estimates of the global average isotope composition for crustal carbon also fall in that range. Assigning -5‰ to $\delta^{13}\text{C}$ -input, a modern value for f_{org} is calculated as 0.2 or expressed as the ratio of $C_{\text{org}}/C_{\text{carb}} = 20/80$. As will be shown later (Chap. 3.7.2) f_{org} has obviously changed during specific periods of the Earth's history (e.g. Hayes et al. 1999). With each molecule of organic carbon being buried, a mole of oxygen is released to the atmosphere. Hence, knowledge of f_{org} is of great value in reconstructing the crustal redox budget.

2.5 Nitrogen

More than 99 % of the known nitrogen on or near the Earth's surface is present as atmospheric N_2 or as dissolved N_2 in the ocean. Only a minor amount is combined with other elements, mainly C, O, and H. Nevertheless, this small part plays a decisive role in the biological realm. Since nitrogen occurs in various oxidation states and in gaseous, dissolved, and solid forms (N_2 , NO_3^- , NO_2^- , NH_3 , NH_4^+), it is a highly suitable element for the search of natural variations in its isotopic composition. Schoenheimer and Rittenberg (1939) were the first to report nitrogen isotopic variations in biological materials. Today, the range of reported $\delta^{15}\text{N}$ -values covers 100 ‰, from about -50 to $+50\text{‰}$. However, most δ -values fall within the much narrower spread from -10 to $+20\text{‰}$, as described in more recent reviews of the exogenic nitrogen cycle by Heaton (1986), Owens (1987), Peterson and Fry (1987) and Kendall (1998).

Nitrogen consists of two stable isotopes, ^{14}N and ^{15}N . Atmospheric nitrogen, given by Rosman and Taylor (1998) has the following composition:

$$^{14}\text{N}: 99.63\%$$

$$^{15}\text{N}: 0.37\%.$$

2.5.1 Analytical Methods

N_2 is used for $^{15}\text{N}/^{14}\text{N}$ isotope ratio measurements, the standard is atmospheric N_2 . Various preparation procedures have been described for the different nitrogen compounds (Bremner and Keeney 1966; Owens 1987; Velensky et al. 1989; Kendall and Grim 1990, and others). In the early days of nitrogen isotope investigations, the extraction and combustion techniques potentially involved chemical treatments that could have introduced isotopic fractionations. More recently, simplified techniques for combustion have come into routine use, so that a precision of $0.1\text{--}0.2\text{‰}$ for $\delta^{15}\text{N}$ determinations can be achieved. Organic nitrogen-compounds

are combusted to CO_2 , H_2O and N_2 in an elemental analyzer. The cryogenically purified N_2 is trapped on molecular sieves for analysis.

More recently methods have been described that are based on the isotope analysis of N_2O . Measurements of bulk $\delta^{15}\text{N}$ -values yield qualitative rather quantitative information on the nitrogen cycle, special techniques are necessary for a separate analysis of nitrate and nitrite in samples containing both species. Sigman et al. (2001) measured N_2O generated by denitrifying bacteria lacking N_2O reductase. McIlvin and Altabet (2005) introduced an alternative approach of the bacteria method. Nitrate is first reduced with a Cd catalyst to nitrite followed by sodium azide treatment to reduce nitrite to N_2O . This method allows sequential analysis of nitrate and nitrite, but azide is toxic and has to be handled with great care.

Compound-specific analysis of amino acids has been described by McClelland and Montoya (2002) studying 16 amino acids in planktonic consumers and their food sources. Some amino acids, like glutamate and aspartate, show ^{15}N -enrichments with increased trophic level, while others like phenylamine, serine and threonine record the N-isotope composition of the system in which organism exist. ^{15}N differences between the two groups can be attributed to differences in metabolic pathways.

Even different preparation techniques have been used for nitrogen in mantle derived samples with N-concentrations being too low to be analysed by conventional techniques. For these samples, static mass spectrometry, in which the gas is left under static conditions in the ion source, a method developed for noble gas analysis and adopted for nitrogen, has been used. As an alternative, Bebout et al. (2007) described a continuous flow technique for nanomole quantities of nitrogen.

2.5.2 Biological Nitrogen Isotope Fractionations

To understand the processes leading to the nitrogen isotope distribution in the geological environment, a short discussion of the biological nitrogen cycle is required. Atmospheric nitrogen, the most abundant form of nitrogen, is the least reactive species of nitrogen. It can, however, be converted to “fixed” nitrogen by bacteria and algae, which, in turn, can be used by biota for degradation to simple nitrogen compounds such as ammonium and nitrate. Thus, microorganisms are responsible for all major conversions in the biological nitrogen cycle, which generally is divided into fixation, nitrification, and denitrification. Other bacteria return nitrogen to the atmosphere as N_2 .

The term *fixation* is used for processes that convert unreactive atmospheric N_2 into reactive nitrogen such as ammonium, usually involving bacteria. Fixation commonly produces organic materials with $\delta^{15}\text{N}$ -values slightly less than 0 ‰ ranging from -3 to +1 (Fogel and Cifuentes 1993) and occurs in the roots of plants by many bacteria. The large amount of energy needed to break the molecular

nitrogen bond makes nitrogen fixation a very inefficient process with little associated N-isotope fractionation.

Nitrification is a multi-step oxidation process mediated by several different autotrophic organisms. Nitrate is not the only product of nitrification, different reactions produce various nitrogen oxides as intermediate species. Nitrification can be described as two partial oxidation reactions, each of which proceeds separately: oxidation by Nitrosomas ($\text{NH}_4 \rightarrow \text{NO}_2^-$) followed by oxidation by Nitrobacter ($\text{NO}_2^- \rightarrow \text{NO}_3^-$). Because the oxidation of nitrite to nitrate is generally rapid, most of the N-isotope fractionations is caused by the slow oxidation of ammonium by Nitrosomas. However, as shown by Casciotti (2009) the second oxidation step from nitrite to nitrate is accompanied by an inverse kinetic isotope fractionation, such that nitrite becomes progressively depleted in ^{15}N as the oxidation reaction proceeds.

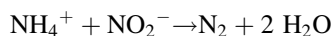
Denitrification (reduction of more oxidized forms to more reduced forms of nitrogen) is a multi-step process with various nitrogen oxides as intermediate compounds resulting from biologically mediated reduction of nitrate. Denitrification takes place in poorly aerated soil and in suboxic water bodies, especially in oxygen minimum zones of the ocean. There is debate about the relative contributions of denitrification in sediments versus in the ocean. Denitrification supposedly balances the natural fixation of nitrogen, if it did not occur, then atmospheric nitrogen would be exhausted in less than 100 million years. Denitrification causes the $\delta^{15}\text{N}$ -values of the residual nitrate to increase exponentially as nitrate concentrations decrease. Experimental investigations have demonstrated that fractionation factors may change from 10 to 30 ‰, with the largest values obtained under lowest reduction rates. Nitrogen isotope fractionations during denitrification in the ocean involves a greater fractionation than in sediments. Table 2.3, which gives a summary of observed N-isotope fractionations.

Noteworthy is the inverse kinetic fractionation during nitrite oxidation, which is different from all other microbial processes in which N-isotope fractionation is involved. Casciotti (2009) argued that the inverse fractionation effect is due to reverse reaction at the enzyme level.

Table 2.3 Nitrogen isotope fractionations for microbial cultures (after Casciotti 2009)

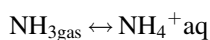
N_2 fixation	$\text{N}_2 \rightarrow \text{N}_{\text{org}}$	-2 to +2 ‰
NH_4^+ assimilation	$\text{NH}_4^+ \rightarrow \text{N}_{\text{org}}$	+14 to +27 ‰
NH_4^+ oxidation (nitrification)	$\text{NH}_4^+ \rightarrow \text{NO}_2^-$	+14 to 38 ‰
Nitrite oxidation (nitrification)	$\text{NO}_2^- \rightarrow \text{NO}_3^-$	-12.8 ‰
Nitrate reduction (denitrification)	$\text{NO}_3^- \rightarrow \text{NO}_2^-$	+13 to +30 ‰
Nitrite reduction (denitrification)	$\text{NO}_2^- \rightarrow \text{NO}$	+5 to +10 ‰
Nitrous oxide reduction (denitrification)	$\text{N}_2\text{O} \rightarrow \text{N}_2$	+4 to +13 ‰
Nitrate reduction (nitrate assimilation)	$\text{NO}_3^- \rightarrow \text{NO}_2^-$	+5 to +10

One very important recent finding in the nitrogen cycle is the discovery of anaerobic ammonium oxidation, briefly called anammox, a dissimilatory process involving the reaction of ammonia with nitrite



which first has been demonstrated using sediment incubations (Thamdrup and Dalsgaard 2002) and later shown to be the major N-loss process in oxygen minimum zone waters.

So far, only kinetic isotope effects have been considered, but isotopic fractionations associated with equilibrium exchange reactions have been demonstrated for the common inorganic nitrogen compounds (Letolle 1980). Of special importance in this respect is the ammonia volatilization reaction:



for which isotope fractionation factors of 1.025–1.035 have been determined (Kirshenbaum et al. 1947; Mariotti et al. 1981). Experimental data by Nitzsche and Stiehl (1984) indicate fractionation factors of 1.0143 at 250 °C and of 1.0126 at 350 °C. During the solution of atmospheric N_2 in ocean water, a very small ^{15}N -enrichment of about 0.1 ‰ occurs (Benson and Parker 1961).

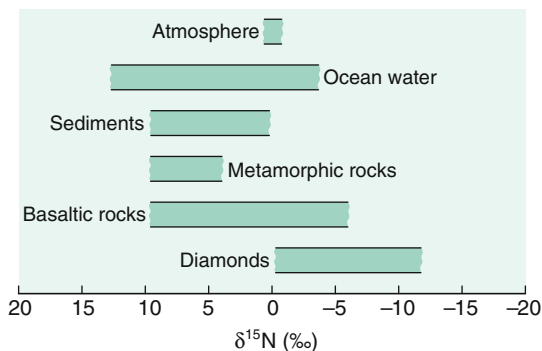
2.5.3 Nitrogen Isotope Distribution in the Earth

Nitrogen is generally regarded as a volatile element with chemical similarities to noble gases. Common belief restricts the dominant nitrogen reservoir to the atmosphere, which is true, if only the earth's surface is considered. Budget estimates of N for the earth as a whole indicate, however, that the dominant reservoir is in the mantle. The average content and speciation of nitrogen in the mantle is poorly constrained. Estimates for average concentrations vary between 0.3 and 36 ppm (Busigny and Bebout 2013).

Mantle nitrogen extracted from MORB glasses (Marty and Humbert 1997; Marty and Zimmermann 1999) and from diamonds (Javoy et al. 1986; Cartigny et al. 1997, 2005; Cartigny and Marty 2013) has an average $\delta^{15}\text{N}$ -value of around –5 ‰ with considerable scatter. Nitrogen isotope values extracted from peridotite xenoliths and mineral separates show large variations with phlogopites being depleted and clinopyroxene and olivine being enriched in ^{15}N (Yokochi et al. 2009). Positive $\delta^{15}\text{N}$ values measured in some MORB samples may reflect the occurrence of subducted nitrogen.

In the crust, during metamorphism of sediments, there is a significant loss of ammonium during devolatilisation, which is associated with a nitrogen fractionation, leaving behind ^{15}N residues (Haendel et al. 1986; Bebout and Fogel 1992; Jia 2006; Plessen et al. 2010). Thus high-grade metamorphic rocks and granites are relatively enriched in ^{15}N and typically have $\delta^{15}\text{N}$ -values between 8 and 10 ‰.

Fig. 2.12 $\delta^{15}\text{N}$ -values of important geological reservoirs (Fig. 2.12, 6th edition, p. 57)



Sadofsky and Bebout (2000) have examined the nitrogen isotope fractionation among coexisting micas, but could not find any characteristic difference between biotite and white mica.

In summary, nitrogen in sediments and crustal rocks exhibits positive $\delta^{15}\text{N}$ -values around 6 ‰, whereas in mantle-derived rocks $\delta^{15}\text{N}$ -values are around -5 ‰.

Figure 2.12 gives an overview about the nitrogen isotope variations in some important reservoirs.

2.5.4 Nitrogen in the Ocean

Nitrogen isotope studies may evaluate the source and fate of nitrogen in the ocean. Nitrogen in the ocean is present in different redox states (nitrate, nitrite, ammonium). Biological processes in the water column may transform one nitrogen compound to the other which is associated with N-isotope fractionations. Nitrogen fixation is regarded as the dominant process for primary production that causes little N isotope fractionation. Thus, nitrogen produced by this process should have a $\delta^{15}\text{N}$ -value close to zero. However, average oceanic $\delta^{15}\text{N}$ is close to 5 ‰ as measured in nitrate, the N-isotope enrichment resulting from denitrification. Denitrification occurring in oxygen depleted zones preferentially reduces ^{14}N , the remaining nitrate thus becomes progressively enriched in ^{15}N . Upwelling of such ^{15}N enriched water masses causes the production of relatively ^{15}N -rich phytoplankton particles that sink to the seafloor. The nitrogen isotope composition of sedimentary organic material, thus, can serve as an indicator of water column nitrogen reactions and of nutrient dynamics (e.g. Farrell et al. 1995).

Nitrogen isotopes in particulate organic nitrogen depends on (i) the isotopic composition of dissolved nitrate, and on (ii) isotope fractionation that occurs during nitrogen uptake by phytoplankton. In the photic zone phytoplankton preferentially incorporates ^{14}N , which results in a corresponding ^{15}N -enrichment in the residual nitrate. The N-isotope composition of settling organic detritus, thus varies

depending on the extent of nitrogen utilization: low ^{15}N contents indicate low relative utilisation, high ^{15}N contents indicate a high utilization.

Denitrification is believed to be enhanced in interglacial times compared to glacial times. Ganeshram et al. (2000) showed that $\delta^{15}\text{N}$ values during interglacials are about 2–3 ‰ heavier than $\delta^{15}\text{N}$ values during glacial times. This relationship has been used as a recorder of paleoproductivity.

Nitrogen isotopes in marine sediments, thus, may reflect nutrient cycles of ancient oceans. However, diagenetic reactions on the seafloor and deeper in the sediments may alter the primary nitrogen isotope signal. Nevertheless, Tesdall et al. (2013) argue that although diagenetic effects have to be taken into account, diagenesis is a secondary effect and therefore bulk sedimentary nitrogen isotope records from the seafloor and subseafloor sediments monitor past changes of the marine nitrogen cycle. They presented a global database of more than 2300 bulk sediment $\delta^{15}\text{N}$ measurements and demonstrated that $\delta^{15}\text{N}$ -values range from 2.5 to 16.6 ‰ with a mean value of 6.7 ‰ which is higher than the average 5 ‰ of nitrate in the ocean (<http://www.ncdc.noaa.gov/paleo/pubs/nicopp/nicopp.html>).

For long, denitrification was believed to be the only mechanism that reduces nitrate to N_2 , however, as found more recently the anaerobic oxidation of ammonia, called anammox reaction, is another mechanism in which bacteria use ammonium to convert nitrite to N_2 . Brunner et al. (2013) demonstrated that N isotope fractionation associated with the anammox reaction fall in the same range as denitrification. They further showed that anammox may be responsible for the large fractionations between nitrate and nitrite in oxygen minimum zones.

In sediments, with increasing thermal degradation of the organic matter, ammonium (NH_4) is liberated which can replace potassium in clay minerals. The nitrogen in the crystal lattice of clay minerals and micas, thus, is derived from decomposing organic matter reflecting the N-isotope composition of organic matter (Scholten 1991; Williams et al. 1995).

2.5.5 Anthropogenic Nitrogen Sources

The nitrogen cycle has been influenced considerably by human activities including agriculture and fossil fuel burning, adding reactive nitrogen to the environment on a local and a global scale. As demonstrated by Hastings et al. (2009, 2013), nitrogen isotopes of reactive nitrogen can be used to trace its origin. For example, Hastings et al. (2009) analysed N isotopes in a 100 m long ice core and observed a decrease from pre-industrial $\delta^{15}\text{N}$ -values of +11 ‰ to present day values of –1 ‰. Other studies have shown that fertilizer, animal wastes or sewage are the main sources of nitrate pollution in the hydrosphere. Under favorable conditions, these N-bearing compounds can be isotopically distinguished from each other (Heaton 1986). Anthropogenic fertilizers have $\delta^{15}\text{N}$ -values in the range –4 to +4 ‰ reflecting their

atmospheric source, whereas animal waste typically has $\delta^{15}\text{N}$ -values $>5\%$. Soil-derived nitrate and fertilizer nitrate commonly have overlapping $\delta^{15}\text{N}$ -values. In another example, Redling et al. (2013) documented foliar uptake and fertilization effects of car nitrogen oxides on vegetation.

2.6 Oxygen

Oxygen is the most abundant element on Earth. It occurs in gaseous, liquid and solid compounds, most of which are thermally stable over large temperature ranges. These facts make oxygen one of the most interesting elements in isotope geochemistry.

Oxygen has three stable isotopes with the following abundances (Rosman and Taylor 1998)

$$^{16}\text{O}: 99.757\%$$

$$^{17}\text{O}: 0.038\%$$

$$^{18}\text{O}: 0.205\%$$

Because of the higher abundance and the greater mass difference, the $^{18}\text{O}/^{16}\text{O}$ ratio is normally determined, which may vary in natural samples by about 10 % or in absolute numbers from about 1 : 475 to 1 : 525. More recently, with improved analytical techniques, the precise measurement of the $^{17}\text{O}/^{16}\text{O}$ ratio also became of interest (see p. 85).

2.6.1 Analytical Methods

CO_2 is the gas generally used for mass-spectrometric analysis. CO and O_2 have also been used in high temperature conversion of organic material and in laser probe preparation techniques. A wide variety of methods have been described to liberate oxygen from the various oxygen-containing compounds.

2.6.1.1 Water

The $^{18}\text{O}/^{16}\text{O}$ ratio of water is usually determined by equilibration of a small amount of CO_2 with a surplus of water at a constant temperature. For this technique, the exact value of the fractionation for the $\text{CO}_2/\text{H}_2\text{O}$ equilibrium at a given temperature is of crucial importance. A number of authors have experimentally determined this fractionation at 25 °C with variable results. A value of 1.0412 was proposed at the 1985 IAEA Consultants Group Meeting to be the best estimate.

It is also possible to quantitatively convert all water oxygen directly to CO_2 by reaction with guanidine hydrochloride (Dugan et al. 1985) which has the advantage

that it is not necessary to assume a value for the $\text{H}_2\text{O}-\text{CO}_2$ isotope fractionation in order to obtain the $^{18}\text{O}/^{16}\text{O}$ ratio. Sharp et al. (2001) described a technique reducing H_2O by reaction with glassy carbon at 1450 °C. O'Neil and Epstein (1966) first described the reduction of water with Br_5F . For the precise measurement of ^{17}O and ^{18}O the method later was modified using CoF_3 (Baker et al. 2002; Barkan and Luz 2005).

As mentioned under Sect. 2.1.1, an alternative method to mass spectrometry is the direct determination of oxygen isotope ratios by laser absorption spectroscopy (Brand et al. 2009a, b and others).

2.6.1.2 Carbonates

The standard procedure for the isotope analysis of carbonates is the reaction with 100 % phosphoric acid at 25 °C first described by McCrea (1950). The following reaction equation:



where Me is a divalent cation, shows that only two-thirds of the carbonate oxygen present in the product CO_2 is liberated, which carries a significant isotope effect being on the order of 10 ‰, but varies up to a few ‰ depending on the cation, the reaction temperature and the preparation procedure. The so-called acid fractionation factor must be precisely known to obtain the oxygen isotope ratio of the carbonate. This can be done by measuring the $\delta^{18}\text{O}$ -value of the carbonate by fluorination with BrF_5 , first described by Sharma and Clayton (1965).

Experimental details of the phosphoric acid method vary significantly among different laboratories. The two most common varieties are the “sealed vessel” and the “acid bath” methods. In the latter method the CO_2 generated is continuously removed, while in the former it is not. Swart et al. (1991) demonstrated that the two methods exhibit a systematic ^{18}O difference between 0.2 and 0.4 ‰ over the temperature range 25 to 90 °C. Of these the “acid-bath” method probably provides the more accurate results. A further modification of this technique is referred to as the “individual acid bath”, in which contaminations from the acid delivery system are minimized. Wachter and Hayes (1985) demonstrated that careful attention must be given to the phosphoric acid. In their experiments best results were obtained by using a 105 % phosphoric acid and a reaction temperature of 75 °C. This high reaction temperature should not be used when attempting to discriminate between mineralogically distinct carbonates by means of differential carbonate reaction rates.

Because some carbonates like magnesite or siderite react very sluggishly at 25 °C, higher reaction temperatures are necessary to extract CO_2 from these minerals. Reaction temperatures have varied up to 90 or even 150 °C (Rosenbaum and Sheppard 1986; Böttcher 1996), but there still exist considerable differences in the fractionation factors determined by various workers. Crowley (2010) showed that for minerals of the CaCO_3 – MgCO_3 group the oxygen isotope composition of CO_2 is a linear function of the reciprocal of reaction temperature. Deviations from this

Table 2.4 Acid fractionation factors for various carbonates determined at 25 °C (modified after Kim et al. 2007)

Mineral	α	References
Calcite	10.30	Kim et al. (2007)
Aragonite	10.63	Kim et al. (2007)
	11.14	Gilg et al. (2007)
Dolomite	11.75	Rosenbaum and Sheppard (1986)
Magnesite	10.79 (50 °C)	Das Sharma et al. (2002)
Siderite	11.63	Carothers et al. (1988)
Witherite	10.57	Kim and O'Neil (1997)

relationship may be attributed to structural state and differences in chemical composition.

Another uncertainty exists for fractionations between aragonite and calcite. Different workers have reported fractionations from negative to positive. Nevertheless there seems to be a general agreement that the fractionation factor for aragonite is about 0.6 ‰ higher than for calcite (Tarutani et al. 1969; Kim and O'Neil 1997), although Grossman and Ku (1986) have reported a value of up to 1.2 ‰. The dolomite-calcite fractionation may vary depending on specific composition (Land 1980). Table 2.4 reports acid fractionation factors for various carbonates.

2.6.1.3 Silicates

Oxygen in silicates and oxides is usually liberated through fluorination with F₂, BrF₅ or ClF₃ in nickel-tubes at 500 to 650 °C (Taylor and Epstein 1962; Clayton and Mayeda 1963; and Borthwick and Harmon 1982) or by heating with a laser (Sharp 1990). Decomposition by carbon reduction at 1000–2000 °C may be suitable for quartz and iron oxides but not for all silicates (Clayton and Epstein 1958). The oxygen is converted to CO₂ over heated graphite or diamond. For an analysis of the three isotope (¹⁶O, ¹⁷O, ¹⁸O) O₂ has to be the analyte gas. Care must be taken to ensure quantitative oxygen yields, which can be a problem in the case of highly refractive minerals like olivine and garnet. Low yields may result in anomalous ¹⁸O/¹⁶O ratios, high yields are often due to excess moisture in the vacuum extraction line.

Today, infrared-laser fluorination, first described by Sharp (1990), most commonly is used for mineral analysis. Alternatively, UV lasers have been used by Wiechert and Hoefs (1995) and Wiechert et al. (2002). A precise SIMS method with a reproducibility of 0.3 ‰ from 15 µm mineral spots has been described by Kita et al. (2009).

2.6.1.4 Phosphates

Phosphates are first dissolved, then precipitated as silver phosphate (Crowson et al. 1991). Ag₃PO₄ is preferred because it is non-hygroscopic and can be precipitated rapidly without numerous chemical purification steps (O'Neil et al. 1994). This

Ag_3PO_4 is then fluorinated (Crowson et al. 1991), reduced with C either in a furnace (O'Neil et al. 1994) or with a laser (Wenzel et al. 2000) or pyrolyzed (Vennemann et al. 2002). Because PO_4 does not exchange oxygen with water at room temperature (Kolodny et al. 1983), the isotopic composition of the Ag_3PO_4 is that of the PO_4 component of the natural phosphate. As summarized by Vennemann et al. (2002) conventional fluorination remains the most precise and accurate analytical technique for Ag_3PO_4 . Laser techniques on bulk materials have also been attempted (Cerling and Sharp 1996; Kohn et al. 1996; Wenzel et al. 2000), but because fossil phosphates invariably contain diagenetic contaminants, chemical processing and analysis of a specific component (CO_3 or PO_4) is ordinarily performed.

2.6.1.5 Sulfates

Sulfates are precipitated as BaSO_4 , and then reduced with carbon at 1000 °C to produce CO_2 and CO. The CO is either measured directly or converted to CO_2 by electrical discharge between platinum electrodes (Longinelli and Craig 1967). Total pyrolysis by continuous flow methods has made the analysis of sulfate oxygen more precise and less time-consuming than the off-line methods. Bao and Thiemens (2000) have used a CO_2 -laser fluorination system to liberate oxygen from barium sulfate.

2.6.1.6 Nitrates

Oxygen isotopes in nitrate may be measured by high-temperature combustion with graphite (Revesz et al. 1997). Since this method is labour-intensive, Sigman et al. (2001) used cultured denitrifying bacteria for the reduction of nitrate. In the analyzed N_2O only one of six oxygen atoms present in the initial nitrate will be measured, therefore potential oxygen isotope fractionations must be adequately taken into account (Casciotti et al. 2002).

2.6.2 Standards

Two different δ -scales are in use: $\delta^{18}\text{O}_{(\text{VSMOW})}$ and $\delta^{18}\text{O}_{(\text{VPDB})}$, because of two different categories of users, who have traditionally been engaged in O-isotope studies. The VPDB scale is used in low-temperature studies of carbonate. The original PDB standard was prepared from a Cretaceous belemnite from the Pee Dee Formation and was the laboratory working standard used at the University of Chicago in the early 1950s when the paleotemperature scale was developed. The original supply of this standard has long been exhausted, therefore secondary standards have been introduced (see Table 2.5), whose isotopic compositions have been calibrated relative to PDB. All other oxygen isotope analyses (waters, silicates, phosphates, sulfates, high-temperature carbonates) are given relative to SMOW.

Table 2.5 $\delta^{18}\text{O}$ -values of commonly used O-isotope standards (data for sulfate and nitrate are from Brand et al. 2009a, b)

Standard	Material	VPDB scale	VSMOW scale
NBS-19	Marble	-2.20	
NBS-20	Limestone	-4.14	
NBS-18	Carbonatite	-23.00	
NBS-28	Quartz		9.60
NBS-30	Biotite		5.10
GISP	Water		-24.75
SLAP	Water		-55.50
NBS-127	Ba sulfate		8.59
USGS 35	Na nitrate		56.81

The conversion equations of $\delta^{18}\text{O}_{(\text{VPDB})}$ versus $\delta^{18}\text{O}_{(\text{VSMOW})}$ and vice versa (Coplen et al. 1983) are:

$$\delta^{18}\text{O}(\text{VSMOW}) = 1.03091 \delta^{18}\text{O}(\text{PDB}) + 30.91$$

and

$$\delta^{18}\text{O}(\text{VPDB}) = 0.97002 \delta^{18}\text{O}(\text{VSMOW}) - 29.98$$

Table 2.5 gives the $\delta^{18}\text{O}$ -values of commonly used oxygen isotope standards on both scales.

2.6.3 Fractionation Processes

Out of the numerous possibilities to fractionate oxygen isotopes in nature, the following are of special significance.

2.6.3.1 Fractionation of Water

Knowledge of the oxygen isotope fractionation between liquid water and water vapor is essential for the interpretation of the isotope composition of different water types. Fractionation factors experimentally determined in the temperature range from 0 to 350 °C have been summarized by Horita and Wesolowski (1994). This is shown in Fig. 2.13.

Addition of salts to water also affects isotope fractionations. The presence of ionic salts in solution changes the local structure of water around dissolved ions. Taube (1954) first demonstrated that the $^{18}\text{O}/^{16}\text{O}$ ratio of CO_2 equilibrated with pure H_2O decreased upon the addition of MgCl_2 , AlCl_3 and HCl , remained more or less unchanged for NaCl , and increased upon the addition of CaCl_2 . The changes vary roughly linearly with the molality of the solute (see Fig. 2.14).

To explain this different fractionation behavior, Taube (1954) postulated different isotope effects between the isotopic properties of water in the hydration

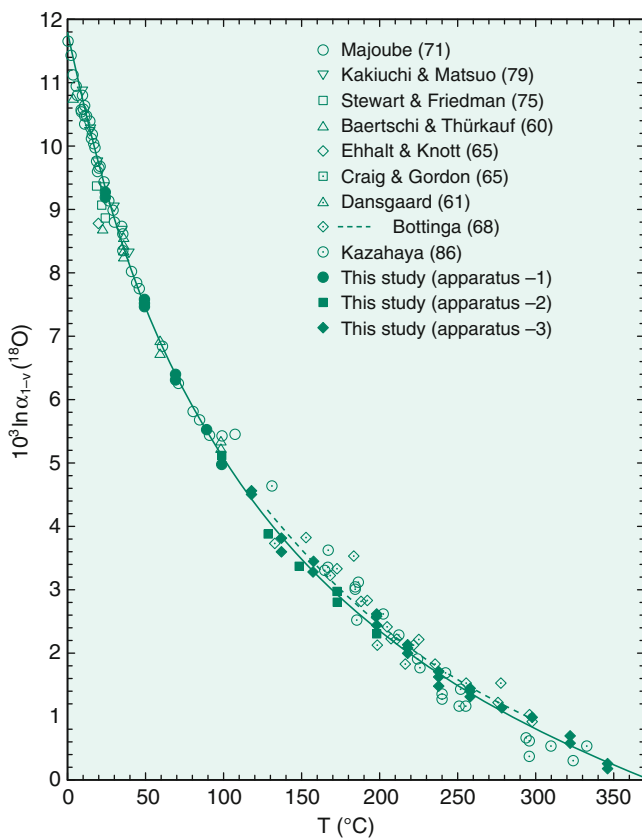


Fig. 2.13 Oxygen isotope fractionation factors between liquid water and water vapour in the temperature range 0–350 °C (after Horita and Wesolowski 1994) (Fig. 2.13, 6th edition p. 62)

sphere of the cation and the remaining bulk water. The hydration sphere is highly ordered, whereas the outer layer is poorly ordered. The relative sizes of the two layers are dependent upon the magnitude of the electric field around the dissolved ions. The strength of the interaction between the dissolved ion and water molecules is also dependent upon the atomic mass of the atom to which the ion is bonded. O’Neil and Truesdell (1991) have introduced the concept of “structure-making” and “structure-breaking” solutes: structure makers yield more positive isotope fractionations relative to pure water whereas structure breakers produce negative isotope fractionations. Any solute that results in a positive isotope fractionation is one that causes the solution to be more structured as is the case for ice structure, when compared to solutes that lead to less structured forms, in which cation–H₂O bonds are weaker than H₂O–H₂O bonds.

As already treated in Sect. 2.1, isotope fractionations, the hydration of ions may play a significant role in hydrothermal solutions and volcanic vapors (Driesner and

Fig. 2.14 Oxygen isotope fractionation between pure water and solutions of various ions (after O’Neil and Truesdell 1991) (Fig. 2.14, 6th edition, p. 63)

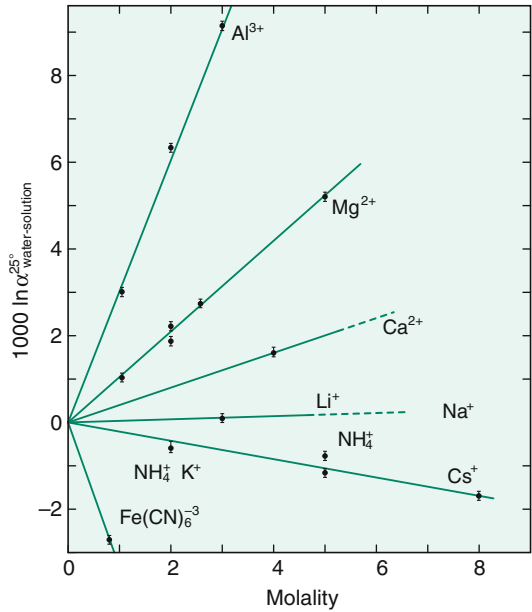


Table 2.6 Experimentally determined oxygen isotope fractionation factors relative to water for the aqueous system $\text{CO}_2\text{--H}_2\text{O}$ between 5 and 40 °C according to $10^3 \ln \alpha = A(10^6/T^{-2}) + B$ (Beck et al. 2005)

	A	B
HCO_3^{-}	2.59	1.89
CO_3^{2-}	2.39	-2.70
$\text{CO}_{2(\text{aq})}$	2.52	12.12

Seward 2000). Such isotope salt effects may change the oxygen isotope fractionation between water and other phases by several permil.

2.6.3.2 CO₂–H₂O System

Of equal importance is the oxygen isotope fractionation in the $\text{CO}_2\text{--H}_2\text{O}$ system. Early work concentrated on the oxygen isotope partitioning between gaseous CO_2 and water (Brenninkmeijer et al. 1983). In more recent work by Usdowski et al. (1991), Beck et al. (2005) and Zeebe (2007), it has been demonstrated that the oxygen isotope composition of the individual carbonate species are isotopically different, which is consistent with experimental work of McCrea (1950) and Usdowski and Hoefs (1993). Table 2.6 summarizes the equations for the temperature dependence between 5 and 40 °C (Beck et al. 2005).

The oxygen isotope fractionation ($1000 \ln \alpha$) between aqueous CO_2 and water at 25 °C is 41.6, dropping to 24.7 at high pH values when CO_3^{2-} is the dominant species (see Fig. 2.15). The pH dependence of the oxygen isotope composition in

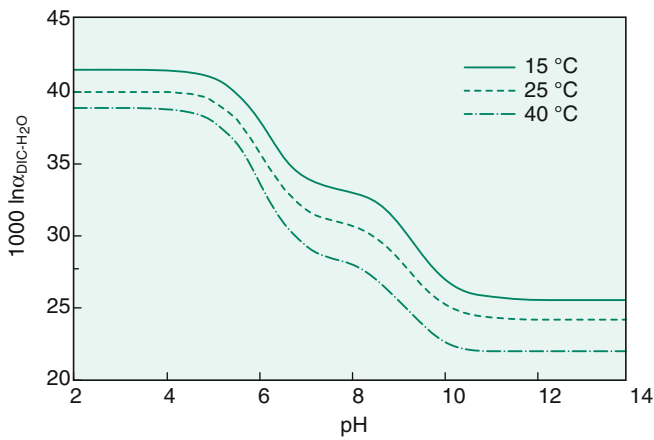


Fig. 2.15 Oxygen isotope fractionations between dissolved inorganic carbon (DIC) and water as function of pH and temperatures (after Beck et al. 2005) (Fig. 2.15, 6th edition, p. 64)

the carbonate-water system has important implications in the derivation of oxygen isotope temperatures.

2.6.3.3 Mineral Fractionations

The oxygen isotope composition of a rock depends on the ¹⁸O contents of the constituent minerals and the mineral proportions. Garlick (1966) and Taylor (1968) arranged coexisting minerals according to their relative tendencies to concentrate ¹⁸O. The list given in Table 2.7 has been augmented by data from Kohn et al. (1998a, b, c).

This order of decreasing ¹⁸O-contents has been explained in terms of the bond-type and strength in the crystal structure. Semi-empirical bond-type calculations have been developed by Garlick (1966) and Savin and Lee (1988) by

Table 2.7 Sequence of minerals in the order (bottom to top) of their increasing tendency to concentrate ¹⁸O

Quartz
Dolomite
K-feldspar, albite
Calcite
Na-rich plagioclase
Ca-rich plagioclase
Muscovite, paragonite, kyanite, glaucophane
Orthopyroxene, biotite
Clinopyroxene, hornblende, garnet, zircon
Olivine
Ilmenite
Magnetite, hematite

assuming that oxygen in a chemical bond has similar isotopic behavior regardless of the mineral in which the bond is located. This approach is useful for estimating fractionation factors. The accuracy of this approach is limited due to the assumption that the isotope fractionation depends only upon the atoms to which oxygen is bonded and not upon the structure of the mineral, which is not strictly true. Kohn and Valley (1998a, b) determined empirically the effects of cation substitutions in complex minerals such as amphiboles and garnets spanning a large range in chemical compositions. Although isotope effects of cation exchange are generally less than 1 ‰ at $T > 500\text{ }^{\circ}\text{C}$, they increase considerably at lower temperatures. Thus; use of amphiboles and garnets for thermometry requires exact knowledge of chemical compositions.

On the basis of these systematic tendencies of ^{18}O enrichment found in nature, significant temperature information can be obtained up to temperatures of $1000\text{ }^{\circ}\text{C}$, and even higher, if calibration curves can be worked out for the various mineral pairs. The published literature contains many calibrations of oxygen isotope geothermometers, most are determined by laboratory experiments, although some are based on theoretical calculations.

Although much effort has been directed toward the experimental determination of oxygen isotope fractionation factors in mineral—water systems, the use of water as an oxygen isotope exchange medium has several disadvantages. Some minerals become unstable in contact with water at elevated temperatures and pressures, leading to melting, breakdown and hydration reactions. Incongruent solubility and ill-defined quench products may introduce additional uncertainties. Most of the disadvantages of water can be circumvented by using calcite as an exchange medium (Clayton et al. 1989; Chiba et al. 1989). Mineral-mineral fractionations—determined by these authors (Table 2.8)—give internally consistent geothermometric information that generally is in accord with independent estimates, such as the theoretical calibrations of Kieffer (1982).

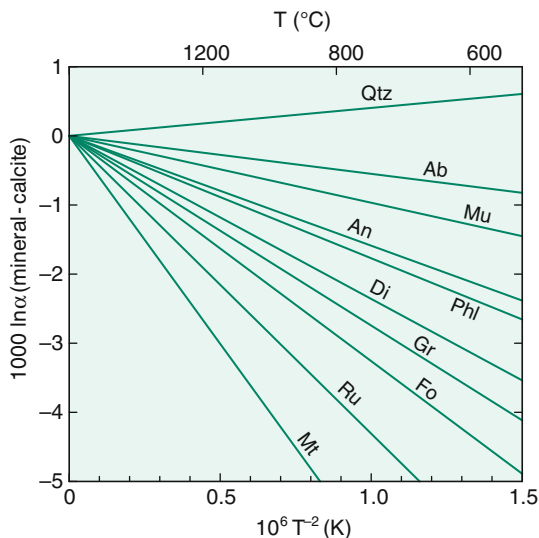
A more recent summary has been given by Chacko et al. (2001) (see Fig. 2.16).

Many isotopic fractionations between low-temperature minerals and water have been estimated by assuming that their temperature of formation and the isotopic composition of the water in which they formed (for example, ocean water) are well known. This is sometimes the only approach available in cases in which the rates of isotope exchange reactions are slow and in which minerals cannot be synthesized in the laboratory at appropriate temperatures.

Table 2.8 Coefficients A for silicate—pair fractionations ($1000 \ln \alpha_{X-Y} = A/T^2$) 10^6 (after Chiba et al. 1989)

	Cc	Ab	An	Di	Fo	Mt
Qtz	0.38	0.94	1.99	2.75	3.67	6.29
Cc		0.56	1.61	2.37	3.29	5.91
Ab			1.05	1.81	2.73	5.35
An				0.76	1.68	4.30
Di					0.92	3.54
Fo						2.62

Fig. 2.16 Oxygen isotope fractionations between various minerals and calcite (after Chacko et al. 2001) (Fig. 2.16, 6th edition, p. 66)



2.6.4 Triple Oxygen Isotope Compositions

Measurements of $^{17}\text{O}/^{16}\text{O}$ ratios potentially expand the utility of $^{18}\text{O}/^{16}\text{O}$ studies, the latter being hampered by difficulties to differentiate between temperature and water composition. Since the natural oxygen isotope ratio of $^{17}\text{O}/^{16}\text{O}$ is close to one half of the $^{18}\text{O}/^{16}\text{O}$ ratio, in the past it was generally assumed that there was no need to measure the rare ^{17}O . However, with improvements in analytical techniques, it became clear that the precise measurement of ^{17}O contents may give additional informations on fractionation processes in the earth's reservoirs. In a diagram $\delta^{17}\text{O}$ versus $\delta^{18}\text{O}$ values; all terrestrial rocks and minerals plot on a line with a coefficient λ 0.52× which was called the Terrestrial Fractionation Line (TFL). Deviations from the TFL reference line are given as $\Delta^{17}\text{O}$ and are termed oxygen isotope anomalies. The coefficient λ differs for equilibrium and kinetic fractionation processes and varies between 0.509 which is the lower limit for kinetic fractionations and 0.530 which is the equilibrium high temperature limit (Young et al. 2002).

For water, for instance, the triple oxygen isotope composition is characterized by an equilibrium fractionation exponent λ between liquid water and water vapour of 0.529 compared to a value of 0.518 for diffusion of water vapour. The global meteoric water line has a slope of 0.528 (Luz and Barkan 2010) (analogous to a slope of 8 of the $\delta\text{D}-\delta^{18}\text{O}$ meteoric water line). For rocks and minerals the slope λ is between 0.524 and 0.526 (Miller et al. 1999; Rumble et al. 2007) and for meteoric waters the slope is 0.528 (Luz and Barkan 2010).

With further analytical improvements, Pack and Herwartz (2014) demonstrated that the concept of a single TFL is invalid and that different reservoirs on Earth are characterized by individual mass fractionation lines with individual slopes and intercepts. Similar conclusions have been reached by Levin et al. (2014) and Passey et al. (2014).

2.6.5 Fluid-Rock Interactions

Oxygen isotope ratio analysis provides a powerful tool for the study of water/rock interaction. The geochemical effect of such an interaction between water and rock or mineral is a shift of the oxygen isotope ratios of the rock and/or the water away from their initial values, given that their compositions are not in equilibrium.

Detailed studies of the kinetics and mechanisms of oxygen isotope exchange between minerals and fluids show that there are three possible exchange mechanisms (Matthews et al. 1983a, b; Gilotti 1985).

- (1) Solution-precipitation. During a solution-precipitation process, larger grains grow at the expense of smaller grains. Smaller grains dissolve and recrystallize on the surface of larger grains which decreases the overall surface area and lowers the total free energy of the system. Isotopic exchange with the fluid occurs while material is in solution.
- (2) Chemical reaction. The chemical activity of one component of both fluid and solid is so different in the two phases that a chemical reaction occurs. The breakdown of a finite portion of the original crystal and the formation of new crystals is implied. The new crystals would form at or near isotopic equilibrium with the fluid.
- (3) Diffusion. During a diffusion process isotopic exchange takes place at the interface between the crystal and the fluid with little or no change in morphology of the reactant grains. The driving force is the random thermal motion of the atoms within a concentration or activity gradient.

In the presence of a fluid phase coupled dissolution—reprecipitation is known to be a much more effective process than diffusion. This has been first demonstrated experimentally by O’Neil and Taylor (1967) and later re-emphasized by Cole (2000) and Fiebig and Hoefs (2002).

The first attempts to quantify isotope exchange processes between water and rocks were made by Sheppard et al. (1971) and Taylor (1974). By using a simple closed-system material balance equation these authors were able to calculate cumulative fluid/rock ratios.

$$W/R = \frac{\delta_{\text{rockf}} - \delta_{\text{rocki}}}{\delta_{\text{H}_2\text{O}_i} - (\delta_{\text{rockf}} - \Delta)}, \quad (2.7)$$

where $\Delta = \delta_{\text{rockf}} - \delta_{\text{H}_2\text{O}_f}$

The equation requires adequate knowledge of both the initial (i) and final (f) isotopic states of the system and describes the interaction of one finite volume of rock with a fluid. The utility of such “zero-dimensional” equations has been questioned by Baumgartner and Rumble (1988), Blattner and Lassey (1989), Nabelek (1991), Bowman et al. (1994) and others. Only under special conditions do one-box models yield information on the amount of fluid that actually flowed through the rocks. If the rock and the infiltrating fluid were not far out of isotopic

equilibrium, then the calculated fluid/rock ratios rapidly approach infinity. Therefore, the equations are sensitive only to small fluid/rock ratios. Nevertheless, the equations can constrain fluid sources. More sophisticated one-dimensional models like the chromatographic or continuum mechanics models (i.e. Baumgartner and Rumble 1988) are physically more plausible and can describe how the isotopic composition of the rock and of the fluid change with time and space. The mathematical models are complex and are based on partial differential equations that must be solved numerically. Examples of fluid-rock interactions in contact metamorphic environments have been presented by Nabelek and Labotka (1993), Bowman et al. (1994) and application to contrasting lithologies by Bickle and Baker (1990) and Cartwright and Valley (1991).

Criss et al. (1987) and Gregory et al. (1989) developed a theoretical framework that describes the kinetics of oxygen isotope exchange between minerals and coexisting fluids. Figure 2.17 shows characteristic patterns in δ - δ plots for some hydrothermally altered granitic and gabbroic rocks. The $^{18}\text{O}/^{16}\text{O}$ arrays displayed on Fig. 2.17 cut across the 45° equilibrium lines at a steep angle as a result of the much faster oxygen isotope exchange of feldspar compared to that of quartz and pyroxene. If a low- ^{18}O fluid such as meteoric or ocean water is involved in the exchange process, the slopes of the disequilibrium arrays can be regarded as “isochrons” where, with continued exchange through time the slopes become less

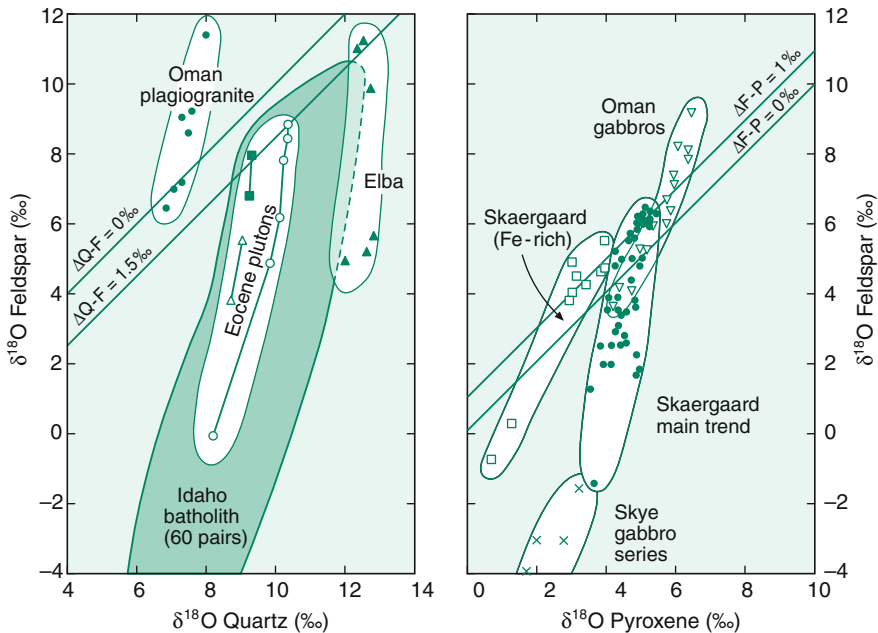
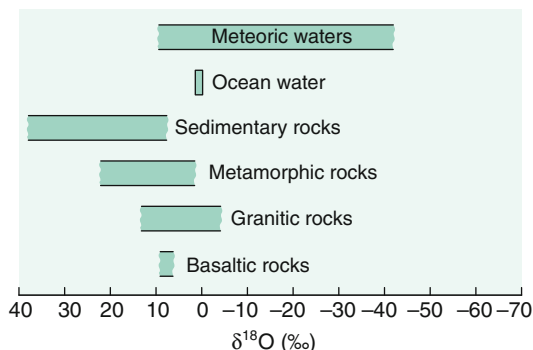


Fig. 2.17 $\delta^{18}\text{O}_{(\text{feldspar})}$ versus $\delta^{18}\text{O}_{(\text{quartz})}$ and versus $\delta^{18}\text{O}_{(\text{pyroxene})}$ plots of disequilibrium mineral pair arrays in granitic and gabbroic rocks. The arrays indicate open-system conditions from circulation of hydrothermal meteoric fluids (after Gregory et al. 1989) (Fig. 2.17, 6th edition, p. 68)

Fig. 2.18 $\delta^{18}\text{O}$ values of important geological reservoirs (Fig. 2.18, 6th edition, p. 68)



steep and approach the 45° equilibrium line. These “times” represent the duration of a particular hydrothermal event.

Figure 2.18 summarizes the naturally observed oxygen isotope variations in important geological reservoirs.

2.7 Magnesium

The oxidation state of magnesium in natural compounds always is two, thus it might be expected that the natural range of Mg isotope composition is comparably small. On the other hand, Mg is incorporated during growth of biogenic CaCO_3 and plays an essential role during photosynthesis indicating that biological fractionations may play an important role for Mg isotopes.

Magnesium is composed of three isotopes (Rosman and Taylor 1998)

$$^{24}\text{Mg} \quad 78.99 \%$$

$$^{25}\text{Mg} \quad 10.00 \%$$

$$^{26}\text{Mg} \quad 11.01 \%$$

Early investigations on Mg isotope variations have been limited by an uncertainty of 1–2 ‰. Catanzaro and Murphy (1966) for instance concluded that terrestrial Mg isotope variations are restricted to a few ‰. The introduction of multicollector-inductively coupled-plasma mass spectrometry (MC-ICP-MS) increased the precision by one order of magnitude and has initiated a new search of natural isotope variations (Galy et al. 2001, 2002). Factors affecting the accuracy of Mg isotopes measured by MC-ICP-MS have been summarized by Teng and Yang (2013). $\delta^{25}\text{Mg}$ and $\delta^{26}\text{Mg}$ values are reported relative to the DSM-3 standard (Galy et al. 2003; Oeser et al. 2014; Teng et al. 2014). Teng et al. (2014) published Mg isotope compositions for 24 reference materials, the long-term reproducibility for $\delta^{25}\text{Mg}$ was 0.05 ‰ and for $\delta^{26}\text{Mg}$ 0.07 ‰. One of the advantages of the

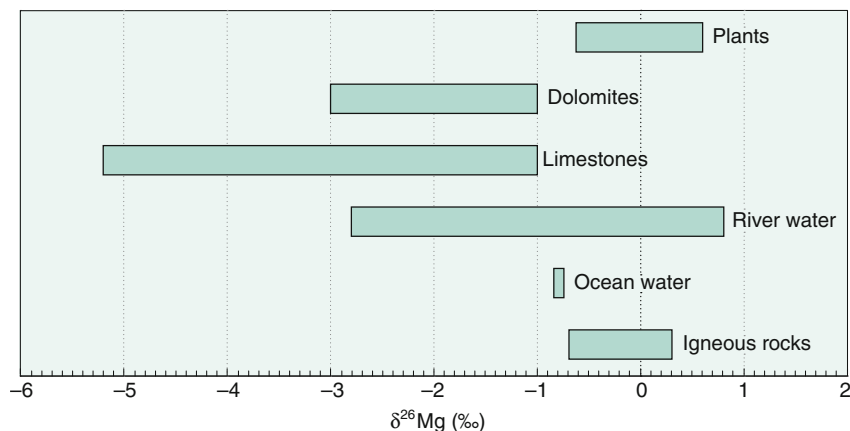


Fig. 2.19 $\delta^{26}\text{Mg}$ values of important geological reservoirs

MC-ICPMS technique is the ability to measure $^{25}\text{Mg}/^{24}\text{Mg}$ and $^{26}\text{Mg}/^{24}\text{Mg}$ ratios independently many times smaller than the magnitude of the natural variations. The relationship between $^{25}\text{Mg}/^{24}\text{Mg}$ and $^{26}\text{Mg}/^{24}\text{Mg}$ ratios is diagnostic of kinetic versus equilibrium fractionations: for equilibrium processes the slope on a three-isotope diagram should be close to 0.521, for kinetic processes the slope should be 0.511 (Young and Galy 2004).

Figure 2.19 summarizes the natural $\delta^{26}\text{Mg}$ isotope variations relative to DSM-3.

2.7.1 High-Temperature Fractionations

Calculations by Schauble (2011) yield systematic ^{26}Mg isotope fractionations among silicates, carbonates and oxides in the order magnesite, dolomite, forsterite, orthoenstatite, diopside, periclase and spinel. Fractionations correlate with coordination numbers, tetrahedral sites tend to have higher $^{26}\text{Mg}/^{24}\text{Mg}$ ratios than octahedral sites: thus, pyrope in which Mg is in eightfold coordination is depleted in heavy Mg isotopes relative to pyroxenes and olivine, in which Mg is in sixfold coordination. Experimentally determined equilibrium isotope fractionations between spinel, forsterite and magnesite by Macris et al. (2013) are consistent with the postulated dependence on coordination numbers. In the temperature range from 600 to 800 °C, Mg isotope fractionations between spinel and forsterite vary from 1.3 to 0.86 ‰ indicating isotope equilibrium. It is still unclear whether small intermineral fractionations among olivine and pyroxenes in mantle rocks represent equilibrium conditions or are products of melt-rock interactions (Xiao et al. 2013). Studies by Teng et al. (2007), Wiechert and Halliday (2007), Young et al. (2009), Handler et al. (2009) and Bourdon et al. (2010) have demonstrated slight differences between basalts and peridotite. Mineral Mg isotope fractionations among

olivine and pyroxene are very small (Handler et al. 2009; Wiechert and Halliday 2007; Yang et al. 2009; Liu et al. 2011), clinopyroxene and phlogopite are more variable and slightly heavier than olivine suggesting that inter-mineral fractionations are controlled by Mg–O bond strengths (Liu et al. 2011). Furthermore, as pointed out by Young et al. (2015), the effects of mineral chemistry are crucial to understand high-temperature mineral Mg isotope distributions.

The Mg isotope composition of the Moon and chondrites are indistinguishable from Earth, suggesting a homogenous Mg-isotope distribution in the solar system and no Mg isotope fractionation during the Moon-forming event (Sedaghatpour et al. 2013). In contrast to the mantle, the upper and lower continental crust is heterogeneous in Mg isotope composition and on average slightly heavier than the mantle (Shen et al. 2009; Li et al. 2010; Liu et al. 2010a, b; Teng et al. 2013). Li et al. (2010) concluded that compared to granites, sediments are heavier and more variable. Such larger variations may result from chemical weathering during which light isotopes are lost to the hydrosphere, leaving ^{26}Mg enriched sedimentary rocks.

Clastic sediments are generally enriched in heavy Mg isotopes with $\delta^{26}\text{Mg}$ values up to 0.92 ‰ (Li et al. 2010). During subduction, clastic sediments generally retain their Mg isotope composition (Li et al. 2014), thus recycling of clastic sediments will introduce Mg enriched in heavy isotopes into the mantle. Carbonates on the hand are significantly depleted in heavy Mg isotopes. Light isotope values in basalts from the North China Craton have been interpreted to indicate recycling of carbonates derived from oceanic crust (Yang et al. 2012a, b).

2.7.2 Fractionations During Weathering

The behaviour of Mg isotopes during weathering is rather complex (Wimpenny et al. 2010; Huang et al. 2012). Mg is soluble and mobile during weathering potentially inducing small fractionations during dissolution and precipitation of minerals. Wimpenny et al. (2010) and Huang et al. (2012) observed that light Mg isotopes are preferentially released during dissolution of basalt leading to enriched residues. Ryu et al. (2011), however, reported little fractionation during dissolution of granite. The different behaviour of Mg isotopes during weathering may reflect crystallographic differences of Mg-sites in minerals.

Compared to dissolution, the behaviour of Mg isotopes during secondary formation of Mg minerals may be even more complex (Huang et al. 2012). Soil and clays are generally heavier than their parent rocks (Tipper et al. 2006a, b, 2010; Opfergelt et al. 2012; Pogge von Strandmann et al. 2014) suggesting that heavy Mg isotopes are preferentially incorporated into the structure of clay minerals or absorbed in soils.

The complex behaviour of Mg during weathering results in large Mg isotope variations of river waters. As summarized by Li et al. (2012) $\delta^{26}\text{Mg}$ values range from -3.80 to $+0.75$ ‰ reflecting differences of catchment lithologies particularly in the proportions of carbonate to silicate rocks. Tipper et al. (2006a) on the other hand observed a total variation in ^{26}Mg of 2.5 ‰ and concluded that the lithology

in the drainage area is of limited significance, instead the major part of the variability has to be attributed to fractionations in the weathering environment.

2.7.3 Ocean Water

The dominant Mg source to the ocean is riverine input, major sinks are removal by hydrothermal fluids, dolomite formation and low-temperature clay formation during alteration of the oceanic crust. The average $\delta^{26}\text{Mg}$ -value of riverine input is -1.09 ‰ (Tipper et al. 2006b).

Because of its relatively long mean residence time, ocean water has a constant isotope composition of -0.80 ‰ that is slightly heavier than average river water resulting from Mg uptake into silicate minerals during weathering. Mg removal from seawater by hydrothermal interaction with the oceanic crust forming smectites and at higher temperatures chlorite does not cause a measurable Mg isotope fractionation. Dolomitisation, however, affects the ocean water, driving seawater to heavier values.

By analyzing pore waters from a large range of oceanographic settings, Higgins and Schrag (2010) demonstrated, that although Mg concentrations in pore waters are very similar in many deep-sea sediments, profiles of $\delta^{26}\text{Mg}$ values are very different, which is best explained by precipitation of Mg-minerals in sediments or underlying crust.

2.7.4 Carbonates

Dolomite is one of the major Mg carbonate that forms under specific environmental conditions. Geske et al. (2015) reported Mg isotope compositions of dolomite from various environments having a total range from -2.49 to -0.45 ‰ and argued that Mg isotope ratios are affected by a variety of factors, making the application of Mg isotopes as a proxy for their depositional and diagenetic environment problematic. On the hand, as observed by Azmy et al. (2013), early diagenetic dolomite inherits its isotope signature from precursor carbonates and diagenetic fluids. Later formed diagenetic dolomite phases may be slightly enriched in ^{26}Mg suggesting that temperature is not the decisive factor, but instead the Mg-isotope composition of the diagenetic fluid.

Mg is present in CaCO_3 in the form of high Mg calcite (4 to ≈ 30 mol%), as low Mg calcite (≤ 4 mol%) and to a minor extent as aragonite (≤ 0.6 mol%). Marine organisms produce a wide range of $\delta^{26}\text{Mg}$ values from -5 to -1 ‰ that are species dependent (Hippler et al. 2009; Li et al. 2012). Since the extent of Mg substitution in CaCO_3 is temperature dependant, Mg/Ca ratios are used as a thermometer for oceanic temperatures. The Mg/Ca temperature dependence, however, does not play

a major play in determining Mg isotope ratios, the observed variability can instead be attributed to mineralogy (Hippler et al. 2009). Mg isotope fractionations between carbonates and water follows the sequence aragonite < dolomite < magnesite < calcite (Saenger and Wang 2014).

Vital effects in low-Mg calcite organisms exhibit no clear temperature dependence affecting the Mg isotope composition (Wang et al. 2013a, b). Most recent benthic and planktonic foraminifera show nearly identical $\delta^{26}\text{Mg}$ ratios (Pogge von Strandmann 2008), making them suitable for investigating past isotopic variations of ocean water. Pogge von Strandmann et al. (2014) measured Mg isotopes from single-species planktonic foraminifera of the past 40 Ma and concluded that seawater Mg has changed from $\delta^{26}\text{Mg}$ of -0.83‰ at present to 0‰ at 15 Ma.

2.7.4.1 Cave Carbonates

Evidence for near equilibrium fractionation has been presented for low-Mg calcite speleothems (Galy et al. 2002). Mg isotope fractionation between speleothems and associated drip waters give a characteristic difference between both phases, which might indicate near equilibrium conditions. Buhl et al. (2007) argued that isotope equilibrium alone cannot explain the Mg isotope data from speleothems. Immenhauser et al. (2010) presented a complete data set of Mg isotopes on solid and liquid phases from a cave. They demonstrated that Mg isotope fractionations depend on a complex interplay of solution residence times, precipitation rates and adsorption effects.

2.7.5 Plants

Magnesium is an essential plant nutrient that is central to photosynthesis. Black et al. (2008) investigated the Mg isotope distribution in wheat and observed a slight enrichment of the whole plant in ^{25}Mg and ^{26}Mg relative to the nutrient solution. These results have been confirmed by Boulou-Bi et al. (2010). Most of the plant Mg is bound in leaves, but the decisive process for the enrichment of ^{26}Mg occurs at the root level. From roots to leaves or shoots a slight ^{26}Mg depletion is observed (Boulou-Bi et al. 2010).

Mg plays a fundamental role in the formation of chlorophyll, in which it is the central ion. The biological process linked to the incorporation of Mg into the chlorophyll molecule induces Mg isotope fractionation, the sign and size of isotope fractionations depend on species and environmental conditions (Black et al. 2006; Ra and Kitagawa 2007; Ra 2010). Ra (2010) observed a 2.4‰ ^{26}Mg variation in phytoplankton from different regions in the northwestern Pacific and related them to different growth rates and phytoplankton heterogeneities.

2.8 Silicon

Silicon has three stable isotopes with the following abundances (Rosman and Taylor 1998):

$$^{28}\text{Si} \quad 92.23 \%$$

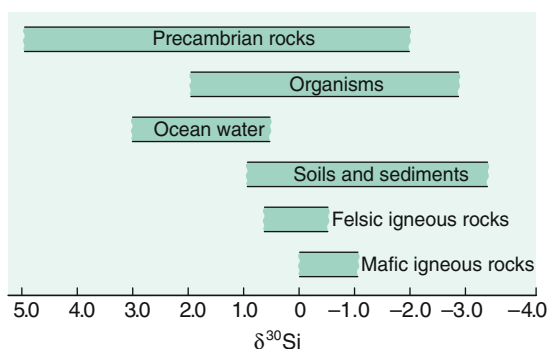
$$^{29}\text{Si} \quad 4.68 \%$$

$$^{30}\text{Si} \quad 3.09 \%$$

Because of its high abundance on Earth, silicon is a very interesting element to be investigated for isotope variations. However, because there is no redox reaction, silicon is always bound to oxygen, relatively small isotope fractionations are to be expected in nature. Early investigations by Douthitt (1982) and more recent ones by Ding (1996) observed a total range of $\delta^{30}\text{Si}$ values in the order of 6 ‰. This range has extended to about 12 ‰ with the lowest $\delta^{30}\text{Si}$ value of -5.7 ‰ in siliceous cements (Basile-Doelsch et al. 2005) and the highest of $+6.1$ ‰ for rice grains (Ding et al. 2006).

Silicon isotope ratios have been generally measured by fluorination (Douthitt 1982; Ding 1996). However, the method is time consuming and potentially hazardous, therefore, more recently MC-ICP-MS techniques have been introduced (Cardinal et al. 2003; Engstrom 2006). Chmeleff et al. (2008) have shown that a UV-femtosecond laser ablation system coupled with MC-ICP-MS gives $\delta^{29}\text{Si}$ - and $\delta^{30}\text{Si}$ -values with very high precision. Determinations with SIMS have been carried out by Robert and Chaussidon (2006), Heck et al. (2011) and others. Independent of the method used, the standard generally is NBS-28 quartz. Figure 2.20 summarizes the naturally occurring silicon isotope variations.

Fig. 2.20 $\delta^{30}\text{Si}$ -values of important geological reservoirs



2.8.1 High-Temperature Fractionations

A number of studies have estimated the $\delta^{30}\text{Si}$ -value of the bulk silicate earth as to be -0.29‰ (Fitoussi et al. 2009; Savage et al. 2010, 2014; Arnytage et al. 2011; Zambardi et al. 2013). This value is identical with the Moon, but isotopically heavier than all types of meteorites. The difference is best explained by Si fractionation during earth's core formation. High pressure, high temperature experiments by Shahar et al. (2009) indicated a 2‰ fractionation between metal and silicate melts (see discussion on p. 211). Similar findings have been reported by Ziegler et al. (2010) by measuring silicon isotope fractionations between Si in metal and silicates in enstatite achondrites. Using a continuous accretion model, the Si isotope fractionation can be used to constrain the amount of Si that entered the Earth's core (Chakrabarti and Jacobsen 2010; Zambardi et al. 2013). Estimated percentages vary somewhat depending on model assumptions, but generally are between 6 and 12 %. However, as demonstrated by Huang et al. (2014), Si isotope fractionations decrease with increasing pressure, thus silicon isotope fractionations obtained experimentally at relatively low pressures may not be applicable to the high pressure conditions of core formation.

Huang et al. (2014) furthermore showed that equilibrium isotope fractionations among mantle minerals are negligible, but may become significant between minerals with different Si coordination numbers, such as Mg-perovskite in 6-coordination and olivine in 4-coordination.

No differences in Si isotope composition are observed between ultramafic rocks and basalts indicating no isotope fractionation during partial melting (Savage et al. 2014). As shown on rocks from the Hekla volcano, Iceland, magmatic differentiation may cause Si isotope fractionation (Savage et al. 2011). $\delta^{30}\text{Si}$ -values become progressively enriched with increasing SiO_2 contents.

Felsic rocks and minerals exhibit small, but systematic ^{30}Si variations increasing with the silicon contents of igneous rocks and minerals. The order of ^{30}Si enrichment in minerals is quartz, feldspar, muscovite and biotite, which is consistent with the order of ^{18}O enrichment. Thus felsic igneous rocks are slightly heavier than mafic igneous rocks.

2.8.2 Cherts

Silicon isotope ratios of quartzites and sandstones are in the range of felsic magmatic and metamorphic rocks reflecting their detrital derivation (Andre et al. 2006). In contrast, microcrystalline quartz from silcretes and clay minerals formed by weathering processes incorporate preferentially light Si isotopes relative to igneous minerals. A wide range of $\delta^{30}\text{Si}$ values from -0.8 to $+5.0\text{‰}$ have been reported for Precambrian cherts (Robert and Chaussidon 2006), much larger than for Phanerozoic cherts. These authors observed a positive correlation of $\delta^{18}\text{O}$ with $\delta^{30}\text{Si}$ values, which they interpreted as reflecting temperature changes in the ocean from about 70 °C

3.5 Ga to about 20 °C 0.8 Ga years ago. In contrast, cherts within BIFs exhibit largely negative $\delta^{30}\text{Si}$ -values from -2.5 to -0.5 ‰ (Andre et al. 2006; Van den Boorn et al. 2010; Steinhöfel et al. 2010) reflecting different sources of silica. These authors argued that variations in $\delta^{30}\text{Si}$ are best explained by mixing between hydrothermal fluids and seawater. Lamina-scale Si isotope heterogeneity within individual chert layers up to 2.2 ‰ may reflect the dynamics of hydrothermal systems.

2.8.3 Chemical Weathering and Mineral Precipitation

Considerable Si isotope fractionation takes place during chemical weathering (Ziegler et al. 2005; Basile-Doelsch et al. 2005; Georg et al. 2006; Cardinal et al. 2010; Opfergelt et al. 2012; Pogge von Strandmann et al. 2014). During dissolution of primary silicate minerals, silicon partitions in about equal proportions into the dissolved phase that is isotopically enriched and into solid secondary phases that are isotopically depleted (Ziegler et al. 2005a, b; Georg et al. 2007). Oelze et al. (2014) demonstrated that preferential adsorption of ^{28}Si on Al-hydroxides may be the cause for the light isotope signature of clay minerals.

Soil-clay mineral formation is, thus, responsible for high $\delta^{30}\text{Si}$ values of continental surface waters and ocean water. For the Yangtze river, Ding et al. (2004) measured a $\delta^{30}\text{Si}$ range from 0.7 to 3.4 ‰, whereas the suspended matter has a more constant composition from 0 to -0.7 ‰. For the Congo, Cardinal et al. (2010) measured low $\delta^{30}\text{Si}$ values close to zero ‰ for small tributaries rich in organic carbon (“black water”) and high $\delta^{30}\text{Si}$ values close to 1 ‰ in large tributaries.

Georg et al. (2009) presented $\delta^{30}\text{Si}$ values of dissolved Si in groundwaters. Of special interest is the observation that $\delta^{30}\text{Si}$ decreases by about 2 ‰ along the groundwater flow path of 100 km deciphering complex Si-cycling, weathering and diagenetic reactions. Thus weathering processes can be regarded as one of the main fractionation mechanism separating silicon isotopes into an isotopically heavy dissolved phase and an isotopically light residue.

2.8.4 Fractionations in Ocean Water

Silicic acid is an important nutrient in the ocean that is required for the growth of mainly diatoms and radiolaria. Silicon incorporation into siliceous organisms is associated with Si isotope fractionation, because ^{28}Si is preferentially removed as the organisms form biogenic silica (de la Rocha et al. 1998, 2003, 2006; Reynolds et al. 2006; Hendry et al. 2010; Egan et al. 2012).

De la Rocha et al. (1997, 1998) observed a 1 ‰ fractionation between dissolved and biogenic silica during opal formation by marine diatoms that does not vary with temperature, at least not among the three species of diatoms investigated by de la Rocha. Varela et al. (2004) observed depletions in ^{30}Si between 1.1 and 1.9 ‰ independent of temperature, pCO_2 or species. Recent culture experiments on polar diatom species by Sutton et al. (2013), however, yielded species dependent

fractionation with silicon isotope values from -0.5 to -2.1 ‰. An increase in opal formation by diatoms results in more positive $\delta^{30}\text{Si}$ -values, whereas a decrease results in more negative δ -values. In this manner variations in ^{30}Si contents of diatoms may provide information on changes of oceanic silicon cycling (De la Rocha et al. 1998).

In early studies it was assumed that dissolution of diatoms—the majority of biogenic silica produced in surface water dissolves before the particles have reached the ocean floor—does not fractionate Si isotopes. However, as shown by Demarest et al. (2009) dissolved silicon is ca 0.55 ‰ depleted in ^{30}Si relative to biogenic SiO_2 . Thus dissolution acts in the opposite sense to production and reduces the net silicon fractionation considerably.

Diatoms as surface dwellers give a surface water signal only. Sponges, however, can be found throughout the water column. The $\delta^{30}\text{Si}$ of sponges is thus a potential proxy to quantify changes in oceanic Si concentrations (Hendry et al. 2010; Wille et al. 2010). As shown by these authors ^{30}Si fractionations during biosilification of sponges depends on silica concentrations in sea water with larger ^{30}Si depletions as silica concentrations increase. Thus, $\delta^{30}\text{Si}$ values of fossil silicified sponges may be used as a proxy for the reconstruction of palaeo Si-concentrations during the past (Hendry et al. 2010; Wille et al. 2010).

2.8.5 Plants

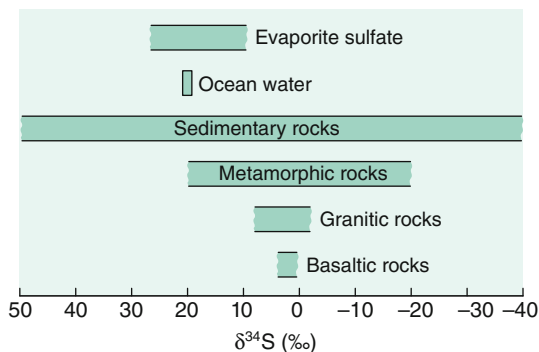
Silicon is an important element for vascular plants favouring growth. Silicon is taken up by terrestrial plants from soil solution, transported into the xylem and deposited as hydrated amorphous silica to form phytoliths that are restored to the soil by decomposition of plant material. Already Douthitt (1982) noted that Si uptake by plants leads to Si isotope fractionation. Plants preferentially incorporate the light Si isotopes; Si concentrations and $\delta^{30}\text{Si}$ -values increase from soil and roots through the stem and leaves. $\delta^{30}\text{Si}$ values range from 1.3 to 6.1 ‰ (Ding et al. 2005, 2008) with large interplant fractionations of 3.5 ‰ between low values in roots and high values in leaves and corn.

2.9 Sulfur

Sulfur has four stable isotopes with the following abundances (De Laeter et al. 2003).

^{32}S :	95.04 ‰
^{33}S :	0.75 ‰
^{34}S :	4.20 ‰
^{36}S :	0.01 ‰

Fig. 2.21 $\delta^{34}\text{S}$ -values of important geological reservoirs (Fig. 2.20, 6th edition, p. 72)



Sulfur is present in nearly all natural environments. It may be a major component in ore deposits, where sulfur is the dominant nonmetal, and as sulfates in evaporites. It occurs as a minor component in igneous and metamorphic rocks, throughout the biosphere in organic substances, in marine waters and sediments as both sulfide and sulfate. These occurrences cover the whole temperature range of geological interest. Thus, it is quite clear that sulfur is of special interest in stable isotope geochemistry.

Thode et al. (1949) and Trofimov (1949) were the first to observe wide variations in the abundances of sulfur isotopes. Variations on the order of 180 ‰ have been documented with the “heaviest” sulfates having $\delta^{34}\text{S}$ -values of greater than +120 ‰ (Hoefs, unpublished results), and the “lightest” sulfides having $\delta^{34}\text{S}$ -values of around -65 ‰. Some of the naturally occurring S-isotope variations are summarized in Fig. 2.21. Reviews of the isotope geochemistry of sulfur have been published by Rye and Ohmoto (1974), Nielsen (1979), Ohmoto and Rye (1979), Ohmoto (1986), Ohmoto and Goldhaber (1997), Seal et al. (2000), Canfield (2001a) and Seal (2006).

For many years the reference standard commonly referred to is sulfur from troilite of the Canyon Diablo iron meteorite (CDT). As Beaudoin et al. (1994) have pointed out, the original CDT is not homogeneous and may display variations in ^{34}S up to 0.4 ‰. Therefore a new reference scale, Vienna-CDT (V-CDT) has been introduced by an advisory committee of IAEA in 1993, recommending an artificially prepared Ag_2S (IAEA-S-1) with a $\delta^{34}\text{S}_{\text{VCDT}}$ of -0.3 ‰ as the new international standard reference material.

2.9.1 Methods

The gas conventionally used for gas-source mass-spectrometric measurement is SO_2 . The introduction of on-line combustion methods (Giesemann et al. 1994) has reduced multistep off-line preparations to one single preparation step, namely the combustion in an elemental analyzer. Sample preparations have become less

dependent on possibly fractionating wet-chemical extraction steps and less time-consuming, thereby reducing minimum sample gas to less than 1 mg.

Puchelt et al. (1971) and Rees (1978) first described a method using SF₆ instead of SO₂ which has some distinct advantages: it has no mass spectrometer memory effect and because fluorine is monoisotopic, no corrections of the raw data of measured isotope ratios are necessary. Comparison of $\delta^{34}\text{S}$ -values obtained using the conventional SO₂ and the laser SF₆ technique has raised serious questions about the reliability of the SO₂ correction for oxygen isobaric interferences (Beaudoin and Taylor 1994). Therefore the SF₆ technique has been revitalized (Hu et al. 2003), demonstrating that SF₆ is an ideal gas for measuring $^{33}\text{S}/^{32}\text{S}$, $^{34}\text{S}/^{32}\text{S}$ and $^{36}\text{S}/^{32}\text{S}$ ratios.

Microanalytical techniques such as laser microprobe (Kelley and Fallick 1990; Crowe et al. 1990; Hu et al. 2003; Ono et al. 2006) and ion microprobe (Chaussidon et al. 1987, 1989; Eldridge et al. 1988, 1993; Kozdon et al. 2010) have become promising tools for determining sulfur isotope ratios.

More recently the use of MC-ICP-MS techniques has been described by Craddock et al. (2008) and Paris et al. (2013). Amrani et al. (2009) developed a MC-ICP-MS method for the analysis of individual sulfur organic compounds. Due to low detection limits, sample sizes are orders of magnitude smaller than for SO₂ and SF₆. MC-ICP-MS requires no chemical pretreatment and allows for simultaneous collection of the individual 4 sulfur isotopes.

2.9.2 Fractionation Mechanisms

Two types of fractionation mechanisms are responsible for the naturally occurring sulfur isotope variations:

- (a) Kinetic isotope effects during microbial processes. Micro-organisms have long been known to fractionate isotopes during their sulfur metabolism, particularly during dissimilatory sulfate reduction, which produces the largest fractionations in the sulfur cycle,
- (b) Various chemical exchange reactions between both sulfate and sulfides and the different sulfides themselves.

2.9.2.1 Equilibrium Reactions

There have been a number of theoretical and experimental determinations of sulfur isotope fractionations between coexisting sulfide phases as a function of temperature. Theoretical studies of fractionations among sulfides have been undertaken by Sakai (1968) and Bachinski (1969), who reported reduced partition function ratios and bond strengths of sulfide minerals and described the relationship of these parameters to isotope fractionation. In a manner similar to that for oxygen in silicates, there is a relative ordering of ^{34}S -enrichment among coexisting sulfide minerals (Table 2.9). Considering the three most common sulfides (pyrite,

Table 2.9 Equilibrium isotope fractionation factors of sulfides with respect to H₂S

Mineral	Chemical composition	A
Pyrite	FeS ₂	0.40
Sphalerite	ZnS	0.10
Pyrrhotite	FeS	0.10
Chalcopyrite	CuFeS ₂	−0.05
Covellite	CuS	−0.40
Galena	PbS	−0.63
Chalcocite	Cu ₂ S	−0.75
Argentite	Ag ₂ S	−0.80

The temperature dependence is given by A/T^2 (after Ohmoto and Rye 1979)

sphalerite and galena) under conditions of isotope equilibrium, pyrite is always the most ³⁴S enriched mineral and galena the most ³⁴S depleted, sphalerite displays an intermediate enrichment in ³⁴S.

The experimental determinations of sulfur isotope fractionations between various sulfides do not exhibit good agreement. The most suitable mineral pair for temperature determination is the sphalerite—galena pair. Rye (1974) has argued that the Czamanske and Rye (1974) fractionation curve gives the best agreement with filling temperatures of fluid inclusions over the temperature range from 370 to 125 °C. By contrast, pyrite—galena pairs do not appear to be suitable for a temperature determination, because pyrite tends to precipitate over larger intervals of ore deposition than galena, implying that these two minerals may frequently not be contemporaneous. The equilibrium isotope fractionations for other sulfide pairs are generally so small that they are not useful as geothermometers. Ohmoto and Rye (1979) critically examined the available experimental data and presented a summary of what they believe to be the best S-isotope fractionation data. These S-isotope fractionations relative to H₂S are shown in Fig. 2.22.

Sulfur isotope temperatures from ore deposits often have been controversial; one of the reasons are strong ³⁴S zonations in sulfide minerals that have been observed by laser probe and ion probe measurements (McKibben and Riciputi 1998).

2.9.2.2 Dissimilatory Sulfate Reduction

Dissimilatory sulfate reduction is conducted by a large group of organisms (over 100 species are known so far, Canfield 2001a), that gain energy for their growth by reducing sulfate while oxidizing organic carbon (or H₂). Sulfate reducers are widely distributed in anoxic environments. They can tolerate temperatures from −1.5 to over 100 °C and salinities from fresh water to brines.

Since the early work with living cultures (Harrison and Thode 1957a, b; Kaplan and Rittenberg 1964) it is well known that sulfate reducing bacteria produce ³²S-depleted sulfide. Despite decades of intense research the factors that determine the magnitude of sulfur isotope fractionation during bacterial sulfate reduction are

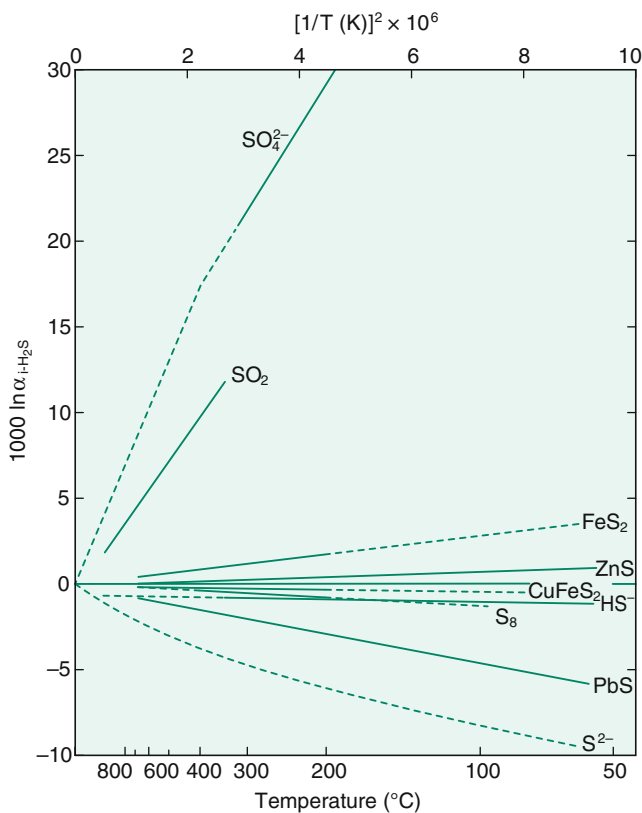


Fig. 2.22 Equilibrium fractionations among sulfur compounds relative to H_2S (solid lines experimentally determined, dashed lines extrapolated or theoretically calculated (after Ohmoto and Rye 1979) (Fig. 2.22, 6th edition, p. 78)

still under debate. The magnitude of isotope fractionation depends on the rate of sulfate reduction with the highest fractionation at low rates and the lowest fractionation at high rates. Kaplan and Rittenberg (1964) and Habicht and Canfield (1997) suggested that fractionations depend on the specific rate ($\text{cell}^{-1} \text{ time}^{-1}$) and not so much on absolute rates ($\text{volume}^{-1} \text{ time}^{-1}$). What is clear, however, is that the rates of sulfate reduction are controlled by the availability of dissolved organic compounds. One parameter which remains unclear is sulfate concentration. While for instance Boudreau and Westrich (1984) argued that the concentration of sulfate becomes important at rather low concentrations (less than 15 % of the seawater value), Canfield (2001b) observed no influence of isotope fractionations on sulfate concentrations for natural populations. Another parameter, that has been assumed to be important is temperature insofar as it regulates in natural populations the sulfate-reducing community (Kaplan and Rittenberg 1964; Brückert et al. 2001). Furthermore differences in fractionation with temperature relate to differences in the

specific temperature response to internal enzyme kinetics as well as cellular properties and corresponding exchange rates of sulfate in and out of the cell of mesophilic sulfate reducing bacteria. Considering different types (including thermophilic) of sulfate-reducers, Canfield et al. (2006), however, found in contrast to earlier belief high fractionations in the low and high temperature range, but lowest fractionations in the intermediate temperature range.

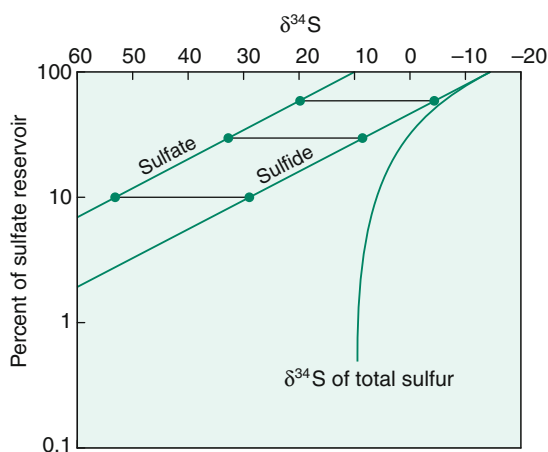
The reaction chain during anaerobic sulfate reduction has been described in detail by Goldhaber and Kaplan (1974). In general, the rate-limiting step is the breaking of the first S–O bond, namely the reduction of sulfate to sulfite. Early laboratory studies with pure cultures of mesophilic sulfate reducing bacteria produced sulfide depleted in ^{34}S by 4 up to 47 ‰ (Harrison and Thode 1957a, b; Kaplan and Rittenberg 1964; Kemp and Thode 1968; McCready et al. 1974; McCready 1975; Bolliger et al. 2001) and for decades this maximum value was considered to be a possible limit for the microbial dissimilatory process (e.g. Canfield and Teske 1996). More recently, sulfur isotope fractionations have been determined from incubations with sediments containing natural populations covering a wide spectrum of environments (from rapidly metabolizing microbial mats to slowly metabolizing coastal sediments; Habicht and Canfield 1997, 2001; Canfield 2001a). Sim et al. (2011) found that the type of organic electron donor is essential in controlling the magnitude of sulfur isotope fractionations of pure culture sulfate reducing bacteria, with complex substrates leading to sulfur isotope discrimination exceeding 47 ‰.

Naturally occurring sulfides in sediments and euxinic waters are commonly depleted in ^{34}S by up to 70 ‰ (Jørgensen et al. 2004), covering the range of experiments with sulfate reducing bacteria (Sim et al. 2011). Recent studies have demonstrated that natural populations are able to fractionate S-isotopes by up to more than 70 ‰ under in situ conditions (Wortmann et al. 2001; Rudnicki et al. 2001; Canfield et al. 2010).

In marine sediments typically 90 % of the sulfide produced during sulfate reduction is reoxidized (Canfield and Teske 1996). The pathways of sulfide oxidation are poorly known, but include biological and abiological oxidation to sulfate, elemental sulfur and other intermediate compounds (Fry et al. 1988). Reoxidation of sulfide often occurs via compounds in which sulfur has intermediate oxidation states (sulfite, thiosulfate, elemental sulfur, polythionates) that do not accumulate, but are readily transformed and can be anaerobically disproportionated by bacteria. Therefore, Canfield and Thamdrup (1994) suggested that through a repeated cycle of sulfide oxidation to sulfur intermediates like elemental sulfur and subsequent disproportionation, bacteria can additionally generate ^{34}S depletions that may add on the isotopic composition of marine sulfides.

Another factor that is of great importance for the preserved sulfur isotope signatures of natural sulfides is whether sulfate reduction took place in a system open or closed with respect to dissolved sulfate. An “open” system has an infinite reservoir of sulfate in which continuous removal from the source produces no detectable loss of material. Typical examples are the Black Sea and local oceanic deeps. In such cases, H_2S is extremely depleted in ^{34}S while consumption and

Fig. 2.23 Rayleigh plot for sulfur isotope fractionations during reduction of sulfate in a closed system. Assumed fractionation factor 1.025, assumed composition of initial sulfate: +10 ‰ (Fig. 2.21, 6th edition, p. 75)



change in ^{34}S remain negligible for the sulfate (Neretin et al. 2003). In a “closed” system, the preferential loss of the lighter isotope from the reservoir has a feedback on the isotopic composition of the unreacted source material. The changes in the ^{34}S -content of residual sulfate and of the H_2S are modeled in Fig. 2.23, which shows that $\delta^{34}\text{S}$ -values of the residual sulfate steadily increase with sulfate consumption (a linear relationship on the log-normal plot). The curve for the derivative H_2S is parallel to the sulfate curve at a distance which depends on the magnitude of the fractionation factor. As shown in Fig. 2.23, H_2S may become isotopically heavier than the original sulfate when about 2/3 of the reservoir has been consumed. The $\delta^{34}\text{S}$ -curve for “total” sulfide asymptotically approaches the initial value of the original sulfate. It should be noted, however, that apparent “closed-system” behavior of covarying sulfate and sulfide $\delta^{34}\text{S}$ -values might be also explained by “open-system” differential diffusion of the different sulfur isotope species (Jørgensen et al. 2004).

Finally it should be mentioned that sulfate is labeled with two biogeochemical isotope systems, sulfur and oxygen. Coupled isotope fractionations of both sulfur and oxygen isotopes have been investigated in experiments (Mizutani and Rafter 1973; Böttcher et al. 2001) and in naturally occurring sediments and aquifers (Fritz et al. 1989; Böttcher et al. 1989; Ku et al. 1999; Aharon and Fu 2000; Wortmann et al. 2001). Böttcher et al. (1998) and Brunner et al. (2005) argued that a characteristic $\delta^{34}\text{S}$ - $\delta^{18}\text{O}$ fractionation slope does not exist, but that the isotope covariations depend on cell-specific sulfate reduction rates and associated oxygen isotope exchange rates with cellular water. Despite the extremely slow oxygen isotope exchange of sulfate with ambient water, $\delta^{18}\text{O}$ in sulfate obviously depend on the $\delta^{18}\text{O}$ of water via an exchange of sulfite with water. Böttcher et al. (1998) and Antler et al. (2013) demonstrated how the fractionation slopes depend on the net sulfate reduction rate: higher rates result in a lower slope meaning that sulfur

isotopes increase faster relative to oxygen isotopes. The critical parameter for the evolution of oxygen and sulfur isotopes in sulfate is the relative difference in rates of sulfate reduction and of intracellular sulfite oxidation.

Recently, Bao (2015) has discussed the triple oxygen isotope composition of sedimentary sulfates, demonstrating that sulfate carries direct signals of ancient atmospheric O₂ and O₃.

2.9.2.3 Thermochemical Reduction of Sulfate

In contrast to bacterial reduction, thermochemical sulfate reduction is an abiotic process with sulfate being reduced to sulfide under the influence of heat rather than bacteria (Trudinger et al. 1985; Krouse et al. 1988). The crucial question, which has been the subject of a controversial debate, is whether thermochemical sulfate reduction can proceed at temperatures as low as about 100 °C, just above the limit of microbiological reduction (Trudinger et al. 1985). There is increasing evidence from natural occurrences that the reduction of aqueous sulfates by organic compounds can occur at temperatures as low as 100 °C, given enough time for the reduction to proceed (Krouse et al. 1988; Machel et al. 1995). S isotope fractionations during thermochemical reduction generally should be smaller than during bacterial sulfate reduction, although experiments by Kiyosu and Krouse (1990) have indicated S-isotope fractionations of 10–20 ‰ in the temperature range of 200–100 °C.

To summarize, bacterial sulfate reduction is characterized by large and heterogeneous ³⁴S-depletions over very small spatial scales, whereas thermogenic sulfate reduction leads to smaller and “more homogeneous” ³⁴S-depletions.

2.9.3 Quadruple Sulfur Isotopes

With respect to quadruple S isotope investigations, a distinction has to be made between large mass-independent S isotope fractionations observed in Archean sulfides and sulfates (Farquhar et al. 2000 and following papers) and much smaller mass-dependent S fractionations being characteristic for biosynthetic pathways. (Farquhar et al. 2003; Johnston 2011; Johnston et al. 2005; Ono et al. 2006, 2007). For long it was thought $\delta^{33}\text{S}$ and $\delta^{36}\text{S}$ values carry no additional information, because sulfur isotope fractionations follow strictly mass-dependent fractionation laws. By studying all sulfur isotopes with very high precision, it was demonstrated that bacterial sulfate reduction follows a mass-dependent relationship that is slightly different from that expected by equilibrium fractionations. On plots $\Delta^{33}\text{S}$ versus $\delta^{34}\text{S}$, mixing of two sulfur reservoirs is non-linear in these coordinates (Young et al. 2002). As a result samples with the same $\delta^{34}\text{S}$ -value can have different $\Delta^{33}\text{S}$ and $\Delta^{36}\text{S}$ values. This opens the possibility to distinguish between different fractionation mechanisms and biosynthetic pathways, even when $\delta^{34}\text{S}$ fractionations are identical (Ono et al. 2006, 2007). Bacterial sulfate reduction shows slightly different fractionation relationships compared to sulfur disproportionation reactions. For

instance, multiple S-isotope measurements of 1.8 Ga sulfates indicate the earliest initiation of microbial S disproportionation (Johnston et al. 2005). In another example, Canfield et al. (2010) demonstrated that S-isotope systematics in an euxinic lake in Switzerland clearly favour microbial reduction as the only reduction pathway. Thus multiple sulfur isotope analyses have great potential in identifying the presence or absence of specific metabolisms in modern environment or may represent a proxy when a particular sulfur metabolism develops in the geologic record.

Large independent S isotope fractionations observed in Archean sulfides and sulfates are a distinctive feature of sedimentary rocks older than 2.4 Ga. It is generally agreed that they indicate the near absence of O_2 and the presence of a reducing gas (likely CH_4 and/or H_2) in the Archean atmosphere. The geologic record of $\Delta^{33}S$ is shown in Fig. 2.24, which is characterized by time dependent magnitudes and signs of MIF-S indicating a temporal structure: ≤ 4 ‰ $\Delta^{33}S$ anomalies in early Archean sulfides, even smaller variations in the mid Archean and very large (≈ 12 ‰) variations in late Archean (see Fig. 2.24). The record of large magnitude $\Delta^{33}S$ values for sulfides terminates abruptly at approximately 2.4 Ga. Besides $\Delta^{33}S$, $\Delta^{36}S$ records also have received a great deal of attention, demonstrating that $\Delta^{36}S$ is preferentially negative down to values lower than -8 ‰.

Experiments that have verified the large $\Delta^{33}S$ and $\Delta^{36}S$ values in the Archean geologic record involve gaseous SO_2 (Farquhar et al. 2000; Claire et al. 2014). The specific chemical reaction that produced the effect observed in Archean samples is unknown, but gas phase reactions involving SO_2 are likely candidates. Farquhar and Wing (2003) and others demonstrated that photolysis of atmospheric SO_2 produces mass-independent S isotope fractionations, if atmospheric O_2 concentrations are very

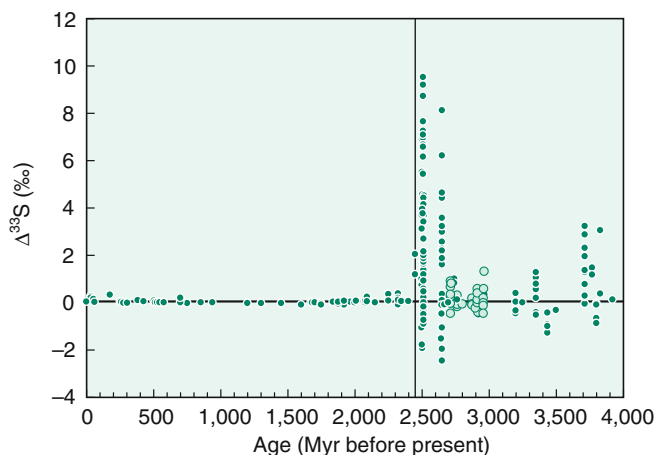


Fig. 2.24 Compilation of $\Delta^{33}S$ versus age for rock samples. Note large $\Delta^{33}S$ before 2.45 Ga, indicated by vertical line, small but measurable $\Delta^{33}S$ after 2.45 Ga (Farquhar et al. 2007) (Fig. 3.29, 6th edition, p. 167)

low. The majority of $\Delta^{33}\text{S}$ and $\Delta^{36}\text{S}$ values scatter around zero, but displays greater variability when $\Delta^{33}\text{S}$ and $\Delta^{36}\text{S}$ are large. Farquhar et al. (2007) and Halevy et al. (2010) attributed these variations to changes in the composition and oxidation state of volcanic sulfur gases. $\Delta^{33}\text{S}/\Delta^{36}\text{S}$ ratios in Archean samples and in products of laboratory photochemical experiments yield characteristic slopes which may be used as fingerprints (Farquhar et al. 2013).

2.10 Chlorine

Chlorine has two stable isotopes with the following abundances (Coplen et al. 2002):

^{35}Cl 75.78 %

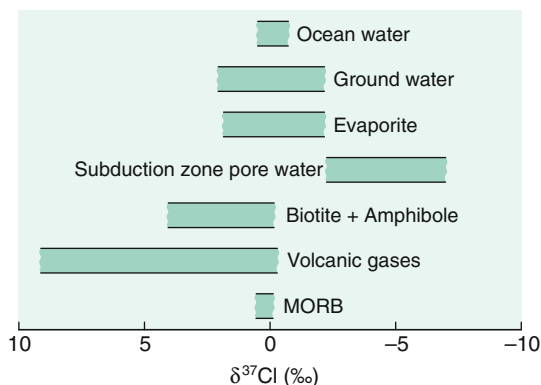
^{37}Cl 24.22 %

Natural isotope variations in chlorine isotope ratios might be expected due to the mass difference between ^{35}Cl and ^{37}Cl as well as to variations in coordination of chlorine in the vapor, aqueous and solid phases. Schauble et al. (2003) calculated equilibrium fractionation factors for some geochemically important species. They showed that the magnitude of fractionations systematically varies with the oxidation state of Cl, but also depends on the oxidation state of elements to which Cl is bound with larger fractionations for 2+ cations than for 1+ cations. Chlorine in silicates appears to be enriched compared to coexisting brines; organic molecules are enriched relative to dissolved Cl^- .

2.10.1 Methods

Measurements of Cl-isotope abundances have been made by different techniques. The first measurements by Hoering and Parker (1961) used gaseous chlorine in the form of HCl. The 81 samples measured exhibited no significant variations relative to the standard ocean chloride. In the early eighties a new technique has been developed by Kaufmann et al. (1984), that uses methylchloride (CH_3Cl). The chloride-containing sample is precipitated as AgCl, reacted with excess methyl iodide, and separated by gas chromatography. The total analytical precision reported is near ± 0.1 % (Long et al. 1993; Eggenkamp 1994; Sharp et al. 2007). The technique requires relatively large quantities of chlorine (>1 mg), which precludes the analysis of materials with low chlorine concentrations. Magenheimer et al. (1994) described a method involving the thermal ionization of Cs_2Cl^+ , which, as argued by Sharp et al. (2007), is very sensitive to analytical artefacts and therefore might lead to erroneous results. In any case both methods are laborintensive and rely on offline chemical conversion reactions. Recent attempts use continuous flow mass-spectrometry (Shouakar-Stash et al. 2005) or use MC-ICPMS techniques (Van Acker et al. 2006).

Fig. 2.25 $\delta^{37}\text{Cl}$ values of important geological reservoirs



δ -values are generally given relative to seawater chloride termed SMOC (Standard Mean Ocean Chloride). Knowledge about chlorine isotope geochemistry has been summarized in a recent book by Eggenkamp (2014). A summary of the observed natural chlorine isotope variations is presented in Fig. 2.25. Ransom et al. (1995) gave a natural variation range in chlorine isotope composition of about 15 ‰ with subduction zone pore waters having $\delta^{37}\text{Cl}$ values as low as -8 ‰ whereas minerals in which Cl substitutes OH have $\delta^{37}\text{Cl}$ values as high as 7 ‰.

2.10.2 Hydrosphere

Chloride (Cl^-) is the major anion in surface- and mantle-derived fluids. It is the most abundant anion in ocean water and in hydrothermal solutions and is the dominant metal complexing agent in ore forming environments (Banks et al. 2000). Despite its variable occurrence, chlorine isotope variations in natural waters commonly are small and close to the chlorine isotope composition of the ocean. This is also true for chlorine from fluid inclusions in hydrothermal minerals which indicate no significant differences between different types of ore deposits such as Mississippi-Valley and Porphyry Copper type deposits (Eastoe et al. 1989; Eastoe and Gilbert 1992).

Relatively large isotopic differences have been found in slow flowing ground-water, where Cl-isotope fractionation is attributed to a diffusion process (Kaufmann et al. 1984; Desaulniers et al. 1986; Kaufmann et al. 1986). Desaulniers et al. (1986) for instance investigated a ground water system, in which chloride diffused upward from saline into fresh water deposits by demonstrating that ^{35}Cl moved about 1.2 ‰ faster than ^{37}Cl .

Cl isotope fractionations between salt minerals and brine have been determined by Eggenkamp et al. (1995), Eastoe et al. (1999, 2007). Halites are enriched by 0.3 ‰ relative to the brine, whereas potassium and magnesium chloride show more or less no fractionation relative to the brine. ^{37}Cl depletions detected in some pore waters have been attributed to processes such as ion filtration, alteration and dehydration

reactions and clay mineral formation (Long et al. 1993; Eggenkamp 1994; Eastoe et al. 2001; Hesse et al. 2006). A pronounced downward depletion of -4‰ in pore waters has been presented by Hesse et al. (2006). Even lower $\delta^{37}\text{Cl}$ -values have been reported in pore waters from subduction-zone environments (Ransom et al. 1995; Spivack et al. 2002). The downward depletion trend might be explained by mixing of shallow ocean water with a deep low ^{37}Cl fluid of unknown origin.

2.10.3 Mantle-Derived Rocks

Controversial results have been reported for chlorine isotopes in mantle-derived rocks. According to Magenheimer et al. (1995) $\delta^{37}\text{Cl}$ -values for MORB glasses show a surprisingly large range. By questioning the findings of Magenheimer et al. (1995), Sharp et al. (2007) argued that the mantle and the crust have very similar isotopic composition. A possible explanation for this apparent discrepancy might be related to analytical artifacts of the TIMS technique (Sharp et al. 2007). Bonifacie et al. (2008) also observed small Cl-isotope variations only in mantle derived rocks. They demonstrated that $\delta^{37}\text{Cl}$ values correlate with chlorine concentrations: Cl-poor basalts have low $\delta^{37}\text{Cl}$ values representing the composition of uncontaminated mantle derived magmas, whereas Cl-rich basalts are enriched in ^{37}Cl being contaminated by ocean water. In contrast to MORB, John et al. (2010) observed with the SIMS technique larger $\delta^{37}\text{Cl}$ variations in OIB glasses which they interpreted as being due to subducting sediments that have developed high $\delta^{37}\text{Cl}$ -values by expelling ^{37}Cl depleted pore fluids.

Barnes et al. (2009) have investigated the serpentinization process in the oceanic lithosphere and interpreted chlorine isotope data to reflect a record of multiple fluid events. Slightly positive $\delta^{37}\text{Cl}$ -values represent typical seawater-hydration conditions under low temperature conditions, negative $\delta^{37}\text{Cl}$ -values result from interaction with porefluids from overlying sediments.

Volcanic gases and associated hydrothermal waters have a large range in $\delta^{37}\text{Cl}$ -values from -2 to $+12\text{‰}$ (Barnes et al. 2006). To evaluate chlorine isotope fractionations in volcanic systems, HCl liquid-vapor experiments performed by Sharp (2006) yield large isotope fractionations of dilute HCl at 100 °C . ^{37}Cl enrichments in fumaroles seem to be due to isotope fractionations between Cl^- in aquatic solution and HCl gas.

Very interesting results have been reported by Sharp et al. (2010) on lunar basalts showing a very large range in $\delta^{37}\text{Cl}$ -values from -1 to $+24\text{‰}$ that have been interpreted to reflect conditions or processes on Moon that do not exist on Earth.

2.10.4 Applications in the Environment

Chlorine isotope studies have been performed to understand the environmental chemistry of anthropogenic organic compounds, such as chlorinated organic solvents or biphenyls. The primary goal of such studies is to identify and quantify

sources and biodegradation processes in the environment. To do this successfully, chlorine isotope values should differ among compounds and manufacturers and indeed the range of reported $\delta^{37}\text{Cl}$ -values is from about -5 to $+6$ ‰ with distinct signatures from different suppliers (van Warmerdam et al. 1995; Jendrzewski et al. 2001).

Perchlorate is another anthropogenic compound, which may contaminate surface and ground waters. The widespread occurrence of perchlorate in the environment makes it necessary to distinguish between a synthetic or a natural origin (Böhlke et al. 2005). The occurrence of natural perchlorate is limited to extremely dry environments, such as the Atacama desert. Synthetic perchlorate is produced by electrolyte oxidation reactions, whereas natural perchlorate is formed by photochemical reactions involving atmospheric ozone. Böhlke et al. (2005) showed that natural perchlorate have the lowest $\delta^{37}\text{Cl}$ -values on Earth, whereas synthetic perchlorate has more “normal” $\delta^{37}\text{Cl}$ -values. During microbial reduction of perchlorate, large kinetic isotope effects have been observed by Sturchio et al. (2003) and Ader et al. (2008), which may document in situ bioremediation.

2.11 Calcium

Calcium has six stable isotopes in the mass range of 40–48 with the following abundances (Taylor and Rosman 1998).

^{40}Ca :	96.94 ‰
^{42}Ca :	0.647 ‰
^{43}Ca :	0.135 ‰
^{44}Ca :	2.08 ‰
^{46}Ca :	0.004 ‰
^{48}Ca :	0.187 ‰

Calcium plays an essential role in biological processes such as the calcification of organisms, and the formation of bones. Its wide natural distribution and the large relative mass difference suggest a large isotope fractionation, which may be caused by mass-dependent fractionations and by radiogenic growth (radioactive decay of ^{40}K to ^{40}Ca , half life of about 1.3 Ga). Felsic Archean rocks with high K/Ca ratios, thus, should show a relative enrichment of ^{40}Ca and, indeed, as demonstrated by Caro et al. (2010), Archean K-rich, Ca-poor rocks show enlarged $^{44}\text{Ca}/^{40}\text{Ca}$ variations.

2.11.1 Analytical Techniques

Early studies on natural Ca isotope variations found no differences or ambiguous results. By using a double-spike technique and by using a mass-dependent law for

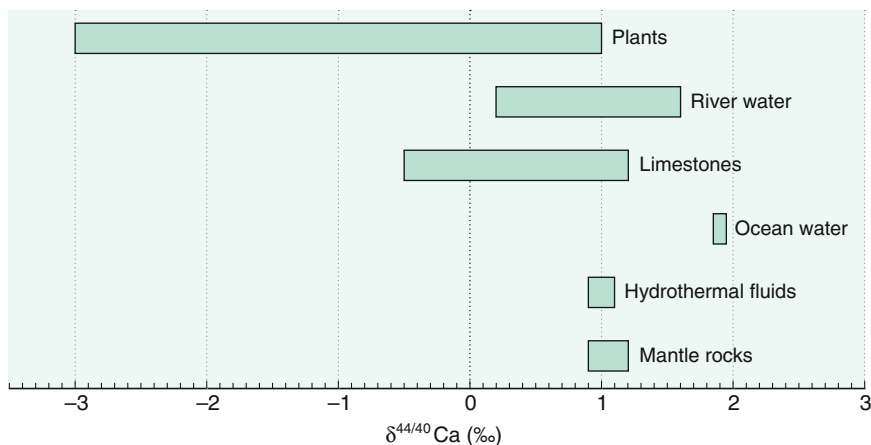


Fig. 2.26 $\delta^{44/40}\text{Ca}$ -values of important geological reservoirs

correction of instrumental mass fractionation, Russell et al. (1978) were the first to demonstrate that differences in the $^{44}\text{Ca}/^{40}\text{Ca}$ ratio are clearly resolvable to a level of 0.5 ‰. More recent investigations by Skulan et al. (1997) and by Zhu and MacDougall (1998), also using the TIMS technique, have improved the precision to about 0.1–0.15 ‰.

MC-ICP-MS techniques have been described by Halicz et al. (1999) using a “hot plasma” and by Fietzke et al. (2004) using a “cool plasma”. SIMS techniques with high spatial resolution and uncertainties of about 0.3 ‰ have been developed by Rollion-Bard et al. (2007) and Kasemann et al. (2008).

Comparing data obtained with different methods and from different laboratories, complications may arise from the use of different δ -values, either $\delta^{44/40}$ or $\delta^{44/42}$, and from the use of different standards. By initiating a laboratory exchange of internal standards, Eisenhauer et al. (2004) have suggested to use NIST SRM 915a as international standard. As the original SRM 915a is not any more available, SRM 915a has been replaced by SRM 915b which is 0.72 ‰ heavier than SRM 915a (Heuser and Eisenhauer 2008). In the following all data are given as $\delta^{44/40}\text{Ca}$ -values. As shown in reviews by DePaolo (2004), Nielsen et al. (2011a, b, c) and Fantle and Tipper (2014), the natural variation range in $\delta^{44/40}\text{Ca}$ -values is about 5 ‰. Figure 2.26 shows natural Ca-isotope variations of important geological reservoirs.

2.11.2 High Temperature Fractionations

Calcium as a lithophile element does not partition into planetary cores, therefore Ca isotopes may reveal genetic links between Earth and meteorites. According to Simon and de Paolo, (2010) and Valdes et al. (2014), Earth, Moon, Mars and differentiated asteroids are indistinguishable from ordinary chondrites, whereas

enstatite chondrites are slightly enriched in heavier Ca isotopes and carbonaceous chondrites are variably depleted in heavier Ca isotopes. Ca isotopes, thus suggest that ordinary chondrites are representative for the material that formed the terrestrial planets.

Huang et al. (2010) and Chen et al. (2014) analysed a suite of terrestrial mantle xenoliths, ocean island basalts, komatiites and carbonatites. Mantle xenoliths vary by about 0.5 ‰ indicating that the mantle is heterogeneous in Ca isotope composition. Ocean island basalts are on average 0.2 ‰ lighter than mantle xenoliths suggesting Ca isotope fractionation during partial melting. During fractional crystallization very limited Ca isotope fractionation seems to occur.

Huang et al. (2010) measured the Ca isotope composition of coexisting clinopyroxene and orthopyroxene in mantle peridotites. $\delta^{44}\text{Ca}$ -values of orthopyroxene are about 0.5 ‰ heavier than clinopyroxene. First principles calculations by Feng et al. (2014) reached very similar conclusions. Combined with data from low-temperature Ca-minerals, Huang et al. (2010) inferred that inter-mineral fractionations are controlled by Ca–O bond strengths. Thus, the Ca-mineral with a shorter Ca–O bond yields a heavier $\delta^{44}\text{Ca}$ -value. Furthermore, these authors estimated that the upper mantle has an average Ca isotope composition slightly higher than the average for basalts. In Hawaiian tholeiites, Huang et al. (2011) observed a 0.3 ‰ variation in $^{44}\text{Ca}/^{40}\text{Ca}$ ratios, which they attributed to recycling of carbonates into the mantle. Besides inter-mineral equilibrium fractionations, high temperature diffusion processes may also affect Ca-isotope fractionations (Richter et al. 2003).

2.11.3 Weathering

Chemical weathering of silicates controls long-term atmospheric CO_2 concentrations coupling the cycles of carbon and calcium. Dissolution of silicates and carbonates does not strongly fractionate Ca isotopes (Fantle and Tipper 2014). Ca ions released during dissolution may be taken up by vegetation, may precipitate as secondary minerals or can be absorbed by clays, oxyhydroxides and humic acids. As shown by Ockert et al. (2013), the absorption of Ca^{2+} on clay minerals favors light Ca isotopes over heavy ones. The largest Ca isotope fractionation in the weathering environment, however, is the uptake by plants.

Ca isotope analysis of rivers represents another approach to identify weathering processes (Tipper et al. 2008, 2010; Fantle and Tipper 2014). From an extensive data compilation, Fantle and Tipper (2014) concluded that the average Ca isotope value of carbonates is 0.60 ‰, whereas average river water has a value of 0.88 ‰ and silicates a value of 0.94 ‰. Since most of the Ca in river water originates from the the dissolution of carbonates and not from silicates, the Ca isotope difference between carbonates and rivers remain unexplained.

2.11.4 Fractionations During Carbonate Precipitation

Calcium carbonates that precipitate from aqueous solutions do not form at isotope equilibrium (DePaolo 2011). Marine carbonates are isotopically depleted in ^{44}Ca relative to seawater (Skulan et al. 1997; Zhu and MacDougall 1998). Experiments on inorganic precipitation of calcite and aragonite (Marriott et al. 2004; Gussone et al. 2003) have demonstrated that Ca isotope fractionation correlates with temperature with an offset of aragonite of about -0.5‰ relative to calcite. During biogenic precipitation, the Ca isotope composition of shells depend on the chemistry of the solution, in which the organisms live and on the process by which Ca is precipitated (Griffith et al. 2008a, b, c). Calcification processes differ among different types of organisms: foraminifera precipitate carbonate in vacuoles from pH-modified seawater, corals pump seawater through various tissues to the site of precipitation. Each step in these processes may cause differences in Ca isotope fractionation.

The magnitude of Ca isotope fractionation during biogenic carbonate precipitation as well as the mechanism—either isotope equilibrium or kinetic effects—remain a matter of debate. Studies by Nägler et al. (2000), Gussone et al. (2005) and Hippler et al. (2006) reported temperature dependent Ca isotope fractionations precipitated in natural environments or under cultured laboratory conditions with a slope of about $0.02\text{‰}/^{\circ}\text{C}$. Temperature dependent fractionations, however, have not been found in all shell secreting organisms (Lemarchand et al. 2004; Sime et al. 2005). Sime et al. (2005) analyzed 12 species of foraminifera and found negligible temperature dependence for all 12 species. These contradictory results indicate a complex physiological control on Ca uptake by calcifying organisms (Eisenhauer et al. 2009).

In the case of dolomite, Holmden (2009) observed a 0.6‰ difference between dolomite and its precursor limestone. Gypsum also preferentially incorporates light Ca compared to dissolved Ca (Harouaka et al. 2014).

2.11.5 Variations with Geologic Time

Zhu and MacDougall (1998) have made the first attempt to investigate the global Ca cycle. They found a homogeneous isotope composition of the ocean, but distinct isotope differences of the sources and sinks and suggested that the ocean is not in steady state. The marine Ca-cycle is characterized by inputs from hydrothermal fluids at oceanic ridge systems and from dissolved Ca delivered by continental weathering and by output through CaCO_3 precipitation, the latter causing the main Ca isotope fractionation. Dissolution of silicate and carbonate rocks during weathering does not strongly fractionate Ca isotopes (Hindshaw et al. 2011). Ca dissolved in rivers shows a very narrow range in Ca isotope composition that is close to the average Ca isotope composition of limestones (Tipper et al. 2010). Hydrothermal solutions to the ocean at ocean ridges are about 1‰ depleted in $\delta^{44/40}\text{Ca}$ values relative to seawater (Amini et al. 2008).

Since the first study of Zhu and MacDougall (1998), several studies have investigated secular changes in the Ca isotope composition of the ocean: De La Rocha and de Paolo (2000b), Fantle and de Paolo (2005) and Fantle (2010) for the Neogene, Steuber and Buhl (2006) for the Cretaceous; Farkas et al. (2007) for the late Mesozoic; and Kasemann et al. (2005a, b) for the Neoproterozoic. Model simulations of the Ca cycle by Farkas et al. (2007) indicated that the observed Ca isotope variations can be produced by variable Ca input fluxes to the oceans. Maximum measured temporal variations in selected age periods are around 1 ‰ in $^{44/40}\text{Ca}$ isotope ratios (see also p. 268 about ocean water history).

High resolution records with 0.3 ‰ excursions for the Permian-Triassic boundary from southern China have been reported by Payne et al. (2010) and by Hinojosa et al. (2012). Shifts in isotope composition could be due to changes in mineralogy (i.e. calcite/aragonite) or to a change in ocean pH-values. By comparing $\delta^{44}\text{Ca}$ -values of conodont apatite with coexisting carbonates, Hinojosa et al. (2012) found a comparable shift in apatite, which argues against a shift in mineralogy, but favors an episode of ocean acidification.

In this context, it is interesting to note, that Griffith et al. (2008a, b, c, 2011) proposed that pelagic barite, containing about 400 ppm Ca, might be an additional recorder of Ca seawater isotope composition through time showing an offset of about 2 ‰ from seawater.

2.11.6 Ca in Plants, Animals and Humans

Vegetation shows the widest range in Ca isotope values, which is larger than variations caused by carbonate precipitation. Studies on higher plants by Page et al. (2008), Wiegand et al. (2005) and Holmden and Belanger (2010) demonstrated systematic Ca isotope fractionations between roots, stemwood and leaves: fine roots yield the lowest $\delta^{44}\text{Ca}$ -values, stemwood are intermediate and leaves have the highest δ -values. Overall variation in ^{44}Ca values from bottom to top in trees is about 0.8 ‰ (Cenki-Tok et al. 2009; Holmden and Belanger 2010). The magnitude of Ca isotope fractionation depends on species and on season (Hindshaw et al. 2013). The preferential uptake of light Ca-isotopes into plants results in an enrichment of Ca in soil solutions. Thus vegetation controls the Ca isotope composition of soil pools (Cenki-Tok et al. 2009).

Experiments under controlled plant growth conditions allow the identification of 3 different Ca isotope fractionation steps (Cobert et al. 2011; Schmitt et al. 2013): (i) preferential ^{40}Ca uptake in the roots, (ii) preferential adsorption of ^{40}Ca on the cell walls during transfer from the roots to the leaves, (iii) additional ^{40}Ca fractionation in the storage organs, which seems to be controlled by the physiology of the plant.

Ca isotope measurements of diet, soft tissues and bone show that bone is considerably lighter than soft tissue and diet. As much as 4 ‰ variation in $^{44}\text{Ca}/^{40}\text{Ca}$ ratios is observed in single organisms (Skulan and DePaolo 1999). Ca isotopes of

bone apatite in animals suggest that Ca isotope composition gets increasingly light as trophic levels increases. Reynard et al. (2010) reported Ca isotope data of modern and archaeological animal and human bones. Sheep at the same location show higher Ca isotope ratios in females than in males which is attributed to lactation by females. Reynard et al. (2010) further demonstrated that human bones are lighter than the local fauna.

2.12 Vanadium

Vanadium has two stable isotopes

^{50}V	0.24 %
^{51}V	99.76 %

Since vanadium exists in four valence states (2^+ , 3^+ , 4^+ , 5^+), it is highly sensitive to reduction-oxidation reactions potentially inducing isotope fractionations.

Nielsen et al. (2011a, b, c) and Prytulak et al. (2011) described a precise MC-ICP-MS technique and reported a $\delta^{51}\text{V}$ isotope variation of 1.2 ‰ for various reference samples. Nielsen et al. (2014) demonstrated that V in the silicate earth is 0.8 ‰ enriched relative to carbonaceous and ordinary chondrites. Although the cause for the enrichment is unknown, Nielsen et al. (2014) postulated that bulk Earth cannot be entirely reconstructed by mixing chondritic meteorites in various proportions. Prytulak et al. (2013) observed a 1 ‰ variation in mafic and ultramafic rocks. Secondary alteration reactions do not appear to induce V isotope fractionations, therefore, V isotopes have the potential to indicate the oxidation state of ancient mantle.

V is enriched in organic matter, especially in crude oils. The analysis of V isotopes in crude oils potentially should be an interesting tool for petroleum geologists. Future vanadium isotope studies certainly will give a more detailed picture of V isotope fractionations.

2.13 Chromium

Chromium has 4 stable isotopes with the following abundances (Rosman and Taylor 1998)

^{50}Cr	4.35 %
^{52}Cr	83.79 %
^{53}Cr	9.50 %
^{54}Cr	2.36 %

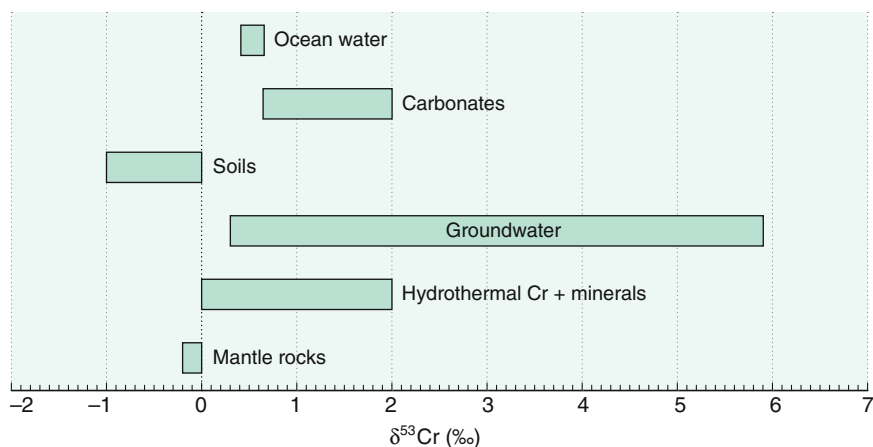


Fig. 2.27 $\delta^{53}\text{Cr}$ -values of important geological reservoirs

Chromium exists in two oxidation states, Cr(III) as a cation Cr^{3+} , and Cr(VI), as an oxyanion (CrO_4^{2-} or HCrO_4^-) having different chemical behaviors: Cr^{3+} is the dominant form in most minerals and in water under reducing conditions, whereas Cr(VI) is stable under oxidizing conditions. Cr(VI) in chromate is highly soluble, mobile and toxic, whereas trivalent chromium, existing as a cation, is largely insoluble and immobile. These properties make Cr isotope investigations very suitable to detect and quantify redox changes in different geochemical reservoirs.

Equilibrium isotope fractionations between Cr(VI) and Cr(III) have been estimated by Schauble et al. (2004), who predicted Cr isotope fractionations >1 ‰ between Cr species with different oxidation states. At 0 °C, Cr isotope fractionations between CrO_4^{2-} and $\text{Cr}(\text{H}_2\text{O})_6^{3+}$ complexes have been calculated to be 7 ‰ with chromate being enriched in ^{53}Cr . However, since isotope equilibration between Cr(VI) and Cr(III) species at low temperatures is slow (Zink et al. 2010), it appears that isotope disequilibrium between Cr-species is common and, therefore, natural Cr isotope fractionations probably are kinetically controlled. Cr isotope variations are measured generally with MC-ICP-MS techniques (Halicz et al. 2008a, b; Schoenberg et al. 2008), $\delta^{53/52}\text{Cr}$ -values are given relative to the NIST SRM 979 standard. Figure 2.27 summarizes average Cr-isotope compositions in important reservoirs.

2.13.1 Mantle Rocks

Mantle xenoliths and ultramafic cumulates have, as first shown by Schoenberg et al. (2008), a $\delta^{53}\text{Cr}$ -value of -0.12 ‰ relative to the certified Cr standard NIST SRM 979 being 0.4 ‰ heavier than various chondritic meteorites (Moynier et al. 2011). The enrichment of the Earth relative to meteorites may be explained by preferential

partitioning of light Cr isotopes into the Earth's core, leaving the mantle enriched in ^{53}Cr . For mantle derived chromites, Farkas et al. (2013) observed a mean $\delta^{53}\text{Cr}$ -value of 0.08 ‰, slightly heavier than for mantle xenoliths possibly suggesting slight Cr fractionations during partial melting. Hydrothermal chromates (crocoites) are considerably enriched with ^{53}Cr contents of up to 2 ‰. During serpentinization of ultramafic rocks, ^{53}Cr will become enriched (Farkas et al. 2013). Thus, oxidative secondary aqueous alteration of ultramafic rocks shifts the primary mantle composition towards heavier ^{53}Cr -values.

2.13.2 Low-Temperature Fractionations

During weathering, oxidation of Cr(III) leads to a ^{53}Cr enrichment in the resulting Cr(VI), leaving soils depleted in ^{53}Cr . Thus, river and ocean water is enriched in heavy Cr-isotopes relative to mantle and crustal rocks indicating Cr isotope fractionation during weathering and transport to the ocean (Bonnand et al. 2013; Frei et al. 2014). Coastal waters are heavier than open ocean waters possibly reflecting in situ reduction of Cr(VI) to Cr(III).

Carbonates encompass the range of Cr-isotopes in seawater (Bonnand et al. 2013). Cr isotopes in marine carbonates, thus, may be a sensitive tracer of weathering of the continental crust as well as of variations of hydrothermal input (Frei et al. 2011).

Frei et al. (2009) used Cr-isotopes to deduce the oxygenation history of the Earth's hydro- and atmosphere. They suggested that the Great Oxidation Event did not lead to a unidirectional increase of oxygen, but instead is better characterized by punctuated fine-scale fluctuations. This view was challenged by Konhauser et al. (2011) arguing that Cr was largely immobile on land till the GOE, but was solubilized in the period that followed. Frei and Polat (2013) interpreted Cr isotope fractionations in 2.0 Ga soils as indicating oxidative weathering on land.

2.13.3 Anthropogenic Cr in the Environment

Extensive industrial use of hexavalent chromate has led to a widespread Cr contamination of soils and groundwater. Reduction of Cr(VI) to Cr(III) may proceed by a variety of abiogenic and microbial processes. All reduction mechanisms induce Cr isotope fractionations with the lighter isotope enriched in the product (Dossing et al. 2011; Sikora et al. 2008). Kitchen et al. (2012) determined experimentally Cr isotope fractionations for Cr-reduction by dissolved Fe(II) up to 4.2 ‰.

Since isotope fractionation during Cr(VI) reduction is little affected by adsorption (Ellis et al. 2004), $^{53}\text{Cr}/^{52}\text{Cr}$ ratios in soils and groundwaters can be used as an indicator of Cr(VI) reduction and pollution. Groundwaters have $\delta^{53}\text{Cr}$ -values ranging from 0.3 to 5.9 ‰ (Ellis et al. 2002, 2004; Berna et al. 2010 and Zink et al. 2010; Izbicki et al. 2012). These authors observed an increase up to 6 ‰ in

$^{53}\text{Cr}/^{52}\text{Cr}$ ratios during the reduction of chromate. In experiments with *Shewanella*, Sikora et al. (2008) observed a Cr isotope fractionation of about 4 ‰ during dissimilatory Cr(VI) reduction. There are other genera of anaerobic and aerobic bacteria that produce comparable isotope fractionations during Cr(VI) reduction (Han et al. 2012). These findings can be applied to quantify Cr(VI) reduction at sites undergoing active remediation.

2.14 Iron

Iron has 4 stable isotopes with the following abundances (Beard and Johnson 1999)

^{54}Fe	5.84 ‰
^{56}Fe	91.76 ‰
^{57}Fe	2.12 ‰
^{58}Fe	0.28 ‰

Iron is the third most abundant element on Earth that participates in a wide range of biotically- and abiotically-controlled redox processes in low- and high-temperature environments. Iron has a variety of important bonding partners and ligands, forming sulfide, oxide and silicate minerals as well as complexes with water. As is well known, bacteria can use Fe during both dissimilatory and assimilatory redox processes. Because of its high abundance and its important role in high and low temperature processes, isotope studies of iron have received the most attention of the transition elements. Since the first investigations on Fe isotope variations by Beard and Johnson (1999), the number of studies on Fe isotope variations has increased exponentially. Reviews on Fe-isotope geochemistry have been given by Anbar (2004a, b), Beard and Johnson (2004), Johnson and Beard (1999), Dauphas and Rouxel (2006) and Anbar and Rouxel (2007). Figure 2.28 summarizes Fe-isotope variations in important geological reservoirs.

2.14.1 Analytical Methods

By using the double-spike SIMS technique, Johnson and Beard (1999) described an analytical procedure with very good precision. Nevertheless, with the introduction of MC-ICP-MS techniques and their ability to measure Fe isotope ratios with little drift, most researchers have concentrated on MC-ICP-MS (Weyer and Schwieters 2003; Arnold et al. 2004a, b; Schoenberg and von Blanckenburg 2005; Dauphas et al. 2009; Craddock and Dauphas 2010; Millet et al. 2012). Fe isotope analysis is highly challenging, because of interferences from $^{40}\text{Ar}^{14}\text{N}^+$, $^{40}\text{Ar}^{16}\text{O}^+$ and $^{40}\text{Ar}^{16}\text{OH}^+$ at masses 54, 56 and 57 respectively. Nevertheless δ -values can be measured routinely with a precision of ± 0.05 ‰ or better (Craddock and Dauphas 2010).

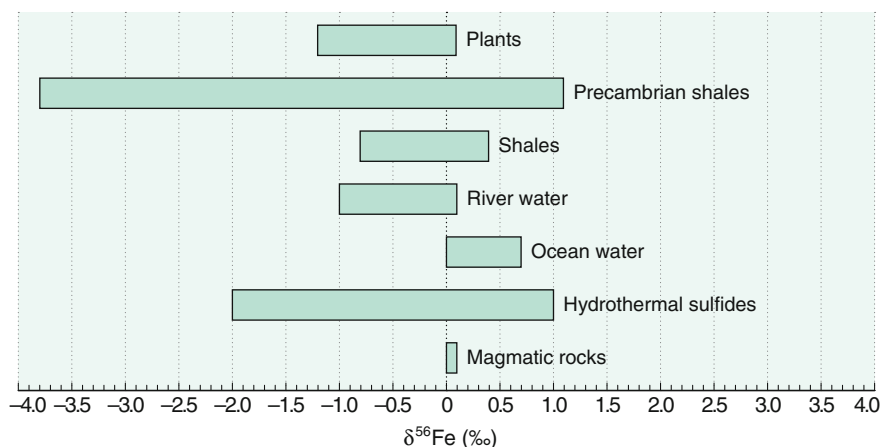


Fig. 2.28 $\delta^{56}\text{Fe}$ -values of important geological reservoirs

Literature data have been presented either in the form of $^{57}\text{Fe}/^{54}\text{Fe}$ or as $^{56}\text{Fe}/^{54}\text{Fe}$ ratios. In the following all data are given as $\delta^{56}\text{Fe}$ values. $\delta^{57}\text{Fe}$ values would be 1.5 times greater than $\delta^{56}\text{Fe}$ values, because only mass-dependent fractionations are expected. Fe isotope ratios are generally reported relative to the IRMM-14 standard, an ultra-pure synthetic Fe metal, or are given to the average composition of various rock types (Beard et al. 2003; Craddock and Dauphas 2010; He et al. 2015). Relative to IRMM-14, igneous rocks have an average composition of $\delta^{56}\text{Fe}$ of 0.09 ‰. The maximum range in $\delta^{56}\text{Fe}$ -values is more than 5 ‰, with low values for sedimentary pyrite and high values in iron oxides from banded iron formations.

2.14.2 Isotope Equilibrium Studies

Equilibrium Fe isotope fractionations for mineral-mineral and mineral-fluid systems have been determined by 3 different approaches: (i) calculations of β -factors based on density functional theory (DFT) (Schauble et al. 2001; Anbar et al. 2005; Blanchard et al. 2009; Rustad and Dixon 2009; Rustad et al. 2010) and (ii) calculations based on Mössbauer spectroscopy and inelastic nuclear resonant X-ray scattering measurements (Polyakov 2007; Polyakov and Soultanov 2011; Dauphas et al. 2012) and (iii) isotope exchange experiments (Skulan et al. 2002; Welch et al. 2003; Shahar et al. 2008; Beard et al. 2010; Saunier et al. 2011; Wu et al. 2011; Frierdich et al. 2014).

Fe isotope fractionations obtained from density functional theory (Blanchard et al. 2009) and from Mossbauer or Inelastic Nuclear Resonant X-ray scattering spectroscopic data (Polyakov et al. 2007; Polyakov and Soultanov 2011) exhibit significant discrepancies. Large discrepancies also exist between calculated and

experimentally determined fractionation factors, especially for mineral-fluid systems. Rustad et al. (2010) achieved better agreement by considering the second hydration shell of Fe dissolved complexes. In a multi direction 3-isotope experimental approach for the $\text{Fe}^{2+}_{\text{aq}}$ —magnetite system, Frierdrich et al. (2014) achieved good agreement with calculated Fe fractionations of Rustad et al. (2010).

First experimental studies at magmatic temperatures, conducted by Schüßler et al. (2007) for equilibrium isotope fractionations between iron sulfide (pyrrhotite) and silicate melt and by Shahar et al. (2008) for fayalite and magnetite demonstrate that Fe isotope fractionations are relatively large at magmatic temperatures and potentially can be used as a geothermometer. Under equilibrium conditions common igneous and metamorphic Fe-minerals should show an order of ^{56}Fe depletion from hematite to magnetite to olivine/pyroxene to ilmenite. For instance, at 800 °C Fe isotope fractionation between magnetite-ilmenite should be around 0.5 ‰ becoming larger with decreasing temperatures. Thus, the pair magnetite-ilmenite potentially may be used as a geothermometer.

Mechanism governing Fe isotope fractionation include precipitation of Fe bearing minerals (Skulan et al. 2002; Butler et al. 2005), isotope exchange between different ligand species (Hill and Schauble 2008; Dideriksen et al. 2008; Wiederhold et al. 2006) and adsorption of dissolved Fe(II) to Fe(III) surfaces (Icopini et al. 2004; Crosby et al. 2007; Jang et al. 2008). Changes in bond partners and/or coordination number also have an effect on isotope fractionation (Hill et al. 2009, 2010), implying that Fe isotope compositions reflect both the redox state and the solution chemistry.

Theoretical calculations and experimental determinations show that Fe(III) bearing phases tend to be enriched in heavy Fe isotopes compared to Fe(II) bearing phases. The largest Fe isotope fractionations have been attributed to redox effects (Johnson et al. 2008). For example, Fe isotope fractionations between Fe(II) and Fe(III) species at 25 °C yield a 2.5–3 ‰ ^{54}Fe depletion in the Fe(II) species. As discussed by Crosby et al. (2005), Fe isotope fractionation results from isotope exchange between Fe(II) and Fe(III) at oxide surfaces explaining why Fe isotope fractionations are very similar for microbial dissimilatory Fe(III) reduction, microbial Fe(II) oxidation and equilibrium between dissolved Fe(II) and Fe(III) species in abiotic systems. This hampers the assertion of Fe isotopes as biosignatures.

2.14.3 Meteorites

Carbonaceous and ordinary chondrites have a uniform bulk Fe isotope composition close to zero ‰ (Craddock and Dauphas 2010; Wang et al. 2013b), whereas the individual Fe components in meteorites are isotopically variable. Chondrules display the largest variation, metals and sulphides show smaller variations (Needham et al. 2009). As shown by Williams et al. (2006) Fe isotope differences between

metal and troilite are in the range of 0.5 ‰—the metal phase being heavier than the sulfide phase troilite, potentially reflecting equilibrium fractionations.

Fe isotopes in meteorites have been used to investigate processes associated with core formation. Iron meteorites are considered to represent remnants of metallic cores of differentiated planetary bodies. Whether core formation fractionates Fe isotopes or not is a matter of debate. Poitrasson et al. (2009) and Hin et al. (2012) experimentally determined no Fe isotope fractionation between Fe–Ni alloy and silicate liquid at temperatures up to 2000 °C.

For the Moon, the bulk iron isotope composition is not well constrained. As shown by Liu et al. (2010a, b), low Ti-basalts have $\delta^{56}\text{Fe}$ values that are 0.1 ‰ lower than high Ti basalts, possibly reflecting differences in mantle sources.

2.14.4 Igneous Rocks

Early studies demonstrated that all terrestrial igneous rocks have homogeneous Fe isotope compositions (Beard and Johnson 1999, 2004). Later studies suggested that igneous processes such as partial melting and crystal fractionation may lead to measurable Fe isotope variations. Weyer et al. (2005) and Weyer and Ionov (2007) found that the Fe isotope composition in mantle peridotites is about 0.1 ‰ lighter than in basalts. Because Fe^{3+} is more incompatible than Fe^{2+} during partial melting and given the fact that Fe^{3+} has higher $\delta^{56}\text{Fe}$ values than Fe^{2+} , liquids should become enriched relative to the solid residue. Dauphas et al. (2009) presented a quantitative model that relates the iron isotope composition of basalts to the degree of partial melting.

Small Fe isotope variations between MORB and OIB have been reported by Teng et al. (2013) that can be explained by fractional crystallization of OIBs. Teng et al. (2008) demonstrated that Fe isotopes fractionate during magmatic differentiation on whole-rock and on crystal scales. They observed that iron in basalts becomes isotopically heavier as more olivine crystallizes, implying that differences in the redox state of Fe play a decisive role. Zoned olivine crystals yield ^{56}Fe isotope fractionations of up to 1.6 ‰, which they interpreted as being due to diffusion between olivines and evolving melt (Teng et al. 2011).

Metasomatism and/or metamorphic/hydrothermal alterations are additional processes that can modify the Fe isotope composition of mantle material (Williams et al. 2005; Weyer and Ionov 2007; Dziony et al. 2014).

In granitic rocks $\delta^{56}\text{Fe}$ values are generally positively correlated with SiO_2 contents (Poitrasson and Freyrier 2005; Heimann et al. 2008). These authors suggested that exsolution of fluids has removed light Fe isotopes causing the enrichment of SiO_2 -rich granitoids. Telus et al. (2012) argued that exsolution alone cannot explain the high $\delta^{56}\text{Fe}$ values in all granitoids, instead fractional crystallization seems to be the major cause of ^{56}Fe enrichment.

2.14.5 Sediments

Marine sediments reflect the average Fe isotope composition of the continental crust, deviations from the mean value are due to biogeochemical processes in the sediments. Under low-temperature conditions the observed natural Fe isotope variations of around 5 ‰ have been attributed to a large number of processes, which can be divided into inorganic reactions and into processes initiated by micro-organisms. Up to 1 ‰ fractionation can result from precipitation of Fe-containing minerals (oxides, carbonates, sulfides) (Anbar and Rouxel 2007). Larger Fe isotope fractionations occur during biogeochemical redox processes, which include dissimilatory Fe(III) reduction (Beard et al. 1999; Icopini et al. 2004; Crosby et al. 2007), anaerobic photosynthetic Fe(II) oxidation (Croal et al. 2004), abiotic Fe (II) oxidation (Bullen et al. 2001) and sorption of aqueous Fe(II) on Fe (III) hydroxides (Balci et al. 2006). Controversy exists whether iron isotope variations observed are controlled by kinetic or equilibrium factors and/or by abiological or microbiological fractionations. This complicates the ability to use iron isotopes to identify microbiological processing in the rock record (Balci et al. 2006). As argued by Johnson et al. (2008) microbiological reduction of Fe^{3+} produces much larger quantities of iron with distinct $\delta^{56}\text{Fe}$ values than abiological processes. Thus a number of studies have interpreted negative $\delta^{56}\text{Fe}$ values in sediments to reflect dissimilatory iron reduction (DIR) (e.g. Bergquist and Boyle 2006; Severmann et al. 2006, 2008, 2010; Teutsch et al. 2009). Coupled Fe and S isotope intergrain variations in pyrite have been used as a proxy for microbial dissimilatory Fe(III) and sulfate reduction (Archer and Vance 2006).

During weathering, Fe is dissolved by ligands and/or bacteria. Fe isotope fractionation may occur during Fe mobilization by Fe reduction or ligand-promoted dissolution or during immobilization of Fe oxy/hydroxides (Fantle and de Paolo 2005; Yesavage et al. 2012 and others). $\delta^{56}\text{Fe}$ values of bulk and HCl-extractable Fe become isotopically lighter as the extent of weathering proceeds; exchangeable Fe is more depleted in ^{56}Fe than Fe in ironhydroxides.

In summary, negative $\delta^{56}\text{Fe}$ -values in sedimentary rocks may reflect ancient DIR (Yamaguchi et al. 2005; Johnson et al. 2008), other studies have, however, favored abiological processes for the occurrence of negative Fe isotope values (Rouxel et al. 2005; Anbar and Rouxel 2007; Guilbaud et al. 2011). Especially large iron isotope fractionations have been found in Proterozoic and Archean banded iron formations (BIFs) and shales (Rouxel et al. 2005; Yamaguchi et al. 2005). In particular BIFs have been used to reconstruct Fe cycling through Archean oceans and the rise of O_2 (atm) during the Proterozoic (see discussion under Sect. 3.8.4 and Fig. 3.30). The pattern shown in Fig. 3.30 distinguishes three stages of Fe isotope evolution, which might reflect redox changes in the Fe cycle (Rouxel et al. 2005). Interplays of the Fe-cycle with the C- and S-record might reflect changing microbial metabolisms during the Earth's history (Johnson et al. 2008).

2.14.6 Ocean and River Water

Dissolved and particulate iron in water occur not only in two oxidation states but in a wide range of chemical species that interact by adsorption/desorption, precipitation/dissolution processes. All these processes potentially fractionate Fe isotopes that may modify the iron isotope composition of waters.

Iron in the ocean is an important micronutrient; the growth of phytoplankton is often limited by low Fe concentrations. Because of its very low concentration, the Fe isotope composition of ocean water is not easily determined. Radic et al. (2011) and John and Adkins (2012) were among the first presenting dissolved and particulate Fe isotope data in depth profiles from the Pacific and Atlantic. Water profiles characterized by positive $\delta^{56}\text{Fe}$ values mainly reflect the continental input with slight transformations in the water column. John and Adkins (2012) demonstrated that dissolved iron in the upper 1500 m is homogeneous with $\delta^{56}\text{Fe}$ values between 0.30 and 0.45 ‰, whereas in the deeper ocean $\delta^{56}\text{Fe}$ -values increase to 0.70 ‰.

Rivers rich in clastic suspended detrital material, like the white waters of the Amazon have a Fe isotope composition close to the continental crust (Poitrasson et al. 2014). Rivers rich in organic material contain a large portion in dissolved Fe form and are depleted in heavy Fe isotopes with significant annual variations (Dos Santos Pinheiro et al. 2014).

Fluids in diagenetic systems are variable in Fe isotope composition with a preferential depletion in ^{56}Fe (Severmann et al. 2006) reflecting the interaction of Fe^{3+} with Fe^{2+} during bacterial iron and sulfate reduction. Processes dominated by sulfate reduction produce high $\delta^{56}\text{Fe}$ values in porewaters, whereas the opposite occurs when dissimilatory iron reduction is the major pathway (Severmann et al. 2006). Fe isotope compositions of pore fluids may reflect the extent of Fe recycling during early diagenesis (Homoky et al. 2011). Fe(II) in pore waters, formed by bacterial Fe(III) reduction, may be reoxidized during sediment suspension events. The resulting fine grained isotopically light FeOOH may be transported back to the deep ocean, a process that has been termed “benthic iron shuttle” (Severmann et al. 2008).

2.14.7 Plants

Although sufficient supply of Fe is essential for all living organisms, iron is one of the most limiting nutrients, because iron in soils exists predominantly in the nearly insoluble Fe (III) form. Therefore, higher plants developed different strategies to make iron available. Guelke and von Blanckenburg (2007) presented evidence that Fe isotope signatures in plants reflect two different strategies that plants have developed to incorporate Fe from the soil. Group I plants induce chemical reactions in the rhizosphere and reduce iron before uptake by incorporating light isotopes in the roots with further depletion during transport to leaves and seeds. Group II plants

transport Fe(III) complexes into plant roots via a specific membrane transport system that do not fractionate Fe relative to Fe in soils (Guelke et al. 2010; Guelke-Stelling and von Blanckenburg 2012). As shown by Kiczka et al. (2010) Fe isotopes may fractionate during remobilization of Fe from old into new plant tissues which may change the Fe isotope composition of leaves and flowers over the season.

2.15 Nickel

Nickel can occur in oxidation states from 4+ to 0, but the 2+ state is essentially the only natural oxidation state. Thus, redox controlled reactions do not play an important role, but instead chemical precipitation, adsorption in aqueous systems and crystallization of Ni-sulfides in magmatic systems might induce fractionations. Since nickel is a bioessential trace element, playing vital roles in enzymes, biological processes also might cause isotope fractionations.

Ni has five stable isotopes

^{58}Ni 68.08

^{60}Ni 26.22

^{61}Ni 1.14

^{62}Ni 3.63

^{64}Ni 0.93

Ni isotopes generally are reported as $\delta^{60/58}\text{Ni}$ values, Gueguen et al. (2013) described an analytical procedure for Ni isotope determinations and determined Ni isotope ratios for various geological reference materials.

2.15.1 Meteorites and Mantle Derived Rocks

The amount of published Ni isotope data is small. First measurements by Cameron et al. (2009) indicated that Ni isotope variations in the mantle and the continental crust are negligible. More recently, Gueguen et al. (2013) and Hofmann et al. (2014) reported Ni isotope fractionations up to 1 ‰ among komatiites and associated Ni-sulfide mineralisations, the latter being depleted in heavy Ni isotopes.

In the metal phase of meteorites, Ni isotopes fractionate between kamacite (Fe-rich phase) and taenite (Ni rich phase), the former being isotopically heavier than the latter (Cook et al. 2007). To investigate potential Ni isotope fractionation between core and mantle, Lazar et al. (2012) determined Ni isotope fractionations between Ni metal and Ni talc silicate. Since the metal has been found to be enriched in the light Ni isotopes, they suggested that Ni isotope fractionations might have occurred during Earth's core segregation.

2.15.2 Water and Organisms

Large fractionations have been observed in the ocean and in organisms. Fujii et al. (2011) investigated theoretically and experimentally Ni isotopes fractionations between inorganic Ni-species and organic ligands and observed Ni isotope fractionations up to 2.5 ‰ controlled by organic ligands.

Dissolved Ni compounds in rivers vary by about 1 ‰ (Cameron and Vance 2014), and are heavier than average continental rocks. Ni dissolved in the ocean has a mean $\delta^{60}\text{Ni}$ -value of 1.44 ‰ (Cameron and Vance 2014) being heavier than riverine Ni. No Ni isotope difference between surface and deep ocean water has been observed.

Gall et al. (2013) observed Ni isotope enrichment of Fe/Mn crusts relative to continental crust and concluded that weathering is accompanied by Ni isotope fractionation resulting in rivers and oceans being isotopically heavy. A depth profile through a sediment core displays large Ni isotope fractionations which might indicate variations in ocean water composition. In another example, Porter et al. (2014) reported Ni isotope variations between 0.15 and 2.5 ‰ in sediments rich in organic carbon. They argued that variable Ni isotope values are controlled by differences in oceanic sources.

Ni plays an essential role in the metabolism of methanogenic archaea. Biological uptake during methanogenic growth produces substantial Ni isotope fractionations resulting in isotopically light cells and heavy residual media (Cameron et al. 2009). As postulated by these authors biological fractionations of Ni may provide a tracer for elucidating the nature of early life.

2.16 Copper

Copper occurs in two oxidation states, Cu^+ and Cu^{++} and rarely in the form of elemental copper. The major Cu-containing minerals are sulfides (chalcopyrite, bornite, chalcocite and others), and, under oxidizing conditions, secondary copper minerals in the form of oxides and carbonates. Cu(I) is the common form in sulfide minerals, whereas Cu(II) is dominant in aqueous solution. Copper is a nutrient element, although toxic for all aquatic photosynthetic microorganisms. Copper may form a great variety of complexes with very different coordinations such as square, trigonal and tetragonal complexes. These properties are ideal prerequisites for relatively large isotope fractionations.

Copper has two stable isotopes

^{63}Cu 69.1 %

^{65}Cu 30.9 %.

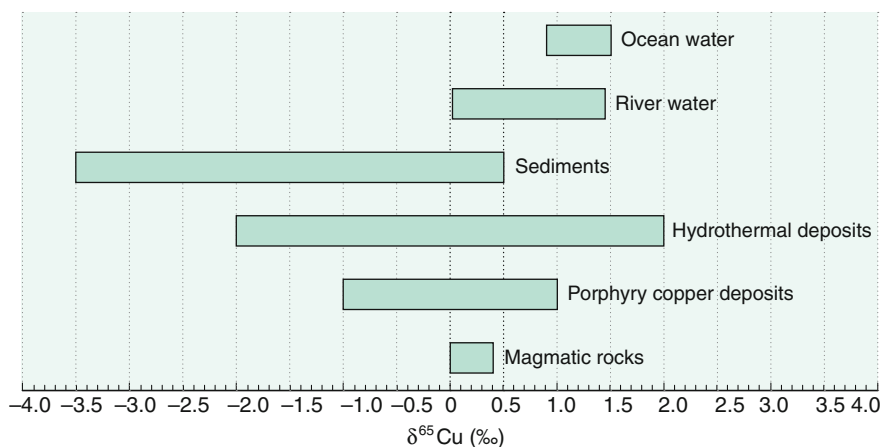


Fig. 2.29 $\delta^{65}\text{Cu}$ -values of important geological reservoirs

Early work of Shields et al. (1965) using the TIMS technique has indicated a total variation of ~ 12 ‰ with the largest variations in low temperature secondary minerals. Later studies using laser-ICP-MS techniques, by Maréchal et al. (1999), Maréchal and Albarede (2002), Zhu et al. (2002), Ruiz et al. (2002), observed a variation range of nearly 10 ‰, which is larger than for Fe. Most samples so far analysed, however, vary between $\delta^{65}\text{Cu}$ values from +2 to -2 ‰ (see Fig. 2.29). The commonly used Cu standard NIST SRM 976 is no longer available, new certified reference materials are ERM-AE633 and ERM-AE647 (Möller et al. 2012).

2.16.1 Low-Temperature Fractionations

Low-temperature processes are the major source of Cu isotope variations; the main processes are: (i) variation of redox conditions, (ii) adsorption on mineral surfaces and organic matter (Pokrovsky et al. 2008; Balistrieri et al. 2008), (iii) inorganic and organic complexation to ligands (Pokrovsky et al. 2008), (iv) biological fractionation by plants and micro-organisms (Weinstein et al. 2011).

Experimental investigations have demonstrated that redox reactions between Cu (I) and Cu(II) species are the principal process that fractionates Cu isotopes (Ehrlich et al. 2004; Zhu et al. 2002). During precipitation of copper without redox change the heavier Cu isotope is preferentially incorporated, however, during Cu(II) reduction precipitated Cu(I) species are 3–5 ‰ lighter than dissolved Cu(II) species. Pokrovsky et al. (2008) observed experimentally a change in sign of Cu isotope fractionations during adsorption from aqueous solutions depending on the kind of surface, either organic or inorganic: on biological cell surfaces a depletion of ^{65}Cu , whereas on hydroxide surfaces an enrichment of ^{65}Cu is observed. In

contrast to abiotic reactions, bacteria preferentially incorporate the lighter Cu isotope into their cells, regardless of experimental conditions (Navarette et al. 2011).

During oxidative weathering of copper rich sulphides, soils become isotopically depleted in ^{65}Cu while porewaters are isotopically enriched (Mathur et al. 2012). Cu isotopes in rivers and seawater indicate that particle-bound Cu are isotopically lighter than dissolved Cu species (Vance et al. 2008). Dissolved Cu in ocean water is heavier than the dissolved riverine input which may be caused by scavenging of light Cu to particulate material, preferentially to Fe–Mn oxides (Vance et al. 2008; Little et al. 2014).

2.16.2 Variations in Ore Deposits

Cu isotopic fractionations at magmatic temperatures appear to be negligible. By analysing native copper grains and whole rock copper in peridotite, Ikehata and Hirata (2012) reported Cu isotope values close to zero ‰ with no differences between Cu metal grains and whole rock copper; thus the Cu isotope composition of mantle and crust appear to be close to zero ‰ (Li et al. 2009a, b).

Various types of Cu-ore deposits have been investigated (Larson et al. 2003; Rouxel et al. 2004a, b; Mathur et al. 2005, 2010; Markl et al. 2006; Li et al. 2010). Early studies showed very limited Cu-isotope variations at high temperatures, but later studies by Maher and Larson (2007) and Li et al. (2010) demonstrated that variations of up to 4 ‰ may occur in porphyry copper deposits. Individual deposits show characteristic Cu isotope zonations that may be caused by fractionations between sulfide, brine and vapour during copper precipitation.

The magnitude of isotope fractionation in copper sulfides increases with secondary alteration and reworking processes (i.e. Markl et al. 2006). Thus copper isotope ratios may be used to decipher details of natural redox processes, but hardly can be used as reliable fingerprints for the source of copper because the variation caused by redox processes within a single deposit is usually much larger than the inter-deposit variation. Experiments by Maher et al. (2011) indicated that the magnitude of Cu-isotope fractionation depend on the pH of the mineralizing fluid and the partitioning of Cu between vapor and liquid. This means that Cu isotope fractionation depend on the physico-chemical conditions during Cu-precipitation. Heavier isotope compositions in supergene Cu minerals and a lighter isotope signature in the leach cap and oxidation zone of an ore deposit can be used as a tool for exploration.

On sites contaminated by acid mine drainage, Borrok et al. (2008) and Kimball et al. (2009) demonstrated systematic copper isotope fractionations between ore minerals and stream water that may be used for ore-prospecting.

2.16.3 Variations in Plants

Copper is an essential micronutrient for plant growth. Cu isotopes may be used to elucidate Cu uptake. Studies by Weinstein et al. (2011), Jouvin et al. (2012) and Ryan et al. (2013) demonstrated that different uptake strategies lead to different Cu isotope fractionations in plants. Tomatoe and oat grown under controlled solution cultures yield Cu isotope fractionations which support previous findings for Fe uptake in strategy 1 and 2 plants (Ryan et al. 2013). Tomatoes preferentially fractionate light ^{63}Cu by about 1 ‰, which is attributed to Cu reduction whereas oat shows minimal Cu fractionation suggesting that Cu uptake and transport is not redox selective.

2.17 Zinc

Zinc has 5 stable isotopes of mass 64, 66, 67, 68 and 70 with the following abundances:

^{64}Zn	48.63 %
^{66}Zn	27.90 %
^{67}Zn	4.10 %
^{68}Zn	18.75 %
^{70}Zn	0.62 %

The JMC-Lyon standard has been the commonly used Zn isotope standard in the past, which however is not longer available. Möller et al. (2012) calibrated IRMM-3702 as the new certified Zn standard, which has a $\delta^{66}\text{Zn}$ -value of 0.29 ‰ relative to the JMC-Lyon standard. In Fig. 2.30 natural Zn isotope variations given as $^{66}\text{Zn}/^{64}\text{Zn}$ ratios are summarized.

The main processes fractionating zinc isotopes are (i) evaporation-condensation processes in which the vapor phase is depleted in the heavier isotopes relative to the solid phase and (ii) sorption processes (Cloquet et al. 2008). Zn isotope fractionation during sorption on Fe hydroxides has been determined by Juillot et al. (2008), Zn-sorption on organic matter has been investigated by Jouvin et al. (2009). The magnitude of isotope fractionation depends on the structure of Zn-complexes on the surface of the solid.

In water, Zn isotope fractionation depends on the ligands present, especially on dissolved phosphate and carbonate. Ab initio calculations of Zn isotope fractionations between aqueous sulfide, chloride and carbonate species by Black et al. (2011) and Fujii et al. (2011) indicate that Zn sulfide complexes are isotopically depleted in heavy Zn isotopes relative to Zn^{2+} and Zn chlorides, whereas carbonates are more enriched than chlorides.

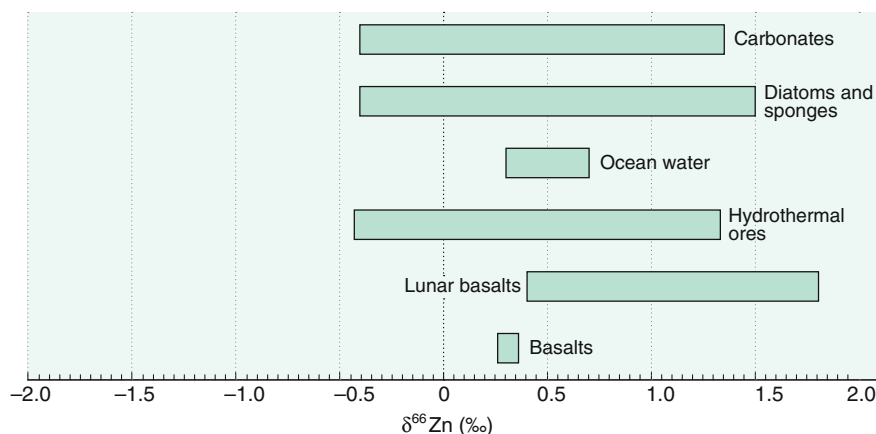


Fig. 2.30 $\delta^{66}\text{Zn}$ -values of important geological reservoirs

2.17.1 Fractionations During Evaporation

Evaporation-condensation processes may cause large fractionations in meteorites (Luck et al. 2005; Wombacher et al. 2008); Paniello et al. (2012) postulated that loss of volatiles in lunar magmatic rocks has lead to an enrichment of heavy Zn isotopes on the Moon relative to Earth.

Significant amounts of Zn may be emitted by degassing from volcanoes. Fumarolic gases and condensates from the Merapi volcano have a relatively large range in Zn isotope compositions. Gaseous Zn samples are enriched in lighter Zn isotopes whereas condensates are enriched in the heavier isotopes (Toutain et al. 2008).

2.17.2 Variations in Mantle Derived Rocks

Early measurements of the $^{66}\text{Zn}/^{64}\text{Zn}$ ratio in mantle—and crustal derived rocks yielded a small variation of about 1 ‰ (Maréchal et al. 1999, 2000; Maréchal and Albarede 2002). One of the main reasons for this small variability appears to be that Zn in natural environments does not participate in redox reactions. It occurs as Zn^{2+} , except, in rare cases, as $\text{Zn}(0)$ metal which is an anthropogenic contaminant.

Recent measurements by Chen et al. (2013a, b) indicate small Zn isotope variations induced by high-temperature igneous processes. By studying two chemically diverse suites of volcanic rocks from Hawaii and Iceland, Chen et al. (2013a, b) concluded that the Earth's mantle is homogeneous in Zn isotope composition and that the bulk silicate earth has a $\delta^{66}\text{Zn}$ -value of 0.28 ‰. Kilauea basalts show small, but systematic Zn isotope enrichment with increasing degree of differentiation.

2.17.3 Ore Deposits

By analyzing sphalerites from ore deposits, Mason et al. (2005), Wilkinson et al. (2005), Kelley et al. (2009), Gagnevin et al. (2012) and Zhou et al. (2014) observed Zn isotope variations of about 1.5 ‰. These studies indicate that early precipitated sphalerites have higher ^{64}Zn -values than late precipitates. The variations have been related to kinetic fractionations during rapid sphalerite precipitation. Gagnevin et al. (2012) explained relatively large Zn-isotope variations at the millimetre scale by mixing of hot hydrothermal fluids with cool brines containing bacterial sulfide. John et al. (2008) reported relatively large Zn isotope fractionation in hydrothermal vent fluids. Low-temperature fluids have heavier $\delta^{66}\text{Zn}$ -values than high temperature fluids. Cooling of vent fluids leads to precipitation of isotopically light sphalerite causing enrichments of the fluid.

2.17.4 Variations in the Ocean

Zinc is an essential micronutrient for phytoplankton, its concentration is controlled by phytoplankton uptake and remineralization. Light Zn isotopes are preferentially incorporated into phytoplankton organic matter, leaving residual Zn in surface water enriched in Zn isotopes (John et al. 2007; Andersen et al. 2011; Hendry and Andersen 2013). Surface waters have a lighter $\delta^{66}\text{Zn}$ signature than deep waters suggesting that absorption of Zn on particle carries heavy Zn out of surface waters (John et al. 2007a). Thus, biological usage and adsorption onto particles are likely to cause isotope fractionations (Gelabert et al. 2006).

In a depth profile of the upper 400 m of Pacific seawater, Bermin et al. (2006) observed small isotope variations which they interpreted as being due to biological recycling. The bulk isotope composition of dissolved Zn in the ocean below 1000 m is around 0.5 ‰, which is heavier than the input from river water (Little et al. 2014; Balistrieri et al. 2008; Chen et al. 2008; Borrok et al. 2009).

Variations of Zn isotopes in marine carbonates have been interpreted to reflect changes in nutrient availability (Pichat et al. 2003; Kunzmann et al. 2013).

2.17.5 Anthropogenic Contamination

Due to anthropogenic activities, many environmental systems are polluted with zinc. The potential of using zinc isotopes to trace Zn contaminations and atmospheric transport was demonstrated by Cloquet et al. (2008), Sonke et al. (2008), Chen et al. (2008) and Weiss et al. (2007). John et al. (2007) measured the Zn isotope composition of various man-made Zn products. They showed that the range of $\delta^{66}\text{Zn}$ values of industrial products is smaller than of Zn ores indicating Zn isotope homogenization during processing and ore purification.

Chen et al. (2008) measured Zn isotope variations along a transect of the Seine. Variations along the river transect showed an increase in Zn concentrations with

highest values in the region of Paris. Less polluted waters have higher $\delta^{66}\text{Zn}$ -values than polluted ones. Roof leaching in the Paris area is a major Zn source.

By analyzing peat profiles, Weiss et al. (2007) concluded that Zn isotopes have the potential to identify atmospheric sources such as zinc derived from mining and smelting. Biogeochemical processes within peat profiles, however, may complicate the interpretation of the record.

2.17.6 Variations in Plants

Zinc is a vital element for most organisms, it plays an essential role in various biochemical processes. The largest variation of Zn isotopes have been found in land plants (Viers et al. 2007; Weiss et al. 2005). As shown by Moynier et al. (2008) and Viers et al. (2007), Zn isotopes fractionate during incorporation of Zn into roots and during transport within plants. The size of the fractionation is species dependent (Viers et al. 2007) and may depend on the height of the plant. The mechanisms of Zn isotope fractionations are not well understood, but may depend on surface absorption, solution speciation and membrane-controlled uptake.

2.18 Germanium

Because of nearly identical ionic radii, Ge may replace Si in minerals and thus may show isotope fractionation behaviour similar to silicon. However, Ge is generally associated to sulfides where it may substitute Zn and Cu at concentrations of more than 1000 ppm, whereas the average concentrations in the earth's crust is around 1 ppm.

Ge has 5 stable isotopes with the following abundances (Rosman and Taylor 1998):

^{70}Ge	20.84 %
^{72}Ge	27.54 %
^{73}Ge	7.73 %
^{74}Ge	36.28 %
^{76}Ge	7.61 %

Early investigations using the TIMS method had an uncertainty of several ‰. Over the past few years advances have been made with the MC-ICP-MS technique with a long term external reproducibility of 0.2–0.4 ‰ (Rouxel et al. 2006; Siebert et al. 2006a). Even better reproducibility has been performed by Luais (2012).

Li et al. (2009a, b) and Li and Liu (2010) estimated isotope fractionation factors among Ge-bearing phases and predicted that sulfides will be depleted in heavy Ge isotopes relative to Ge-oxides. Based on a few measurements of basalts and granites

Rouxel et al. (2006) concluded that the bulk silicate earth has a homogeneous isotope composition. However, chemical sediments like sponges and authigenic glauconites are enriched in $\delta^{74}\text{Ge}$ by about 2 ‰. This suggests that Ge in seawater—similar to silicon—is isotopically enriched in ^{74}Ge relative to the bulk earth. Ge isotopes thus might offer new insights into the biogeochemistry of the present and past ocean, but more data are needed.

Relatively high Ge concentrations have been reported in coal seams. Qi et al. (2011) observed $\delta^{74}\text{Ge}$ variations of more than 7 ‰ in coals and their combustion products. They showed that coal combustion fractionates Ge isotopes, with soot being more depleted in ^{74}Ge than slags.

2.19 Selenium

Selenium is an essential trace element for animals and humans having a narrow concentration range between sufficiency and toxicity (Schilling et al. 2011). It occurs in four oxidation states that differ in their nutritional and toxic behaviour. Selenium to some extent is chemically similar to sulfur, therefore, one might expect relatively large fractionations of selenium isotopes in nature. Six stable selenium isotopes are known with the following abundances (Coplen et al. 2002)

^{74}Se	0.89 %
^{76}Se	9.37 %
^{77}Se	7.63 %
^{78}Se	23.77 %
^{80}Se	49.61 %
^{82}Se	8.73 %

In general $^{82}\text{Se}/^{76}\text{Se}$ ratios have been measured. Because of the 7 ‰ mass difference between ^{76}Se and ^{82}Se and numerous microbial and inorganic Se redox transformations, interest in selenium isotope studies has grown in recent years.

An early study by Krouse and Thode (1962), using SeF_6 gas, required relatively large quantities of Se, limiting the applications of selenium isotopes. Johnson et al. (1999) developed a double-spike solid-source technique that corrects for fractionations during sample preparation and mass spectrometry, yielding an overall reproducibility of ± 0.2 ‰. This technique brings sample requirements down to submicrogram levels. Even lower Se amounts (10 ng) are required for measurements with the MC-ICP-MS technique (Rouxel et al. 2002) using a commercial Se solution as standard. Carignan and Wen (2007) published $\delta^{82}\text{Se}$ -values relative to the NIST SRM 3149 standard. Figure 2.31 summarizes Se isotope variations in specific reservoirs.

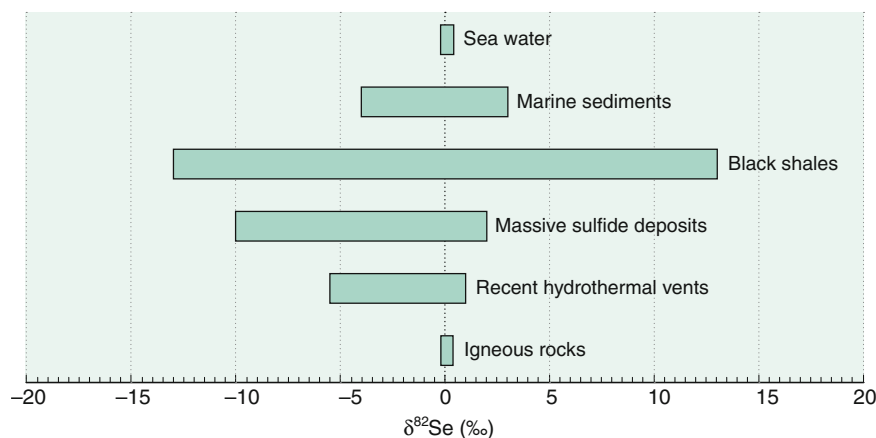


Fig. 2.31 $\delta^{82}\text{Se}$ -values of important geological reservoirs

2.19.1 Fractionation Processes

Selenium oxyanions can be reduced by certain microbes. Reduction proceeds in 3 steps with Se(IV) and Se(0) species as stable intermediates (Johnson 2004). Se isotope fractionation experiments by Herbel et al. (2000) indicate about 5 ‰ fractionations during reduction of selenate to selenite. Little or no fractionation has been observed during selenite sorption, oxidation of reduced Se in soils, or Se volatilization by algae.

Johnson and Bullen (2003) investigated Se isotope fractionations induced by inorganic reduction of selenate by Fe(II)-Fe(III) hydroxide sulfate (“green rust”). The overall fractionation is 7.4 ‰, which is larger than during bacterial selenate reduction. This indicates that the magnitude of Se isotope fractionations depends on the specific reaction mechanism. Mitchell et al. (2013) determined Se isotope fractionations during sorption to iron oxides and to iron sulfides: fractionations to iron oxides are generally very small, whereas fractionations to sulfides are much larger.

2.19.2 Natural Variations

Mantle-derived rocks have a $\delta^{82}\text{Se}$ composition close to zero. Rouxel et al. (2002) measured several igneous rocks and a few iron meteorites, which all lie within 0.6 ‰ of the NIST-SRM 3149 standard. Selenium may become enriched in recent hydrothermal vent sulfides, in which Se may be derived from leaching of igneous rocks or of Se-rich organic sediments. Layton-Matthews et al. (2013) reported a wide range of $\delta^{82}\text{Se}$ values in ancient seafloor hydrothermal deposits. Very negative values are probably due to Se loss from carbonaceous shales during hydrothermal activity.

Although Se and S share similar geochemical behaviour; in the oceanic environment, Se behaves different to S, where it exists as Se VI and Se IV oxyanions

and—most important—as dissolved organic Se. Mitchell et al. (2012) observed in marine shales with low organic carbon content a small range in $\delta^{82}\text{Se}$ values, whereas in black shales with high Se concentrations larger Se isotope variations occur (Wen and Carigman 2011). In a profile of very Se-rich carbonaceous shales, Zhu et al. (2014) observed a range in $^{82/76}\text{Se}$ -values from -14.2 to $+11.4$ ‰, suggesting multiple cycles of oxidation and reduction.

2.20 Bromine

Bromine has two stable isotopes with nearly equal abundances (Berglund and Wieser 2011).

^{79}Br 50.69 %

^{81}Br 49.31 %

The most common natural form of bromine is the bromide anion (Br^-). Although higher oxidation states of bromine exist in nature, little is known about the Br isotope composition of bromine oxyanions.

Eggenkamp and Coleman (2000) measured Br isotope values in the form of gaseous CH_3Br . Xiao et al. (1993) used positive thermal ionization mass spectrometry for the measurement of Cs_2Br^+ . Bromine in organic compounds have been analysed with MC-ICP-MS techniques (Hitzfeld et al. 2011; Holmstrand et al. 2010). The standard in use is SMOB (Standard Mean Ocean Bromine).

Bromide concentrations in most geological settings are too low for a precise isotope measurement, a notable exception are sedimentary formation waters. Although no direct Br isotope measurements of salt minerals are known, indirect evidence from porewaters suggest that evaporites have $\delta^{81}\text{Br}$ -values between 0.5 and 1.0 ‰ (Eggenkamp 2014).

Of special interest are high bromine concentrations in very saline deep groundwaters from old crystalline shields. Shouakar-Stash et al. (2007) and Stotler et al. (2010), observed very large Br-isotope variations from -0.80 to $+3.35$ ‰ that do not indicate a simple marine origin, but favor complex water/rock interactions.

Another interesting aspect of bromine isotope geochemistry is that of all brominated organic compounds in the stratosphere, methyl bromide is the most important contributor to stratospheric ozone depletion. CH_3Br may originate from natural and anthropogenic sources. Horst et al. (2013) determined the Br isotope composition of methyl bromide at two locations in Sweden. Subarctic samples in northern Sweden were more negative than samples in the Stockholm area. The CH_3Br concentration in northern Sweden was 2–3 times lower than in the Stockholm area, possibly indicating industrial contamination of the latter area. CH_3Br emissions from plants are about 2 ‰ depleted in ^{81}Br relative to bromine in the plant (Horst et al. 2014).

2.21 Strontium

Sr has 4 stable isotopes.

^{84}Sr	0.56 %
^{86}Sr	9.86 %
^{87}Sr	7.00 %
^{88}Sr	82.58 %

In the past, isotopes of Sr mainly have been used as a geochronometer. Due to radioactive decay of ^{87}Rb to ^{87}Sr , the $^{87}\text{Sr}/^{86}\text{Sr}$ ratio of a sample together with the Rb/Sr concentration ratio carries geochronologic information. Conventional $^{87}\text{Sr}/^{86}\text{Sr}$ measurements by thermal ionisation mass-spectrometry (TIMS) use the $^{88}\text{Sr}/^{86}\text{Sr}$ ratio for internal instrumental mass fractionations. Normalization to a fixed $^{88}\text{Sr}/^{86}\text{Sr}$ ratio assumes that this ratio is constant for natural samples. However, as shown by Fietzke and Eisenhauer (2006), this is not the case. MC-ICP-MS and double spike TIMS methods document $^{88}\text{Sr}/^{86}\text{Sr}$ variations in terrestrial and meteoritic samples (Fietzke and Eisenhauer 2006; Krabbenhöft et al. 2009; Neymark et al. 2014). Figure 2.32 demonstrates the range of natural variations of $\delta^{88/86}\text{Sr}$ -values relative to the SrCO_3 standard SRM987.

2.21.1 Silicates

Earth, Mars and Moon have indistinguishable bulk Sr isotope compositions, exceptions are some carbonaceous chondrites being depleted in heavy Sr isotopes (Moynier et al. 2010). The bulk Earth has a $\delta^{88}\text{Sr}$ -value of 0.27 ‰. With respect to magmatic rocks, first measurements by Halicz et al. (2008a, b) and Charlier et al.

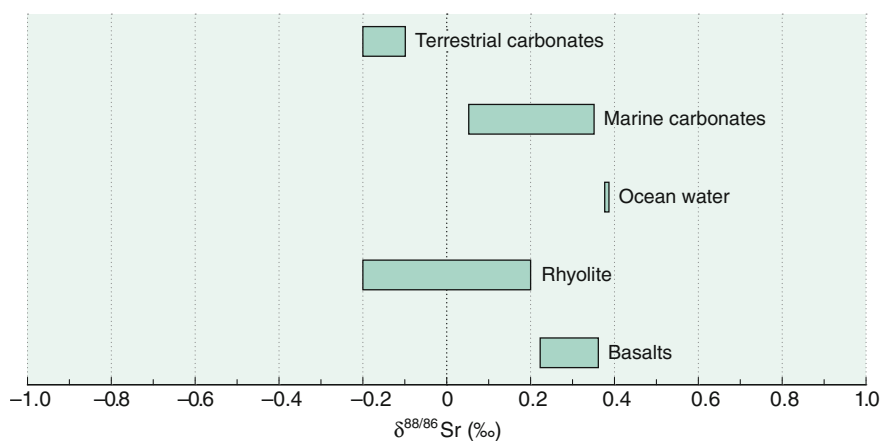


Fig. 2.32 $\delta^{88/86}\text{Sr}$ -values of important geological reservoirs

(2012) indicated that basaltic rocks have a rather uniform value of +0.3 ‰ whereas more evolved rocks—andesites to rhyolites—have lighter values from −0.2 to +0.2 ‰. Charlier et al. (2012) interpreted the observed Sr isotope variations as resulting from isotope fractionations during fractional crystallization in which ^{88}Sr becomes enriched in plagioclase and K-feldspar.

2.21.2 Carbonates

One of the main Sr isotope fractionation processes is the preferential uptake of lighter Sr isotopes during carbonate precipitation. Sr isotope fractionations during inorganic precipitation of calcite depend primarily on precipitation rates resulting in larger fractionations at higher rates (Böhm et al. 2012). Carbonate precipitating organisms generally fractionate $^{88}\text{Sr}/^{86}\text{Sr}$ ratios by 0.1–0.2 ‰ relative to ocean water; the magnitude of Sr isotope fractionation is species dependent. Larger depletions in heavy isotopes have been observed in planktonic foraminifera (Böhm et al. 2012; Stevenson et al. 2014). For tropical corals, Fietzke and Eisenhauer (2006) and Rüggeburg et al. (2008) used $^{88}\text{Sr}/^{86}\text{Sr}$ ratios to reconstruct oceanic surface temperatures. For cold-water corals, however, Raddatz et al. (2013) observed no temperature dependence, instead Sr isotope ratios reflect sea water composition with an offset of −0.2 ‰.

Knowledge of the magnitude of Sr fractionations during carbonate precipitation opens the possibility to quantify the output carbonate flux from the ocean (Krabbenhöft et al. 2010), which is not possible on the basis of $^{87}\text{Sr}/^{86}\text{Sr}$ ratios because ocean water and carbonates are very similar in $^{87}\text{Sr}/^{86}\text{Sr}$ ratios.

By analysing biogenic fossil carbonates, mostly brachiopods, Vollstädt et al. (2014) concluded that seawater throughout the Phanerozoic has varied in $\delta^{88/86}\text{Sr}$ values by 0.25–0.60 ‰, which they interpreted to result from varying amounts of buried carbonates.

In contrast to marine carbonates, terrestrial carbonates, i.e. speleothems, display negative $^{88}\text{Sr}/^{86}\text{Sr}$ ratios from −0.1 to −0.2 ‰ (Halicz et al. 2008a, b).

2.21.3 Rivers and Plants

By analysing Sr dissolved in rivers, the behaviour of $^{88/86}\text{Sr}$ during weathering has been investigated (Krabbenhöft et al. 2010; de Souza et al. 2010; Wei et al. 2013). Krabbenhöft et al. (2010) demonstrated that large rivers are quite variable in $\delta^{88}\text{Sr}$. De Souza et al. (2010) concluded that Sr released during weathering of silicate rocks does not indicate any Sr-isotope fractionation. By analyzing a river from South China, large seasonal Sr-isotope differences depend on the amount of precipitation (Wei et al. 2013).

Plants are isotopically lighter by 0.2–0.5 ‰ than corresponding soils (De Souza et al. 2010). $\delta^{88}\text{Sr}$ values of foliar tissues (leaves, flowers) are isotopically depleted relative to roots and stem which is opposite to the trend observed for Ca isotopes (Wiegand et al. 2005; Page et al. 2008).

2.22 Molybdenum

Mo consists of 7 stable isotopes that have the following abundances:

^{92}Mo	15.86 %,
^{94}Mo	9.12 %,
^{95}Mo	15.70 %,
^{96}Mo	16.50 %,
^{97}Mo	9.45 %,
^{98}Mo	23.75 %,
^{100}Mo	9.62 %.

Either $^{97}\text{Mo}/^{95}\text{Mo}$ or $^{98}\text{Mo}/^{95}\text{Mo}$ ratios have been reported in the literature. Therefore care has to be taken when comparing Mo isotope values. Mo isotope data, given in the following as $\delta^{98}\text{Mo}$ values, are generally reported relative to internal laboratory standards calibrated against ocean water (Mean Ocean Molybdenum (MOMo), Barling et al. 2001; Siebert et al. 2003). More recently, Nägler et al. (2014) proposed that NIST SRM 3134 should be accepted as international standard with a $\delta^{98}\text{Mo}$ value of +0.25 ‰ relative to MOMo.

What makes Mo particular interesting, is its use as a potential proxy for the redox history of the oceans and the atmosphere (Barling et al. 2001; Siebert et al. 2003; Wille et al. 2007; Dahl et al. 2010a, b; Herrmann et al. 2012; Scott and Lyons 2012 besides others). Figure 2.33 summarizes natural Mo isotope variations.

2.22.1 Molybdenites

Limited data from igneous and clastic sedimentary rocks show very small isotope variations (Siebert et al. 2003). Larger variations have been found in molybdenites (MoS_2), an accessory mineral in many magmatic rocks (Hannah et al. 2007; Mathur et al. 2010a, b). According to Mathur et al. (2010a, b) Mo isotope variations depend on the type of ore deposit; molybdenites from porphyry coppers have lighter Mo isotope composition relative to other ore deposits. Greber et al. (2011) observed isotope variations of 1.35 ‰ in a single molybdenite deposit which is larger than the overall Mo isotope variation in igneous rocks. By analysing molybdenites from the well-known porphyry copper deposit of Questa, New Mexico, Greber et al. (2014) subdivided three stages during which Mo isotope fractionations may occur, all lead to molybdenites being heavier than the magmatic source. This implies that Mo isotope compositions of molybdenites are not necessarily representative of the average isotope composition of igneous rocks.

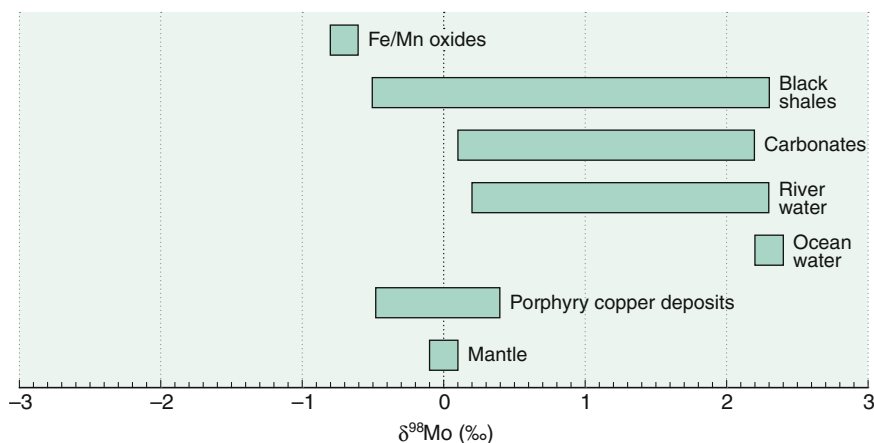


Fig. 2.33 $\delta^{98/95}\text{Mo}$ -values of important geological reservoirs

2.22.2 Sediments

Marine sediments show a large range in isotope composition (Siebert et al. 2006a, b; Poulson et al. 2006). As summarized by Poulson Brucker et al. (2009) Mo in sediments originates from 3 different sources:

- (1) A small riverine fraction. The isotope composition of Mo input from rivers has been investigated by Archer and Vance (2008) and Neubert et al. (2011). They found a large range of $\delta^{98}\text{Mo}$ values from 0.2 to 2.3 ‰ that are heavier than the average continental crust. Along streams no significant modification of Mo isotope signatures is observed (Neubert et al. 2011). Thus catchment lithology probably controls the delivery of Mo to the ocean. Pearce et al. (2010), on the other hand, argued that Mo isotope differences might be explained by retention of light Mo isotopes in soils.
- (2) Mo associated with biological material that is delivered to the seafloor. The relationship between organic matter and Mo is complex, because Mo is not only incorporated into cells, but is also absorbed to organic material in the water column (Poulson Brucker et al. 2009; Kowalski et al. 2013). As demonstrated by Kowalski et al. (2013), Mo isotope fractionations in tidal systems of the North Sea are caused by biological activity. Zerkle et al. (2011) reported cyanobacterial assimilation of Mo that produce considerable isotope fractionations comparable to those in sedimentary organic matter.
- (3) Mo absorbed to Fe/Mn oxides under oxic conditions and Mo bounded through complexation with sulfides under anoxic conditions. Absorbed Mo has a light composition ($\delta^{98}\text{Mo} -0.7$ ‰) being 3 ‰ depleted relative to seawater (Barling et al. 2001; Siebert et al. 2003, Anbar 2004b; Anbar and Rouxel 2007 and others). In euxinic waters, i.e. below 400 m in the Black Sea, molybdate is converted to MoS_4^{2-} that is completely removed to the sediment thus resulting

in a sediment isotope signature of seawater (Neubert et al. 2008; Nägler et al. 2011). Black shales in general formed in an anoxic environment have a Mo isotope composition nearly identical to ocean water (Barling et al. 2001; Arnold et al. 2004a, b; Nägler et al. 2005). In suboxic and weakly euxinic waters, the removal of Mo is not quantitative leading to isotope fractionations that are superimposed by effects associated with particle scavenging yielding Mo-isotope values intermediate between Fe–Mn crusts and euxinic black shales (McManus et al. 2002, 2006; Nägler et al. 2005; Poulson et al. 2006; Siebert et al. 2003, 2006b). Thus, the Mo isotope composition of black shales only reflects the seawater composition when a critical sulfidity is reached.

2.22.3 Palaeoredox Proxy

Because of its long residence time, Mo in ocean water has a uniform isotope composition with a $\delta^{98}\text{Mo}$ value of 2.3 ‰ (Anbar 2004b; Anbar and Rouxel 2007). The Mo isotope composition of ancient oceans has been inferred from black shales assuming that the C-org rich sediments accumulated in euxinic settings (Gordon et al. 2009). However, not all black shales represent euxinic conditions. In recent Black Sea sediments, incomplete removal of Mo from seawater may lead to a Mo isotope depletion of ^{98}Mo in anoxic sediments (Neubert et al. 2008). Therefore when reconstructing paleoenvironments it is important to distinguish between euxinic and non-euxinic black shales.

Nevertheless, variations in the Mo isotope compositions of black shales, have been used as a palaeoredox proxy showing changes of reducing marine conditions throughout periods of Earth's history (Arnold et al. 2004a, b; Siebert et al. 2005; Wille et al. 2007; Pearce et al. 2008; Gordon et al. 2009; Dahl et al. 2010a, b, 2011). In a compilation of Mo-isotope values from black shales, Dahl et al. (2010a, b) postulated two episodes of global ocean oxygenation: the emergence of the Ediacaran fauna at around 550 Ma, and the diversification of vascular plants at around 400 Ma. However, as shown by Gordon et al. (2009) the reconstruction of the Mo isotope composition of ancient oceans from organic rich-shales requires independent evidence of local euxinia.

2.22.4 Carbonates

As an alternative tool for the reconstruction of past ocean chemistry, Voegelin et al. (2009, 2010) analyzed the Mo isotopic composition of carbonates. They observed a large spread in $\delta^{98}\text{Mo}$ -values of biogenic carbonates, which they attributed to vital effects. In contrast inorganic carbonates closely approach modern ocean Mo-values and are not controlled by local redox conditions. Voegelin et al. (2009) concluded that the Mo-isotopic composition of inorganic carbonates may be used to characterize the Mo isotopic composition of past oceanic water masses.

2.23 Cadmium

Cadmium has 8 stable isotopes:

^{106}Cd	1.25 %
^{108}Cd	0.89
^{110}Cd	12.49
^{111}Cd	12.80
^{112}Cd	24.13
^{113}Cd	12.22
^{114}Cd	28.73
^{116}Cd	7.49

Either $^{114}\text{Cd}/^{110}\text{Cd}$ or $^{112}\text{Cd}/^{110}\text{Cd}$ ratios have been reported in the literature, analytical techniques are MC-ICP-MS or double-spike TIMS (Schmitt et al. 2009). Comparing datasets from different laboratories is difficult, because no generally agreed standard exists. Different laboratories have used different commercially available Cd-solutions. Recently, Rehkämper et al. (2011) and Abouchami et al. (2013) suggested NIST SRM 3108 as certified reference material. δ -values reported here are $^{114/110}\text{Cd}$ ratios given relative to SRM 3108 (see Fig. 2.34). A recent review of Cd isotope variations has been published by Rehkämper et al. (2011).

Cd isotope variations are generated mainly by two fractionation processes: (i) partial evaporation/condensation processes in planetary objects and during refining of ore minerals, and (ii) biological utilization of Cd in the oceanic water column. Rocks and minerals show rather constant Cd isotope compositions

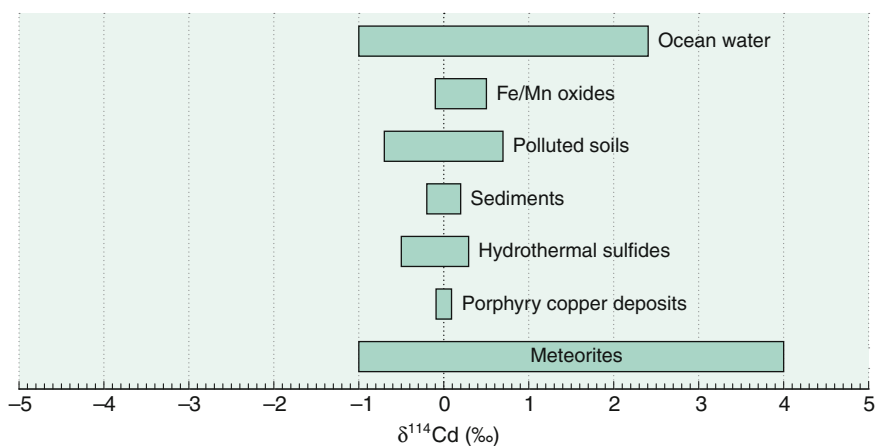


Fig. 2.34 $\delta^{114/110}\text{Cd}$ -values of important geological reservoirs

(Wombacher et al. 2003, 2008). Schmitt et al. (2009) observed in basalts and loess very small differences, suggesting small Cd isotope differences in mantle and crustal rocks.

2.23.1 Extraterrestrial Materials

Cd isotope variations in extraterrestrial material may be caused by kinetic fractionations during evaporation/condensation processes. Carbonaceous chondrites have relative constant Cd isotope compositions (Rehkämper et al. 2011). In contrast, ordinary chondrites and many enstatite chondrites show very large Cd isotope variations with a range in $\delta^{114}\text{Cd}$ values from -8 to $+16$ ‰ (Wombacher et al. 2008). The large range of Cd isotopes in ordinary chondrites obviously results from evaporation/condensation processes, which has been supported by experiments evaporating Cd in vacuo (Wombacher et al. 2004).

The Moon seems to have the same Cd isotope composition as the Earth. Lunar soils are enriched in heavy Cd isotopes, indicating kinetically controlled cadmium loss from the soils.

2.23.2 Marine Environment

Rivers are thought to be the most important source of marine Cd. Rivers in Siberia, analyzed by Lambelet et al. (2013), show a Cd isotope composition close to the continental crust implying that weathering does not produce a measurable Cd isotope fractionation.

Cd in the ocean is a micronutrient, its distribution resembles that of phosphate. Large Cd isotope variations are observed in oceanic surface waters, the most ^{114}Cd enriched values, up to 4 ‰, correlate with waters most depleted in Cd concentration. Rather uniform $\delta^{114}\text{Cd}$ values of 0.3 ‰ were determined for waters below 1000 m water depth (Lacan et al. 2006; Rippberger et al. 2007; Horner et al. 2010; Abouchami et al. 2011; Yang et al. 2012a, b; Gault-Ringold et al. 2012; Xue et al. 2013).

Phytoplankton in surface waters preferentially incorporates isotopically light Cd making the surface ocean isotopically heavy. On the other hand, Yang et al. (2012a, b) observed no net biological fractionation between phytoplankton and ocean water, and suggested that mixing of different water masses might be an important process. Abouchami et al. (2011) observed distinct Cd isotope boundaries in southern Ocean water masses, thereby tracing surface ocean circulation regimes.

Carbonates precipitated from ocean water show very little Cd isotope fractionation and therefore might be used as a tracer for the Cd isotope composition of oceans in the past (Horner et al. 2011). Schmitt et al. (2009) and Horner et al. (2010) reported Cd isotopes for Fe–Mn crusts and demonstrated that nearly all samples were indistinguishable from oceanic deep waters. Thus, Fe–Mn crusts

might potentially be used as a proxy of ancient deep-water Cd isotope composition (Wasylenki et al. 2014).

2.23.3 Pollution Indicator

Soils sampled near ore refineries may be enriched in Cd concentration exhibiting characteristic δ -values (Cloquet et al. 2006). Since Cd isotopes fractionate during evaporation, measurable Cd isotope fractionations should occur during coal burning and sulfide smelting and refining, and indeed, Shiel et al. (2010) observed a 1 ‰ fractionation in $\delta^{114}\text{Cd}$ values during smelting of Zn and Pb ores. Thus, Cd isotope ratios can be used to identify their anthropogenic origin.

2.24 Tin

Tin has 10 stable isotopes, more than any other element, covering the mass range from 112 to 124.

^{112}Sn	0.97
^{114}Sn	0.66
^{115}Sn	0.34
^{116}Sn	14.54
^{117}Sn	7.68
^{118}Sn	24.22
^{119}Sn	8.59
^{120}Sn	32.58
^{122}Sn	4.63
^{124}Sn	5.79

Tin has two oxidation states, Sn(II) and Sn(IV). Cassiterite (SnO_2) is the major tin mineral, but tin also occurs in complex sulfide minerals. Organotin compounds are used in industry, most prominently in the production of polyvinyl chloride as heat and light stabilizer. Due to their widespread use, large amounts of organotin compounds have entered the environment.

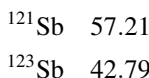
Early studies using TIMS could not detect measurable Sn isotope fractionations due to the high ionization potential of Sn. However, with the introduction of MC-ICP-MS, precise Sn isotope measurements become possible (Clayton et al. 2002; Hausteine et al. 2010; Yamazaki et al. 2013). These authors demonstrated that cassiterites from ore deposits in Europe and Asia exhibit relatively large Sn isotope

variations. Hausteine et al. (2010) used Sn isotope signatures in cassiterites for the provenance of ancient tin.

Polyakov et al. (2005) concluded from synchrotron radiation experiments that large tin isotope fractionations should be found between tin compounds of different oxidation states. Investigating Sn isotope fractionations during methylation reactions, Malinovsky et al. (2009) demonstrated that under irradiation of UV light, synthesis and decomposition of methyltin is accompanied by mass-dependent and mass-independent tin isotope fractionations. In summary, although the data base is poor, future Sn isotope studies appear to be promising.

2.25 Antimony

Antimony has two stable isotopes with high abundances



In nature, antimony occurs mainly as sulfide, particularly as stibnite, Sb_2S_3 ; oxides are far less common, although the main industrial use is as Sb_2O_3 . Antimony is moderately volatile and occurs in two oxidation states, Sb(V) and Sb(III).

The most extensive study about Sb isotope variations has been presented by Rouxel et al. (2003) using a MC-ICP-MS technique. More recently, modified MC-ICP techniques have been published by Tanimizu et al. (2011) and Lobo et al. (2013).

By analysing water samples and a suite of sedimentary and magmatic rocks including hydrothermal sulfides from deep-sea vents, Rouxel et al. (2003) observed a total range in $^{123}\text{Sb}/^{121}\text{Sb}$ ratios of 1.6 ‰ with the largest variations occurring in hydrothermal sulfides. Redox changes from Sb being reduced in vent fluids to oxidized Sb in seawater may cause the Sb fractionations, which have been confirmed experimentally during the reduction of Sb(V) to Sb(III).

An interesting aspect of Sb isotope geochemistry is its potential use of provenancing ancient pre-Roman and Roman glass. Sb had been added to obtain colour and opacity in glass. Lobo et al. (2013) demonstrated that different Sb sources had been used for glass production in the Roman era.

2.26 Tellurium

Tellurium occurs in nature in four oxidation states: as two oxyanions, tellurate and tellurite, and in two reduced forms, as native tellurium and as metal telluride. As a chalcophile element, tellurium might show similar behaviour in isotope fractionation with sulfur.

Tellurium has 8 stable isotopes with the following abundances

^{120}Te	0.10 ‰
^{122}Te	2.60
^{123}Te	0.91
^{124}Te	4.82
^{125}Te	7.14
^{126}Te	19.0
^{128}Te	31.6
^{130}Te	33.7

By measuring $^{130/122}\text{Te}$ ratios in gaseous TeF_6 , Smithers and Krouse (1968) first demonstrated that inorganic and microbiological reductions of tellurite to elemental tellurium causes isotope fractionations with depletions in the heavy isotope in the reaction product. Due to considerable memory effects and other chemical disadvantages, the method has been abandoned. Fehr et al. (2004) introduced a MC-ICP-MS method for tellurium. They found no differences in isotope composition between meteorites and terrestrial tellurides. By measuring $^{130}\text{Te}/^{125}\text{Te}$ ratios with a modified MC-ICP-MS technique, Fornadel et al. (2014) demonstrated that tellurides and native tellurium in ore deposits reveal isotope differences up to 1.64 ‰ with significant variations within individual deposits.

2.27 Barium

Barium consists of 7 naturally occurring isotopes:

^{130}Ba	0.11
^{132}Ba	0.10
^{134}Ba	2.42
^{135}Ba	6.59
^{136}Ba	7.85
^{137}Ba	11.23
^{138}Ba	71.70

Since barium belongs to the earth alkaline elements, its chemical and isotopic behaviour should be closely related to Ca and Sr isotopes. Barium in nature occurs as discrete minerals such as barite and witherite (BaCO_3), but also may substitute potassium in common minerals, especially feldspars. In the ocean, Ba shows a nutrient-type behaviour being associated with organic matter. The wide occurrence

of Ba in low- and high-temperature environments makes Ba an interesting element to look for isotope variations.

Early studies on Ba isotopes concentrated on meteorites (Eugster et al. 1969). More recently, by measuring $^{137}\text{Ba}/^{134}\text{Ba}$ ratios with a MC-ICP-MS technique, von Allmen et al. (2010), Böttcher et al. (2012) and Pretet et al. (2015) reported that Ba minerals and standards vary by up to 0.5 ‰. Distinct differences in Ba-isotope compositions have been reported for barites of different origins (von Allmen et al. 2010).

Besides biological reactions, mineral precipitation and sorption-desorption processes may induce Ba isotope fractionations. Pretet et al. (2015) demonstrated that during inorganic and organic precipitation of carbonates light Ba isotopes are preferentially incorporated, similar to Ca and Sr isotopes. Corals from different oceanic localities show considerable Ba isotope variations which may suggest a heterogeneous Ba isotope composition of seawater. Future Ba isotope measurements may provide a better understanding of the biogeochemical Ba cycle.

2.28 Mercury

Mercury has seven stable isotopes with the following abundances (Rosman and Taylor 1998)

^{196}Hg	0.15
^{198}Hg	9.97
^{199}Hg	16.87
^{200}Hg	23.10
^{201}Hg	13.18
^{202}Hg	29.86
^{204}Hg	6.87

Due to the relative uniform isotope abundances in the mass range ^{198}Hg to ^{204}Hg , several possibilities exist for the measurement of Hg isotope ratios; in most studies δ -values are given as $^{202}\text{Hg}/^{198}\text{Hg}$ ratios. Since the first description of a precise MC-ICP-MS technique (Lauretta et al. 2001), the number of Hg-isotope studies has grown exponentially. Reviews have been presented by Bergquist and Blum (2009), Yin et al. (2010), Blum (2011) and Blum et al. (2014). The large interest in Hg isotopes relies on two factors: (i) due to its ability to be transported over long distances in the atmosphere, mercury is a global pollutant and (ii) large mass independent isotope fractionations have been observed besides mass-dependent fractionations (Sonke 2011 and others).

The biogeochemical cycle of Hg is complex including different redox states and various chemical speciations affecting its mobility and toxicity. Mercury can exist as stable HgS (cinnabar) and in the form of Hg–S complexes, in methylated form (methylmercury) and in gaseous and aerosol phases in the atmosphere. Emissions are dominated by anthropogenic activity (coal combustion), but inputs from volcanic and hydrothermal emissions are also significant. Atmospheric Hg can be converted into methylmercury by bacteria that may accumulate in aquatic food webs potentially causing severe health problems.

Large $\delta^{202/198}\text{Hg}$ -isotope fractionations have been observed in natural samples (Bergquist and Blum 2009 and others), far larger than anticipated. The natural Hg isotope variation encompasses 7 ‰, from $\delta^{202}\text{Hg}$ –4.5 to +2.5 ‰ relative to NIST 3133 (Zambardi et al. 2009).

Bucharenko (2001) and Schauble (2007) demonstrated that isotope variations are controlled by nuclear volume and magnetic shift isotope effects being negligible for the light elements.

2.28.1 MDF and MIF Fractionation Processes

Most equilibrium and kinetic processes for Hg are mass dependent fractionations (MDF), i.e. Hg reacting during microbial transformations (Kritee et al. 2007, 2009); as for other elements, MDF depend on the type of organism, temperature, growth rate etc. On the other hand, experiments during abiotic photoreduction show MDF and mass independent fractionations, MIF, that have been observed for the odd isotopes ^{199}Hg and ^{201}Hg (Bergquist and Blum 2009). Experiments identified photoreduction of aquatic inorganic Hg^{2+} and photodegradation of monomethylmercury as MIF inducing reactions (Sonke 2011).

The magnitude of the observed MIF due to the nuclear volume effect is generally small. As predicted by Bucharenko et al. (2004) and Schauble (2007) and confirmed in experiments by Zheng and Hintelmann (2010), nuclear volume effects have been reported for the Hg liquid-vapor transition (Estrade et al. 2009; Ghosh et al. 2013), in which a small enrichment of the odd over the even isotopes takes place (Sonke and Blum 2013) (<0.2 ‰ for $\Delta^{199}\text{Hg}$ and $\Delta^{201}\text{Hg}$) resulting in $\Delta^{199}\text{Hg}/\Delta^{201}\text{Hg}$ ratios of 1.5–2 (Estrade et al. 2009; Zheng and Hintelmann 2010). Larger MIFs have been observed during photochemical reduction of Hg (Bergquist and Blum 2009), in which magnetic isotope effects are the major fractionation process. The largest positive MIF of Hg isotopes (odd mass excess) probably is caused by photochemical degradation of methylmercury in water, which is transferred to the biosphere, in specific to fish (Bergquist and Blum 2009; Blum and Bergquist 2007, 2009). The largest negative MIF (odd mass deficit) is caused by photochemical reduction of inorganic Hg.

MIF reactions may yield a characteristic signature insofar that only odd isotopes (^{199}Hg , ^{201}Hg) deviate significantly from MDF. The ratio $\Delta^{199}\text{Hg}/\Delta^{201}\text{Hg}$ seems to be diagnostic of the process causing the MIF (Bergquist and Blum 2009). Recent

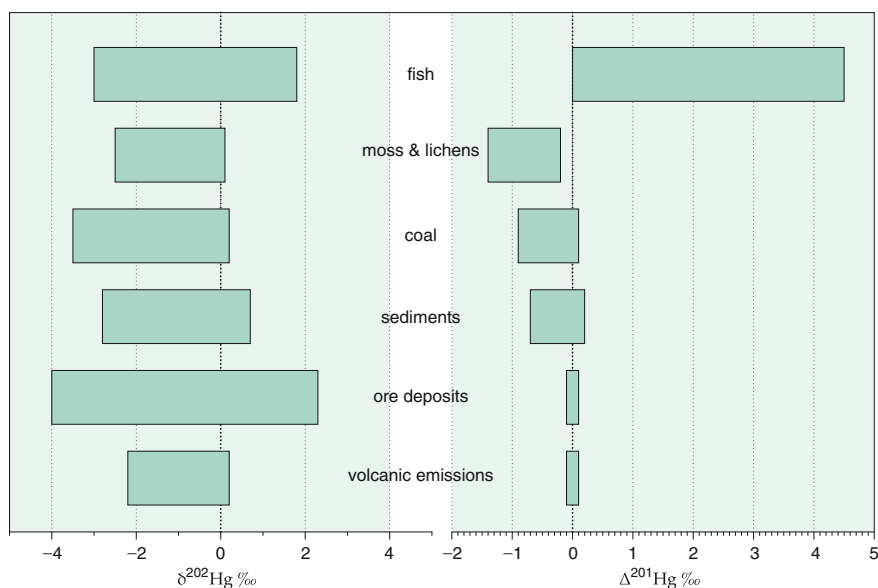


Fig. 2.35 $\delta^{202/198}\text{Hg}$ and $\Delta^{201}\text{Hg}$ values of important geological reservoirs

studies of atmospheric Hg samples show, however, that even isotopes of Hg may also show small non-mass dependent fractionations (Chen et al. 2012; Rolison et al. 2013). The mechanism for the even isotope mass independent fractionations remain, however, unclear.

For the calculation of odd and even numbered MIF values, Blum and Bergquist (2007) gave the following definitions.

$$\Delta^{199}\text{Hg} = \delta^{199}\text{Hg} - (\delta^{202}\text{Hg} \times 0.2520)$$

$$\Delta^{200}\text{Hg} = \delta^{200}\text{Hg} - (\delta^{202}\text{Hg} \times 0.5024)$$

$$\Delta^{201}\text{Hg} = \delta^{201}\text{Hg} - (\delta^{202}\text{Hg} \times 0.7520)$$

$$\Delta^{204}\text{Hg} = \delta^{204}\text{Hg} - (\delta^{202}\text{Hg} \times 1.4930)$$

Figure 2.35 summarizes MDF and MIF Hg isotope variations in important reservoirs (modified from Bergquist and Blum 2009).

2.28.2 Variations in Rocks

Hg has two common oxidation states: Hg(0) exists primarily in gaseous form and Hg(II) exists as highly particle-reactive gaseous, aqueous and solid species. Dissolved Hg(II) has affinities for sulfides and organic matter.

Isotope variations of mercury in common magmatic rocks are very small. A larger range does occur in Hg ore deposits and in hydrothermal springs (Smith

et al. 2008). Smith et al. (2008) postulated that boiling of hydrothermal fluids and separation of a Hg-bearing vapour phase are responsible for the observed isotope variations. Sherman et al. (2009) investigated the Guaymas and Yellowstone hydrothermal systems. They reported considerable isotope fractionations, in the Guaymas system solely being mass-dependent, whereas at Yellowstone small mass-independent fractionations occur which may be due to the presence of light facilitating photochemical reactions.

Sapropels—sediments deposited during periods of high primary productivity—may record the Hg isotopic composition of the ocean by quantitative sequestration of Hg by organic matter. Sapropels from the Mediterranean gave $\delta^{202}\text{Hg}$ values from -1.0 to -0.6 ‰ (Gehrke et al. 2009).

Mosses and lichens are passive filters of atmospheric particulates, which may monitor atmospheric Hg emissions. Carignan et al. (2009) demonstrated that they are characterized by negative MIF. Snow samples also may be regarded as good collectors of atmospheric Hg particulates (Sherman et al. 2010).

2.28.3 Environmental Pollutant

The geochemical cycle of mercury is characterized by atmospheric transport over long distances. Mercury exists in 3 species in the atmosphere: (i) elemental Hg (Hg^0) having a residence time of about 1 year in the atmosphere, (ii) divalent reactive gaseous Hg^{2+} and (iii) Hg bound to particles. These species are linked together by abundant oxidation and reduction processes. Hg^0 comprises more than 90 % of total atmospheric Hg and is relatively stable allowing large scale mixing, whereas the other two species are much more reactive and deposit readily.

Besides natural inputs from volcanic and hydrothermal emissions, anthropogenic sources dominate Hg emissions with coal combustion being the largest contributor. Because elementary Hg is extremely volatile, mercury easily exchanges between water and air and between land and air, resulting in global dispersion.

Hg MDF and MIF signatures in moss, peat, coal and soils demonstrate that a large part of the Hg surface reservoir has been affected by anthropogenic activities offering the possibility to use Hg isotopes as a fingerprint (Sonke 2011) and to quantify the relative contributions of Hg deposition from local, regional and global sources. As suggested by Kritee et al. (2007, 2009), Hg isotopes may distinguish between different sources of mercury emissions based on the magnitude of isotope fractionations. Sonke et al. (2010) investigated mercury pollution from two European metal refineries and showed that heavy Hg isotopes are preferentially retained in slag residues. Ma et al. (2013) investigated Hg emissions from a heavy metal smelter in Manitoba. Hg isotope variations observed in sediment cores can be explained by mixing of a natural endmember ($\delta^{202}\text{Hg} -2.4$ ‰) and an anthropogenic endmember emitted from the smelter ($\delta^{202}\text{Hg} -0.9$). Sediment cores 5 and 73 km away from the smelter reveal decreasing Hg concentrations and characteristic shifts in Hg isotope values. Even at the distance of 73 km 70 % of the Hg in the sediments originated from the smelter. In comparable studies, Stetson et al. (2009)

and Yin et al. (2013) have reached similar conclusions by investigating Hg pollution and Hg isotope fractionation in the vicinity of Ag, Au and Hg mines.

At the global scale, anthropogenic emissions are dominated by coal fired power plants. Biswas et al. (2008) demonstrated that coal deposits in the United States, China and Kazakhstan have characteristic Hg isotope values that can be used to discriminate among Hg sources. $\delta^{202}\text{Hg}$ in coal vary by 3 ‰ and $\Delta^{201}\text{Hg}$ by 0.9 ‰. Combining the two variables may result in a characteristic fingerprint for coal deposits.

2.29 Thallium

The geochemical behaviour of thallium is largely controlled by its large ionic radius, which makes it highly incompatible during magmatic processes. Tl exists in two valence states as Tl^+ and Tl^{3+} . Because of its high redox potential, the oxidized form is uncommon in natural environments, but seems to play an important role during adsorption processes. Furthermore Tl is a highly volatile element favoring kinetic fractionations during degassing processes.

Thallium has two stable isotopes with masses 203 and 205.

^{203}Tl 29.52

^{205}Tl 70.48

The small relative mass difference between the two Tl isotopes predicts little Tl isotope fractionations. However, the so far observed Tl isotope variation is larger than 3 ‰ (Rehkämper et al. 2002; Nielsen et al. 2006). Responsible for the large variation are Tl isotope fractionations between seawater and Fe–Mn oxyhydroxides and fractionations during low temperature alterations of the oceanic crust.

The generally used standard is NIST 997 Tl metal. It is important to note that Tl isotope ratios are generally given in the ϵ -notation (variations in parts per 10,000), in the following Tl isotope ratios are given, however, as δ -values. A recent review about the Tl isotope geochemistry has been published by Nielsen and Rehkämper (2011). Figure 2.36 summarizes natural Tl isotope variations

2.29.1 Igneous Rocks

During magmatic processes (crystal fractionation, crustal assimilation etc.) little fractionations seem to occur. Nielsen et al. (2005, 2006, 2007) demonstrated that the continental crust does not differ from the mantle. By analysing igneous rocks in the vicinity of porphyry copper deposits, Baker et al. (2010) reported a variation range of about 0.6 ‰ due to hydrothermal alteration processes.

Because Tl is a volatile trace element, it becomes enriched in volcanic condensates. As shown by Baker et al. (2009) gaseous volcanic emissions are more variable in Tl isotope composition than igneous rocks, but have a mean value being indistinguishable from the estimated mantle composition. The larger variability may

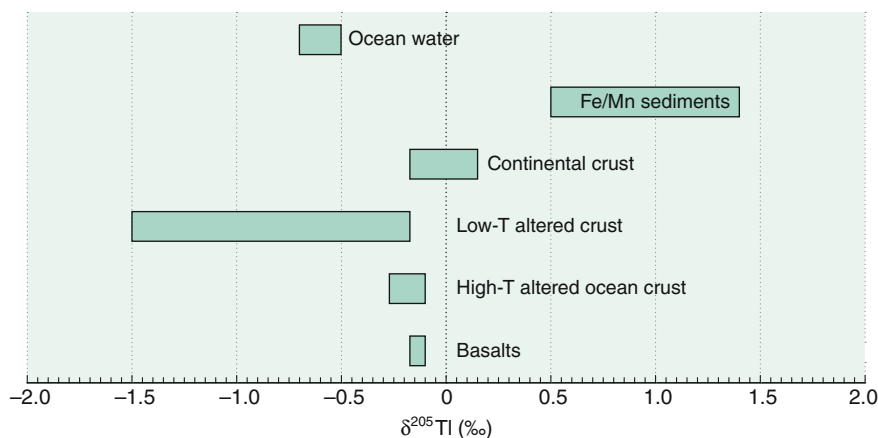


Fig. 2.36 $\delta^{205}\text{Tl}$ -values of important geological reservoirs

result from partial evaporation during mantle degassing. As indicated in late magmatic/hydrothermal veins, Hettmann et al. (2014) demonstrated that fluids released during degassing are enriched in ^{205}Tl .

Since most geochemical reservoirs except Fe–Mn marine sediments and low temperature seawater altered basalts are more or less invariant in Tl isotope composition, admixing of small amounts of Fe–Mn sediments or low-temperature altered oceanic crust into the mantle should induce small Tl isotope fractionations in mantle derived rocks (Nielsen et al. 2006, 2007). Thus, Tl isotopes may have potential to distinguish between different admixtures to arc lavas. Lavas from the Mariana arc, however, overlap with MORB basalts in Tl isotope composition (Prytulak et al. 2013a, b); thus, no external input can be detected.

2.29.2 Fractionations in the Ocean

No significant Tl isotope fractionations occur during weathering. Dissolved and particulate components in river water do not differ from those of the continental crust (Nielsen et al. 2005). The oceans, however, are depleted in ^{203}Tl compared to the continental crust. A systematic 2 ‰ difference between Fe–Mn crusts enriched in ^{205}Tl and seawater has been observed by Rehkämper et al. (2002), which seems to be due to a fractionation effect during adsorption of Tl onto Fe–Mn particles (Rehkämper et al. 2004).

Variations of Tl concentrations and isotope compositions of seawater over time may depend on different rates of Tl removal via scavenging on Fe–Mn oxyhydroxides and via uptake during low temperature alteration of oceanic crust (Nielsen et al. 2009, 2011a, b, c). Nielsen et al. (2009) observed that growth layers of two Fe–Mn crusts from the Pacific Ocean show a systematic change Tl isotope

composition with age, which they explained by time-dependent changes in Tl-isotope composition of seawater. Low Tl isotope ratios during the age range between 55 and 45 Ma might be explained by a fourfold increase of Fe–Mn oxide precipitation compared to present day.

The potential to use Tl isotopes as a paleoredox proxy has been shown by Nielsen et al. (2011a, b, c). Early diagenetic pyrite deposited in an oxic water column display Tl isotope ratios heavier than seawater, whereas pyrite deposited under euxinic conditions have a Tl isotope composition close to seawater, due to reduced precipitation of Fe/Mn oxides in a sulfidic water column.

2.30 Uranium

Natural uranium is mainly composed of two long-lived radioactive isotopes:

$$\begin{array}{ll} {}^{235}\text{U} & 0.72\% \\ {}^{238}\text{U} & 99.27\% \end{array}$$

In the past uranium isotopes have been widely used as a chronological tool. Present day isotope fractionation between ${}^{235}\text{U}$ and ${}^{238}\text{U}$ has been considered to be insignificant. The ratio ${}^{238}\text{U}/{}^{235}\text{U}$ has been assumed to be a constant with a value of 137.88. However, precise measurements by Hiess et al. (2012) on a suite of uranium-bearing minerals commonly used for U–Pb geochronology, e.g. zircons, exhibit isotope variations in $\delta^{238}\text{U}$ values larger than 5 ‰.

Uranium exists in two oxidation states having different solubilities. Under oxidizing conditions, U is typically present as soluble hexavalent uranyl ion UO_2^{2+} , under reducing conditions U occurs in the tetravalent state, forming relatively insoluble complexes. These properties favor natural isotope variations. Fractionations occur due to mass-independent nuclear volume fractionations, resulting from the differences in nuclear size and shape (Schauble 2007; Abe et al. 2008). Schauble (2007) showed that as a function of oxidation state enriched $\delta^{238}\text{U}$ values occur in reduced species, opposite to fractionations generally observed.

Using MC-ICP-MS techniques, Stirling et al. (2007), Weyer et al. (2008), Bopp et al. (2009), Montoya-Pino et al. (2010) reported $\delta^{238}\text{U}$ variations of more than 1 ‰ in various rock types (see Fig. 2.37). Several standards are in use, δ -values measured with a precision better than 0.1 ‰ are given relative to the SRM 950a standard.

2.30.1 Fractionation Processes

Uranium isotope fractionations mainly are attributed to biogenic or abiogenic reduction of U(VI) to U(IV). Basu et al. (2014) determined experimentally uranium isotope fractionations of up to 1 ‰ during microbial U(VI) reduction. Diverse

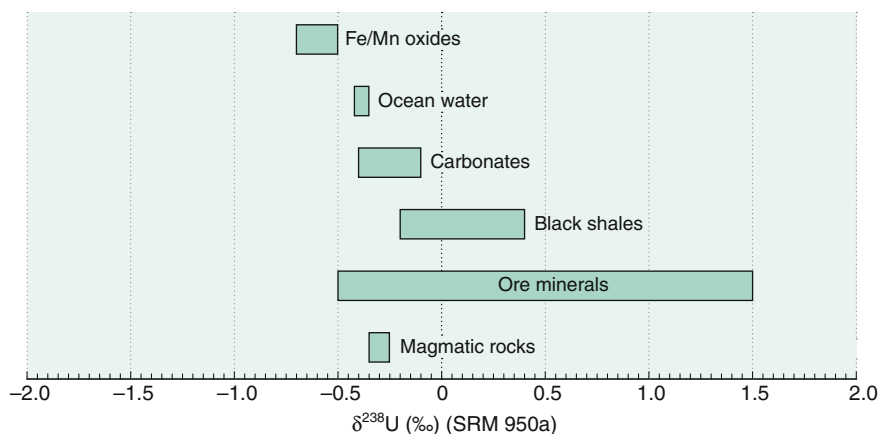


Fig. 2.37 $\delta^{238}\text{U}$ -values of important geological reservoirs

microorganisms are capable of reducing U(VI) to U(IV) inducing isotope fractionations that is opposite in direction observed during reduction of nitrate, sulphate and chromate: ^{238}U preferentially partitions into U(IV) phases, whereas ^{235}U is enriched in U(VI) phases. Thus, heavy $\delta^{238}\text{U}$ values are observed for black shales, which contain the reduced form of U, and light isotope values are observed for Fe/Mn oxides.

Another process causing significant U isotope fractionation occurs between seawater and Fe–Mn oxides. Brennacka et al. (2013) postulated that U fractionation is due to coordination changes during absorption. As the redox change of U does not change during absorption, a difference in the coordination environment between dissolved and absorbed U is obviously responsible for the isotope fractionation.

2.30.2 Characteristic U Signatures

Uranium in the ocean occurs mainly in the soluble U(VI) form with a $\delta^{238}\text{U}$ -value of -0.4 ‰ (Weyer et al. 2008). Under oxic conditions U may be removed through adsorption on Fe/Mn oxides depleted in ^{238}U , shifting oceanic U to heavier values. Under anoxic conditions, sediments enrich ^{238}U shifting ocean water to lighter U isotope values.

The potential of uranium isotopes as a paleo-redox tracer has been investigated by Montoya-Pino et al. (2010), Brennecke et al. (2011), Kendall et al. (2013) and Noordmann et al. (2015). Montoya-Pino et al. (2010) demonstrated that U isotope variations in black shales can be used to quantify the extent of marine anoxia. Black shales from the Cretaceous (Oceanic Anoxic Event 2) are systematically lighter in ^{238}U than modern Black Sea shales which corresponds to a threefold increase of oceanic anoxia relative to the present ocean.

Measurements by Stirling et al. (2007) and Weyer et al. (2008) on recent and fossil corals suggested that carbonates might record the isotope composition of seawater of the geologic past. On the other hand, as argued by Romaniello et al. (2013), $\delta^{238}\text{U}$ values of ancient carbonates, affected by diagenetic processes, may be enriched in ^{238}U due to U accumulation under anoxic pore water conditions.

Large differences of nearly 2 ‰ have been observed between uranium ores formed at low and at high temperatures (Bopp et al. 2009; Uvarova et al. 2015; Murphy et al. 2014): magmatic ores vary from -0.7 to -0.3 ‰ whereas sandstone-type low temperature ores have $\delta^{238}\text{U}$ -values around $+0.4$ ‰. Isotope variations seem to be controlled by the isotope composition of the U source and the efficiency of U reduction. Up to 5 ‰ fractionations have been observed in U mineralised sediment—groundwater systems (Murphy et al. 2014). ^{238}U preferentially enriches in the sediment, leading to depletions in the groundwater.

References

- Abe M, Suzuki T, Fujii Y, Hada M, Hirao K (2008) An ab initio molecular orbital study of the nuclear volume effects in uranium isotope fractionations. *J Chem Phys* 129:164309
- Abelson PH, Hoering TC (1961) Carbon isotope fractionation in formation of amino acids by photosynthetic organisms. *Proc Natl Acad Sci USA* 47:623
- Abouchami W, Galer S et al (2013) A common reference material for cadmium isotope studies—NIST SRM 3108. *Geostand Geoanal Res* 37:5–17
- Abouchami W, Galer S, de Baar H, Alderkamp A, Middag R, Laan P, Feldmann H, Andreae M (2011) Modulation of the southern ocean cadmium isotope signature by ocean circulation and primary productivity. *Earth Planet Sci Lett* 305:83–91
- Ader M, Chaudhuri S, Coates JD, Coleman M (2008) Microbial perchlorate reduction: a precise laboratory determination of the chlorine isotope fractionation and its possible biochemical basis. *Earth Planet Sci Lett* 269:604–612
- Aharon P, Fu B (2000) Microbial sulfate reduction rates and sulfur and oxygen isotope fractionation at oil and gas seeps in deepwater Gulf of Mexico. *Geochim Cosmochim Acta* 64:233–246
- Amini M, Eisenhauer A, Böhm F, Fietzke J, Bach W, Garbe-Schoenberg D, Rosner M, Bock B, Lackschewitz K, Hauff F (2008) Calcium isotope ($\delta^{44/40}\text{Ca}$) fractionation along hydrothermal pathways, Logatchev field (Mid-Atlantic Ridge, $14^{\circ}45'\text{N}$). *Geochim Cosmochim Acta* 72:4107–4122
- Amrani A, Sessions AL, Adkins JF (2009) Compound-specific $\delta^{34}\text{S}$ analysis of volatile organics by coupled GC/Multicollector-ICPMS. *Anal Chem* 81:9027–9034
- Anbar AD (2004a) Iron stable isotopes: beyond biosignatures. *Earth Planet Sci Lett* 217:223–236
- Anbar AD (2004b) Molybdenum stable isotopes: observations, interpretations and directions. *Rev Mineral Geochem* 55:429–454
- Anbar AD, Jarzecki AA, Spiro TG (2005) Theoretical investigation of iron isotope fractionation between $\text{Fe}(\text{H}_2\text{O})_6^{3+}$ and $\text{Fe}(\text{H}_2\text{O})_6^{2+}$: implications for iron stable isotope geochemistry. *Geochim Cosmochim Acta* 69:825–837
- Anbar AD, Rouxel O (2007) Metal stable isotopes in paleoceanography. *Ann Rev Earth Planet Sci* 35:717–746
- Andersen MB, Vance D, Archer C, Anderson RF, Ellwood MJ, Allen CS (2011) The Zn abundance and isotopic composition of diatom frustules, a proxy for Zn availability in ocean surface seawater. *Earth Planet Sci Lett* 301:137–145

- Andre L, Cardinal D, Alleman LY, Moorbath S (2006) Silicon isotopes in 3.8 Ga west Greenland rocks as clues to the Eoarchaeal supracrustal Si cycle. *Earth Planet Sci Lett* 245:162–173
- Antler G, Turchyn AV, Rennie V, Herut B, Sivan O (2013) Coupled sulphur and oxygen isotope insight into bacterial sulphate reduction in the natural environment. *Geochim Cosmochim Acta* 118:98–117
- Archer C, Vance D (2006) Coupled Fe and S isotope evidence for Archean microbial Fe(III) and sulphate reduction. *Geology* 34:153–156
- Archer C, Vance D (2008) The isotopic signature of the global riverine molybdenum flux and anoxia in the ancient oceans. *Nat Geosci* 1:597–600
- Arnold GL, Anbar AD, Barling J, Lyons TW (2004a) Molybdenum isotope evidence for widespread anoxia in Mid-Proterozoic oceans. *Science* 304:87–90
- Arnold GL, Weyer S, Anbar AD (2004b) Fe isotope variations in natural materials measured using high mass resolution multiple collector ICPMS. *Anal Chem* 76:322–327
- Azmy K, Lavoie D, Wang Z, Brand U, Al-Aasm I, Jackson S, Girard I (2013) Magnesium-isotope and REE compositions of Lower Ordovician carbonates from eastern Laurentia: implications for the origin of dolomites and limestones. *Chem Geol* 356:64–75
- Bachinski DJ (1969) Bond strength and sulfur isotope fractionation in coexisting sulfides. *Econ Geol* 64:56–65
- Baker L, Franchi IA, Maynard J, Wright IP, Pillinger CT (2002) A technique for the determination of $^{18}\text{O}/^{16}\text{O}$ and $^{17}\text{O}/^{16}\text{O}$ isotopic ratios in water from small liquid and solid samples. *Anal Chem* 74:1665–1673
- Baker RG, Rehkämper M, Hinkley TK, Nielsen SG, Poutain JP (2009) Investigation of thallium fluxes from subaerial volcanism- implications for the present and past mass balance of thallium in the oceans. *Geochim Cosmochim Acta* 73:6340–6359
- Baker RG, Rehkämper M, Ihlenfeld C, Oates CJ, Coggon R (2010) Thallium isotope variations in an ore-bearing continental igneous setting: Collahuasi Formation, northern Chile. *Geochim Cosmochim Acta* 74:4405–4416
- Balci N, Bullen TD, Witte-Lien K, Shanks WC, Motelica M, Mandernack KW (2006) Iron isotope fractionation during microbially simulated Fe(II) oxidation and Fe(III) precipitation. *Geochim Cosmochim Acta* 70:622–639
- Balistrieri L, Borrok DM, Wanty RB, Ridley WI (2008) Fractionation of Cu and Zn isotopes during adsorption onto amorphous Fe(III) oxyhydroxide: experimental mixing of acid rock drainage and ambient river water. *Geochim Cosmochim Acta* 72:311–328
- Banks DA, Green R, Cliff RA, Yardley BWD (2000) Chlorine isotopes in fluid inclusions: determination of the origins of salinity in magmatic fluids. *Geochim Cosmochim Acta* 64:1785–1789
- Bao H (2015) Sulfate: a time capsule for bEarth's O_2 , O_3 and H_2O . *Chem Geol* 395:108–118
- Bao H, Thiemens MH (2000) Generation of O_2 from BaSO_4 using a CO_2 -laser fluorination system for simultaneous $\delta^{18}\text{O}$ and $\delta^{17}\text{O}$ analysis. *Anal Chem* 72:4029–4032
- Barkan E, Luz B (2005) High precision measurements of $^{17}\text{O}/^{16}\text{O}$ and $^{18}\text{O}/^{16}\text{O}$ ratios in H_2O . *Rapid Commun Mass Spectr* 19:3737–3742
- Barling J, Arnold GL, Anbar AD (2001) Natural mass-dependent variations in the isotopic composition of molybdenum. *Earth Planet Sci Lett* 193:447–457
- Barnes JD, Paulick H, Sharp ZD, Bach W, Beaudoin G (2009) Stable isotope ($\delta^{18}\text{O}$, δD , $\delta^{37}\text{Cl}$) evidence for multiple fluid histories in mid-Atlantic abyssal peridotites (ODP Leg 209). *Lithos* 110:83–94
- Barnes JD, Sharp ZD, Fischer TP (2006) Chlorine stable isotope systematics and geochemistry along the Central American and Izu-Bonin-Mariana volcanic arc. *Eos Trans AGU* 87(52), Fall Meet Suppl V52B-08
- Barth S (1998) Application of boron isotopes for tracing source of anthropogenic contamination in groundwater. *Water Res* 32:685–690
- Basile-Doelsch I, Meunier JD, Parron C (2005) Another continental pool in the terrestrial silicon cycle. *Nature* 433:399–402

- Basu A, Sanford RA, Johnson TM, Lundstrom CC, Löffler FE (2014) Uranium isotopic fractionation factors during U(VI) reduction by bacterial isolates. *Geochim Cosmochim Acta* 136:100–113
- Baumgartner LP, Rumble D (1988) Transport of stable isotopes. I. Development of a kinetic continuum theory for stable isotope transport. *Contr Mineral Petrol* 98:417–430
- Beard BL, Handler RM, Scherer MM, Wu L, Czaja AD, Heimann A, Johnson CM (2010) Iron isotope fractionation between aqueous ferrous iron and goethite. *Earth Planet Sci Lett* 295:241–250
- Beard BL, Johnson CM (1999) High-precision iron isotope measurements of terrestrial and lunar materials. *Geochim Cosmochim Acta* 63:1653–1660
- Beard BL, Johnson CM (2004) Fe isotope variations in the modern and ancient Earth and other planetary bodies. *Rev Mineral Geoch* 55:319–357
- Beard BL, Johnson CM, Cox L, Sun H, Nealson KH, Aguilar C (1999) Iron isotope biosphere. *Science* 285:1889–1892
- Beard BL, Johnson CM, Skulan JL, Nealson KH, Cox L, Sun H (2003) Application of Fe isotopes to tracing the geochemical and biological cycling of Fe. *Chem Geol* 195:87–117
- Beaudoin G, Taylor BE (1994) High precision and spatial resolution sulfur-isotope analysis using MILES laser microprobe. *Geochim Cosmochim Acta* 58:5055–5063
- Beaudoin G, Taylor BE, Rumble D, Thiemens M (1994) Variations in the sulfur isotope composition of troilite from the Canyon Diablo iron meteorite. *Geochim Cosmochim Acta* 58:4253–4255
- Bebout GE, Fogel ML (1992) Nitrogen isotope compositions of metasedimentary rocks in the Catalina Schist, California: implications for metamorphic devolatilization history. *Geochim Cosmochim Acta* 56:2839–2849
- Bebout GE, Idleman BD, Li L, Hilkert A (2007) Isotope-ratio-monitoring gas chromatography methods for high-precision isotopic analysis of nanomole quantities of silicate nitrogen. *Chem Geol* 240:1–10
- Beck WC, Grossman EL, Morse JW (2005) Experimental studies of oxygen isotope fractionation in the carbonic acid system at 15°, 25°, and 40 °C. *Geochim Cosmochim Acta* 69:3493–3503
- Benson BB, Parker PDM (1961) Nitrogen/argon and nitrogen isotope ratios in aerobic sea water. *Deep Sea Res* 7:237–253
- Berglund M, Wieser ME (2011) Isotopic compositions of the elements 2009 (IUPAC Technical Report). *Pure Appl Chem* 83:397–410
- Bergquist BA, Blum JD (2009) The odds and evens of mercury isotopes: applications of mass-dependent and mass-independent isotope fractionation. *Elements* 5:353–357
- Bergquist BA, Boyle EA (2006) Iron isotopes in the Amazon River system: weathering and transport signatures. *Earth Planet Sci Lett* 248:54–68
- Bermin J, Vance D, Archer C, Statham PJ (2006) The determination of the isotopic composition of Cu and Zn in seawater. *Chem Geol* 226:280–297
- Berna EC, Johnson TM, Makdisi RS, Basu A (2010) Cr stable isotopes as indicators of Cr (VI) reduction in groundwater: a detailed time-series study of a point-source plume. *Environ Sci Technol* 44:1043–1048
- Bickle MJ, Baker J (1990) Migration of reaction and isotopic fronts in infiltration zones: assessments of fluid flux in metamorphic terrains. *Earth Planet Sci Lett* 98:1–13
- Bidigare RR et al (1997) Consistent fractionation of ^{13}C in nature and in the laboratory: growth-rate effects in some haptophyte algae. *Global Biogeochem Cycles* 11:279–292
- Bigeleisen J (1965) Chemistry of isotopes. *Science* 147:463–471
- Bigeleisen J, Perlman ML, Prosser HC (1952) Conversion of hydrogenic materials for isotopic analysis. *Anal Chem* 24:1356
- Biswas A, Blum JD, Bergquist BA, Keeler GJ, Xie Z (2008) Natural mercury isotope variation in coal deposits and organic soils. *Environ Sci Technol* 42:8303–8309
- Black JR, Epstein E, Rains WD, Yin Q-Z, Casey WD (2008) Magnesium isotope fractionation during plant growth. *Environ Sci Tech* 42:7831–7836

- Black JR, Kavner A, Schauble EA (2011) Calculation of equilibrium stable isotope partition function ratios for aqueous zinc complexes and metallic zinc. *Geochim Cosmochim Acta* 75:769–783
- Blanchard M, Poitrasson F, Meheut M, Lazzari M, Mauri F, Balan E (2009) Iron isotope fractionation between pyrite (FeS_2), hematite (Fe_2O_3) and siderite (FeCO_3): a first-principles density functional theory study. *Geochim Cosmochim Acta* 73:6565–6578
- Blattner P, Lassey KR (1989) Stable isotope exchange fronts, Damköhler numbers and fluid to rock ratios. *Chem Geol* 78:381–392
- Blum JD, Sherman LS, Johnson MW (2014) Mercury isotopes in earth and environmental sciences. *Ann Rev Earth Planet Sci* 42:249–269
- Blum JD (2011) Applications of stable mercury isotopes to biogeochemistry. In: Baskaran M (Ed) *Handbook of environmental isotope geochemistry*. Springer, New York, pp 229–246
- Bolliger C, Schroth MH, Bernasconi SM, Kleikemper J, Zeyer J (2001) Sulfur isotope fractionation during microbial reduction by toluene-degrading bacteria. *Geochim Cosmochim Acta* 65:3289–3299
- Bonifacie M, Jendrzejewski N, Agrinier P, Humler E, Coleman M, Javoy M (2008) The chlorine isotope composition of the Earth's mantle. *Science* 319:1518–1520
- Bonnand P, James RH, Parkinson IJ, Connelly DP, Fairchild IJ (2013) The chromium isotopic composition of seawater and marine carbonates. *Earth Planet Sci Lett* 382:10–20
- Bopp CJ, Lundstrom CC, Johnson TM, Glessner JJ (2009) Variations in $^{238}\text{U}/^{235}\text{U}$ in uranium ore deposits: isotopic signatures of the U reduction process? *Geology* 37:611–614
- Borrok DM, Nimick DA, Wanty RB, Ridley WI (2008) Isotope variations of dissolved copper and zinc in stream water affected by historical mining. *Geochim Cosmochim Acta* 72:329–344
- Borrok DM, Wanty RB, Ridley WI, Lamothe PJ, Kimball BA, Verplanck PL, Runkel RL (2009) Application of iron and zinc isotopes to track the sources and mechanisms of metal loading in a mountain watershed. *Appl Geochem* 24:1270–1277
- Borthwick J, Harmon RS (1982) A note regarding ClF_3 as an alternative to BrF_5 for oxygen isotope analysis. *Geochim Cosmochim Acta* 46:1665–1668
- Bottinga Y (1969) Calculated fractionation factors for carbon and hydrogen isotope exchange in the system calcite-carbon dioxide-graphite-methane-hydrogen-water-vapor. *Geochim Cosmochim Acta* 33:49–64
- Boudreau BP, Westrich JT (1984) The dependence of bacterial sulfate reduction on sulfate concentration in marine sediments. *Geochim Cosmochim Acta* 48:2503–2516
- Boulou-Bi EB, Poszwa A, Leyval C, Vigier N (2010) Experimental determination of magnesium isotope fractionation during higher plant growth. *Geochim Cosmochim Acta* 74:2523–2537
- Bourdon B, Tipper ET, Fitoussi C, Stracke A (2010) Chondritic Mg isotope composition of the Earth. *Geochim Cosmochim Acta* 74:5069–5083
- Bowman JR, Willett SD, Cook SJ (1994) Oxygen isotope transport and exchange during fluid flow. *Am J Sci* 294:1–55
- Brand W, Coplen TB et al (2009a) Comprehensive inter-laboratory calibration of reference materials for $\delta^{18}\text{O}$ versus VSMOW using various on-line high-temperature conversion techniques. *Rapid Comm Mass Spectrom* 23:999–1019
- Brand W, Geilmann H, Crosson ER, Rella CW (2009b) Cavity ring-down spectroscopy versus high-temperature conversion isotope ratio mass spectrometry: a case study on $\delta^2\text{H}$ and $\delta^{18}\text{O}$ of pure water samples and alcohol/water mixtures. *Rapid Comm Mass Spectrom* 23:1879–1884
- Brand W (2002) Mass spectrometer hardware for analyzing stable isotope ratios. In: de Groot P (ed) *Handbook of stable isotope analytical techniques*. Elsevier, New York
- Bremner JM, Keeney DR (1966) Determination and isotope ratio analysis of different forms of nitrogen in soils. III. *Soil Sci Soc Am Proc* 30:577–582
- Brennecke GA, Wasylenko LE, Bargar JR, Weyer S, Anbar AD (2011) Uranium isotope fractionation during adsorption to Mn-oxyhydroxides. *Environ Sci Technol* 45:1370–1375
- Brennikmeijer CAM, Kraft MP, Mook WG (1983) Oxygen isotope fractionation between CO_2 and H_2O . *Isotope Geosci* 1:181–190

- Brooker R, Blundy J, James R (2004) Trace element and Li isotope systematics in zabargad peridotites: evidence of ancient subduction processes in the Red Sea mantle. *Chem Geol* 212:179–204
- Brunner B, Bernasconi SM, Kleikemper J, Schroth MH (2005) A model of oxygen and sulfur isotope fractionation in sulfate during bacterial sulfate reduction. *Geochim Cosmochim Acta* 69:4773–4785
- Brunner B, Contreras S and 9 others (2013) Nitrogen isotope effects induced by anammox bacteria. *PNAS* 1310488110
- Brüchert V, Knoblauch C, Jörgensen BB (2001) Controls on stable sulfur isotope fractionation during bacterial sulfate reduction in Arctic sediments. *Geochim Cosmochim Acta* 65:763–776
- Bucharenko AI (2001) Magnetic isotope effect: nuclear spin control of chemical reactions. *J Phys Chem A* 105:9995–10011
- Buhl D, Immenhauser A, Smeulders G, Kabiri L, Richter DK (2007) Time series $\delta^{26}\text{Mg}$ analysis in speleothem calcite: kinetic versus equilibrium fractionation, comparison with other proxies and implications for palaeoclimate research. *Chem Geol* 244:715–729
- Burgoyne TW, Hayes JM (1998) Quantitative production of H_2 by pyrolysis of gas chromatographic effluents. *Anal Chem* 70:5136–5141
- Burton KW, Vigier N (2011) Lithium isotopes as tracers in marine and terrestrial environments. In: Baskaran M (ed) *Handbook environment isotope geochemistry*. Springer, New York, pp 41–59
- Busigny V, Bebout GE (2013) Nitrogen in the silicate earth: speciation and isotopic behavior during mineral-fluid interactions. *Elements* 9:353–358
- Butler IB, Archer C, Vance D, Oldroyd A, Rickard D (2005) Fe isotope fractionation on FeS formation in ambient aqueous solution. *Earth Planet Sci Lett* 236:430–442
- Böhlke JK, Sturchio NC, Gu B, Horita J, Brown GM, Jackson WA, Batista J, Hatzinger PB (2005) Perchlorate isotope forensics. *Anal Chem* 77:7838–7842
- Böhm F, Eisenhauer A, Tang J, Dietzel M, Krabbenhöft A, Kisakürek B, Horn C (2012) Strontium isotope fractionation of planktic foraminifera and inorganic calcite. *Geochim Cosmochim Acta* 93:300–314
- Böttcher ME (1996) $^{18}\text{O}/^{16}\text{O}$ and $^{13}\text{C}/^{12}\text{C}$ fractionation during the reaction of carbonates with phosphoric acid: effects of cationic substitution and reaction temperature. *Isotopes Environ Health Stud* 32:299–305
- Böttcher ME, Brumsack HJ, Lange GJ (1998) Sulfate reduction and related stable isotope (^{34}S , ^{18}O) variations in interstitial waters from the eastern Mediterranean. *Proc Ocean Drill Progr, Scientific Res* 160:365–373
- Böttcher ME, Thamdrup B, Vennemann TW (2001) Oxygen and sulfur isotope fractionation during anaerobic bacterial disproportionation of elemental sulfur. *Geochim Cosmochim Acta* 65:1601–1609
- Böttcher M, Geprägs P, Neubert N, von Allmen K, Pretet C, Samankassou E, Nägler Tf (2012) Barium isotope fractionation during experimental formation of the double carbonate $\text{BaMn}(\text{CO}_3)_2$ at ambient temperature. *Isotopes in environmental and health studies*. doi:[10.1080/10256016.2012.673489](https://doi.org/10.1080/10256016.2012.673489)
- Cameron V, Vance D, Archer C, House CH (2009) A biomarker based on the stable isotopes of nickel. *PNAS* 106:10944–10948
- Cameron V, Vance D (2014) Heavy nickel isotope compositions in rivers and oceans. *Geochim Cosmochim Acta* (in press)
- Canfield DE (2001a) Biogeochemistry of sulfur isotopes. *Rev Mineral* 43:607–636
- Canfield DE (2001b) Isotope fractionation by natural populations of sulfate-reducing bacteria. *Geochim Cosmochim Acta* 65:1117–1124
- Canfield DE, Farquhar J, Zerkle AL (2010) High isotope fractionations during sulfate reduction in a low-sulfate euxinic ocean analog. *Geology* 38:415–418
- Canfield DE, Olsen CA, Cox RP (2006) Temperature and istic control of isotope fractionation by a sulfate reducing bacterium. *Geochim Cosmochim Acta* 70:548–561

- Canfield DE, Teske A (1996) Late Proterozoic rise in atmospheric oxygen concentration inferred from phylogenetic and sulphur-isotope studies. *Nature* 382:127–132
- Canfield DE, Thamdrup B (1994) The production of ^{34}S depleted sulfide during bacterial disproportion to elemental sulfur. *Science* 266:1973–1975
- Cardinal D, Gaillardet J, Hughes HJ, Opfergelt S, Andre L (2010) Contrasting silicon isotope signatures in rivers from the Congo Basin and the specific behaviour of organic-rich waters. *Geophys Res Lett* 37:L12403
- Carignan J, Estrade N, Sonke J, Donard O (2009) Odd isotope deficit in atmospheric Hg measured in lichens. *Environ Sci Technol* 43:5660–5664
- Carignan J, Wen H (2007) Scaling NIST SRM 3149 for Se isotope analysis and isotopic variations of natural samples. *Chem Geol* 242:347–350
- Caro G, Papanastassiou DA, Wasserburg GJ (2010) $^{40}\text{K}/^{40}\text{Ca}$ isotopic constraints on the oceanic calcium cycle. *Earth Planet Sci Lett* 296:124–132
- Cartigny P (2005) Stable isotopes and the origin of diamond. *Elements* 1:79–84
- Cartigny P, Boyd SR, Harris JW, Javoy M (1997) Nitrogen isotopes in peridotitic diamonds from Fuxian, China: the mantle signature. *Terra Nova* 9:175–179
- Cartigny P, Marty B (2013) Nitrogen isotopes and mantle geodynamics: the emergence of life and the atmosphere-crust-mantle connection. *Elements* 9:359–366
- Cartwright I, Valley JW (1991) Steep oxygen isotope gradients at marble-metagranite contacts in the NW Adirondacks Mountains, N.Y. *Earth Planet Sci Lett* 107:148–163
- Casciotti KL (2009) Inverse kinetic isotope fractionation during bacterial nitrite oxidation. *Geochim Cosmochim Acta* 73:2061–2076
- Casciotti KL, Sigman DM, Galanter Hastings M, Böhlke JK, Hilkert A (2002) Measurement of the oxygen isotopic composition of nitrate in seawater and freshwater using the denitrifier method. *Anal Chem* 74:4905–4912
- Catanzaro EJ, Murphy TJ (1966) Magnesium isotope ratios in natural samples. *J Geophys Res* 71:1271
- Cenki-Tok B, Chabaux F, Lemarchand D, Schmitt A, Pierret M, Viville D, Bagard M, Stille P (2009) The impact of water-rock interaction and vegetation on calcium isotope fractionation in soil- and stream waters of a small, forested catchment (the Strengbach case). *Geochim Cosmochim Acta* 73:2215–2228
- Cerling TE, Sharp ZD (1996) Stable carbon and oxygen isotope analyses of fossil tooth enamel using laser ablation. *Palaeo Palaeo Palaeoecol* 126:173–186
- Cerling TE, Harris JM (1999) Carbon isotope fractionation between diet and bioapatite in ungulate mammals and implications for ecological and paleocological studies. *Oecologia* 120:347–363
- Chacko T, Cole DR, Horita J (2001) Equilibrium oxygen, hydrogen and carbon fractionation factors applicable to geologic systems. *Rev Mineral Geochem* 43:1–81
- Chacko T, Riciputi LR, Cole DR, Horita J (1999) A new technique for determining equilibrium hydrogen isotope fractionation factors using the ion microprobe: application to the epidote-water system. *Geochim Cosmochim Acta* 63:1–10
- Chakrabarti B, Jacobsen S (2010) Silicon isotopes in the inner solar system: implications for core formation, solar nebula processes and partial melting. *Geochim Cosmochim Acta* 74:6921–6933
- Chan LH, Alt JC, Teagle DAH (2002) Lithium and lithium isotope profiles through the upper oceanic crust: a study of seawater-basalt exchange at ODP Sites 504B and 896A. *Earth Planet Sci Lett* 201:187–201
- Chan LH, Edmond JM, Thompson G (1993) A lithium isotope study of hot-springs and metabasalts from midocean ridge hydrothermal systems. *J Geophys Res* 98:9653–9659
- Charlier BL, Nowell GM, Parkinson IJ, Kelley SP, Pearson DG, Burton KW (2012) High temperature strontium stable isotope behaviour in the early solar system and planetary bodies. *Earth Planet Sci Lett* 329–330:31–40
- Chaussidon M, Albarede F (1992) Secular boron isotope variations in the continental crust: an ion microprobe study. *Earth Planet Sci Lett* 108:229–241

- Chaussidon M, Albarede F, Sheppard SMF (1987) Sulphur isotope heterogeneity in the mantle from ion microprobe measurements of sulphide inclusions in diamonds. *Nature* 330:242–244
- Chaussidon M, Albarede F, Sheppard SMF (1989) Sulphur isotope variations in the mantle from ion microprobe analysis of microsulphide inclusions. *Earth Planet Sci Lett* 92:144–156
- Chaussidon M, Marty B (1995) Primitive boron isotope composition of the mantle. *Science* 269:383–386
- Chen JB, Gaillardet J, Louvat P (2008) Zinc isotopes in the Seine river waters, France: a probe of anthropogenic contamination. *Environ Sci Technol* 42:6494–6501
- Chen JB, Hintelmann H, Feng XB, Dimcock B (2012) Unusual fractionation of both odd and even mercury isotopes in precipitation from Peterborough, ON, Canada. *Geochim Cosmochim Acta* 90:33–46
- Chen H, Nguyen BM, Moynier F (2013b) Zinc isotopic composition of iron meteorites: absence of isotope anomalies and origin of the volatile element depletion. *Meteor Planet Sci* 48:2441–2450
- Chen H, Savage PS, Teng FZ, Helz RT, Moynier F (2013a) Zinc isotopic fractionation during magmatic differentiation and the isotopic composition of bulk Earth. *Earth Planet Sci Lett* 369–370:34–42
- Chen H, Savage PS, Valdes M, Puchtel IS, Day JM, Moreira M, Jackson M, Moynier F (2014) Heterogeneity of calcium isotopes in Earth's mantle. *Goldschmidt 2014 Abstracts*, p 400
- Chetelat B, Gaillardet J, Freydier F (2009) Use of B isotopes as a tracer of anthropogenic emissions in the atmosphere of Paris, France. *Appl Geochem* 24:810–820
- Chiba H, Chacko T, Clayton RN, Goldsmith JR (1989) Oxygen isotope fractionations involving diopside, forsterite, magnetite and calcite: application to geothermometry. *Geochim Cosmochim Acta* 53:2985–2995
- Chmieleff J, Horn I, Steinhöfel G, von Blanckenburg F (2008) In situ determination of precise stable Si isotope ratios by UV-femtosecond laser ablation high-resolution multi-collector ICP-MS. *Chem Geol* 249:155–160
- Claire MW, Kasting JF, Domagal-Goldman SD, Stueken EE, Buick R, Meadows VS (2014) Modeling the signature of sulphur mass-independent fractionation produced in the Archean atmosphere. *Geochim Cosmochim Acta* 141:365–380
- Clayton RN, Anderson P, Gale NH, Gills G, Whitehouse MJ (2002) Precise determination of the isotopic composition of Sn using MC-ICP-MS. *J Anal At Spectrom* 17:1248–1256
- Clayton RN, Epstein S (1958) The relationship between $^{18}\text{O}/^{16}\text{O}$ ratios in coexisting quartz, carbonate and iron oxides from various geological deposits. *J Geol* 66:352–373
- Clayton RN, Goldsmith JR, Mayeda TK (1989) Oxygen isotope fractionation in quartz, albite, anorthite and calcite. *Geochim Cosmochim Acta* 53:725–733
- Clayton RN, Mayeda TK (1963) The use of bromine pentafluoride in the extraction of oxygen from oxides and silicates for isotopic analysis. *Geochim Cosmochim Acta* 27:43–52
- Cloquet C, Carignan J, Lehmann MF, Vanhaecke F (2008) Variation in the isotopic composition of zinc in the natural environment and the use of zinc isotopes in biogeosciences: a review. *Anal Bioanal Chem* 390:451–463
- Cloquet C, Carignan J, Libourel G, Sterckeman T, Perdrix E (2006) Tracing source pollution in soils using cadmium and lead isotopes. *Environ Sci Technol* 40:2525–2530
- Cobert F, Schmitt AD, Bourgeade P, Labolle F, Badot PM, Chabaux F, Stille P (2011) Experimental identification of Ca isotopic fractionations in higher plants. *Geochim Cosmochim Acta* 75:5467–5482
- Cole DR (2000) Isotopic exchange in mineral-fluid systems IV: the crystal chemical controls on oxygen isotope exchange rates in carbonate-H₂O and layer silicate-H₂O systems. *Geochim Cosmochim Acta* 64:921–933
- Coleman ML, Sheppard TJ, Durham JJ, Rouse JE, Moore GR (1982) Reduction of water with zinc for hydrogen isotope analysis. *Anal Chem* 54:993–995
- Cook DL, Wadhwa M, Clayton RN, Dauphas N, Janney PE, Davis AM (2007) Mass-dependent fractionation of nickel isotopes in meteoritic metal. *Meteorit Planet Sci* 42:2067–2077

- Coplen TB et al (2002) Isotope abundance variations of selected elements. *Pure Appl Chem* 74:1987–2017
- Coplen TB, Hanshaw BB (1973) Ultrafiltration by a compacted clay membrane. I. Oxygen and hydrogen isotopic fractionation. *Geochim Cosmochim Acta* 37:2295–2310
- Coplen TB, Kendall C, Hopple J (1983) Comparison of stable isotope reference samples. *Nature* 302:236–238
- Craddock PR, Dauphas N (2010) Iron isotopic compositions of geological reference materials and chondrites. *Geostand Geoanal Res* 35:101–123
- Craddock PR, Rouxel OJ, Ball LA, Bach W (2008) Sulfur isotope measurement of sulfate and sulfide by high-resolution MC-ICP-MS. *Chem Geol* 253:102–113
- Craig H (1961a) Isotopic variations in meteoric waters. *Science* 133:1702–1703
- Craig H (1961b) Standard for reporting concentrations of deuterium and oxygen-18 in natural waters. *Science* 133:1833–1834
- Criss RE, Gregory RT, Taylor HP (1987) Kinetic theory of oxygen isotopic exchange between minerals and water. *Geochim Cosmochim Acta* 51:1099–1108
- Criss RE (1999) Principles of stable isotope distribution. Oxford University Press, Oxford
- Croal LR, Johnson CM, Beard BL, Newman DK (2004) Iron isotope fractionation by Fe(II)-oxidizing photoautotrophic bacteria. *Geochim Cosmochim Acta* 68:1227–1242
- Crosby HA, Johnson CM, Roden EE, Beard BL (2005) Fe(II)-Fe(III) electron/atom exchange as a mechanism for Fe isotope fractionation during dissimilatory iron oxide reduction. *Environ Sci Tech* 39:6698–6704
- Crosby HA, Roden EE, Johnson CE, Beard BL (2007) The mechanisms of iron isotope fractionation produced during dissimilatory Fe(III) reduction by *Shewanella putrefaciens* and *Geobacter sulfurreducens*. *Geobiology* 5:169–189
- Crowe DE, Valley JW, Baker KL (1990) Micro-analysis of sulfur isotope ratios and zonation by laser microprobe. *Geochim Cosmochim Acta* 54:2075–2092
- Crowley SF (2010) Effect of temperature on the oxygen isotope composition of carbon dioxide ($\delta^{18}\text{O}_{\text{CO}_2}$) prepared from carbonate minerals by reaction with polyphosphoric acid: an example of the rhombohedral CaCO_3 - MgCO_3 group minerals. *Geochim Cosmochim Acta* 74:6406–6421
- Crowson RA, Showers WJ, Wright EK, Hoering TC (1991) Preparation of phosphate samples for oxygen isotope analysis. *Anal Chem* 63:2397–2400
- Czamanske GK, Rye RO (1974) Experimentally determined sulfur isotope fractionations between sphalerite and galena in the temperature range 600 °C to 275 °C. *Econ Geol* 69:17–25
- Dahl TW, Anbar AD, Gordon GW, Rosing MT, Frei R, Canfield DE (2010a) The behavior of molybdenum and its isotopes across the chemocline and in the sediments of sulfidic Lake Cadagno, Switzerland. *Geochim Cosmochim Acta* 74:144–163
- Dahl TW, Canfield DE, Rosing MT, Frei RE, Gordon GW, Knoll AH, Anbar AD (2011) Molybdenum evidence for expansive sulfidic water masses in ≈ 750 Ma oceans. *Earth Planet Sci Lett* 311:264–274
- Dahl TW, Hammarlund EU et al (2010b) Devonian rise in atmospheric oxygen correlated to the radiations of terrestrial plants and large predatory fish. *PNAS* 107:17911–17915
- Dauphas N, Craddock PR, Asimov PD, Bennett VC, Nutman A, Ohnenstetter D (2009a) Iron isotopes may reveal the redox conditions of mantle melting from Archean to Present. *Earth Planet Sci Lett* 288:255–267
- Dauphas N, Pourmand A, Teng FZ (2009b) Routine isotopic analysis of iron by HR-MC-ICPMS: how precise and how accurate? *Chem Geol* 267:175–184
- Dauphas N, Roskosz M et al (2012) A general moment NRIXS approach to the determination of equilibrium Fe isotope fractionation factors: application to goethite and jarosite. *Geochim Cosmochim Acta* 94:254–275
- Dauphas N, Rouxel O (2006) Mass spectrometry and natural variations in iron isotopes. *Mass Spectrom Rev* 25:515–550

- De Laeter JR, Böhlke JK, De Bièvre P, Hidaka H, Peiser HS, Rosman KJR, Taylor PD (2003) Atomic weights of the elements: review 2000 (IUPAC Technical Report). *Pure Appl Chem* 75:683–2000
- De La Rocha C (2003) Silicon isotope fractionation by marine sponges and the reconstruction of the silicon isotope composition of ancient deep water. *Geology* 31:423–426
- De La Rocha CL, Brzezinski MA, De Niro MJ (1997) Fractionation of silicon isotopes by marine diatoms during biogenic silica formation. *Geochim Cosmochim Acta* 61:5051–5056
- De La Rocha CL, Brzezinski MA, De Niro MJ, Shemesh A (1998) Silicon-isotope composition of diatoms as an indicator of past oceanic change. *Nature* 395:680–683
- De La Rocha CL, De Paolo DJ (2000) Isotopic evidence for variations in the marine calcium cycle over the Cenozoic. *Science* 289:1176–1178
- De Souza GF, Reynolds B, Kiczka M, Bourdon B (2010) Evidence for mass-dependent isotopic fractionation of strontium in a glaciated granitic watershed. *Geochim Cosmochim Acta* 74:2596–2614
- DeNiro MJ, Epstein S (1977) Mechanism of carbon isotope fractionation associated with lipid synthesis. *Science* 197:261–263
- DePaolo D (2004) Calcium isotope variations produced by biological, kinetic, radiogenic and nucleosynthetic processes. *Rev Mineral Geochem* 55:255–288
- DePaolo D (2011) Surface kinetic model for isotopic and trace element fractionation during precipitation of calcite from aqueous solution. *Geochim Cosmochim Acta* 75:1039–1056
- Demarest MS, Brzezinski MA, Beucher CP (2009) Fractionation of silicon isotopes during biogenic silica dissolution. *Geochim Cosmochim Acta* 73:5572–5583
- Desaulniers DE, Kaufmann RS, Cherry JO, Bentley HW (1986) ^{37}Cl – ^{35}Cl variations in a diffusion-controlled groundwater system. *Geochim Cosmochim Acta* 50:1757–1764
- Dideriksen K, Baker JA, Stipp SLS (2008) Equilibrium Fe isotope fractionation between inorganic aqueous Fe(III) and the siderophore complex, Fe(III)-desferrioxamine B. *Earth Planet Sci Lett* 269:280–290
- Ding T, Ma GR, Shui MX, Wan DF, Li RH (2005) Silicon isotope study on rice plants from the Zhejiang province, China. *Chem Geol* 218:41–50
- Ding T, Wan D, Wang C, Zhang F (2004) Silicon isotope compositions of dissolved silicon and suspended matter in the Yangtze River, China. *Geochim Cosmochim Acta* 68:205–216
- Ding TP, Zhou JX, Wan DF, Chen ZY, Wang CY, Zhang F (2008) Silicon isotope fractionation in bamboo and its significance to the biogeochemical cycle of silicon. *Geochim Cosmochim Acta* 72:1381–1395
- Ding T et al (1996) Silicon isotope geochemistry. Geological Publishing House, Beijing
- Dohmen R, Kasemann SA, Coogan L, Chakraborty S (2010) Diffusion of Li in olivine. Part I: Experimental observations and a multi species diffusion model. *Geochim Cosmochim Acta* 74:274–292
- Dos Santos Pinheiro GM, Poitras F, Sondag F, Cochonneau G, Cruz Vieira L (2014) Contrasting iron isotopic compositions in river suspended particulate matter: the Negro and the Amazon annual river cycles. *Earth Planet Sci Lett* 394:168–178
- Dossing LN, Dideriksen K, Stipp SL, Frei R (2011) Reduction of hexavalent chromium by ferrous iron: a process of chromium isotope fractionation and its relevance to natural environments. *Chem Geol*
- Douthitt CB (1982) The geochemistry of the stable isotopes of silicon. *Geochim Cosmochim Acta* 46:1449–1458
- Driesner T (1997) The effect of pressure on deuterium-hydrogen fractionation in high-temperature water. *Science* 277:791–794
- Driesner T, Seward TM (2000) Experimental and simulation study of salt effects and pressure/density effects on oxygen and hydrogen stable isotope liquid-vapor fractionation for 4–5 molal aqueous NaCl and KCl solutions to 400° C. *Geochim Cosmochim Acta* 64:1773–1784
- Dugan JP, Borthwick J, Harmon RS, Gagnier MA, Glahn JE, Kinsell EP, McLeod S, Viglino JA (1985) Guadine hydrochloride method for determination of water oxygen isotope ratios and

- the oxygen-18 fractionation between carbon dioxide and water at 25 °C. *Anal Chem* 57:1734–1736
- Dziony W, Horn I, Lattard D, Koepke J, Steinhoefel G, Schuessler J, Holtz F (2014) In-situ Fe isotope ratio determination in Fe-Ti oxides and sulphides from drilled gabbros and basalt from the IODP Hole 1256D in the eastern equatorial Pacific. *Chem Geol* 363:101–113
- Eastoe CJ, Gilbert JM, Kaufmann RS (1989) Preliminary evidence for fractionation of stable chlorine isotopes in ore-forming hydrothermal deposits. *Geology* 17:285–288
- Eastoe CJ, Guilbert JM (1992) Stable chlorine isotopes in hydrothermal processes. *Geochim Cosmochim Acta* 56:4247–4255
- Eastoe CJ, Long A, Knauth LP (1999) Stable chlorine isotopes in the Palo Duro basin, Texas: evidence for preservation of Permian evaporate brines. *Geochim Cosmochim Acta* 63:1375–1382
- Eastoe CJ, Long A, Land LS, Kyle JR (2001) Stable chlorine isotopes in halite and brine from the Gulf Coast Basin: brine genesis and evolution. *Chem Geol* 176:343–360
- Eastoe CJ, Peryt TM, Petrychenko OY, Geisler-Cussey D (2007) Stable chlorine isotopes in Phanerozoic evaporates. *Appl Geochem* 22:575–588
- Egan KE, Rickaby RE, Leng H, Hendry KE, Hemoso M, Sloane HJ, Bostock H, Halliday RN (2012) Diatom silicon isotopes as a proxy for silicic acid utilisation: a southern ocean core top calibration. *Geochim Cosmochim Acta* 96: 174–192
- Eggenkamp HGM, Coleman M (2000) Rediscovery of classical methods and their application to the measurement of stable bromine isotopes in natural samples. *Chem Geol* 167:393–402
- Eggenkamp HGM, Kreulen R, Koster van Groos AF (1995) Chlorine stable isotope fractionation in evaporates. *Geochim Cosmochim Acta* 59:5169–5175
- Eggenkamp HGM (1994) $\delta^{37}\text{Cl}$: the geochemistry of chlorine isotopes. Thesis, University of Utrecht
- Eggenkamp HGM (2014) The geochemistry of stable chlorine and bromine isotopes. Springer, New York
- Ehrlich S, Butler I, Halicz L, Rickard D, Oldroyd A, Matthews A (2004) Experimental study of the copper isotope fractionation between aqueous Cu(II) and covellite, CuS. *Chem Geol* 209:259–269
- Eisenhauer A et al (2004) Proposal for an international agreement on Ca notation as result of the discussion from the workshops on stable isotope measurements in Davos (Goldschmidt 2002) and Nice (EUG 2003). *Geostand Geoanal Res* 28:149–151
- Eisenhauer A, Kisakürek B, Böhm F (2009) Marine calcification: an alkali earth metal isotope perspective. *Elements* 5:365–368
- Eldridge CS, Compston W, Williams IS, Both RA, Walshe JL, Ohmoto H (1988) Sulfur isotope variability in sediment hosted massive sulfide deposits as determined using the ion microprobe SHRIMP. I. An example from the Rammelsberg ore body. *Econ Geol* 83:443–449
- Eldridge CS, Williams IS, Walshe JL (1993) Sulfur isotope variability in sediment hosted massive sulfide deposits as determined using the ion microprobe SHRIMP. II. A study of the H.Y.C. deposit at McArthur River, Northern Territory, Australia. *Econ Geol*. 88:1–26
- Elliott T, Jeffcoate AB, Bouman C (2004) The terrestrial Li isotope cycle: light-weight constraints on mantle convection. *Earth Planet Sci Lett* 220:231–245
- Ellis AS, Johnson TM, Bullen TD (2002) Chromium isotopes and the fate of hexavalent chromium in the environment. *Science* 295:2060–2062
- Ellis AS, Johnson TM, Bullen TD (2004) Using chromium stable isotope ratios to quantify Cr(VI) reduction: lack of sorption effects. *Environ Sci Technol* 38:3604–3607
- Emrich K, Ehhalt DH, Vogel JC (1970) Carbon isotope fractionation during the precipitation of calcium carbonate. *Earth Planet Sci Lett* 8:363–371
- Engstrom E, Rodushkin I, Baxter DC, Ohlander B (2006) Chromatographic purification for the determination of dissolved silicon isotopic compositions in natural waters by high-resolution multicollector inductively coupled mass spectrometry. *Anal Chem* 78:250–257

- Estrade N, Carignan J, Sonke JE, Donard O (2009) Mercury isotope fractionation during liquid-vapor evaporation experiments. *Geochim Cosmochim Acta* 73:2693–2711
- Eugster O, Tera F, Wasserburg GJ (1969) Isotopic analyses of barium in meteorites and in terrestrial samples. *J Geophys Res* 74:3897–3908
- Fantle MS (2010) Evaluating the Ca isotope proxy. *Am J Sci* 310:194–210
- Fantle MS, de Paolo DJ (2005) Variations in the marine Ca cycle over the past 20 million years. *Earth Planet Sci Lett* 237:102–117
- Fantle MS, Tipper ET (2014) Calcium isotopes in the global biogeochemical Ca cycle: implications for development of a Ca isotope proxy. *Earth Sci Rev* 129:148–177
- Farkas J, Buhl D, Blenkinsop J, Veizer J (2007) Evolution of the oceanic calcium cycle during the late Mesozoic: evidence from $\delta^{44/40}\text{Ca}$ of marine skeletal carbonates. *Earth Planet Sci Lett* 253:96–111
- Farkas J, Chrastny V, Novak M, Cadkova E, Pasava J, Chakrabarti R, Jacobsen S, Ackerman L, Bullen TD (2013) Chromium isotope variations ($\delta^{53/52}\text{Cr}$) in mantle-derived sources and their weathering products: implications for environmental studies and the evolution of $\delta^{53/52}\text{Cr}$ in the Earth's mantle over geologic time. *Geochim Cosmochim Acta* 123:74–92
- Farquhar J, Bao H, Thiemens M (2000) Atmospheric influence of Earth's earliest sulfur cycle. *Science* 289:756–759
- Farquhar J, Day JM, Hauri EH (2013) Anomalous sulphur isotopes in plume lavas reveal deep mantle storage of Archaean crust. *Nature* 496:490–493
- Farquhar GD, Ehleringer JR, Hubick KT (1989) Carbon isotope discrimination and photosynthesis. *Ann Rev Plant Physiol Plant Mol Biol* 40:503–537
- Farquhar J, Johnston DT, Wing BA, Habicht KS, Canfield DE, Airieau S, Thiemens MH (2003) Multiple sulphur isotope interpretations for biosynthetic pathways: implications for biological signatures in the sulphur isotope record. *Geobiology* 1:27–36
- Farquhar J, Kim ST, Masterson A (2007) Implications from sulfur isotopes of the Nakhla meteorite for the origin of sulfate on Mars. *Earth Planet Sci Lett* 264:1–8
- Farrell JW, Pedersen TF, Calvert SE, Nielsen B (1995) Glacial-interglacial changes in nutrient utilization in the equatorial Pacific Ocean. *Nature* 377:514–517
- Fehr MA, Rehkämper M, Halliday AN (2004) Application of MC-ICP-MS to the precise determination of tellurium isotope compositions in chondrites, iron meteorites and sulphides. *Inter J Mass Spectr* 232:83–94
- Feng C, Qin T, Huang S, Wu Z, Huang F (2014) First principles investigations of equilibrium calcium isotope fractionation between clinopyroxene and Ca-doped orthopyroxene. *Geochim Cosmochim Acta* 143:132–142
- Fiebig J, Hoefs J (2002) Hydrothermal alteration of biotite and plagioclase as inferred from intragranular oxygen isotope- and cation-distribution patterns. *Eur J Mineral* 14:49–60
- Fietzke J, Eisenhauer A et al (2004) Direct measurement of $^{44}\text{Ca}/^{40}\text{Ca}$ ratios nby MC-ICP-MS using the cool plasma technique. *Chem Geol* 206:11–20
- Fietzke J, Eisenhauer A (2006) Determination of temperature-dependent stable strontium isotope ($^{88}\text{Sr}/^{86}\text{Sr}$) fractionation via bracketing standard MC-ICP-MS. *Geochem Geophys Geosys* 7(8). doi:[10.1029/2006GC001243](https://doi.org/10.1029/2006GC001243)
- Fogel ML, Cifuentes LA (1993) Isotope fractionation during primary production. In: Engel MH, Macko SA (eds) *Organic geochemistry*. Plenum Press, New York, pp 73–98
- Fornadel AP, Spry GP, Jackson SE, Mathur RD, Chapman JB, Girard I (2014) Methods for the determination of stable Te isotopes of minerals in the system Au-Ag-Te by MC-ICP-MS. *J Anal At Spectrom* 29:623–637
- Foster GI, Pogge von Strandmann PA, Rae JW (2010) Boron and magnesium isotopic compositions of seawater. *Geochem Geophys Geosys* 11. doi:[10.1029/2010GC003201](https://doi.org/10.1029/2010GC003201)
- Freeman KH (2001) Isotopic biogeochemistry of marine organic carbon. *Rev Mineral Geochem* 43:579–605

- Frei R, Gaucher C, Dossing LN, Sial AN (2011) Chromium isotopes in carbonates—a tracer for climate change and for reconstructing the redox state of ancient seawater. *Earth Planet Sci Lett* 312:114–125
- Frei R, Gaucher C, Poulton SW, Canfield DE (2009) Fluctuations in Precambrian atmospheric oxygenation recorded by chromium isotopes. *Nature* 461:250–253
- Frei R, Poiret D, Frei KM (2014) Weathering on land and transport of chromium to the ocean in a subtropical region (Misiones, NW Argentina): a chromium stable isotope perspective. *Chem Geol* 381:110–124
- Frei R, Polat A (2013) Chromium isotope fractionation during oxidative weathering—implications from the study of a paleoproterozoic (ca. 1.9 Ga) paleosol, Schreiber Beach, Ontario, Canada. *Precam Res* 224:434–453
- Friedman I (1953) Deuterium content of natural waters and other substances. *Geochim Cosmochim Acta* 4:89–103
- Friedrich AJ, Beard BL, Scherer MM, Johnson CM (2014) Determination of the Fe(II) aq-magnetite equilibrium iron isotope fractionation factor using the three-isotope method and a multi-direction approach to equilibrium. *Earth Planet Sci Lett* 391:77–86
- Fritz P, Basharmel GM, Drimmie RJ, Ibsen J, Qureshi RM (1989) Oxygen isotope exchange between sulphate and water during bacterial reduction of sulphate. *Chem Geol* 79:99–105
- Fry B, Ruf W, Gest H, Hayes JM (1988) Sulphur isotope effects associated with oxidation of sulfide by O₂ in aqueous solution. *Chem Geol* 73:205–210
- Fujii T, Moynier F, Dauphas N, Abe M (2011b) Theoretical and experimental investigation of nickel isotope fractionation in species relevant to modern and ancient oceans. *Geochim Cosmochim Acta* 75:469–482
- Fujii T, Moynier F, Pons ML, Albarede F (2011a) The origin of Zn isotope fractionation in sulfides. *Geochim Cosmochim Acta* 75:7632–7643
- Gagnevin D, Boyce AJ, Barrie CD, Menuge JF, Blakeman RJ (2012) Zn, Fe, and S isotope fractionation in a large hydrothermal system. *Geochim Cosmochim Acta* 88:183–198
- Galimov EM (2006) Isotope organic geochemistry. *Org Geochem* 37:1200–1262
- Galimov EM (1985a) The biological fractionation of isotopes. Academic Press Inc, Orlando
- Gall L, Williams HM, Siebert C, Halliday AN, Herrington RJ, Hein JR (2013) Nickel isotopic compositions of ferromanganese crusts and the constancy of deep ocean inputs and continental weathering effects. *Earth Planet Sci Lett*
- Galy A et al (2003) Magnesium isotope heterogeneity of the isotopic standard SRM980 and new reference materials for magnesium-isotope-ratio measurements. *J Anal At Spectr* 18:1352–1356
- Galy A, Bar-Matthews M, Halicz L, O’Nions RK (2002) Mg isotopic composition of carbonate: insight from speleothem formation. *Earth Planet Sci Lett* 201:105–115
- Galy A, Belshaw NS, Halicz L, O’Nions RK (2001) High-precision measurement of magnesium isotopes by multiple-collector inductively coupled plasma mass spectrometry. *Inter J Mass Spectr* 208:89–98
- Ganeshram RS, Pedersen TF, Calvert SE, McNeill GW, Fontugue MR (2000) Glacial-interglacial variability in denitrification in the world’s oceans: causes and consequences. *Paleoceanography* 15:361–376
- Gao Y, Casey JF (2011) Lithium isotope composition of ultramafic geological reference materials JP-1 and DTS-2. *Geostand Geoanal Res* 36:75–81
- Gao Y, Vils F et al (2012) Downhole variation of lithium and oxygen isotopic compositions of oceanic crust at East Pacific Rise, ODP Site 1256. *Geochem Geophys Geosystems* 13. doi:[10.1029/2012GC004207](https://doi.org/10.1029/2012GC004207)
- Garlick GD (1966) Oxygen isotope fractionation in igneous rocks. *Earth Planet Sci Lett* 1:361–368
- Gault-Ringold M, Adu T, Stirling C, Frew RD, Hunter KA (2012) Anomalous biogeochemical behaviour of cadmium in subantarctic surface waters: mechanistic constraints from cadmium isotopes. *Earth Planet Sci Lett* 341–344:94–103

- Gehre M, Hoefling R, Kowski P, Strauch G (1996) Sample preparation device for quantitative hydrogen isotope analysis using chromium metal. *Anal Chem* 68:4414–4417
- Gehrke GE, Blum JD, Meyers PA (2009) The geochemical behaviour and isotope composition of Hg in a mid-Pleistocene western Mediterranean sapropel. *Geochim Cosmochim Acta* 73:1651–1665
- Gelabert A, Pokrovsky OS, Viers J, Schott J, Boudou A, Feurtet-Mazel A (2006) Interaction between zinc and marine diatom species: surface complexation and Zn isotope fractionation. *Geochim Cosmochim Acta* 70:839–857
- Georg RB, Halliday AN, Schauble EA, Reynolds BC (2007) Silicon in the Earth's core. *Nature* 447:1102–1106
- Georg RB, Reynolds BC, Frank M, Halliday AN (2006) Mechanisms controlling the silicon isotopic compositions of river water. *Earth Planet Sci Lett* 249:290–306
- Georg RB, Zhu C, Reynolds BC, Halliday AN (2009) Stable silicon isotopes of groundwater, feldspars and clay coating in the Navajo sandstone aquifer, Black Mesa, Arizona, USA. *Geochim Cosmochim Acta* 73:2229–2241
- Geske A, Goldstein RH, Mavromatis V, Richter DK, Buhl D, Kluge T, John CM, Immenhauser A (2015) The magnesium isotope ($\delta^{26}\text{Mg}$) signature of dolomites. *Geochim Cosmochim Acta* 149:131–151
- Ghosh S, Schauble EA, Lacrampe Coulome G, Blum JD, Bergquist BA (2013) Estimation of nuclear volume dependent fractionation of mercury isotopes in equilibrium liquid-vapor evaporation experiment. *Chem Geol* 366:5–12
- Giesenmann A, Jäger HA, Norman AL, Krouse HR, Brand WA (1994) On-line sulphur isotope determination using an elemental analyzer coupled to a mass spectrometer. *Anal Chem* 66:2816–2819
- Giletti BJ (1985) The nature of oxygen transport within minerals in the presence of hydrothermal water and the role of diffusion. *Chem Geol* 53:197–206
- Godfrey JD (1962) The deuterium content of hydrous minerals from the East Central Sierra Nevada and Yosemite National Park. *Geochim Cosmochim Acta* 26:1215–1245
- Goldhaber MB, Kaplan IR (1974) The sedimentary sulfur cycle. In: Goldberg EB (ed) *The sea*, vol IV. Wiley and Sons, New York
- Gordon GW, Lyons TW, Arnold GL, Roe J, Sageman BB, Anbar AD (2009) When do black shales tell molybdenum isotope tales? *Geology* 37:535–538
- Graham CM, Harmon RS, Sheppard SMF (1984) Experimental hydrogen isotope studies: hydrogen isotope exchange between amphibole and water. *Am Mineral* 69:128–138
- Graham CM, Sheppard SMF, Heaton THE (1980) Experimental hydrogen isotope studies. I. Systematics of hydrogen isotope fractionation in the systems epidote-H₂O, zoisite-H₂O and AlO(OH)-H₂O. *Geochim Cosmochim Acta* 44:353–364
- Greber ND, Hofmann BD, Voegelin AR, Villa IM, Nägler TF (2011) Mo isotope compositions in Mo-rich high- and low-T hydrothermal systems from the Swiss Alps. *Geochim Cosmochim Acta* 75:6600–6609
- Greber ND, Pettke T, Nägler TF (2014) Magmatic-hydrothermal molybdenum isotope fractionation and its relevance to the igneous crustal signature. *Lithos* 190–191:104–110
- Gregory RT, Criss RE, Taylor HP (1989) Oxygen isotope exchange kinetics of mineral pairs in closed and open systems: applications to problems of hydrothermal alteration of igneous rocks and Precambrian iron formations. *Chem Geol* 75:1–42
- Griffith EM, Paytan A, Eisenhauer A, Bullen TD, Thomas E (2011) Seawater calcium isotope ratios across the Eocene-Oligocene transition. *Geology* 39:683–686
- Griffith EM, Paytan A, Kozdon R, Eisenhauer A, Ravelo AC (2008a) Influences on the fractionation of calcium isotopes in planktonic foraminifera. *Earth Planet Sci Lett* 268:124–136
- Griffith EM, Payton A, Caldeira K, Bullen TD, Thomas E (2008c) A dynamic marine calcium cycle during the past 28 million years. *Science* 322:1671–1674
- Griffith EM, Schauble EA, Bullen TD, Paytan A (2008b) Characterization of calcium isotopes in natural and synthetic barite. *Geochim Cosmochim Acta* 72:5641–5658

- Grossman EL, Ku T-L (1986) Oxygen and carbon isotope fractionation in biogenic aragonite: temperature effects. *Chem Geol* 59:59–74
- Gueguen B, Rouxel O, Ponzevera E, Bekker A, Fouquet Y (2013) Nickel isotope variations in terrestrial silicate rocks and geological reference materials measured by MC-ICP-MS. *Geostand Geoanal Res* 37:297–317
- Guelke M, von Blanckenburg F (2007) Fractionation of stable iron isotopes in higher plants. *Environ Sci Technol* 41:1896–1901
- Guelke M, von Blanckenburg F, Schoenberg R, Staubwasser M, Stuetzel H (2010) Determining the stable Fe isotope signature of plant-available iron in soils. *Chem Geol* 277:269–280
- Guelke-Stelling M, von Blanckenburg F (2012) Fe isotope fractionation caused by translocation of iron during growth of bean and oat as models of strategy I and II plants. *Plant Soil* 352:217–231
- Guerrot C, Millot R, Robert M, Negrel P (2011) Accurate and high-precision determination of boron isotopic ratios at low concentration by MC-ICP-MS (Neptune). *Geostand Geoanal Res* 35:275–284
- Guilbaud R, Butler IB, Ellam RM (2011) Abiotic pyrite formation produces a large Fe isotope fractionation. *Science* 332:1548–1551
- Gussone N et al (2003) Model for kinetic effects on calcium isotope fractionations ($\delta^{44}\text{Ca}$) in inorganic aragonite and cultured planktonic foraminifera. *Geochim Cosmochim Acta* 67:1375–1382
- Gussone N et al (2005) Calcium isotope fractionation in calcite and aragonite. *Geochim Cosmochim Acta* 69:4485–4494
- Habicht KS, Canfield DE (1997) Sulfur isotope fractionation during bacterial sulfate reduction in organic-rich sediments. *Geochim Cosmochim Acta* 61:5351–5361
- Habicht KS, Canfield DE (2001) Isotope fractionation by sulfate-reducing natural populations and the isotopic composition of sulfide in marine sediments. *Geology* 29:555–558
- Haendel D, Mühle K, Nitzsche HIM, Stiehl G, Wand U (1986) Isotopic variations of the fixed nitrogen in metamorphic rocks. *Geochim Cosmochim Acta* 50:749–758
- Halevy I, Johnston DT, Schrag DP (2010) Explaining the structure of the Archean mass-independent sulfur isotope record. *Science* 329:204–207
- Halicz L, Galy A, Belshaw N et al (1999) High-precision measurement of calcium isotopes in carbonates and related materials by multiple collector inductively coupled plasma mass spectrometry (MC-ICP-MS). *J Anal At Spectr* 14:1835–1838
- Halicz L, Segal I, Fruchter N, Stein M, Lazar B (2008b) Strontium stable isotopes fractionate in the soil environment? *Earth Planet Sci Lett* 272:405–411
- Halicz L, Yang L, Teplyakov N, Burg A, Sturgeon R, Kolodny Y (2008a) High precision determination of chromium isotope ratios in geological samples by MC-ICP-MS. *J Anal At Spectrom* 23:1622–1627
- Han R, Qin L, Brown ST, Christensen JN, Beller HR (2012) Differential isotopic fractionation during Cr(VI) reduction by an aquifer-derived bacterium under aerobic versus denitrifying conditions. *Appl Environ Microbiol* 78:2462–2464
- Handler MR, Baker JA, Schiller M, Bennett VC, Yaxley GM (2009) Magnesium stable isotope composition of Earth's upper mantle. *Earth Planet Sci Lett* 282:306–313
- Hannah JL, Stein HJ, Wieser ME, de Laeter JR, Varner MD (2007) Molybdenum isotope variations in molybdenite: vapor transport and Rayleigh fractionation of Mo. *Geology* 35:703–706
- Harouaka K, Eisenhauer A, Fantle MS (2014) Experimental investigation of Ca isotopic fractionation during abiotic gypsum precipitation. *Geochim Cosmochim Acta* 129:157–176
- Harrison AG, Thode HG (1957a) Kinetic isotope effect in chemical reduction of sulphate. *Faraday Soc Trans* 53:1648–1651
- Harrison AG, Thode HG (1957b) Mechanism of the bacterial reduction of sulphate from isotope fractionation studies. *Faraday Soc Trans* 54:84–92
- Hastings MG, Jarvis JC, Steig EJ (2009) Anthropogenic impacts on nitrogen isotopes of ice-core nitrate. *Science* 324:1238

- Hastings MG, Casciotti KL, Elliott EM (2013) Stable isotopes as tracers of anthropogenic nitrogen sources, deposition, and impacts. *Elements* 9: 339–34
- Haustein M, Gillis C, Pernicka E (2010) Tin isotopy – a new method for solving old questions. *Archaeometry* 52:816–832
- Hayes JM (1993) Factors controlling ^{13}C contents of sedimentary organic compounds: principle and evidence. *Mar Geol* 113:111–125
- Hayes JM, Strauss H, Kaufman AJ (1999) The abundance of ^{13}C in marine organic matter and isotopic fractionation in the global biogeochemical cycle of carbon during the past 800 Ma. *Chem Geol* 161:103–125
- Hayes JM (2001) Fractionation of carbon and hydrogen isotopes in biosynthetic processes. In: Valley JW, Cole DR (eds) *Stable isotope geochemistry*. *Rev Mineral Geochem* 43:225–277
- He Y, Ke S, Teng FZ, Wang T, Wu H, Lu Y, Li S (2015) High precision iron isotope analysis of geological standards by high resolution MC-ICPMS. *Geostand Geoanal Res* (in press)
- Heaton THE (1986) Isotopic studies of nitrogen pollution in the hydrosphere and atmosphere: a review. *Chem Geol* 59:87–102
- Heck PR, Huberty JM, Kita NT, Ushikubo T, Kozdon R, Valley JW (2011) SIMS analysis of silicon and oxygen isotope ratios for quartz from Archean and Paleoproterozoic banded iron formations. *Geochim Cosmochim Acta* 75:5879–5891
- Heimann A, Beard BL, Johnson CM (2008) The role of volatile exsolution and sub-solidus fluid/rock interactions in producing high $^{56}\text{Fe}/^{54}\text{Fe}$ ratios in siliceous igneous rocks. *Geochim Cosmochim Acta* 72:4379–4396
- Hemming NG, Hanson GN (1992) Boron isotopic composition in modern marine carbonates. *Geochim Cosmochim Acta* 56:537–543
- Hendry KR, Andersen MB (2013) The zinc isotopic composition of siliceous marine sponges: investigating nature's sediment traps. *Chem Geol* 354:33–41
- Hendry KR, Georg RB, Rickaby R, Robinson LR, Halliday AN (2010) Deep ocean nutrients during the last glacial maximum deduced from sponge silicon isotopic compositions. *Earth Planet Sci Lett* 292:290–300
- Herbel MJ, Johnson TM, Oremland RS, Bullen TD (2000) Fractionation of selenium isotopes during bacterial respiratory reduction of selenium oxyanions. *Geochim Cosmochim Acta* 64:3701–3710
- Herrmann AD, Kendall B, Algeo TJ, Gordon GW, Wasylenki LE, Anbar AD (2012) Anomalous molybdenum isotope trends in Upper Pennsylvanian euxinic facies: significance for the use of $\delta^{98}\text{Mo}$ as a global marine redox proxy. *Chem Geol* 324–325:87–98
- Hervig RL, Moore GM, Williams LB, Peacock SM, Holloway JR, Roggensack K (2002) Isotopic and elemental partitioning of boron between hydrous fluid and silicate melt. *Am Mineral* 87:769–774
- Hesse R, Egeberg PK, Frøpe SK (2006) Chlorine stable isotope ratios as tracer for pore-water advection rates in a submarine gas-hydrate field: implication for hydrate concentration. *Geofluids* 6:1–7
- Hettmann K, Marks MA, Kreissig K, Zack T, Wenzel T, Rehkämper M, Jacob DE, Markl G (2014) The geochemistry of Tl and its isotopes during magmatic and hydrothermal processes: the peralkaline Ilimaussaq complex, southwest Greenland. *Chem Geol*
- Heuser A, Eisenhauer A (2008) The calcium isotope composition ($\delta^{44/40}\text{Ca}$) of NIST SRM 915a and NIST SRM 1486. *Geostand Newslett J Geostand Geoanal* 32:311–315
- Hiess J, Condon DJ, McLean N, Noble SR (2012) $^{238}\text{U}/^{235}\text{U}$ systematics in terrestrial uranium-bearing minerals. *Science* 335:1610–1614
- Higgins JA, Schrag DP (2010) Constraining magnesium cycling in marine sediments using magnesium isotopes. *Geochim Cosmochim Acta* 74:5039–5053
- Hill P, Schauble E (2008) Modeling the effects of bond environment on equilibrium iron isotope fractionation in ferric aquo-chloro complexes. *Geochim Cosmochim Acta* 72:1939–1958

- Hill P, Schauble E, Shahar A, Tonui E, Young ED (2009) Experimental studies of equilibrium iron isotope fractionation in ferric aquo-chloro complexes. *Geochim Cosmochim Acta* 73:2366–2381
- Hill P, Schauble E, Young ED (2010) Effects of changing solution chemistry on $\text{Fe}^{3+}/\text{Fe}^{2+}$ isotope fractionation in aqueous Fe-Cl solution. *Geochim Cosmochim Acta* 74:6669–6705
- Hin RC, Schmidt MW, Bourdon B (2012) Experimental evidence for the absence of iron isotope fractionation between metal and silicate liquids at 1GPa and 1250–1300 °C and its cosmochemical consequences. *Geochim Cosmochim Acta* 93:164–181
- Hindshaw RS, Reynolds BC, Wiederhold JG, Kretzschmar R, Bourdon B (2013) Calcium isotope fractionation in alpine plants. *Biogeochemistry* 112:373–388
- Hindshaw RS, Reynolds BC, Wiederhold JG, Kretzschmar R, Bourdon B (2011) Calcium isotopes in a proglacial weathering environment: Damma glacier, Switzerland. *Geochim Cosmochim Acta* 75:106–118
- Hinojosa JL, Brown ST, Chen J, DePaolo DJ, Paytan A, Shen SZ, Payne J (2012) Evidence for end-Permian ocean acidification from calcium isotopes in biogenic apatite. *Geology*
- Hippler D, Buhl D, Witbaard R, Richter DK, Immenhauser A (2009) Towards a better understanding of magnesium-isotope ratios from marine skeletal carbonates. *Geochim Cosmochim Acta* 73:6134–6146
- Hippler D, Eisenhauer A, Nägler TF (2006) Tropical Atlantic SST history inferred from Ca isotope thermometry over the last 140 ka. *Geochim Cosmochim Acta* 70:90–100
- Hitzfeld KL, Gehre M, Richnow HH (2011) A novel online approach to the determination of isotope ratios for organically bound chlorine, bromine and sulphur. *Rapid Commun Mass Spectr* 25:3114–3122
- Hoering T, Parker PL (1961) The geochemistry of the stable isotopes of chlorine. *Geochim Cosmochim Acta* 23:186–199
- Hofmann A, Bekker A, Dirks P, Gueguen B, Rumble D, Rouxel O (2014) Comparing orthomagmatic and hydrothermal mineralization models for komatiite-hosted nickel deposits in Zimbabwe using multiple-sulfur, iron and nickel isotope data. *Miner Deposita* 49:75–100
- Holmden C (2009) Ca isotope study of Ordovician dolomite, limestone, and anhydrite in the Williston basin: Implications for subsurface dolomitization and local Ca cycling. *Chem Geol* 268:180–188
- Holmden C, Belanger N (2010) Ca isotope cycling in a forested ecosystem. *Geochim Cosmochim Acta* 74:995–1015
- Holmstrand H, Unger M, Carrizo D, Andersson P, Gustafsson Ö (2010) Compound specific bromine isotope analysis of brominated diphenyl ethers using GC-ICP-MC-MS. *Rapid Commun Mass Spectr* 24:2135–2142
- Homoky WB, Severmann S, Mills RA, Statham PJ, Fones GR (2011) Pore-fluid Fe isotopes reflect the extent of benthic Fe redox recycling: evidence from continental shelf and deep-sea sediments. *Geology* 37:751–754
- Horita J (1988) Hydrogen isotope analysis of natural waters using an H_2 -water equilibration method: a special implication to brines. *Chem Geol* 72:89–94
- Horita J, Driesner T, Cole DR (1999) Pressure effect on hydrogen isotope fractionation between brucite and water at elevated temperatures. *Science* 286:1545–1547
- Horita J, Wesolowski DJ (1994) Liquid-vapor fractionation of oxygen and hydrogen isotopes of water from the freezing to the critical temperature. *Geochim Cosmochim Acta* 58:3425–3437
- Horita J, Wesolowski DJ, Cole DR (1993) The activity-composition relationship of oxygen and hydrogen isotopes in aqueous salt solutions. I. Vapor-liquid water equilibration of single salt solutions from 50 to 100 °C. *Geochim Cosmochim Acta* 57:2797–2817
- Horner TJ, Schönbachler M, Rehkämpfer M et al (2010) Ferromanganese crusts as archives of deep water Cd isotope composition. *Geochem Geophys Geosyst* 11:Q04001
- Horner T, Rickaby R, Henderson G (2011) Isotopic fractionation of cadmium into calcite. *Earth Planet Sci Lett* 312:243–253

- Horst A, Andersson P, Thornton BJ, Holmstrand H, Wishkerman A, Keppler F, Gustafsson Ö (2014) Stable bromine isotope composition of methyl bromide released from plant matter. *Geochim Cosmochim Acta* 125:186–195
- Horst A, Thornton BJ, Holmstrand H, Andersson P, Crill PM, Gustafsson Ö (2013) Stable bromine isotopic composition of atmospheric CH₃Br. *Tellus Ser B Chem Phys Meteor* 65:21040
- Hu GX, Rumble D, Wang PL (2003) An ultraviolet laser microprobe for the in-situ analysis of multisulfur isotopes and its use in measuring Archean sulphur isotope mass-independent anomalies. *Geochim Cosmochim Acta* 67:3101–3118
- Huang S, Farkas J, Jacobsen SB (2010) Calcium isotopic fractionation between clinopyroxene and orthopyroxene from mantle peridotites. *Earth Planet Sci Lett* 292:337–344
- Huang S, Farkas J, Jacobsen S (2011) Stable calcium isotopic compositions of Hawaiian shield lavas: evidence for recycling of ancient marine carbonates into the mantle. *Geochim Cosmochim Acta* 75:4987–4997
- Huang KJ, Teng FZ, Wei GJ, Ma JL, Bao ZY (2012) Adsorption- and desorption-controlled magnesium isotope fractionation during extreme weathering of basalt in Hainan Island, China. *Earth Planet Sci Lett* 359–360:73–83
- Huang F, Wu Z, Huang S, Wu F (2014) First-principles calculations of equilibrium silicon isotope fractionation among mantle minerals. *Geochim Cosmochim Acta* 140:509–520
- Huh Y, Chan L-H, Zhang L, Edmond JM (1998) Lithium and its isotopes in major world rivers: implications for weathering and the oceanic budget. *Geochim Cosmochim Acta* 62:2039–2051
- Icopini GA, Anbar AD, Ruebush SS, Tien M, Brantley SL (2004) Iron isotope fractionation during microbial reduction of iron: the importance of adsorption. *Geology* 32:205–208
- Ikehata K, Hirata T (2012) Copper isotope characteristics of copper-rich minerals from the Horoman peridotite complex, Hokkaido, Northern Japan. *Econ Geol* 107:1489–1497
- Immenhauser A, Buhl D, Richter D, Niedermayer A, Riechelmann D, Dietzel M, Schulte U (2010) Magnesium isotope fractionation during low-Mg calcite precipitation in a limestone cave – field study and experiments. *Geochim Cosmochim Acta* 74:4346–4364
- Ingraham NL, Criss RE (1998) The effect of vapor pressure on the rate of isotopic exchange between water and vapour. *Chem Geol* 150:287–292
- Izbicki JA, Bullen TD, Martin P, Schroth B (2012) Delta chromium-53/52 isotopic composition of native and contaminated groundwater, Mojave Desert, USA. *Appl Geochem* 27:841–853
- James RH, Palmer MR (2000) The lithium isotope composition of international rock standards. *Chem Geol* 166:319–326
- Jang JH, Mathur R, Liermann LJ, Ruebush S, Brantley SL (2008) An iron isotope signature related to electron transfer between aqueous ferrous iron and goethite. *Chem Geol* 250:40–48
- Javoy M, Pineau F, Delorme H (1986) Carbon and nitrogen isotopes in the mantle. *Chem Geol* 57:41–62
- Jeffcoate AB, Elliott T, Kasemann SA, Ionov D, Cooper K, Brooker R (2007) Li isotope fractionation in peridotites and mafic melts. *Geochim Cosmochim Acta* 71:202–218
- Jeffcoate AB, Elliott T, Thomas A, Bouman C (2004) Precise, small sample size determination of lithium isotope isotopic compositions of geological reference materials and modern seawater by MC-ICP-MS. *Geostand Geoanal Res* 28:161–172
- Jendzejewski N, Eggenkamp HGM, Coleman ML (2001) Characterisation of chlorinated hydrocarbons from chlorine and carbon isotopic compositions: scope of application to environmental problems. *Appl Geochem* 16:1021–1031
- Jia Y (2006) Nitrogen isotope fractionations during progressive metamorphism: A case study from the Paleozoic Cooma metasedimentary complex, southeastern Australia. *Geochim Cosmochim Acta* 70:5201–5214
- Jiang SY, Palmer MR (1998) Boron isotope systematics of tourmaline from granites and tourmalines: a synthesis. *Eur J Mineral* 10:1253–1265

- John SG, Geis RW, Saito MA, Boyle EA (2007a) Zinc isotope fractionation during high-affinity and low-affinity zinc transport by the marine diatom *Thalassiosira oceanica*. *Limnol Oceanogr* 52:2710–2714
- John SG, Park JG, Zhang Z, Boyle EA (2007b) The isotopic composition of some common forms of anthropogenic zinc. *Chem Geol* 245:61–69
- John SG, Rouxel OJ, Craddock PR, Engwall AM, Boyle EA (2008) Zinc stable isotopes in seafloor hydrothermal vent fluids and chimneys. *Earth Planet Sci Lett* 269:17–28
- John SG, Adkins J (2012) The vertical distribution of iron stable isotopes in the North Atlantic near Bermuda. *Global Biogeochem Cycles* 26:GB2034
- John T, Layne GD, Haase KM, Barnes JD (2010) Chlorine isotope evidence for crustal recycling into the Earth's mantle. *Earth Planet Sci Lett*
- Johnson TM (2004) A review of mass-dependent fractionation of selenium isotopes and implications for other heavy stable isotopes. *Chem Geol* 204:201–214
- Johnson CM, Beard BL (1999) Correction of instrumentally produced mass fractionation during isotopic analysis of Fe by thermal ionization mass spectrometry. *Int J Mass Spectr* 193:87–99
- Johnson CM, Beard BL, Roden EE (2008) The iron isotope fingerprints of redox and biogeochemical cycling in modern and ancient Earth. *Ann Rev Earth Planet Sci* 36:457–493
- Johnson TM, Bullen TD (2003) Selenium isotope fractionation during reduction by Fe(II)-Fe(III) hydroxide-sulfate (green rust). *Geochim Cosmochim Acta* 67:413–419
- Johnson TM, Herbel MJ, Bullen TD, Zawislanski PT (1999) Selenium isotope ratios as indicators of selenium sources and oxyanion reduction. *Geochim Cosmochim Acta* 63:2775–2783
- Johnston DT (2011) Multiple sulphur isotopes and the evolution of the Earth's sulphur cycle. *Earth Sci Rev* 106:161–183
- Johnston DT, Farquhar J, Wing BA, Kaufman AJ, Canfield DE, Habicht KS (2005) Multiple sulphur isotope fractionations in biological systems: a case study with sulphate reducers and sulphur disproportionators. *Am J Sci* 305:645–660
- Jouvin D, Louvat P, Juillot F, Marechal CN, Benedetti MF (2009) Zinc isotopic fractionation: why organic matters. *Environ Sci Tech* 43:5747–5754
- Jouvin D, Weiss DJ, Mason TF, Bravin MN, Louvat P, Zhao F, Ferec F, Hinsinger P, Benedetti MF (2012) Stable isotopes of Cu and Zn in higher plants: evidence for Cu reduction at the root surface and two conceptual models for isotopic fractionation processes. *Environ Sci Technol* 46:2652–2660
- Juillot F, Marechal C, Ponthieu M, Cacaly S, Morin G, Benedetti M, Hazemann JL, Proux O, Guyot F (2008) Zn isotopic fractionation caused by sorption on goethite and 2-Line ferrihydrite. *Geochim Cosmochim Acta* 72:4886–4900
- Jørgensen BB, Böttcher MA, Lüschen H, Neretin LN, Volkov II (2004) Anaerobic methane oxidation and a deep H₂S sink generate isotopically heavy sulfides in Black Sea sediments. *Geochim Cosmochim Acta* 68:2095–2118
- Kakihana H, Kotaka M, Shohei S, Nomura M, Okamoto N (1977) Fundamental studies on the ion-exchange separation of boron isotopes. *Bull Chem Soc Japan* 50:158–163
- Kaplan IR, Rittenberg SC (1964) Microbiological fractionation of sulphur isotopes. *J Gen Microbiol* 34:195–212
- Kasemann SA, Jeffcoate AB, Elliott T (2005a) Lithium isotope composition of basalt glass reference material. *Ann Chem* 77:5251–5257
- Kasemann S, Schmidt D, Pearson P et al (2008) Biological and ecological insights into Ca isotopes in planktic foraminifera as a paleotemperature proxy. *Earth Planet Sci Lett* 271:292–302
- Kasemann SA, Hawkesworth CJ, Prave AR, Fallick AE, Pearson PN (2005b) Boron and calcium isotope composition in Neoproterozoic carbonate rocks from Namibia: evidence for extreme environmental change. *Earth Planet Sci Lett* 231:73–86
- Kaufmann RS, Long A, Bentley H, Campbell DJ (1986) Chlorine isotope distribution of formation water in Texas and Louisiana. *Bull Am Assoc Petrol Geol* 72:839–844
- Kaufmann RS, Long A, Bentley H, Davis S (1984) Natural chlorine isotope variations. *Nature* 309:338–340

- Kelley SP, Fallick AE (1990) High precision spatially resolved analysis of $\delta^{34}\text{S}$ in sulphides using a laser extraction technique. *Geochim Cosmochim Acta* 54:883–888
- Kelley KD, Wilkinson JJ, Chapman JB, Crowther HL, Weiss DJ (2009) Zinc isotopes in sphalerite from base metal deposits in the Red Dog district, northern Alaska. *Econ Geol* 104:767–773
- Kemp ALW, Thode HG (1968) The mechanism of the bacterial reduction of sulphate and of sulphite from isotopic fractionation studies. *Geochim Cosmochim Acta* 32:71–91
- Kendall B, Brennecke GA, Weyer S, Anbar AD (2013) Uranium isotope fractionation suggests oxidative uranium mobilization at 2.50 Ga. *Chem Geol* 362:105–114
- Kendall C, Grim E (1990) Combustion tube method for measurement of nitrogen isotope ratios using calcium oxide for total removal of carbon dioxide and water. *Anal Chem* 62:526–529
- Kendall C (1998) Tracing nitrogen sources and cycling in catchments. In: Kendall C, McDonnell JJ (eds) *Isotope tracers in catchment hydrology*. Elsevier Science, Amsterdam, pp 519–576
- Kerstel ER, Gagliardi G, Gianfrani L, Meijer HA, van Trigt R, Ramaker R (2002) Determination of the $^2\text{H}/^1\text{H}$, $^{17}\text{O}/^{16}\text{O}$ and $^{18}\text{O}/^{16}\text{O}$ isotope ratios in water by means of tunable diode laser spectroscopy at 1.39 μ . *Spectrochim Acta A* 58:2389–2396
- Kiczka M, Wiederhold JG, Kraemer SM, Bourdon B, Kretzschmar R (2010) Iron isotope fractionation during Fe uptake and translocation in Alpine plants. *Environ Sci Technol* 44:6144–6150
- Kieffer SW (1982) Thermodynamic and lattice vibrations of minerals: 5. Application to phase equilibria, isotopic fractionation and high-pressure thermodynamic properties. *Rev Geophys Space Phys* 20:827–849
- Kim S-T, Mucci A, Taylor BE (2007) Phosphoric acid fractionation factors for calcite and aragonite between 25 and 75 °C. *Chem Geol* 246:135–146
- Kim S-T, O'Neil JR (1997) Equilibrium and nonequilibrium oxygen isotope effects in synthetic carbonates. *Geochim Cosmochim Acta* 61:3461–3475
- Kimball BE, Mathur R, Dohnalkova AC, Wall AJ, Runkel RL, Brantley SL (2009) Copper isotope fractionation in acid mine drainage. *Geochim Cosmochim Acta* 73:1247–1263
- Kirshenbaum I, Smith JS, Crowell T, Graff J, McKee R (1947) Separation of the nitrogen isotopes by the exchange reaction between ammonia and solutions of ammonium nitrate. *J Chem Phys* 15:440–446
- Kita NT, Ushikubo T, Fu B, Valley JW (2009) High precision SIMS oxygen isotope analysis and the effect of sample topography. *Chem Geol* 264:43–57
- Kitchen JW, Johnson TM, Bullen TD, Zhu J, Raddatz A (2012) Chromium isotope fractionation factors for reduction of Cr(VI) by aqueous Fe(II) and organic molecules. *Geochim Cosmochim Acta* 89:190–201
- Kitchen NE, Valley JW (1995) Carbon isotope thermometry in marbles of the Adirondack Mountains, New York. *J Metamorph Geol* 13:577–594
- Kiyosu Y, Krouse HR (1990) The role of organic acid in the abiogenic reduction of sulfate and the sulfur isotope effect. *Geochemical J* 24:21–27
- Klochko K, Kaufman AJ, Yao W, Byrne RH, Tossell JA (2006) Experimental measurement of boron isotope fractionation in seawater. *Earth Planet Sci Lett* 248:276–285
- Kohn MJ, Schoeninger MJ, Valley JW (1996) Herbivore tooth oxygen isotope compositions: effects of diet and physiology. *Geochim Cosmochim Acta* 60:3889–3896
- Kohn MJ, Valley JW (1998a) Oxygen isotope geochemistry of amphiboles: isotope effects of cation substitutions in minerals. *Geochim Cosmochim Acta* 62:1947–1958
- Kohn MJ, Valley JW (1998b) Effects of cation substitutions in garnet and pyroxene on equilibrium oxygen isotope fractionations. *J Metam Geol* 16:625–639
- Kohn MJ, Valley JW (1998c) Obtaining equilibrium oxygen isotope fractionations from rocks: theory and examples. *Contr Mineral Petrol* 132:209–224
- Kolodny Y, Luz B, Navon O (1983) Oxygen isotope variations in phosphate of biogenic apatites, I. Fish bone apatite—rechecking the rules of the game. *Earth Planet Sci Lett* 64:393–404
- Konhauser KO, Lalonde SV et al (2011) Aerobic bacterial pyrite oxidation and acid rock drainage during the great oxidation event. *Nature* 478:369–374

- Kowalski N, Dellwig O et al (2013) Pelagic molybdenum concentration anomalies and the impact of sediment resuspension on the molybdenum budget in two tidal systems of the North Sea. *Geochim Cosmochim Acta* 119:198–211
- Kowalski PM, Jahn S (2011) Prediction of equilibrium Li isotope fractionation between minerals and aqueous solutions at high p and T: an efficient ab initio approach. *Geochim Cosmochim Acta* 75:6112–6123
- Kozdon R, Kita RN, Huberty JM, Fournelle JH, Johnson CA, Valley JW (2010) In situ sulfur isotope analysis of sulfide minerals by SIMS: precision and accuracy with application to thermometry of similar to 3.5 Ga Pilbara cherts. *Chem Geol* 275:243–253
- Krabbenhöft A, Eisenhauer A et al (2010) Constraining the marine strontium budget with natural isotope fractionations ($^{87}\text{Sr}/^{86}\text{Sr}$, $\delta^{88/86}\text{Sr}$) of carbonates, hydrothermal solutions and river waters. *Geochim Cosmochim Acta* 74:4097–4109
- Krabbenhöft A, Fietzke J, Eisenhauer A, Liebetrau V, Böhm F, Vollstaedt H (2009) Determination of radiogenic and stable strontium isotope ratios ($^{87}\text{Sr}/^{86}\text{Sr}$; $\delta^{88/86}\text{Sr}$) by thermal ionization mass spectrometry applying an $^{87}\text{Sr}/^{84}\text{Sr}$ double spike. *J Anal At Spectr* 24:1267–1271
- Kritee K, Barkay T, Blum JD (2009) Mass-dependent stable isotope fractionation of mercury during mer mediated microbial degradation of monoethylmercury. *Geochim Cosmochim Acta* 73:1285–1296
- Kritee K, Blum JD, Johnson MW, Bergquist BA, Barkay T (2007) Mercury stable isotope fractionation during reduction of Hg(II) to Hg(0) by mercury resistant microorganisms. *Environ Sci Technol* 41:1889–1895
- Krouse HR, Thode HG (1962) Thermodynamic properties and geochemistry of isotopic compounds of selenium. *Can J Chem* 40:367–375
- Krouse HR, Viau CA, Eliuk LS, Ueda A, Halas S (1988) Chemical and isotopic evidence of thermochemical sulfate reduction by light hydrocarbon gases in deep carbonate reservoirs. *Nature* 333:415–419
- Ku TCW, Walter LM, Coleman ML, Blake RE, Martini AM (1999) Coupling between sulfur recycling and syndepositional carbonate dissolution: evidence from oxygen and sulfur isotope composition of pore water sulfate, South Florida Platform, USA. *Geochim Cosmochim Acta* 63:2529–2546
- Kunzmann M, Halverson GP, Sossi PA, Raub TD, Payne JL, Kirby J (2013) Zn isotope evidence for immediate resumption of primary productivity after snowball Earth. *Geology* 41:27–30
- Lacan F, Francois R, Ji Y, Sherrell RM (2006) Cadmium isotopic composition in the ocean. *Geochim Cosmochim Acta* 70:5104–5118
- Lambelet M, Rehkämper M, van de Flierdt T, Xue Z, Kreissig K, Coles B, Porecelli D, Andersson P (2013) Isotopic analysis of Cd in the mixing zone of Siberian rivers with the Arctic Ocean—new constraints on marine Cd cycling and the isotopic composition of riverine Cd. *Earth Planet Sci Lett* 361:64–73
- Land LS (1980) The isotopic and trace element geochemistry of dolomite: the state of the art. In: Concepts and models of dolomitization. *Soc Econ Paleontol Min Spec Publ* 28:87–110
- Larson PB, Maher K, Ramos FC, Chang Z, Gaspar M, Meinert LD (2003) Copper isotope ratios in magmatic and hydrothermal ore-forming processes. *Chem Geol* 201:337–350
- Lauretta DS, Klaue B, Blum JD, Buseck PR (2001) Mercury abundances and isotopic compositions in the Murchison (CM) and Allende (CV) carbonaceous chondrites. *Geochim Cosmochim Acta* 65:2807–2816
- Laws EA, Bidigare RR, Popp BN (1997) Effect of growth rate and CO₂ concentration on carbon isotope fractionation by the marine diatom *Phaeodactylum tricornutum*. *Limnol Oceanogr* 42:1552–1560
- Laws EA, Popp BN, Bidigare RR, Kennicutt MC, Macko SA (1995) Dependence of phytoplankton carbon isotopic composition on growth rate and CO_{2aq}: theoretical considerations and experimental results. *Geochim Cosmochim Acta* 59:1131–1138
- Layton-Matthews D, Leybourne M, Peter JM, Scott SD, Cousens B, Eglington BM (2013) Multiple sources of selenium in ancient seafloor hydrothermal systems: compositional and Se,

- S and Pb isotopic evidence from volcanic-hosted and volcanic-sediment hosted massive sulphide deposits of the Finlayson Lake district, Yukon, Canada. *Geochim Cosmochim Acta* 117:313–331
- Lazar C, Young ED, Manning CE (2012) Experimental determination of equilibrium nickel isotope fractionation between metal and silicate from 500 °C to 950 °C. *Geochim Cosmochim Acta* 86:276–295
- Le Roux PJ, Shirey SB, Benton L, Hauri EH, Mock TD (2004) In situ, multiple-multiplier, laser ablation ICP-MS measurement of boron isotopic composition ($\delta^{11}\text{B}$) at the nanogram level. *Chem Geol* 203:123–138
- Leeman WP, Tonarini S, Chan LH, Borg LE (2004) Boron and lithium isotopic variations in a hot subduction zone—the southern Washington Cascades. *Chem Geol* 212:101–124
- Lehmann M, Siegenthaler U (1991) Equilibrium oxygen- and hydrogen-isotope fractionation between ice and water. *J Glaciol* 37:23–26
- Lemarchand D, Gaillardet J, Lewin E, Allegre CJ (2000) The influence of rivers on marine boron isotopes and implications for reconstructing past ocean pH . *Nature* 408:951–954
- Lemarchand D, Gaillardet J, Lewin E, Allègre CJ (2002) Boron isotope systematics in large rivers: implications for the marine boron budget and paleo- pH reconstruction over the Cenozoic. *Chem Geol* 190:123–140
- Lemarchand E, Schott J, Gaillardet J (2005) Boron isotopic fractionation related to boron sorption on humic acid and the structure of surface complexes formed. *Geochim Cosmochim Acta* 69:3519–3533
- Lemarchand E, Schott J, Gaillardet J (2007) How surface complexes impact boron isotopic fractionation: evidence from Fe and Mn oxides sorption experiments. *Earth Planet Sci Lett* 260:277–296
- Lemarchand D, Wasserburg GJ, Papanastassiou DA (2004) Rate-controlled calcium isotope fractionation in synthetic calcite. *Geochim Cosmochim Acta* 68:4665–4678
- Letolle R (1980) Nitrogen-15 in the natural environment. In: Fritz P, Fontes JCh (eds) *Handbook of environmental isotope geochemistry*. Elsevier, Amsterdam, pp 407–433
- Levin NE, Raub TD, Dauphas N, Eiler JM (2014) Triple-oxygen-isotope variations in sedimentary rocks. *Geochim Cosmochim Acta* 139:173–189
- Li W, Chakraborty S, Beard BL, Romanek CS, Johnson CM (2012) Magnesium isotope fractionation during precipitation of inorganic calcite under laboratory conditions. *Earth Planet Sci Lett* 333–314:304–316
- Li W, Jackson SE, Pearson NJ, Alard O, Chappell BW (2009a) The Cu isotope signature of granites from the Lachlan Fold Belt, SE Australia. *Chem Geol* 258:38–49
- Li X, Liu Y (2010) First principles study of Ge isotopic fractionation during adsorption onto Fe (III)-oxyhydroxide surfaces. *Chem Geol* 278:15–22
- Li W-Y, Teng F-Z, Ke S, Rudnick R, Gao S, Wu F-Y, Chappell B (2010) Heterogeneous magnesium isotopic composition of the upper continental crust. *Geochim Cosmochim Acta* 74:6867–6884
- Li X, Zhao H, Tang M, Liu Y (2009b) Theoretical prediction for several important equilibrium Ge isotope fractionation factors and geological implications. *Earth Planet Sci Lett* 287:1–11
- Li W-Y, Teng FZ, Wing BA, Xiao Y (2014) Limited magnesium isotope fractionation during metamorphic dehydration in metapelites from the Onawa contact aureole, Maine. *Geochem Geophys Geosys* 15(10). doi:[10.1002/2013GC004992](https://doi.org/10.1002/2013GC004992)
- Liebscher A, Meixner A, Romer R, Heinrich W (2005) Liquid-vapor fractionation of boron and boron isotopes: experimental calibration at 400 °C/23 Mpa to 450 °C/42Mpa. *Geochim Cosmochim Acta* 69:5693–5704
- Little SH, Vance D, Walker-Brown C, Landing WM (2014) The oceanic mass balance of copper and zinc isotopes, investigated by analysis of their inputs, and outputs to ferromanganese oxide sediments. *Geochim Cosmochim Acta* 125:653–672

- Liu Y, Spicuzza MJ, Craddock PR, Day JM, Valley JW, Dauphas N, Taylor LA (2010a) Oxygen and iron isotope constraints on near-surface fractionation effects and the composition of lunar mare basalt source regions. *Geochim Cosmochim Acta* 74:6249–6262
- Liu SA, Teng FZ, He Y, Ke S, Li S (2010b) Investigation of magnesium isotope fractionation during granite differentiation: implication for Mg isotopic composition of the continental crust. *Earth Planet Sci Lett* 297:646–654
- Liu SA, Teng FZ, Yang W, Wu FY (2011) High-temperature inter-mineral magnesium isotope fractionation in mantle xenoliths from the North China craton. *Earth Planet Sci Lett* 308:131–140
- Lobo L, Degryse P, Shortland A, Vanhaecke F (2013) Isotopic analysis of antimony using multi-collector ICP-mass spectrometry for provenance determination of Roman glass. *J Anal At Spectrom* 28: 1213–129
- Long A, Eastoe CJ, Kaufmann RS, Martin JG, Wirt L, Fincey JB (1993) High precision measurement of chlorine stable isotope ratios. *Geochim Cosmochim Acta* 57:2907–2912
- Longinelli A, Craig H (1967) Oxygen-18 variations in sulfate ions in sea-water and saline lakes. *Science* 156:56–59
- Louvat P, Bouchez J, Paris G (2011) MC-ICP-MS isotope measurements with direct injection nebulisation (d-DIHEN): optimisation and application to boron in seawater and carbonate samples. *Geostand Geoanal Res* 35:75–88
- Luais B (2012) Germanium chemistry and MC-ICPMS isotopic measurements of Fe-Ni, Zn alloys and silicate matrices: insights into deep Earth processes. *Chem Geol*
- Luck JM, Ben Othman D, Albarede F (2005) Zn and Cu isotopic variations in chondrites and iron meteorites: early solar nebula reservoirs and parent-body processes. *Geochim Cosmochim Acta* 69:5351–5363
- Lundstrom CC, Chaussidon M, Hsui AT, Keleman P, Zimmermann M (2005) Observations of Li isotope variations in the Trinity ophiolite: evidence for isotope fractionation by diffusion during mantle melting. *Geochim Cosmochim Acta* 69:735–751
- Luz B, Barkan E (2010) Variations of $^{17}\text{O}/^{16}\text{O}$ and $^{18}\text{O}/^{16}\text{O}$ in meteoric waters. *Geochim Cosmochim Acta* 74:6276–6286
- Lécuyer C, Grandjean P, Reynard B, Albarede F, Telouk P (2002) $^{11}\text{B}/^{10}\text{B}$ analysis of geological materials by ICP-MS Plasma 54: application to boron fractionation between brachiopod calcite and seawater. *Chem Geol* 186:45–55
- Ma J, Hintelmann H, Kirk JL, Muir DC (2013) Mercury concentrations and mercury isotope composition in lake sediment cores *Chem Geol*. 336:96–102
- Machel HG, Krouse HR, Sassen P (1995) Products and distinguishing criteria of bacterial and thermochemical sulfate reduction. *Appl Geochemistry* 10:373–389
- MacrisCA Young ED, Manning CE (2013) Experimental determination of equilibrium magnesium isotope fractionation between spinel, forsterite and magnesite from 600 to 800 °C. *Geochim Cosmochim Acta* 118:18–32
- Magenheim AJ, Spivack AJ, Michael PJ, Gieskes JM (1995) Chlorine stable isotope composition of the oceanic crust: implications for earth's distribution of chlorine. *Earth Planet Sci Lett* 131:427–432
- Magenheim AJ, Spivack AJ, Volpe C, Ranson B (1994) Precise determination of stable chlorine isotope ratios in low-concentration natural samples. *Geochim Cosmochim Acta* 58:3117–3121
- Maher K, Jackson S, Mountain B (2011) Experimental evaluation of the fluid-mineral fractionation of Cu isotopes at 250 °C and 300 °C. *Chem Geol* 286:229–239
- Maher K, Larson P (2007) Variation in copper isotope ratios and controls on fractionation in hypogene skarn mineralization at Corocochuayco and Tintaya, Peru. *Econ Geol* 102:225–237
- Malinovsky D, Moens L, Vanhaecke F (2009) Isotopic fractionation of Sn during methylation and demethylation in aqueous solution. *Environ Sci Tech* 43: 4399–4404
- Mariotti A, Germon JC, Hubert P, Kaiser P, Letolle R, Tardieux P (1981) Experimental determination of nitrogen kinetic isotope fractionation: some principles, illustration for the denitrification and nitrification processes. *Plant Soil* 62:413–430

- Markl G, von Blanckenburg F, Wagner T (2006b) Iron isotope fractionation during hydrothermal ore deposition and alteration. *Geochim Cosmochim Acta* 70:3011–3030
- Markl G, Lahaye Y, Schwinn G (2006a) Copper isotopes as monitors of redox processes in hydrothermal mineralization. *Geochim Cosmochim Acta* 70:4215–4228
- Marriott CS, Henderson GM, Belshaw NS, Tudhope AW (2004) Temperature dependence of $\delta^7\text{Li}$, $\delta^{44}\text{Ca}$ and Li/Ca during growth of calcium carbonate. *Earth Planet Sci Lett* 222:615–624
- Marschall HR, Altherr R, Kalt A, Ludwig T (2008) Detrital, metamorphic and metasomatic tourmaline in high-pressure metasediments from Syros (Greece): intra-grain boron isotope patterns determined by secondary-ion mass spectrometry. *Contr Mineral Petrol* 155:703–717
- Marschall HR, Jiang SY (2011) Tourmaline isotopes: no element left behind. *Elements* 7:313–319
- Marty B, Humbert F (1997) Nitrogen and argon isotopes in oceanic basalts. *Earth Planet Sci Lett* 152:101–112
- Marty B, Zimmermann L (1999) Volatiles (He, C, N, Ar) in mid-ocean ridge basalts: assesment of shallow-level fractionation and characterization of source composition. *Geochim Cosmochim Acta* 63:3619–3633
- Maréchal CN, Albarede F (2002) Ion-exchange fractionation of copper and zinc isotopes. *Geochim Cosmochim Acta* 66:1499–1509
- Maréchal CN, Télouk P, Albarède F (1999) Precise analysis of copper and zinc isotopic compositions by plasma-source mass spectrometry. *Chem Geol* 156:251–273
- Maréchal CN, Nicolas E, Douchet C, Albarède F (2000) Abundance of zinc isotopes as a marine biogeochemical tracer. *Geochem Geophys Geosys* 3:1:1999GC000029
- Mason TFD et al (2005) Zn and Cu isotopic variability in the Alexandrinka volcanic-hosted massive sulphide (VHMS) ore deposit, Urals, Russia. *Chem Geol* 221:170–187
- Mathur R, Brantley S, Anbar A, Munizaga F, MaksaeV R, Vervoort J, Hart G (2010a) Variations of Mo isotopes from molybdenite in high-temperature hydrothermal ore deposits. *Mineral Deposita* 45:43–50
- Mathur R, Dendas M, Titley S, Phillips A (2010b) Patterns in the copper isotope composition of minerals in porphyry copper deposits in southwestern United States. *Econ Geol* 105:1457–1467
- Mathur R, Jin L, Prush V, Paul J, Ebersole C, Fornadel A, Williams JZ, Brantley S (2012) Cu isotopes and concentrations during weathering of black shale of the Marcellus Formation, Huntington County, Pennsylvania (USA). *Chem Geol* 304–305:175–184
- Mathur R, Ruiz J, Titley S, Liermann L, Buss H, Brantley S (2005) Cu isotopic fractionation in the supergene environment with and without bacteria. *Geochim Cosmochim Acta* 69:5233–5246
- Matthews A, Goldsmith JR, Clayton RN (1983a) Oxygen isotope fractionation between zoisite and water. *Geochim Cosmochim Acta* 47:645–654
- Matthews A, Goldsmith JR, Clayton RN (1983b) On the mechanics and kinetics of oxygen isotope exchange in quartz and feldspars at elevated temperatures and pressures. *Geol Soc Am Bull* 94:396–412
- Matthews DE, Hayes JM (1978) Isotope-ratio-monitoring gas chromatography-mass spectrometry. *Anal Chem* 50:1465–1473
- McClelland JW, Montoya JP (2002) Trophic relationships and the nitrogen isotope composition of amino acids in plankton. *Ecology* 83:2173–2180
- McCrea JM (1950) On the isotopic chemistry of carbonates and a paleotemperature scale. *J Chem Phys* 18:849–857
- McCready RGL (1975) Sulphur isotope fractionation by *Desulfovibrio* and *Desulfotomaculum* species. *Geochim Cosmochim Acta* 39:1395–1401
- McCready RGL, Kaplan IR, Din GA (1974) Fractionation of sulfur isotopes by the yeast *Saccharomyces cerevisiae*. *Geochim Cosmochim Acta* 38:1239–1253
- McIlvin MR, Altabet MA (2005) Chemical conversion of nitrate and nitrite to nitrous oxide for nitrogen and oxygen isotopic analysis in freshwater and seawater. *Anal Chem* 77:5589–5595
- McKibben MA, Riciputi LR (1998) Sulfur isotopes by ion microprobe. In: Applications of microanalytical techniques to understanding mineralizing processes. *Rev Econ Geol* 7:121–140

- McManus J et al (2006) Molybdenum and uranium geochemistry in continental margin sediments: palaeoproxy potential. *Geochim Cosmochim Acta* 70:4643–4662
- McManus J, Nägler T, Siebert C, Wheat CG, Hammond D (2002) Oceanic molybdenum isotope fractionation: diagenesis and hydrothermal ridge flank alteration. *Geochem Geophys Geosyst* 3:1078. doi:[10.1029/2002GC000356](https://doi.org/10.1029/2002GC000356)
- McMullen CC, Cragg CG, Thode HG (1961) Absolute ratio of $^{11}\text{B}/^{10}\text{B}$ in Searles Lake borax. *Geochim Cosmochim Acta* 23:147
- Miller MF, Franchi IA, Sexton AS, Pillingier CT (1999) High precision $\delta^{17}\text{O}$ isotope measurements of oxygen from silicates and other oxides: method and applications. *Rapid Commun Mass Spect* 13:1211–1217
- Millet MA, Baker JA, Payne CE (2012) Ultra-precise stable Fe isotope measurements by high resolution multi-collector inductively coupled mass spectrometry with a ^{57}Fe - ^{58}Fe double spike. *Chem Geol* 304–305:18–25
- Millot R, Guerrot C, Vigier N (2004) Accurate and high-precision measurement of lithium isotopes in two reference materials by MC-ICP-MS. *Geostand Geoanal Res* 28:153–159
- Millot R, Petelet-Giraud E, Guerrot C, Negrel P (2010b) Multi-isotopic composition ($\delta^7\text{Li}$ - $\delta^{11}\text{B}$ - δD - $\delta^{18}\text{O}$) of rainwaters in France: origin and spatio-temporal characterization. *Appl Geochem* 25:1510–1524
- Millot R, Vigier N, Gaillardet J (2010a) Behaviour of lithium and its isotopes during weathering in the Mackenzie Basin, Canada. *Geochim Cosmochim Acta* 74:3897–3912
- Misra S, Froelich PN (2012) Lithium isotope history of Cenozoic seawater: changes in silicate weathering and reverse weathering. *Science* 335:818–823
- Mitchell K, Couture RM, Johnson TM, Mason PRD, Van Cappellen P (2013) Selenium sorption and isotope fractionation: iron(III) oxides versus iron (II) sulfides. *Chem Geol* 342:21–28
- Mitchell K, Mason P, Van Cappellen P, Johnson TM, Gill BC, Owens JD, Diaz J, Ingall E, Reichart GJ, Lyons T (2012) Selenium as paleo-oceanographic proxy: a first assessment. *Geochim Cosmochim Acta* 89:302–317
- Mizutani Y, Rafter TA (1973) Isotopic behavior of sulfate oxygen in the bacterial reduction of sulfate. *Geochem J* 6:183–191
- Monson KD, Hayes JM (1982) Carbon isotopic fractionation in the biosynthesis of bacterial fatty acids. Ozonolysis of unsaturated fatty acids as a means of determining the intramolecular distribution of carbon isotopes. *Geochim Cosmochim Acta* 46:139–149
- Montoya-Pino C, Weyer S, Anbar AD, Pross J, Oschmann J, van de Schootbrugge B, Arz HW (2010) Global enhancement of ocean anoxia during Oceanic Anoxic Event 2: a quantitative approach using U isotopes. *Geology* 38:315–318
- Mook WG, Bommerson JC, Stavermann WH (1974) Carbon isotope fractionation between dissolved bicarbonate and gaseous carbon dioxide. *Earth Planet Sci Lett* 22:169–174
- Moriguti T, Nakamura E (1998) Across-arc variation of Li-isotopes in lavas and implications for crust /mantle recycling at subduction zones. *Earth Planet Sci Lett* 163:167–174
- Moynier F, Agranier A, Hezel DC, Bouvier A (2010) Sr stable isotope composition of Earth, the Moon, Mars, Vesta and meteorites. *Earth Planet Sci Lett* 300:359–366
- Moynier F, Yin QZ, Schauble E (2011) Isotopic evidence of Cr partitioning into Earth's core. *Science* 331:1417–1420
- Moynier F, Pichat S, Pons ML, Fike D, Balter V, Albarède F (2008) Isotope fractionation and transport mechanisms of Zn in plants. *Chem Geol* 267:125–130
- Murphy MJ, Stirling CH, Kaltenbach A, Turner SP, Schaefer BF (2014) Fractionation of ^{238}U / ^{235}U by reduction during low temperature uranium mineralization processes. *Earth Planet Sci Lett* 388:306–317
- Méheut M, Lazzeri M, Balan E, Mauri F (2010) First-principles calculation of H/D isotopic fractionation between hydrous minerals and water. *Geochim Cosmochim Acta* 74:3874–3882
- Möller K, Schoenberg R, Pedersen RB, Weiss D, Dong S (2012) Calibration of the new certified reference materials ERM-AE633 and ERM-AE647 for copper and IRMM-3702 for zinc isotope amount ratio determinations. *Geostand Geoanal Res* 36:177–199

- Nabelek PI, Labotka TC (1993) Implications of geochemical fronts in the Notch Peak contact-metamorphic aureole, Utah, USA. *Earth Planet Sci Lett* 119:539–559
- Nabelek PI (1991) Stable isotope monitors. In: *Contact metamorphism*. *Rev Mineral* 26:395–435
- Nakano T, Nakamura E (2001) Boron isotope geochemistry of metasedimentary rocks and tourmalines in a subduction zone metamorphic suite. *Phys Earth Planet Inter* 127:233–252
- Navarette JU, Borrok DM, Viveros M, Elzey JT (2011) Copper isotope fractionation during surface adsorption and intracellular incorporation by bacteria. *Geochim Cosmochim Acta* 75:784–799
- Needham AW, Porcelli D, Russell SS (2009) An Fe isotope study of ordinary chondrites. *Geochim Cosmochim Acta* 73:7399–7413
- Neretin LN, Böttcher ME, Grinenko VA (2003) Sulfur isotope geochemistry of the Black Sea water column. *Chem Geol* 200:59–69
- Neubert N, Heri AR, Voegelin AR, Schlunegger F, Villa IM (2011) The molybdenum isotopic composition in river water; constraints from small catchments. *Earth Planet Sci Lett* 304:180–190
- Neubert N, Nägler TF, Böttcher ME (2008) Sulfidity controls molybdenum isotope fractionation into euxinic sediments: evidence from the modern Black Sea. *Geology* 36:775–778
- Neymark LA, Premo WR, Mel'nikov NN, Emsbo P (2014) Precise determination of $\delta^{88}\text{Sr}$ in rocks, minerals and waters by double-spike TIMS: a powerful tool in the study of geological, hydrological and biological processes. *J Anal At Spectr* 29:65–75
- Nielsen SG et al (2005) Thallium isotope composition of the upper continental crust and rivers—an investigation of the continental sources of dissolved marine thallium. *Geochim Cosmochim Acta* 69:2007–2019
- Nielsen SG, Goff M, Hesselbo SP, Jenkyns HC, LaRowe DE, Lee CT (2011b) Thallium isotopes in early diagenetic pyrite—a paleoredox proxy? *Geochim Cosmochim Acta* 75:6690–6704
- Nielsen H (1979) Sulfur isotopes. In: Jäger E, Hunziker J (eds) *Lectures in isotope geology*. Springer, Berlin, pp 283–312
- Nielsen SG, Mar-Gerrison S, Gannoun A, LaRowe D, Klemm V, Halliday A, Burton KW, Hein JR (2009) Thallium isotope evidence for a permanent increase in marine organic carbon export in the early Eocene. *Earth Planet Sci Lett* 278:297–307
- Nielsen SG, Prytulak J, Halliday AN (2011c) Determination of precise and accurate $^{51}\text{V}/^{50}\text{V}$ isotope ratios by MC-ICP-MS, Part 1: Chemical separation of vanadium and mass spectrometric protocols. *Geostand Geoanal Res* 35:293–306
- Nielsen SG, Prytulak J, Wood BJ, Halliday AN (2014) Vanadium isotopic difference between the silicate Earth and meteorites. *Earth Planet Sci Lett* 389:167–175
- Nielsen SG, Rehkämper M, Brandon AD, Norman MD, Turner S, O'Reilly SY (2007) Thallium isotopes in Iceland and Azores lavas—implications for the role of altered crust and mantle geochemistry. *Earth Planet Sci Lett* 264:332–345
- Nielsen SG, Rehkämper M, Norman MD, Halliday AN, Harrison D (2006) Thallium isotopic evidence for ferromanganese sediments in the mantle source of Hawaiian basalts. *Nature* 439:314–317
- Nielsen SG, Rehkämper M (2011) Thallium isotopes and their application to problems in earth and environmental science. In: Baskaran M (ed) *Handbook of environmental isotope geochemistry*, vol 1. Springer, New York, pp 247–269
- Nielsen LC, Druhan JL, Yang W, Brown ST, DePaolo DJ (2011) Calcium isotopes as tracers of biogeochemical processes. In: *Handbook of environmental isotope geochemistry*. Springer, New York, pp 105–124
- Nishio Y, Nakai S, Yamamoto J, Sumino H, Matsumoto T, Prikhod'ko VS, Arai S (2004) Lithium isotope systematics of the mantle derived ultramafic xenoliths: implications for EM1 origin. *Earth Planet Sci Letters* 217:245–261
- Nitzsche HM, Stiehl G (1984) Untersuchungen zur Isotopenfraktionierung des Stickstoffs in den Systemen Ammonium/Ammoniak und Nitrid/Stickstoff. *ZFI Mitt* 84:283–291

- Noordmann J, Weyer S, Montoya-Pino C, Dellwig O, Neubert N, Eckert S, Paetzel M, Böttcher ME (2015) Uranium and molybdenum isotope systematics in modern euxinic basins: case studies from the central Baltic Sea and the Kyllaren fjord (Norway). *Chem Geol* (in press)
- Nägler TF et al (2014) Proposal for an international molybdenum isotope reference standard and data representation. *Geostand Geoanal Res* 38:149–151
- Nägler TF, Neubert N, Böttcher ME, Dellwig O, Schnetger B (2011) Molybdenum isotope fractionation in pelagic euxinia: evidence from the modern Black and Baltic Seas. *Chem Geol* 289:1–11
- Nägler TF, Siebert C, Lüschen H, Böttcher ME (2005) Sedimentary Mo isotope records across the Holocene fresh-brackish water transition of the Black Sea. *Chem Geol* 219:283–295
- Nägler TF, Eisenhauer A, Müller A, Hemleben C, Kramers J (2000) The $\delta^{44}\text{Ca}$ -temperature calibration on fossil and cultured *Globigerinoides sacculifer*: new tool for reconstruction of past sea surface temperatures. *Geochim Geophys Geosyst* 3:1(2000GC000091)
- Ockert C, Gussone N, Kaufhold S, Teichert BM (2013) Isotope fractionation during Ca exchange on clay minerals in a marine environment. *Geochim Cosmochim Acta* 112:374–388
- Oelze M, von Blanckenburg F, Hoellen D, Dietzel M, Bouchez J (2014) Si stable isotope fractionation during adsorption and the competition between kinetic and equilibrium isotope fractionation: implications for weathering systems. *Chem Geol* (in press)
- Oeser M, Weyer S, Horn I, Schuth S (2014) High-precision Fe and Mg isotope ratios of silicate reference glasses determined in situ by femtosecond LA-MC-ICP-MS and by solution nebulisation MC-ICP-MS. *Geostand Geoanal Res* 38:311–328
- Ohmoto H (1986) Stable isotope geochemistry of ore deposits. *Rev Mineral* 16:491–559
- Ohmoto H, Goldhaber MB (1997) Sulfur and carbon isotopes. In: Barnes HL (ed) *Geochemistry of hydrothermal ore deposits*, 3rd edn. Wiley Interscience, New York, pp 435–486
- Ohmoto H, Rye RO (1979) *Isotopes of sulfur and carbon*. In: *Geochemistry of hydrothermal ore deposits*, 2nd edn. Holt Rinehart and Winston, New York
- Ono S, Shanks WC, Rouxel OJ, Rumble D (2007) S-33 constraints on the seawater sulphate contribution in modern seafloor hydrothermal vent sulfides. *Geochim Cosmochim Acta* 71:1170–1182
- Ono S, Wing BA, Johnston D, Farquhar J, Rumble D (2006) Mass-dependent fractionation of quadruple sulphur isotope system as a new tracer of sulphur biogeochemical cycles. *Geochim Cosmochim Acta* 70:2238–2252
- Opfergelt S, Georg RB, Delvaux B, Cabidoche YM, Burton KW, Halliday AN (2012) Mechanism of magnesium isotope fractionation in volcanic soil weathering sequences, Guadeloupe. *Earth Planet Sci Lett* 341–344:176–185
- Owens NJP (1987) Natural variations in ^{15}N in the marine environment. *Adv Mar Biol* 24:390–451
- O’Leary MH (1981) Carbon isotope fractionation in plants. *Phytochemistry* 20:553–567
- O’Neil JR, Epstein S (1966) A method for oxygen isotope analysis of milligram quantities of water and some of its applications. *J Geophys Res* 71:4955–4961
- O’Neil JR, Roe LJ, Reinhard E, Blake RE (1994) A rapid and precise method of oxygen isotope analysis of biogenic phosphate. *Isr J Earth Sci* 43:203–212
- O’Neil JR, Taylor HP (1967) The oxygen isotope and cation exchange chemistry of feldspars. *Am Mineral* 52:1414–1437
- O’Neil JR, Truesdell AH (1991) Oxygen isotope fractionation studies of solute-water interactions. In: *Stable isotope geochemistry: a tribute to Samuel Epstein*. *Geochemical Soc Spec Publ* 3:17–25
- Pack A, Herwartz D (2014) The triple oxygen isotope composition of the Earth mantle and $\Delta^{17}\text{O}$ variations in terrestrial rocks. *Earth Planet Sci Lett* (inpress)
- Pagani M, Lemarchand D, Spivack A, Gaillardet J (2005) A critical evaluation of the boron isotope- p_{H} proxy: the accuracy of ancient ocean p_{H} estimates. *Geochim Cosmochim Acta* 69:953–961
- Page B, Bullen T, Mitchell M (2008) Influences of calcium availability and tree species on Ca isotope fractionation in soil and vegetation. *Biogeochemistry* 88:1–13

- Palmer MR, Slack JF (1989) Boron isotopic composition of tourmaline from massive sulfide deposits and tourmalinites. *Contr Mineral Petrol* 103:434–451
- Palmer MR, Spivack AJ, Edmond JM (1987) Temperature and pH controls over isotopic fractionation during the absorption of boron on marine clays. *Geochim Cosmochim Acta* 51:2319–2323
- Paniello RC, Day JM, Moynier F (2012) Zinc isotopic evidence for the origin of the Moon. *Nature* 490:376–379
- Paris G, Sessions A, Subhas AV, Adkins JF (2013) MC-ICP-MS measurement of $d^{34}\text{S}$ and $D^{33}\text{S}$ in small amounts of dissolved sulphate. *Chem Geol* 345:50–61
- Park R, Epstein S (1960) Carbon isotope fractionation during photosynthesis. *Geochim Cosmochim Acta* 21:110–126
- Parkinson IJ, Hammond SJ, James RH, Rogers NW (2007) High-temperature lithium isotope fractionation: insights from lithium isotope diffusion in magmatic systems. *Earth Planet Sci Lett* 257:609–621
- Passey BH, Hu H, Ji H, Montanari S, Li G, Henkes GA, Levin NE (2014) Triple oxygen isotopes in biogenic and sedimentary carbonates. *Geochim Cosmochim Acta* 141:1–25
- Payne JL, Turchyn AV, Paytan A, DePaolo DJ, Lehrmann DJ, Yu M, Wei J (2010) Calcium isotope constraints on the end-Permian mass extinction. *PNAS* 107:8543–8548
- Pearce CR, Burton KW, Pogge von Strandmann PA, James RH, Gislason SR (2010) Molybdenum isotope behaviour accompanying weathering and riverine transport in a basaltic terrain. *Earth Planet Sci Lett* 295:104–114
- Pearce CR, Cohen AS, Coe AL, Burton KW (2008) Molybdenum isotope evidence for global ocean anoxia coupled with perturbations to the carbon cycle during the Early Jurassic. *Geology* 36:231–234
- Pearson PN, Palmer MR (1999) Middle Eocene seawater pH and atmospheric carbon dioxide. *Science* 284:1824–1826
- Pearson PN, Palmer MR (2000) Atmospheric carbon dioxide concentrations over the past 60 million years. *Nature* 406:695–699
- Peterson BJ, Fry B (1987) Stable isotopes in ecosystem studies. *Ann Rev Ecol Syst* 18:293–320
- Pichat S, Douchet C, Albarede F (2003) Zinc isotope variations in deep-sea carbonates from the eastern equatorial Pacific over the last 175 ka. *Earth Planet Sci Lett* 210:167–178
- Pistiner JS, Henderson GM (2003) Lithium-isotope fractionation during continental weathering processes. *Earth Planet Sci Lett* 214:327–339
- Plessen B, Harlov DE, Henry D, Guidotti CV (2010) Ammonium loss and nitrogen isotopic fractionation in biotite as a function of metamorphic grade in metapelites from western Maine, USA. *Geochim Cosmochim Acta* 74:4759–4771
- Pogge von Strandmann PA, Forshaw J, Schmidt DN (2014) Modern and Cenozoic records of magnesium behaviour from foraminiferal Mg isotopes. *Biogeosci Discuss* 11:7451–7464
- Pogge von Strandmann PA, Burton KW, James RH, van Calsteren P, Gislason SR, Sigfusson B (2008) The influence of weathering processes on riverine magnesium isotopes in a basaltic terrain. *Earth Planet Sci Lett* 276:187–197
- Poitrasson F, Cruz Vieira L et al (2014) Iron isotope composition of the bulk waters and sediments from the Amazon River basin. *Chem Geol* 377:1–11
- Poitrasson F, Freydier R (2005) Heavy iron isotope composition of granites determined by high resolution MC-ICP-MS. *Chem Geol* 222:132–147
- Poitrasson F, Roskosz M, Corgne A (2009) No iron isotope fractionation between molten alloys and silicate melt to 2000 °C and 7.7 GPa: experimental evidence and implications for planetary differentiation and accretion. *Earth Planet Sci Lett* 278:376–385
- Pokrovsky OS, Viers J, Emnova EE, Kompantseva EI, Freydier R (2008) Copper isotope fractionation during its interaction with soil and aquatic microorganisms and metal oxy(hydr) oxides: possible structural control. *Geochim Cosmochim Acta* 72:1742–1757

- Polyakov VB, Clayton RN, Horita J, Mineev SD (2007) Equilibrium iron isotope fractionation factors of minerals: reevaluation from the data of nuclear inelastic resonant X-ray scattering and Mossbauer spectroscopy. *Geochim Cosmochim Acta* 71:3833–3846
- Polyakov VB, Mineev SD, Clayton RN, Hu G, Mineev KS (2005) Determination of tin equilibrium fractionation factors from synchrotron radiation experiments. *Geochim Cosmochim Acta* 69:5531–5536
- Polyakov VB, Soultanov DM (2011) New data on equilibrium iron isotope fractionation among sulfides: constraints on mechanisms of sulfide formation in hydrothermal and igneous systems. *Geochim Cosmochim Acta* 75:1957–1974
- Popp BN, Laws EA, Bidigare RR, Dore JE, Hanson KL, Wakeham SG (1998) Effect of phytoplankton cell geometry on carbon isotope fractionation. *Geochim Cosmochim Acta* 62:69–77
- Porter SJ, Selby D, Cameron V (2014) Characterising the nickel isotopic composition of organic-rich marine sediments. *Chem Geol* 387:12–21
- Poulson RL, Siebert C, McManus J, Berelson WM (2006) Authigenic molybdenum isotope signatures in marine sediments. *Geology* 34:617–620
- Poulson-Brucker RL, McManus J, Severmann S, Berelson WM (2009) Molybdenum behaviour during early diagenesis: insights from Mo isotopes. *Geochem Geophys Geosys* 10(Q06010):1–25
- Pretet C, van Zuilen K, Nögler TF, Reynaud S, Immenhauser A, Böttcher ME, Samankassou E (2015) The barium isotope composition of corals: a potential proxy for seawater? *Chem Geol* (in press)
- Prytulak J, Nielsen SG et al (2013b) The stable vanadium isotope composition of the mantle and mafic lavas. *Earth Planet Sci Lett* 365:177–189
- Prytulak J, Nielsen RG, Halliday AN (2011) Determination of precise and accurate $^{51}\text{V}/^{50}\text{V}$ isotope ratios by multi-collector ICP-MS, Part 2: Isotope composition of six reference materials plus the Allende chondrite and verification tests. *Geostand Geoanal Res* 35:307–318
- Prytulak J, Nielsen SG, Plank T, Barker M, Elliott T (2013a) Assessing the utility of thallium and thallium isotopes for tracing subduction zone inputs to the Mariana arc. *Chem Geol* 345:139–149
- Puchelt H, Sabels BR, Hoering TC (1971) Preparation of sulfur hexafluoride for isotope geochemical analysis. *Geochim Cosmochim Acta* 35:625–628
- Qi HW, Rouxel O, Hu RZ, Bi XW, Wen HJ (2011) Germanium isotopic systematics in Ge-rich coal from the Lincang Ge deposit, Yunnan, Southwestern China. *Chem Geol* 286:252–265
- Ra K (2010) Determination of Mg isotopes in chlorophyll *a* for marine bulk phytoplankton from the northwestern Pacific ocean. *Geochem Geophys Geosys* 11(12):Q12011. doi:[10.1029/2010GC003350](https://doi.org/10.1029/2010GC003350)
- Ra K, Kitagawa H (2007) Magnesium isotope analysis of different chlorophyll forms in marine phytoplankton using multi-collector ICP-MS. *J Anal At Spectrom* 22:817–821
- Raddatz J, Liebetrau V et al (2013) Stable Sr-isotope, Sr/Ca, Mg/Ca, Li/Ca and Mg/Li ratios in the scleractinian cold-water coral *Lophelia pertusa*. *Chem Geol* 352:143–152
- Radic A, Lacan F, Murray JW (2011) Iron isotopes in the seawater of the equatorial Pacific Ocean: new constraints for the oceanic iron cycle. *Earth Planet Sci Lett* 306:1–10
- Ransom B, Spivack AJ, Kastner M (1995) Stable Cl isotopes in subduction-zone pore waters: implications for fluid-rock reactions and the cycling of chlorine. *Geology* 23:715–718
- Redling K, Elliott E, Bain D, Sherwell J (2013) Highway contributions to reactive nitrogen deposition: tracing the fate of vehicular NO_x using stable isotopes and plant biomonitors. *Biogeochemistry* 116:261–274
- Rees CE (1978) Sulphur isotope measurements using SO₂ and SF₆. *Geochim Cosmochim Acta* 42:383–389
- Rehkämper M, Frank M, Hein JR, Halliday A (2004) Cenozoic marine geochemistry of thallium deduced from isotopic studies of ferromanganese crusts and pelagic sediments. *Earth Planet Sci Lett* 219:77–91

- Rehkämper M, Frank M, Hein JR, Porcelli D, Halliday A, Ingri J, Libetrau V (2002) Thallium isotope variations in seawater and hydrogenetic, diagenetic and hydrothermal ferromanganese deposits. *Earth Planet Sci Lett* 197:65–81
- Rehkämper M, Wombacher F, Horner TJ, Xue Z (2011) Natural and anthropogenic Cd isotope variations. In: Baskaran M (ed) *Handbook of environmental isotope geochemistry*. Springer, New York, pp 125–154
- Revesz K, Böhlke JK, Yoshinari T (1997) Determination of ^{18}O and ^{15}N in nitrate. *Anal Chem* 69:4375–4380
- Reynard LM, Henderson GM, Hedges RE (2010) Calcium isotope ratios in animal and human bone. *Geochim Cosmochim Acta* 74:3735–3750
- Reynolds BC, Frank M, Halliday AN (2006) Silicon isotope fractionation during nutrient utilization in the North Pacific. *Earth Planet Sci Letters* 244:431–443
- Richet P, Bottinga Y, Javoy M (1977) A review of H, C, N, O, S, and Cl stable isotope fractionation among gaseous molecules. *Ann Rev Earth Planet Sci* 5:65–110
- Richter FM, Davis AM, DePaolo D, Watson BE (2003) Isotope fractionation by chemical diffusion between molten basalt and rhyolite. *Geochim Cosmochim Acta* 67:3905–3923
- Rippberger S, Rehkämper VM, Porcelli D, Halliday AN (2007) Cadmium isotope fractionation in seawater – a signature of biological activity. *Earth Planet Sci Lett* 261:670–684
- Robert F, Chaussidon M (2006) A paleotemperature curve for the Precambrian oceans based on silicon isotopes in cherts. *Nature* 443:969–972
- Rolison JM, Landing WM, Luke W, Cohen M, Salters VJ (2013) Isotopic composition of species-specific atmospheric Hg in a coastal environment. *Chem Geol* 336:37–49
- Rollion-Bard C, Blamart D, Trebosc J, Tricot G, Mussi A, Cuif JP (2011) Boron isotopes as pH proxy: a new look at boron speciation in deep-sea corals using ^{11}B MAS NMR and EELS. *Geochim Cosmochim Acta* 75:1003–1012
- Rollion-Bard C, Erez J (2010) Intra-shell boron isotope ratios in the symbiont-bearing benthic foraminifera *Amphistegina lobifera*: implications for d^{11}B vital effects and paleo-pH reconstructions. *Geochim Cosmochim Acta* 74:1530–1536
- Rollion-Bard C, Vigier N, Spezzaferri S (2007) In-situ measurements of calcium isotopes by ion microprobe in carbonates and application to foraminifera. *Chem Geol* 244:679–690
- Romanek CS, Grossman EL, Morse JW (1992) Carbon isotope fractionation in synthetic aragonite and calcite: effects of temperature and precipitation rate. *Geochim Cosmochim Acta* 56:419–430
- Romaniello SJ, Herrmann AD, Anbar AD (2013) Uranium concentrations and $^{238}\text{U}/^{235}\text{U}$ isotope ratios in modern carbonates from the Bahamas: assessing a novel paleoredox proxy. *Chem Geol* 362:305–316
- Rose EF, Chaussidon M, France-Lanord C (2000) Fractionation of boron isotopes during erosion processes: the example of Himalayan rivers. *Geochim Cosmochim Acta* 64:397–408
- Rosenbaum J, Sheppard SMF (1986) An isotopic study of siderites, dolomites and ankerites at high temperatures. *Geochim Cosmochim Acta* 50:1147–1150
- Rosman JR, Taylor PD (1998) Isotopic compositions of the elements (technical report): commission on atomic weights and isotopic abundances. *Pure Appl Chem* 70:217–235
- Rouxel O, Bekker A, Edwards KJ (2005) Iron isotope constraints on the Archean and Proterozoic ocean redox state. *Science* 307:1088–1091
- Rouxel O, Fouquet Y, Ludden JN (2004a) Copper isotope systematics of the Lucky Strike, Rainbow and Logatchev seafloor hydrothermal fields on the Mi-Atlantic Ridge. *Econ Geol* 99:585–600
- Rouxel O, Fouquet Y, Ludden JN (2004b) Subsurface processes at the Lucky Strike hydrothermal field, Mid-Atlantic Ridge: evidence from sulfur, selenium and iron isotopes. *Geochim Cosmochim Acta* 68:2295–2311
- Rouxel O, Galy A, Elderfield H (2006) Germanium isotope variations in igneous rocks and marine sediments. *Geochim Cosmochim Acta* 70:3387–3400

- Rouxel O, Ludden J, Carignan J, Marin L, Fouquet Y (2002) Natural variations in Se isotopic composition determined by hydride generation multiple collector inductively coupled plasma mass spectrometry. *Geochim Cosmochim Acta* 66:3191–3199
- Rouxel O, Ludden J, Fouquet Y (2003) Antimony isotope variations in natural systems and implications for their use as geochemical tracers. *Chem Geol* 200:25–40
- Rozanski K, Araguas-Araguas L, Gonfiantini R (1993) Isotopic patterns in modern global precipitation. In: *Climate change in continental isotopic records*. *Geophys Monograph* 78:1–36
- Robinson M, Clayton RN (1969) Carbon-13 fractionation between aragonite and calcite. *Geochim Cosmochim Acta* 33:997–1002
- Rudnick RL, Ionov DA (2007) Lithium elemental and isotopic disequilibrium in minerals from peridotite xenoliths from far-east Russia: product of recent melt/fluid-rock interaction. *Earth Planet Sci Lett* 256:278–293
- Rudnick RL, Tomaschak PB, Njo HB, Gardner LR (2004) Extreme lithium isotopic fractionation during continental weathering revealed in saprolites from South Carolina. *Chem Geol* 212:45–57
- Rudnicki MD, Elderfield H, Spiro B (2001) Fractionation of sulfur isotopes during bacterial sulfate reduction in deep ocean sediments at elevated temperatures. *Geochim Cosmochim Acta* 65:777–789
- Ruiz J, Mathur R, Young S, Brantley S (2002) Controls of copper isotope fractionation. *Geochim Cosmochim Acta Spec Suppl* 66:A654
- Rumble D, Miller MF, Franchi IA, Greenwood RC (2007) Oxygen three-isotope fractionation lines in terrestrial silicate minerals: an inter-laboratory comparison of hydrothermal quartz and eclogitic garnet. *Geochim Cosmochim Acta* 71:3592–3600
- Russell WA, Papanastassiou DA, Tombrello TA (1978) Ca isotope fractionation on the Earth and other solar system materials. *Geochim Cosmochim Acta* 42:1075–1090
- Rustad JR, Casey WH, Yin QZ, Bylaska EJ, Felmy AR, Bogatko SA, Jackson VE, Dixon DA (2010) Isotopic fractionation of $\text{Mg}_{(\text{aq})}^{2+}$, $\text{Ca}_{(\text{aq})}^{2+}$ and $\text{Fe}_{(\text{aq})}^{2+}$ with carbonate minerals. *Geochim Cosmochim Acta* 74:6301–6323
- Rustad JR, Dixon DA (2009) Prediction of iron-isotope fractionation between hematite ($\alpha\text{-Fe}_2\text{O}_3$) and ferric and ferrous iron in aqueous solution from density functional theory. *J Phys Chem* 113:12249–12255
- Ryan BM, Kirby JK, Degryse F, Harris H, McLaughlin MJ, Scheiderich K (2013) Copper speciation and isotopic fractionation in plants: uptake and translocation mechanism. *New Phytol* 199:367–378
- Rye RO (1974) A comparison of sphalerite-galena sulfur isotope temperatures with filling-temperatures of fluid inclusions. *Econ Geol* 69:26–32
- Ryu JS, Jacobson AD, Holmden C, Lundstrom C, Zhang Z (2011) The major ion, $\delta^{44/40}\text{Ca}$, $\delta^{44/42}\text{Ca}$ and $\delta^{26/24}\text{Mg}$ geochemistry of granite weathering at pH = 1 and T = 25 °C: power-law processes and the relative reactivity of minerals. *Geochim Cosmochim Acta* 75:6004–6026
- Rüggeburg A, Fietzke J, Liebetrau V, Eisenhauer A, Dullo WC, Freiwald A (2008) Stable strontium isotopes ($\delta^{88/86}\text{Sr}$) in cold-water corals—a new proxy for reconstruction of intermediate ocean water temperatures. *Earth Planet Sci Lett* 269:570–575
- Saccoccia PJ, Seewald JS, Shanks WC (2009) Oxygen and hydrogen isotope fractionation in serpentine-water and talc-water systems from 250 to 450 °C, 50 MPa. *Geochim Cosmochim Acta* 73:6789–6804
- Sachse D, Billault I et al (2012) Molecular paleohydrology: interpreting the hydrogen-isotopic composition of lipid biomarkers from photosynthesizing organisms. *Ann Rev Earth Planet Sci* 40:221–249
- Sadofsky SJ, Bebout GE (2000) Ammonium partitioning and nitrogen isotope fractionation among coexisting micas during high-temperature fluid-rock interaction. Examples from the New England Appalachians. *Geochim Cosmochim Acta* 64:2835–2849
- Saenger C, Wang Z (2014) Magnesium isotope fractionation in biogenic and abiogenic carbonates: implications for paleoenvironmental proxies. *Quart J Rev* 90:1–21

- Sakai H (1968) Isotopic properties of sulfur compounds in hydrothermal processes. *Geochem J* 2:29–49
- Sanyal A, Nugent M, Reeder RJ, Bijma J (2000) Seawater p_H control on the boron isotopic composition of calcite: evidence from inorganic calcite precipitation experiments. *Geochim Cosmochim Acta* 64:1551–1555
- Sauer PE, Eglinton TI, Hayes JM, Schimmelmann A, Sessions AL (2001) Compound-specific D/H ratios of lipid biomarkers from sediments as a proxy for environmental and climatic conditions. *Geochim Cosmochim Acta* 65:213–222
- Saunier G, Pokrovski GS, Poitrasson F (2011) First experimental determination of iron isotope fractionation between hematite and aqueous solution at hydrothermal conditions. *Geochim Cosmochim Acta* 75:6629–6654
- Savage PS, Armytage R, Georg RB, Halliday AN (2014) High temperature silicon isotope geochemistry. *Lithos* 190–191:500–519
- Savage PS, Georg RB, Williams HM, Burton KW, Halliday AN (2011) Silicon isotope fractionation during magmatic differentiation. *Geochim Cosmochim Acta* 75:6124–6139
- Savin SM, Lee M (1988) Isotopic studies of phyllosilicates. *Rev Mineral* 19:189–223
- Schauble EA (2007) Role of nuclear volume in driving equilibrium stable isotope fractionation of mercury, thallium and other very heavy elements. *Geochim Cosmochim Acta* 71:2170–2189
- Schauble EA (2011) First principles estimates of equilibrium magnesium isotope fractionation in silicate, oxide, carbonate and hexaaquamagnesium(2+) crystals. *Geochim Cosmochim Acta* 75:844–869
- Schauble EA, Rossman GR, Taylor HP (2001) Theoretical estimates of equilibrium Fe isotope fractionations from vibrational spectroscopy. *Geochim Cosmochim Acta* 65:2487–2498
- Schauble ES, Rossman GR, Taylor HP (2003) Theoretical estimates of equilibrium chlorine-isotope fractionations. *Geochim Cosmochim Acta* 67:3267–3281
- Schauble EA, Rossman GR, Taylor HP (2004) Theoretical estimates of equilibrium chromium isotope fractionations. *Chem Geol* 205:99–114
- Scheele N, Hoefs J (1992) Carbon isotope fractionation between calcite, graphite and CO_2 . *Contr Mineral Petrol* 112:35–45
- Schilling K, Johnson TM, Wilcke W (2011) isotope fractionation of selenium during fungal biomethylation by *Alternaria alternata*. *Environ Sci Technol* 45:2670–2676
- Schimmelmann A, Sessions AL, Mastalerz M (2006) Hydrogen isotopic (D/H) composition of organic matter during diagenesis and thermal maturation. *Ann Rev Earth Planet Sci* 34:501–533
- Schmidt M, Maseyk K, Lett C, Biron P, Richard P, Bariac T, Seibt U (2010) Concentration effects on laser based $\delta^{18}O$ and δ^2H measurements and implications for the calibration of vapour measurements with liquid standards. *Rapid Comm Mass Spectrom* 24:3553–3561
- Schmitt AD, Galer SJ, Abouchami W (2009) Mass-dependent cadmium isotopic variations in nature with emphasis on the marine environment. *Earth Planet Sci Lett* 277:262–272
- Schmitt AD, Cobert F, Bourgeade P et al (2013) Calcium isotope fractionation during plant growth under a limited nutrient supply. *Geochim Cosmochim Acta*
- Schoenberg R, von Blanckenburg F (2005) An assessment of the accuracy of stable Fe isotope ratio measurements on samples with organic and inorganic matrices by high-resolution multicollector ICP-MS. *Int J Mass Spectr* 242:257–272
- Schoenberg R, Zink S, Staubwasser M, von Blanckenburg F (2008) The stable Cr isotope inventory of solid Earth reservoirs determined by double-spike MC-ICP-MS. *Chem Geol* 249:294–306
- Schoenheimer R, Rittenberg D (1939) Studies in protein metabolism: I. General considerations in the application of isotopes to the study of protein metabolism. The normal abundance of nitrogen isotopes in amino acids. *J Biol Chem* 127:285–290
- Schüßler JA, Schoenberg R, Behrens H, von Blanckenburg F (2007) The experimental calibration of iron isotope fractionation factor between pyrrhotite and peralkaline rhyolitic melt. *Geochim Cosmochim Acta* 71:417–433

- Scott C, Lyons TW (2012) Contrasting molybdenum cycling and isotopic properties in euxinic versus non-euxinic sediments and sedimentary rocks: refining the paleoproxies. *Chem Geol* 300:61–77
- Seal RR (2006) Sulfur isotope geochemistry of sulfide minerals. *Rev Mineral Geochem* 61:633–677
- Seal RR, Alpers CN, Rye RO (2000) Stable isotope systematics of sulfate minerals. *Rev Mineral* 40:541–602
- Sedaghatpour F, Teng FZ, Liu Y, Sears DW, Taylor LA (2013) Magnesium isotope composition of the Moon. *Geochim Cosmochim Acta* 120:1–16
- Seitz HM, Brey GP, Lahaye Y, Durali S, Weyer S (2004) Lithium isotope signatures of peridotite xenoliths and isotope fractionation at high temperature between olivine and pyroxene. *Chem Geol* 212:163–177
- Seitz HM, Brey GP, Zipfel J, Ott U, Weyer S, Durali S, Weinbruch S (2007) Lithium isotope composition of ordinary and carbonaceous chondrites and differentiated planetary bodies: bulk solar system and solar reservoirs. *Earth Planet Sci Lett* 260:582–596
- Sessions AL, Burgoyne TW, Schimmelmann A, Hayes JM (1999) Fractionation of hydrogen isotopes in lipid biosynthesis. *Org Geochem* 30:1193–1200
- Severmann S, Johnson CM, Beard BL, McManus J (2006) The effect of early diagenesis on the Fe isotope composition of porewaters and authigenic minerals in continental margin sediments. *Geochim Cosmochim Acta* 70:2006–2022
- Severmann S, Lyons TW, Anbar A, McManus J, Gordon G (2008) Modern iron isotope perspective on the benthic iron shuttle and the redox evolution of ancient oceans. *Geology* 36:487–490
- Severmann S, McManus J, Berelson WM, Hammond DE (2010) The continental shelf benthic flux and its isotope composition. *Geochim Cosmochim Acta* 74:3984–4004
- Shahar A, Young ED, Manning CE (2008) Equilibrium high-temperature Fe isotope fractionation between fayalite and magnetite: an experimental calibration. *Earth Planet Sci Lett* 268:330–338
- Shahar A, Ziegler K, Young ED, Riccolaeu A, Schauble E, Fei Y (2009) Experimentally determined Si isotope fractionation between silicate and Fe metal and implications for the Earth's core formation. *Earth Planet Sci Lett* 288:228–234
- Sharma T, Clayton RN (1965) Measurement of $^{18}\text{O}/^{16}\text{O}$ ratios of total oxygen of carbonates. *Geochim Cosmochim Acta* 29:1347–1353
- Sharp ZD (1990) A laser-based microanalytical method for the in situ determination of oxygen isotope ratios of silicates and oxides. *Geochim Cosmochim Acta* 54:1353–1357
- Sharp ZD, Atudorei V, Durakiewicz T (2001) A rapid method for determination of hydrogen and oxygen isotope ratios from water and hydrous minerals. *Chem Geol* 178:197–210
- Sharp ZD, Barnes JD, Brearley AJ, Chaussidon M, Fischer TP, Kamenetsky VS (2007) Chlorine isotope homogeneity of the mantle, crust and carbonaceous chondrites. *Nature* 446:1062–1065
- Sharp ZD, Shearer CK, McKeegan KD, Barnes JD, Wang YD (2010) The chlorine isotope composition of the Moon and implications for an anhydrous mantle. *Science* 329:1050–1053
- Shen B, Jacobson B, Lee CT, Yin QZ, Mourtou DM (2009) The Mg isotopic systematics of granitoids in continental arcs and implications for the role of chemical weathering in crust formation. *PNAS* 106:20652–20657
- Sheppard SMF, Nielsen RL, Taylor HP (1971) Hydrogen and oxygen isotope ratios in minerals from Porphyry Copper Deposits. *Econ Geol* 66:515–542
- Sherman LS, Blum JD, Johnson KP, Keeler GJ, Barres JA, Douglas TA (2010) Mass-independent fractionation of mercury isotopes in Arctic snow driven by sunlight. *Nat Geosci* 3:173–177
- Sherman LS, Blum JD, Nordstrom DK, McCleskey RB, Barkay T, Vetriani C (2009) Mercury isotope composition of hydrothermal systems in the Yellowstone Plateau volcanic field and Guaymas Basin sea-floor rift. *Earth Planet. Sci Lett* 279:86–96
- Shiel AE, Weis D, Orians KJ (2010) Evaluation of zinc, cadmium and lead isotope fractionation during smelting and refining. *Sci Tot Environ* 408:2357–2368
- Shields WR, Goldich SS, Garner EI, Murphy TJ (1965) Natural variations in the abundance ratio and the atomic weight of copper. *J Geophys Res* 70:479–491

- Shouakar-Stash O, Alexeev SV, Frape SK, Alexeeva LP, Drimmie RJ (2007) Geochemistry and stable isotope signatures including chlorine and bromine isotopes of the deep groundwaters of the Siberian Platform, Russia. *Appl Geochem* 22:589–605
- Shouakar-Stash O, Drimmie RJ, Frape SK (2005) Determination of inorganic chlorine stable isotopes by continuous flow isotope mass spectrometry. *Rapid Commun Mass Spectr* 19:121–127
- Siebert C, Kramers JD, Meisel T, Morel P, Nögler TF (2005) PGE, Re-Os and Mo isotope systematics in Archean and early Proterozoic sedimentary systems as proxies for redox conditions of the early Earth. *Geochim Cosmochim Acta* 69:1787–1801
- Siebert C, McManus J, Bice A, Poulson R, Berelson WM (2006b) Molybdenum isotope signatures in continental margin sediments. *Earth Planet Sci Lett* 241:723–733
- Siebert C, Nögler TF, von Blanckenburg F, Kramers JD (2003) Molybdenum isotope records as potential proxy for paleoceanography. *Earth Planet Sci Lett* 211:159–171
- Siebert C, Ross A, McManus J (2006a) Germanium isotope measurements of high-temperature geothermal fluids using double-spike hydride generation MC-ICP-MS. *Geochim Cosmochim Acta* 70:3986–3995
- Sigman DM, Casciotti KL, Andreani M, Barford C, Galanter M, Böhlke JK (2001) A bacterial method for the nitrogen isotopic analysis of nitrate in seawater and freshwater. *Anal Chem* 73:4145–4153
- Sikora ER, Johnson TM, Bullen TD (2008) Microbial mass-dependent fractionation of chromium isotopes. *Geochim Cosmochim Acta* 72:3631–3641
- Sim MS, Bosak T, Ono S (2011) Large sulfur isotope fractionation does not require disproportionation. *Science* 333:74–77
- Sime NG, De la Rocha C, Galy A (2005) Negligible temperature dependence of calcium isotope fractionation in 12 species of planktonic foraminifera. *Earth Planet Sci Lett* 232:51–66
- Simon JL, dePaolo DJ (2010) Stable calcium isotopic composition of meteorites and rocky planets. *Earth Planet Sci Lett* 289:457–466
- Skulan JL, Beard BL, Johnson CM (2002) Kinetic and equilibrium isotope fractionation between aqueous Fe(III) and hematite. *Geochim Cosmochim Acta* 66:2505–2510
- Skulan JL, DePaolo DJ, Owens TL (1997) Biological control of calcium isotopic abundances in the global calcium cycle. *Geochim Cosmochim Acta* 61:2505–2510
- Skulan JL, DePaolo DJ (1999) Calcium isotope fractionation between soft and mineralised tissues as a monitor of calcium use in vertebrates. *PNAS* 96:13709–13713
- Slack JF, Palmer MR, Stevens BPJ, Barnes RG (1993) Origin and significance of tourmaline-rich rocks in the Broken Hill district, Australia. *Econ Geol* 88:505–541
- Smith CN, Kesler SE, Blum JD, Rytuba JR (2008) Isotope geochemistry of mercury in source rocks, mineral deposits and spring deposits of the California Coast Ranges, USA. *Earth Planet Sci Lett* 269:398–406
- Smith MP, Yardley BWD (1996) The boron isotopic composition of tourmaline as a guide to fluid processes in the southwestern England orefield: an ion microprobe study. *Geochim Cosmochim Acta* 60:1415–1427
- Smithers RM, Krouse HR (1968) Tellurium isotope fractionation study. *Can J Chem* 46:583–591
- Sonke JE (2011) A global model of mass independent mercury stable isotope fractionation. *Geochim Cosmochim Acta* 75:4577–4590
- Sonke JE, Blum JD (2013) Advances in mercury stable isotope geochemistry. *Chem Geol* 366:1–4
- Sonke JE, Schäfer J et al (2010) Sedimentary mercury stable isotope records of atmospheric and riverine pollution from two major European heavy metal refineries. *Chem Geol* 279:90–100
- Sonke JE, Sivry Y et al (2008) Historical variations in the isotopic composition of atmospheric zinc deposition from a zinc smelter. *Chem Geol* 252:145–157
- Spivack AJ, Edmond JM (1986) Determination of boron isotope ratios by thermal ionization mass spectrometry of the dicesium metaborate cation. *Anal Chem* 58:31–35
- Spivack AJ, Kastner M, Ransom B (2002) Elemental and isotopic chloride geochemistry in the Nankai trough. *Geophysical Res Lett* 29:1661. doi:[10.1029/2001GL014122](https://doi.org/10.1029/2001GL014122)

- Stetson SJ, Gray JE, Wanty RB, MacLary DL (2009) Isotope variability of mercury in ore, mine-waste calcine, and leachates of mine-waste calcine from areas mined for mercury. *Environ Sci Technol* 43:7331–7336
- Steuber T, Buhl D (2006) Calcium-isotope fractionation in selected modern and ancient marine carbonates. *Geochim Cosmochim Acta* 70:5507–5521
- Stevenson EI, Hermoso M, Rickaby RE, Tyler JJ, Minoletti F, Parkinson IJ, Mokadem F, Burton KW (2014) Controls on stable strontium isotope fractionation in coccolithophores with implications for the marine Sr cycle. *Geochim Cosmochim Acta* 128:225–235
- Stirling CH, Andersen MB, Potter EK, Halliday AN (2007) Low-temperature isotopic fractionation of uranium. *Earth Planet Sci Lett* 264:208–225
- Stotler RL, Frape SK, Shouakar-Stash O (2010) An isotopic survey of $d^{81}\text{Br}$ and $d^{37}\text{Cl}$ of dissolved halides in the Canadian and Fennoscandian shields. *Chem Geol* 274:38–55
- Sturchio NC, Hatzinger PB, Atkins MD, Suh C, Heraty LJ (2003) Chlorine isotope fractionation during microbial reduction of perchlorate. *Environ Sci Technol* 37:3859–3863
- Sutton JN, Varela DE, Brzezinski MA, Beucher CP (2013) Species-dependent silicon isotope fractionation by marine diatoms. *Geochim Cosmochim Acta* 104:300–309
- Suzuoki T, Epstein S (1976) Hydrogen isotope fractionation between OH-bearing minerals and water. *Geochim Cosmochim Acta* 40:1229–1240
- Swart PK, Burns SJ, Leder JJ (1991) Fractionation of the stable isotopes of oxygen and carbon in carbon dioxide during the reaction of calcite with phosphoric acid as a function of temperature and technique. *Chem Geol* 86:89–96
- Swihart GH, Moore PB (1989) A reconnaissance of the boron isotopic composition of tourmaline. *Geochim Cosmochim Acta* 53:911–916
- Tanimizu M, Araki Y, Asaoka S, Takahashi Y (2011) Determination of natural isotopic variation in antimony using inductively coupled plasma mass spectrometry for an uncertainty estimation of the standard atomic weight of antimony. *Geochem J* 45:27–32
- Tarutani T, Clayton RN, Mayeda TK (1969) The effect of polymorphism and magnesium substitution on oxygen isotope fractionation between calcium carbonate and water. *Geochim Cosmochim Acta* 33:987–996
- Taube H (1954) Use of oxygen isotope effects in the study of hydration ions. *J Phys Chem* 58:523
- Taylor HP (1968) The oxygen isotope geochemistry of igneous rocks. *Contr Mineral Petrol* 19:1–71
- Taylor HP (1974) The application of oxygen and hydrogen isotope studies to problems of hydrothermal alteration and ore deposition. *Econ Geol* 69:843–883
- Taylor HP, Epstein S (1962) Relation between $^{18}\text{O}/^{16}\text{O}$ ratios in coexisting minerals of igneous and metamorphic rocks. I Principles and experimental results. *Geol Soc Am Bull* 73:461–480
- Taylor TI, Urey HC (1938) Fractionation of the lithium and potassium isotopes by chemical exchange with zeolites. *J Chem Phys* 6:429–438
- Telus M, Dauphas N, Moynier F, Tissot F, Teng FZ, Nabelek PI, Craddock PR, Groat LA (2012) Iron, zinc, magnesium and uranium isotopic fractionation during continental crust differentiation: the tale from migmatites, granitoids and pegmatites. *Geochim Cosmochim Acta* 97:247–265
- Teng FZ et al (2004) Lithium isotope composition and concentration of the upper continental crust. *Geochim Cosmochim Acta* 68:4167–4178
- Teng FZ, Dauphas N, Helz R (2008) Iron isotope fractionation during magmatic differentiation in Kilauea Iki lava lake. *Science* 320:1620–1622
- Teng FZ, Dauphas N, Helz RT, Gao S, Huang S (2011) Diffusion-driven magnesium and iron isotope fractionation in Hawaiian olivine. *Earth Planet Sci Lett* 308:317–324
- Teng FZ, Dauphas N, Huang S, Marty B (2013) Iron isotope systematics of oceanic basalts. *Geochim Cosmochim Acta* 107:12–26
- Teng FZ, McDonough WF, Rudnick RL, Walker RJ (2006) Diffusion-driven extreme lithium isotopic fractionation in country rocks of the Tin Mountain pegmatite. *Earth Planet Sci Lett* 243:701–710

- Teng FZ, McDonough WF, Rudnick RL, Wing BA (2007a) Limited lithium isotopic fractionation during progressive metamorphic dehydration in metapelites: a case study from the Onawa contact aureole, Maine. *Chem Geol* 239:1–12
- Teng FZ, Rudnick RL, McDonough WF, Wu FY (2009) Lithium isotope systematics of A-type granites and their mafic enclaves: further constraints on the Li isotopic composition of the continental crust. *Chem Geol* 262:415–424
- Teng FZ, Wadhwa M, Helz RT (2007b) Investigation of magnesium isotope fractionation during basalt differentiation: implications for a chondritic composition of the terrestrial mantle. *Earth Planet Sci Lett* 261:84–92
- Teng FZ, Yang W (2013) Comparison of factors affecting the accuracy of high-precision magnesium isotope analysis by multi-collector inductively coupled plasma mass spectrometry. *Rapid Commun Mass Spectrom* 28:19–24
- Teng FZ et al. (2014) Magnesium isotopic compositions of international geological reference materials. *Geostand Geoanal Res* (in press)
- Tesdal JE, Galbraith ED, Kienast M (2013) Nitrogen isotopes in bulk marine sediments: linking seafloor observations with subseafloor records. *Biogeosciences* 10:101–118
- Teutsch N, Schmid M, Muller B, Halliday AN, Burgmann H, Wehrli B (2009) Large iron isotope fractionation at the oxic-anoxic boundary in lake Nyos. *Earth Planet Sci Lett* 285:52–60
- Thamdrup B, Dalsgaard T (2002) Production of N_2 through anaerobic ammonium oxidation coupled to nitrate reduction in marine sediments. *Appl Environ Microbiol* 68:1312–1318
- Thode HG, Macnamara J, Collins CB (1949) Natural variations in the isotopic content of sulphur and their significance. *Can J Res* 27B:361
- Tipper ET, Galy A, Bickle MJ (2006a) Riverine evidence for a fractionated reservoir of Ca and Mg on the continents: implications for the oceanic Ca cycle. *Earth Planet Sci Lett* 247:267–279
- Tipper ET, Galy A, Bickle MJ (2008) Calcium and magnesium isotope systematics in rivers draining the Himalaya-Tibetan-Plateau region: lithological or fractionation control? *Geochim Cosmochim Acta* 72:1057–1075
- Tipper ET, Galy A, Gaillardet J, Bickle MJ, Elderfield H, Carder EA (2006b) The magnesium isotope budget of the modern ocean: constraints from riverine magnesium isotope ratios. *Earth Planet Sci Lett* 250:241–253
- Tipper ET, Gaillardet J, Galy A, Louvat P, Bickle MJ, Capmas F (2010) Calcium isotope ratios in the world's largest rivers: a constraint on the maximum imbalance of oceanic calcium fluxes. *Global Biogeochemical Cycles* 24:10.1029/2009GB003574
- Tomaschak PB, Ryan JG, Defant MJ (2000) Lithium isotope evidence for light element decoupling in the Panama subarc mantle. *Geology* 28:507–510
- Tomaschak PB, Tera F, Helz RT, Walker RJ (1999) The absence of lithium isotope fractionation during basalt differentiation: new measurements by multicollector sector ICP-MS. *Geochim Cosmochim Acta* 63:907–910
- Tomaschak PB, Widom E, Benton LD, Goldstein SL, Ryan JG (2002) The control of lithium budgets in island arcs. *Earth Planet Sci Lett* 196:227–238
- Tomaszack PB (2004) Lithium isotopes in earth and planetary sciences. *Rev Mineral Geochem*
- Tonarini S, Leeman WP, Leat PT (2011) Subduction erosion of forearc mantle wedge implicated in the genesis of the South Sandwich Island (SSI) arc: evidence from boron isotope systematics. *Earth Planet Sci Lett* 301:275–284
- Toutain JP, Sonke J et al (2008) Evidence for Zn isotopic fractionation at Merapi volcano. *Chem Geol* 253:74–82
- Trofimov A (1949) Isotopic constitution of sulfur in meteorites and in terrestrial objects. *Dokl Akad Nauk SSSR* 66:181 (in Russian)
- Trudinger PA, Chambers LA, Smith JW (1985) Low temperature sulphate reduction: biological versus abiological. *Can J Earth Sci* 22:1910–1918
- Truesdell AH (1974) Oxygen isotope activities and concentrations in aqueous salt solution at elevated temperatures: Consequences for isotope geochemistry. *Earth Planet Sci Lett* 23:387–396

- Turner JV (1982) Kinetic fractionation of carbon-13 during calcium carbonate precipitation. *Geochim Cosmochim Acta* 46:1183–1192
- Urey HC, Brickwedde FG, Murphy GM (1932) A hydrogen isotope of mass 2 and its concentration. *Phys Rev* 40:1
- Usdowski E, Hoefs J (1993) Oxygen isotope exchange between carbonic acid, bicarbonate, carbonate, and water: a re-examination of the data of McCrea (1950) and an expression for the overall partitioning of oxygen isotopes between the carbonate species and water. *Geochim Cosmochim Acta* 57:3815–3818
- Uzdowski E, Michaelis J, Böttcher MB, Hoefs J (1991) Factors for the oxygen isotope equilibrium fractionation between aqueous CO₂, carbonic acid, bicarbonate, carbonate, and water. *Z Phys Chem* 170:237–249
- Uvarova YA, Kyser TK, Geagea ML, Chipley D (2015) Variations in the uranium isotopic composition of uranium ores from different types of uranium deposits. *Geochim Cosmochim Acta* (in press)
- Valdes MC, Moreira M, Foriel J, Moynier F (2014) The nature of Earth's building blocks as revealed by calcium isotopes. *Earth Planet Sci Lett* 394:135–145
- Valley JW, O'Neil JR (1981) ¹³C/¹²C exchange between calcite and graphite: a possible thermometer in Greville marbles. *Geochim Cosmochim Acta* 45:411–419
- Van Acker M, Shahar A, Young ED, Coleman ML (2006) GC/Multiple Collector-ICPMS method for chlorine stable isotope analysis of chlorinated aliphatic hydrocarbons. *Anal Chem* 78:4663–4667
- Van den Boorn SH, van Bergen MJ, Vroon PZ, de Vries ST, Nijman W (2010) Silicon isotope and trace element constraints on the origin of ≈ 3.5 Ga cherts: implications for Early Archaean marine environments. *Geochim Cosmochim Acta* 74:1077–1103
- Van Warmerdam EM, Frapre SK, Aravena R, Drimmie RJ, Flatt H, Cherry JA (1995) Stable chlorine and carbon isotope measurements of selected chlorinated organic solvents. *Appl Geochem* 10:547–552
- Vance D, Archer C, Bermin J, Perkins J, Statham PC, Lohan MC, Ellwood MJ, Mills RA (2008) The copper isotope geochemistry of rivers and oceans. *Earth Planet Sci Lett* 274:204–213
- Varela DE, Pride CJ, Brzezinski MA (2004) Biological fractionation of silicon isotopes in southern ocean surface waters. *Glob Biogeochem Cycles* 18. doi:10.1029/2003GB002140
- Velinsky DJ, Pennock JR, Sharp JH, Cifuentes LA, Fogel ML (1989) Determination of the isotopic composition of ammonium-nitrogen at the natural abundance level from estuarine waters. *Mar Chem* 26:351–361
- Vengosh A, Chivas AR, McCulloch M, Starinsky A, Kolodny Y (1991a) Boron isotope geochemistry of Australian salt lakes. *Geochim Cosmochim Acta* 55:2591–2606
- Vengosh A, Heumann KG, Juraske S, Kashner R (1994) Boron isotope application for tracing sources of contamination in groundwater. *Environ Sci Tech* 28:1968–1974
- Vengosh A, Starinsky A, Kolodny Y, Chivas AR (1991b) Boron isotope geochemistry as a tracer for the evolution of brines and associated hot springs from the Dead Sea, Israel. *Geochim Cosmochim Acta* 55:1689–1695
- Vennemann TW, Fricke HC, Blake RE, O'Neil JR, Colman A (2002) Oxygen isotope analysis of phosphates: a comparison of techniques for analysis of Ag₃PO₄. *Chem Geol* 185:321–336
- Vennemann T, O'Neil JR (1996) Hydrogen isotope exchange reactions between hydrous minerals and hydrogen: I. A new approach for the determination of hydrogen isotope fractionation at moderate temperatures. *Geochim Cosmochim Acta* 60:2437–2451
- Viers J et al (2007) Evidence of Zn isotope fractionation in a soil-plant system of a pristine tropical watershed (Nsimi, Cameroon). *Chem Geol* 239:124–137
- Voegelin AR, Nägler TF, Beukes NJ, Lacassie JP (2010) Molybdenum isotopes in late Archean carbonate rocks: implications for early Earth oxygenation. *Precamb Res* 182:70–82
- Voegelin AR, Nägler TF, Samankassou E, Villa IM (2009) Molybdenum isotopic composition of modern and Carboniferous carbonates. *Chem Geol* 265:488–498
- Vogel JC, Grootes PM, Mook WG (1970) Isotopic fractionation between gaseous and dissolved carbon dioxide. *Z Physik* 230:225–238

- Vollstädt H, Eisenhauer A et al. (2014) The Phanerozoic $\delta^{88/86}\text{Sr}$ record of seawater: new constraints on past changes in oceanic carbonate fluxes. *Geochim Cosmochim Acta* 128:249–265
- Von Allmen K, Böttcher ME, Samankassou E, Nägler TF (2010) Barium isotope fractionation in the global barium cycle: first evidence from barium minerals and precipitation experiments. *Chem Geol* 277:70–77
- Wachter EA, Hayes JM (1985) Exchange of oxygen isotopes in carbon dioxide-phosphoric acid systems. *Chem Geol* 52:365–374
- Wang Z, Hu P, Gaetani G, Liu C, Saenger C, Cohen A, Hart S (2013b) Experimental calibration of Mg isotope fractionation between aragonite and seawater. *Geochim Cosmochim Acta* 102:113–123
- Wang Y, Sessions AL, Nielsen JR, Goddard WA (2009a) Equilibrium $^2\text{H}/^1\text{H}$ fractionations in organic molecules. I. Calibration of ab initio calculations. *Geochim Cosmochim Acta* 73:7060–7075
- Wang Y, Sessions AL, Nielsen RJ, Goddard WA (2009b) Equilibrium $^2\text{H}/^1\text{H}$ fractionations in organic molecules. II: Linear alkanes, alkenes, ketones, carboxylic acids, esters, alcohols and ethers. *Geochim Cosmochim Acta* 73:7076–7086
- Wang Y, Sessions AL, Nielsen RJ, Goddard WA (2013a) Equilibrium $^2\text{H}/^1\text{H}$ fractionation in organic molecules. III Cyclic ketones and hydrocarbons. *Geochim Cosmochim Acta* 107:82–95
- Wanner C, Sonnenthal EL, Liu XM (2014) Seawater $\delta^7\text{Li}$: a direct proxy for global CO_2 consumption by continental silicate weathering? *Chem Geol* 381:154–167
- Wasylenki LE, Swihart JW, Romaniello SJ (2014) Cadmium isotope fractionation during adsorption to Mn oxyhydroxide at low and high ionic strength. *Geochim Cosmochim Acta* 140:212–226
- Wei G, Ma J, Liu Y, Xie L, Lu W, Deng W, Ren Z, Zeng T, Yang Y (2013) Seasonal changes in the radiogenic and stable strontium isotopic composition of Xijiang River: implications for chemical weathering. *Chem Geol* 343:67–75
- Weinstein C, Moynier F, Wang K, Paniello R, Foriel J, Catalano J, Pichat S (2011) Isotopic fractionation of Cu in plants. *Chem Geol* 286:266–271
- Weiss DJ, Mason TFD, Zhao FJ, Kirk GJD, Coles BJ, Horstwood MSA (2005) Isotopic discrimination of zinc in higher plants. *New Phytol* 165:703–710
- Weiss DJ, Rausch N, Mason TFD, Coles BJ, Wilkinson JJ, Ukonmaanaho L, Arnold T, Nieminen TM (2007) Atmospheric deposition and isotope biogeochemistry of zinc in ombrotrophic peat. *Geochim Cosmochim Acta* 71:3498–3517
- Welch SA, Beard BL, Johnson CM, Braterman PS (2003) Kinetic and equilibrium Fe isotope fractionation between aqueous Fe(II) and Fe(III). *Geochim Cosmochim Acta* 67:4231–4250
- Wen H, Carignan J (2011) Selenium isotopes trace the source and redox processes in the black shale-hosted Se-rich deposits in China. *Geochim Cosmochim Acta* 75:1411–1427
- Wenzel B, Lecuyer C, Joachimski MM (2000) Comparing oxygen isotope records of Silurian calcite and phosphate— $\delta^{18}\text{O}$ composition of brachiopods and conodonts. *Geochim Cosmochim Acta* 69:1859–1872
- Weyer S, Anbar AD, Brey GP, Münker C, Mezger K (2005) Iron isotope fractionation during planetary differentiation. *Earth Planet Sci Lett* 240:251–264
- Weyer S, Anbar AD, Gerdes A, Gordon GW, Algeo TJ, Boyle EA (2008) Natural fractionation of $^{238}\text{U}/^{235}\text{U}$. *Geochim Cosmochim Acta* 72:345–3359
- Weyer S, Ionov D (2007) Partial melting and melt percolation in the mantle: the message from Fe isotopes. *Earth Planet Sci Lett* 259:119–133
- Weyer S, Schwieters JB (2003) High precision Fe isotope measurements with high mass resolution MC-ICPMS. *Inter J Mass Spectr* 226:355–368
- Wiechert U, Fiebig J, Przybilla R, Xiao Y, Hoefs J (2002) Excimer laser isotope-ratio-monitoring mass spectrometry for in situ oxygen isotope analysis. *Chem Geol* 182:179–194
- Wiechert U, Halliday AN (2007) Non-chondritic magnesium and the origin of the inner terrestrial planets. *Earth Planet Sci Lett* 256:360–371

- Wiechert U, Hoefs J (1995) An excimer laser-based microanalytical preparation technique for in-situ oxygen isotope analysis of silicate and oxide minerals. *Geochim Cosmochim Acta* 59:4093–4101
- Wiederhold JG, Kraemer SM, Teutsch N, Borer PM, Halliday AN, Kretzschmar R (2006) Iron isotope fractionation during proton-promoted, ligand-controlled and reductive dissolution of goethite. *Environ Sci Tech* 40:3787–3793
- Wiegand BA, Chadwick OA, Vitousek PM, Wooden JH (2005) Ca cycling and isotopic fluxes in forested ecosystems in Hawaii. *Geophys Res Lett* 32:L11404
- Wilkinson JJ, Weiss DJ, Mason TF, Coles BJ (2005) Zinc isotope variation in hydrothermal systems: preliminary evidence from the Irish Midlands ore field. *Econ Geol* 100:583–590
- Wille M, Kramers JD, Nägler TF, Beukes NJ, Schroder S, Meiser T, Lacassie JP, Voegelin AR (2007) Evidence for a gradual rise of oxygen between 2.6 and 2.5 Ga from Mo isotopes and Re-PGE signatures in shales. *Geochim Cosmochim Acta* 71:2417–2435
- Wille M, Sutton J, Ellwood MJ, Sambridge M, Maher W, Eggins S, Kelly M (2010) Silicon isotopic fractionation in marine sponges: a new model for understanding silicon isotope variations in sponges. *Earth Planet Sci Lett* 292:281–289
- Williams LB, Ferrell RE, Hutcheon I, Bakel AJ, Walsh MM, Krouse HR (1995) Nitrogen isotope geochemistry of organic matter and minerals during diagenesis and hydrocarbon migration. *Geochim Cosmochim Acta* 59:765–779
- Williams LB, Hervig RL (2004) Boron isotopic composition of coals: a potential tracer of organic contaminated fluids. *Appl Geochem* 19:1625–1636
- Williams LB, Hervig RL, Holloway JR, Hutcheon I (2001) Boron isotope geochemistry during diagenesis. Part I. Experimental determination of fractionation during illitization of smectite. *Geochim Cosmochim Acta* 65:1769–1782
- Williams HM, Markowski A, Quitte G, Halliday AN, Teutsch N, Levasseur S (2006) Fe isotope fractionations in iron meteorites: new insight into metal-sulphide segregation and planetary accretion. *Earth Planet Sci Lett* 250:486–500
- Williams HM, Peslier AH, McCammon C, Halliday AN, Levasseur S, Teutsch N, Burg JP (2005) Systematic iron isotope variations in mantle rocks and minerals: the effects of partial melting and oxygen fugacity. *Earth Planet Sci Lett* 235:435–452
- Wimpenny J, Gislason SR, James RH, Gannoun A, Pogge von Strandmann P, Burton KW (2010) The behavior of Li and Mg isotopes during primary phase dissolution and secondary mineral formation in basalt. *Geochim Cosmochim Acta* 74:5259–5279
- Wombacher F, Rehkämper M, Mezger K (2004) Dependence of the mass-dependence in cadmium isotope fractionation during evaporation. *Geochim Cosmochim Acta* 68:2349–2357
- Wombacher F, Rehkämper M, Mezger K (2008) Cadmium stable isotope cosmochemistry. *Geochim Cosmochim Acta* 72:646–667
- Wombacher F, Rehkämper M, Mezger K, Münker C (2003) Stable isotope compositions in geological materials and meteorites determined by multiple-collector ICPMS. *Geochim Cosmochim Acta* 67:4639–4654
- Wortmann UG, Bernasconi SM, Böttcher ME (2001) Hypersulfidic deep biosphere indicates extreme sulfur isotope fractionation during single-step microbial sulfate reduction. *Geology* 29:647–650
- Wu L, Beard BL, Roden EE, Johnson CM (2011) Stable iron isotope fractionation between aqueous Fe (II) and hydrous ferric oxide. *Environ Sci Technol* 45:1845–1852
- Wunder B, Meixner A, Romer RL, Feenstra A, Schettler G, Heinrich W (2007) Lithium isotope fractionation between Li-bearing staurolite, Li-mica and aqueous fluids: an experimental study. *Chem Geol* 238:277–290
- Wunder B, Meixner A, Romer R, Heinrich W (2006) Temperature-dependent isotopic fractionation of lithium between clinopyroxene and high-pressure hydrous fluids. *Contrib Mineral Petrol* 151:112–120

- Wunder B, Meixner A, Romer R, Wirth R, Heinrich W (2005) The geochemical cycle of boron: constraints from boron isotope partitioning experiments between mica and fluid. *Lithos* 84:206–216
- Xiao YK, Liu WG, Qi HP, Zhang CG (1993) A new method for the high-precision isotopic measurement of bromine by thermal ionization mass spectrometry. *Int J Mass Spectrom Ion Proc* 123:117–123
- Xiao Y, Teng FZ, Zhang HF, Yang W (2013) Large magnesium isotope fractionation in peridotite xenoliths from eastern North China craton: product of melt-rock interaction. *Geochim Cosmochim Acta* 115:241–261
- Xue Z, Rehkämper M, Horner TJ, Abouchami W, Middag R, van de Fliert T, de Baar HJ (2013) Cadmium isotope variations in the Southern Ocean. *Earth Planet Sci Lett* 382:161–172
- Yamaguchi KE, Johnson CM, Beard BL, Ohmoto H (2005) Biogeochemical cycling of iron in the Archean-Paleoproterozoic Earth: constraints from iron isotope variations in sedimentary rocks from the Kapvaal and Pilbara cratons. *Chem Geol* 218:135–169
- Yamazaki E, Nakai S, Yokoyama T, Ishihara S, Tang HF (2013) Tin isotopic analysis of cassiterites from southeastern and eastern Asia. *Geochem J* 47:21–35
- Yang S-C, Lee D-C, Ho L-Y (2012b) The isotopic composition of cadmium in the water column of the South China Sea. *Geochim Cosmochim Acta* 98:66–77
- Yang W, Teng FZ, Zhang HF (2009) Chondritic magnesium isotopic composition of the terrestrial mantle: a case study of peridotite xenoliths from the North China craton. *Earth Planet Sci Lett* 288:475–482
- Yang W, Teng FZ, Zhang HF, Li SG (2012a) Magnesium isotopic systematics of continental basalts from the North China craton: implications for tracing subducted carbonate in the mantle. *Chem Geol* 328:185–194
- Yesavage T, Fantle MS, Vervoort J, Mathur R, Jin L, Liermann LJ, Brantley SL (2012) Fe cycling in the Shale Hills Critical Zone Observatory, Pennsylvania: an analysis of biogeochemical weathering and Fe isotope fractionation. *Geochim Cosmochim Acta* 99:18–38
- Yin R, Feng X, Shi W (2010) Application of the stable isotope system to the study of sources and fate of Hg in the environment: a review. *Appl Geochem* 25:1467–1477
- Yin R, Feng X, Wang J, Li P, Liu J, Zhang Y, Chen J, Zheng L, Hu T (2013) Mercury speciation and mercury isotope fractionation during ore roasting process and their implication to source identification of downstream sediment in the Wanshan mercury mining area, SW China. *Chem Geol* 366:39–46
- Yokochi R, Marty B, Chazot G, Burnard P (2009) Nitrogen in peridotite xenoliths: lithophile behaviour and magmatic isotope fractionation. *Geochim Cosmochim Acta* 73:4843–4861
- Young ED, Galy A (2004) The isotope geochemistry and cosmochemistry of magnesium. *Rev Mineral Geochem* 55:197–230
- Young ED, Galy A, Nagahara H (2002) Kinetic and equilibrium mass-dependent isotope fractionation laws in nature and their geochemical and cosmochemical significance. *Geochim Cosmochim Acta* 66:1095–1104
- Young ED, Manning CE, Schauble EA, Shahar A, Macris CA, Lazar C, Jordan M (2015) High-temperature equilibrium isotope fractionation of non-traditional isotopes: experiments, theory and applications. *Chem Geol* 395:176–195
- Young MB, McLaughlin K, Kendall C, Stringfellow W, Rollow M, Elsbury K, Donald E, Payton A (2009) Characterizing the oxygen isotopic composition of phosphate sources to aquatic ecosystems. *Environ Sci Technol* 43:5190–5196
- Zambardi T, Poitrasson F, Corgne A, Meheut M, Quitte Anand M (2013) Silicon isotope variations in the inner solar system: implications for planetary formation, differentiation and composition. *Geochim Cosmochim Acta* 121:67–83
- Zambardi T, Sonke JE, Toutain JP, Sortino F, Shinohara H (2009) Mercury emissions and stable isotope compositions at Vulcano Island (Italy). *Earth Planet Sci Lett* 277:236–243
- Zeebe RE (2005) Stable boron isotope fractionation between dissolved $B(OH)_3$ and $B(OH)_4^-$. *Geochim Cosmochim Acta* 69:2753–2766

- Zeebe RE (2007) An expression for the overall oxygen isotope fractionation between the sum of dissolved inorganic carbon and water. *Geochim Geophys Geosys* 8: [10.1029/2007GC001663](https://doi.org/10.1029/2007GC001663)
- Zerkle AL, Schneiderich K, Maresca JA, Liermann LJ, Brantley SL (2011) Molybdenum isotope fractionation by cyanobacterial assimilation during nitrate utilization and N₂ fixation. *Geobiology* 9:94–106
- Zhang L, Chan LH, Gieskes JM (1998) Lithium isotope geochemistry of pore waters from Ocean Drilling Program Sites 918 and 919, Irminger Basin. *Geochim Cosmochim Acta* 62:2437–2450
- Zhang J, Quay PD, Wilbur DO (1995) Carbon isotope fractionation during gas-water exchange and dissolution of CO₂. *Geochim Cosmochim Acta* 59:107–114
- Zheng W, Hintelmann H (2010) Nuclear field shift effects in isotope fractionation of mercury during abiotic reduction in the absence of light. *J Phys Chem A* 114:4238–4245
- Zhou JX, Huang ZL, Zhou MF, Zhu XK, Muchez P (2014) Zinc, sulphur and lead isotopic variations in carbonate-hosted Pb-Zn sulfide deposits, southwest China. *Ore Geol Rev* 58:41–54
- Zhu XK et al (2002) Mass fractionation processes of transition metal isotopes. *Earth Planet Sci Lett* 200:47–62
- Zhu JM, Johnson TM, Clark SK, Zhu XK, Wang XL (2014) Selenium redox cycling during weathering of Se-rich shales: a selenium isotope study. *Geochim Cosmochim Acta* 126:228–249
- Zhu P, MacDougall JD (1998) Calcium isotopes in the marine environment and the oceanic calcium cycle. *Geochim Cosmochim Acta* 62:1691–1698
- Ziegler K, Chadwick OA, Brzezinski MA, Kelly EF (2005a) Natural variations of $\delta^{30}\text{Si}$ ratios during progressive basalt weathering. *Geochim Cosmochim Acta* 69:4597–4610
- Ziegler K, Chadwick OA, White AF, Brzezinski MA (2005b) $\delta^{30}\text{Si}$ systematics in a granitic saprolite, Puerto Rico. *Geology* 33:817–820
- Ziegler K, Young ED, Schauble E, Wasson JT (2010) Metal-silicate silicon isotope fractionation in enstatite meteorites and constraints on Earth's core formation. *Earth Planet Sci Lett* 295:487–496
- Zink S, Schoenberg R, Staubwasser M (2010) Isotopic fractionation and reaction kinetics between Cr(III) and Cr(VI) in aqueous media. *Geochim Cosmochim Acta* 74:5729–5745

<http://www.springer.com/978-3-319-19715-9>

Stable Isotope Geochemistry

Hoefs, J.

2015, XV, 389 p. 101 illus., 98 illus. in color., Hardcover

ISBN: 978-3-319-19715-9